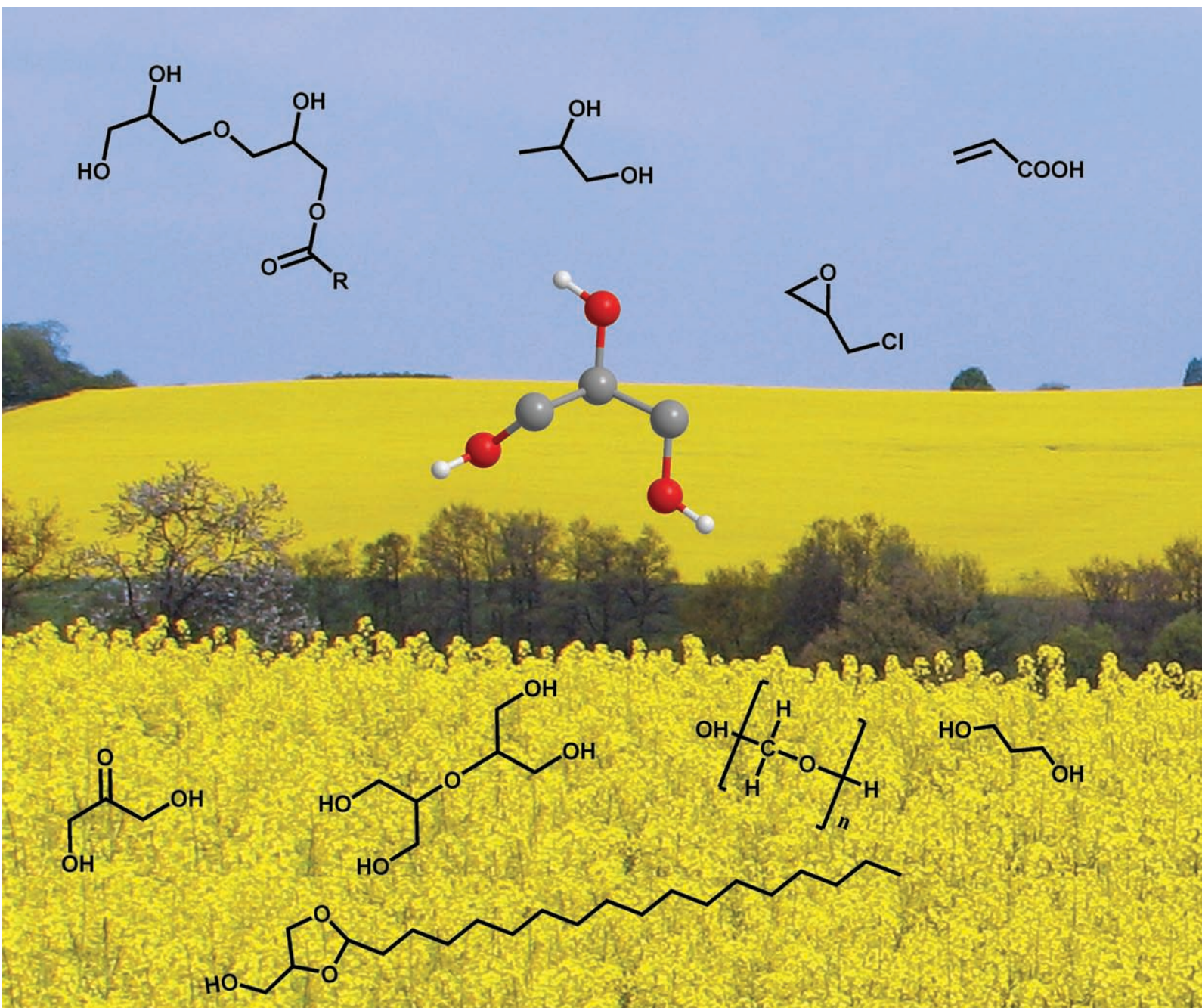


Green Chemistry

Cutting-edge research for a greener sustainable future

www.rsc.org/greenchem

Volume 10 | Number 1 | January 2008 | Pages 1–140



ISSN 1463-9262

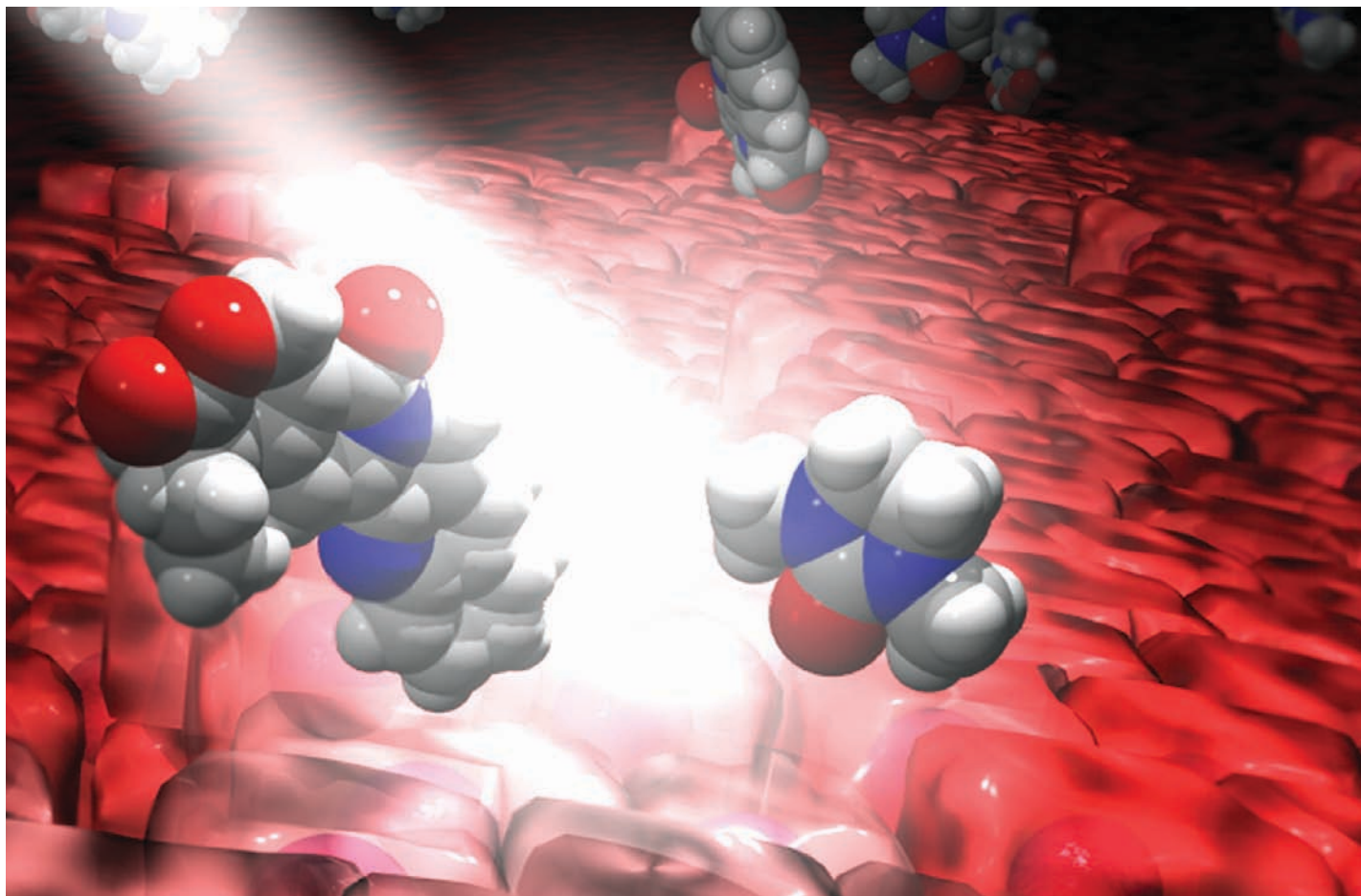
Behr *et al.*
New derivatives of glycerol

Dunn *et al.*
Green chemistry tools

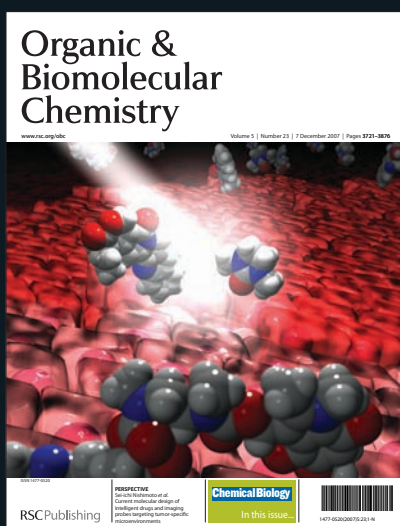


1463-9262(2008)10:1;1-H

RSC Publishing



Organic & Biomolecular Chemistry...



OBC has achieved tremendous success since the first issue was published in January 2003. Can any other 'young' journal boast such highly cited papers, published quickly after independent peer review to such exacting standards?

- Now one of the leading journals in the field, impact factor 2.874*
- Short publication times – average 21 days from acceptance for papers, and 13 days for communications
- Enhanced HTML articles – hyperlinked compound information, ontology terms linked to definitions and related articles, links to IUPAC Gold Book terms, and more . . .

* 2006 Thomson Scientific (ISI) Journal Citation Reports®

... high quality - high impact!

RSC Publishing

www.rsc.org/obc

Registered Charity Number 207890

Green Chemistry

Cutting-edge research for a greener sustainable future

www.rsc.org/greenchem

RSC Publishing is a not-for-profit publisher and a division of the Royal Society of Chemistry. Any surplus made is used to support charitable activities aimed at advancing the chemical sciences. Full details are available from www.rsc.org

IN THIS ISSUE

ISSN 1463-9262 CODEN GRCHFJ 10(1) 1-140 (2008)



Cover

See Behr *et al.*, pp. 13–30.
One plant, reams of opportunities! This cover shows that glycerol which is formed as a surplus by-product in the production of biodiesel from rapeseed oil, can be utilized as the raw material of various important intermediates.
Image reproduced by permission of Arno Behr from *Green Chem.*, 2008, **10**, 13.

CHEMICAL TECHNOLOGY

T1

Chemical Technology highlights the latest applications and technological aspects of research across the chemical sciences.

Chemical Technology

January 2008/Volume 5/Issue 1

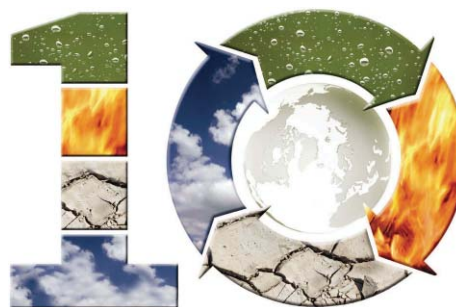
www.rsc.org/chemicaltechnology

EDITORIAL

11

Celebrating the tenth year of the *Green Chemistry* journal

This year *Green Chemistry* enters its tenth year of publishing. Martyn Poliakoff, Chair of the Editorial Board, Walter Leitner, Scientific Editor, and Sarah Ruthven, RSC Editor, take a glimpse at the exciting year ahead.



EDITORIAL STAFF

Editor

Sarah Ruthven

Assistant editor

Sarah Dixon

Publishing assistant

Ruth Bircham

Team leader, serials production

Stephen Wilkes

Technical editor

Edward Morgan

Production administration coordinator

Sonya Spring

Administration assistantsClare Davies, Donna Fordham, Kirsty Lunnon,
Julie Thompson**Publisher**

Emma Wilson

Green Chemistry (print: ISSN 1463-9262; electronic: ISSN 1463-9270) is published 12 times a year by the Royal Society of Chemistry, Thomas Graham House, Science Park, Milton Road, Cambridge, UK CB4 0WF.

All orders, with cheques made payable to the Royal Society of Chemistry, should be sent to RSC Distribution Services, c/o Portland Customer Services, Commerce Way, Colchester, Essex, UK CO2 8HP. Tel +44 (0) 1206 226050; E-mail sales@rscdistribution.org

2008 Annual (print + electronic) subscription price: £947; US\$1799. 2008 Annual (electronic) subscription price: £852; US\$1695. Customers in Canada will be subject to a surcharge to cover GST. Customers in the EU subscribing to the electronic version only will be charged VAT.

If you take an institutional subscription to any RSC journal you are entitled to free, site-wide web access to that journal. You can arrange access via Internet Protocol (IP) address at www.rsc.org/ip. Customers should make payments by cheque in sterling payable on a UK clearing bank or in US dollars payable on a US clearing bank. Periodicals postage paid at Rahway, NJ, USA and at additional mailing offices. Airfreight and mailing in the USA by Mercury Airfreight International Ltd., 365 Blair Road, Avenel, NJ 07001, USA.

US Postmaster: send address changes to Green Chemistry, c/o Mercury Airfreight International Ltd., 365 Blair Road, Avenel, NJ 07001. All despatches outside the UK by Consolidated Airfreight.

PRINTED IN THE UK

Advertisement sales: Tel +44 (0) 1223 432246; Fax +44 (0) 1223 426017; E-mail advertising@rsc.org

Green Chemistry

Cutting-edge research for a greener sustainable future

www.rsc.org/greenchem

Green Chemistry focuses on cutting-edge research that attempts to reduce the environmental impact of the chemical enterprise by developing a technology base that is inherently non-toxic to living things and the environment.

EDITORIAL BOARD

Chair

Professor Martyn Poliakoff
Nottingham, UK

Scientific Editor

Professor Walter Leitner
RWTH-Aachen, Germany

Associate Editors

Professor C. J. Li
McGill University, Canada

Members

Professor Paul Anastas
Yale University, USA
Professor Joan Brennecke
University of Notre Dame, USA
Professor Mike Green
Sasol, South Africa
Professor Buxing Han
Chinese Academy of Sciences,
China

Dr Alexei Lapkin
Bath University, UK
Dr Janet Scott
Unilever, UK
Professor Tom Welton
Imperial College, UK

ADVISORY BOARD

James Clark, York, UK
Avelino Corma, Universidad
Politécnica de Valencia, Spain
Mark Harmer, DuPont Central
R&D, USA
Herbert Hugl, Lanxess Fine
Chemicals, Germany
Roshan Jachuck,
Clarkson University, USA
Makato Misono, nite,
Japan

Colin Raston,
University of Western Australia,
Australia
Robin D. Rogers, Centre for Green
Manufacturing, USA
Kenneth Seddon, Queen's
University, Belfast, UK
Roger Sheldon, Delft University of
Technology, The Netherlands
Gary Sheldrake, Queen's
University, Belfast, UK

Pietro Tundo, Università ca
Foscari di Venezia, Italy

INFORMATION FOR AUTHORS

Full details of how to submit material for publication in Green Chemistry are given in the Instructions for Authors (available from <http://www.rsc.org/authors>). Submissions should be sent *via* ReSource: <http://www.rsc.org/resource>.

Authors may reproduce/republish portions of their published contribution without seeking permission from the RSC, provided that any such republication is accompanied by an acknowledgement in the form: (Original citation) – Reproduced by permission of the Royal Society of Chemistry.

© The Royal Society of Chemistry 2008. Apart from fair dealing for the purposes of research or private study for non-commercial purposes, or criticism or review, as permitted under the Copyright, Designs and Patents Act 1988 and the Copyright and Related Rights Regulations 2003, this publication may only be reproduced, stored or transmitted, in any form or by any means, with the prior permission in writing of the Publishers or in the case of reprographic reproduction in accordance with the terms of licences issued by the Copyright Licensing Agency in the UK. US copyright law is applicable to users in the USA.

The Royal Society of Chemistry takes reasonable care in the preparation of this publication but does not accept liability for the consequences of any errors or omissions.

Ⓢ The paper used in this publication meets the requirements of ANSI/NISO Z39.48-1992 (Permanence of Paper).

Royal Society of Chemistry: Registered Charity No. 207890

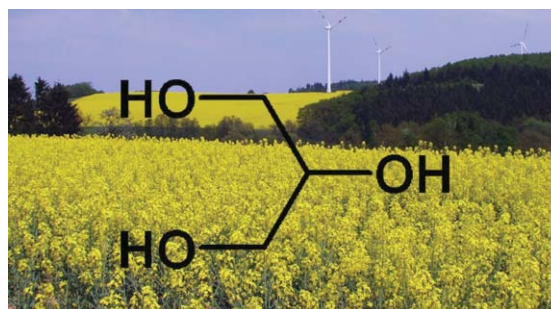
CRITICAL REVIEW

13

Improved utilisation of renewable resources: New important derivatives of glycerol

Arno Behr,* Jens Eilting, Ken Irawadi, Julia Leschinski and Falk Lindner

The increasing availability of glycerol due to the fast growing production of biodiesel has led to an immense interest in the usage of this alcohol as starting material for chemical syntheses. The present review gives a detailed survey of the manifold uses of glycerol especially considering novel catalytic pathways.



PERSPECTIVE

31

Green chemistry tools to influence a medicinal chemistry and research chemistry based organisation

Kim Alfonsi, Juan Colberg, Peter J. Dunn,* Thomas Fevig, Sandra Jennings, Timothy A. Johnson, H. Peter Kleine, Craig Knight, Mark A. Nagy, David A. Perry* and Mark Stefaniak

This article describes the development of green chemistry solvent selection and reagent selection tools, and the successful use of those tools in a large pharmaceutical company.

Preferred	Usable	Undesirable
Water	Cyclohexane	Pentane
Acetone	Heptane	Hexane(s)
Ethanol	Toluene	Di-isopropyl ether
2-Propanol	Methylcyclohexane	Diethyl ether
Ethyl acetate	Methyl <i>t</i> -butyl ether	Dichloromethane
Isopropyl acetate	Isocetane	Dichloroethane
Methanol	Acetonitrile	Chloroform
Methyl ethyl ketone	2-MethylTHF	Dimethyl formamide
1-Butanol	Tetrahydrofuran	<i>N</i> -Methylpyrrolidinone
<i>t</i> -Butanol	Xylenes	Pyridine
	Dimethyl sulfoxide	Dimethyl acetate
	Acetic acid	Dioxane
	Ethylene glycol	Dimethoxyethane
		Benzene
		Carbon tetrachloride

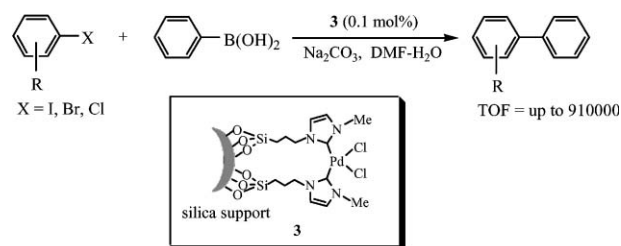
COMMUNICATIONS

37

Highly effective silica gel-supported *N*-heterocyclic carbene–Pd catalyst for Suzuki–Miyaura coupling reaction

Huili Qiu, Shaheen M. Sarkar, Dong-Hwan Lee and Myung-Jong Jin*

The immobilized *N*-heterocyclic carbene–Pd complex onto silica gel exhibited excellent catalytic activity in the coupling reaction of aryl halides with arylboronic acid. The heterogeneous Pd catalyst could be recycled without a significant loss of catalytic activity.

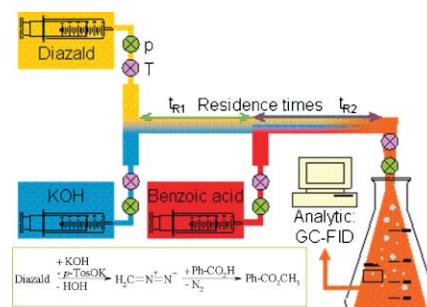


41

Making diazomethane accessible for R&D and industry: generation and direct conversion in a continuous micro-reactor set-up

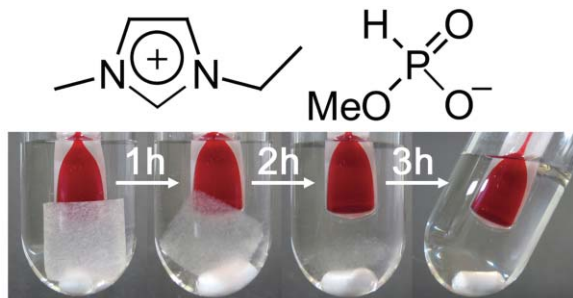
Michael Struempel, Bernd Ondruschka, Ralf Daute and Annegret Stark*

A simple micro-reactor set-up is presented, demonstrating for the first time the potential of Diazald[®], a diazomethane precursor, as a reactant for the production of pharmaceuticals and fine chemicals on an industrial scale.



COMMUNICATIONS

44



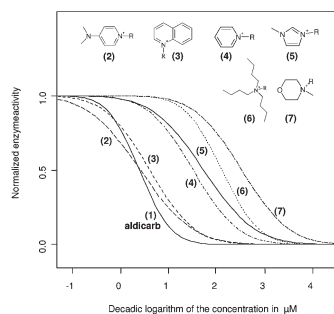
Cellulose dissolution with polar ionic liquids under mild conditions: required factors for anions

Yukinobu Fukaya, Kensaku Hayashi, Masahisa Wada and Hiroyuki Ohno*

N -Ethyl- N' -methylimidazolium methylphosphonate enables us to solubilize 4 wt% cellulose without pretreatments and heating.

PAPERS

47

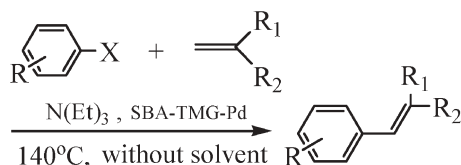


Qualitative and quantitative structure activity relationships for the inhibitory effects of cationic head groups, functionalised side chains and anions of ionic liquids on acetylcholinesterase

Jürgen Arning,* Stefan Stolte, Andrea Bösch, Frauke Stock, William-Robert Pitner, Urs Welz-Biermann, Bernd Jastorff and Johannes Ranke

Different head groups, alkyl and functionalised alkyl side chains and a set of commonly used anion species of ionic liquids were tested in an acetylcholinesterase inhibition screening assay.

59

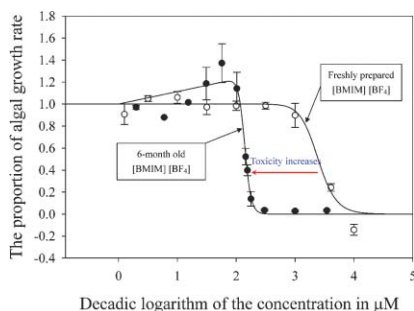


Solvent-free Heck reaction catalyzed by a recyclable Pd catalyst supported on SBA-15 via an ionic liquid

Xiumin Ma, Yinxi Zhou, Jicheng Zhang, Anlian Zhu, Tao Jiang* and Buxing Han*

The Pd catalyst supported on 1,1,3,3-tetramethylguanidinium (TMG)-modified molecular sieve SBA-15 is a very active and stable catalyst for the Heck coupling reaction in solvent-free conditions. It is easy to separate the supported catalyst from the reaction mixture and reuse it.

67



Influence of anions on the toxic effects of ionic liquids to a phytoplankton *Selenastrum capricornutum*

Chul-Woong Cho, Thi Phuong Thuy Pham, You-Chul Jeon and Yeoung-Sang Yun*

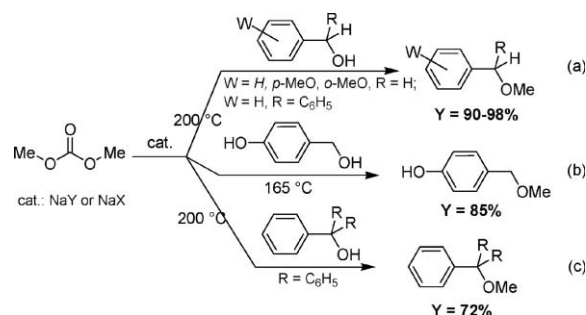
Toxicity of fluoride-containing ionic liquid [BMIM][BF₄] to algal growth can increase due to hydrolysis of anions. Extreme care should thus be taken when discharging ionic liquids into aquatic environments as they can remain for a long time.

73

The methylation of benzyl-type alcohols with dimethyl carbonate in the presence of Y- and X-faujasites: selective synthesis of methyl ethers

Maurizio Selva,* Enrico Militello and Massimo Fabris

In the presence of NaY or NaX faujasites, a genuinely green procedure is described by using the non-toxic dimethyl carbonate (DMC) for a highly selective synthesis of methyl ethers of benzyl-type alcohols.

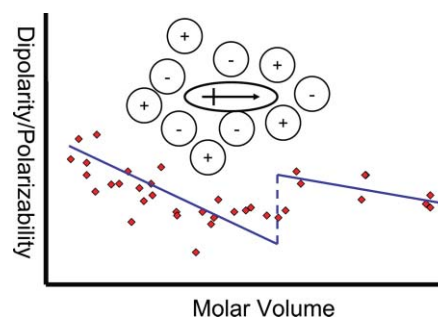


80

The relationship between solvent polarity and molar volume in room-temperature ionic liquids

Mark N. Kobrač*

A recently-developed theoretical method is used to estimate the molar volume of a series of ionic liquids, and the variation of experimentally-measured ϵ and π^* values with molar volume is explored.

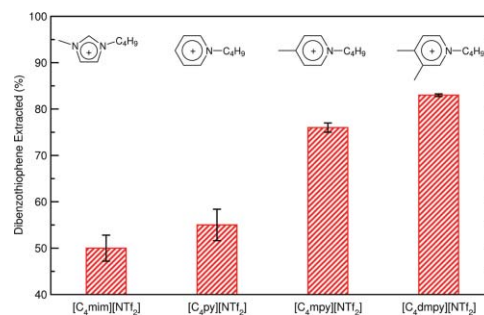


87

Desulfurisation of oils using ionic liquids: selection of cationic and anionic components to enhance extraction efficiency

John D. Holbrey,* Ignacio López-Martín, Gadi Rothenberg, Kenneth R. Seddon, Guadalupe Silvero and Xi Zheng

Extraction of dibenzothiophene from dodecane is enhanced using ionic liquids with ring-substituted alkylpyridinium over those with imidazolium cations, the extraction efficiency follows the order: dimethylpyridinium > methylpyridinium > pyridinium ~ imidazolium ~ pyrrolidinium.

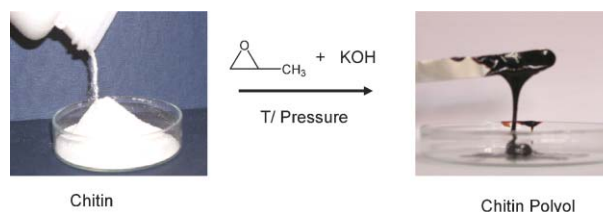


93

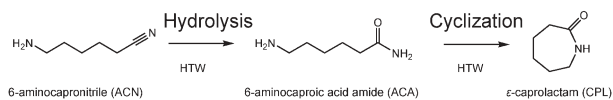
The bulk oxypropylation of chitin and chitosan and the characterization of the ensuing polyols

Susana Fernandes, Carmen Sofia Rocha Freire,* Carlos Pascoal Neto and Alessandro Gandini

A simple and highly efficient process was optimized to transform solid polysaccharides into reactive liquid polyols, without the need of any solvent or separation-purification procedures.



98

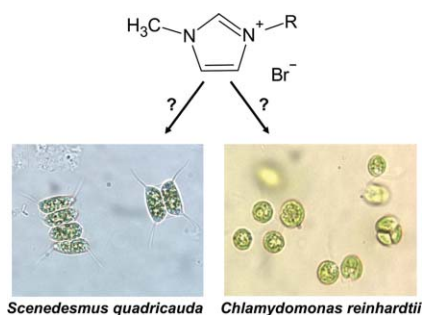


The continuous synthesis of ϵ -caprolactam from 6-aminocapronitrile in high-temperature water

Chong Yan, Joan Fraga-Dubreuil, Eduardo Garcia-Verdugo, Paul A. Hamley, Martyn Poliakoff,* Ian Pearson and A. Stuart Coote

An alternative and clean method for the production of ϵ -caprolactam is reported, using high-temperature water both as solvent and catalyst. The overall yield reaches 90% within a short residence time (<2 min).

104

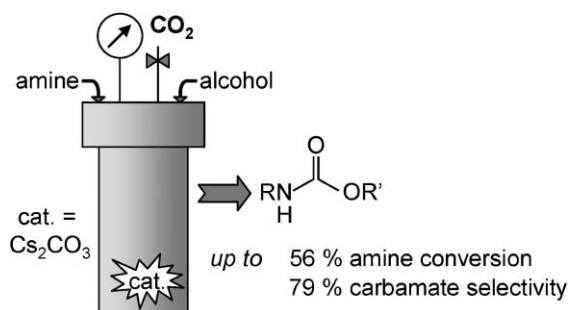


Toxicity of imidazolium ionic liquids to freshwater algae

Konrad J. Kulacki* and Gary A. Lamberti

The effects of ionic liquids on two freshwater algae, *Scenedesmus quadricauda* and *Chlamydomonas reinhardtii*, have been examined under high and low nutrient test conditions.

111

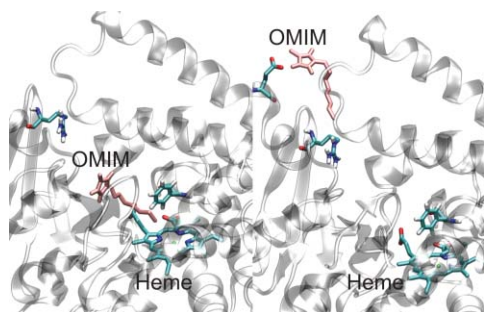


Green synthesis of carbamates from CO_2 , amines and alcohols

Angelica Ion, Charlie Van Doorslaer, Vasile Parvulescu, Pierre Jacobs and Dirk De Vos*

Basic catalysts such as cesium carbonate are effective in converting a large range of amines and alcohols to the corresponding carbamates, in presence or absence of dehydrating agents.

117



Ionic liquid effects on the activity of monooxygenase P450 BM-3

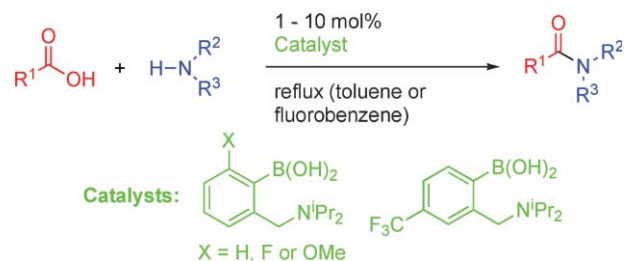
Kang Lan Tee, Danilo Roccatano, Stefan Stolte, Jürgen Arning, Bernd Jastorff and Ulrich Schwaneberg*

Hydroxylation activity of P450 BM-3 monooxygenase in the presence of ten different ionic liquids as cosolvents.

Synthesis, evaluation and application of novel bifunctional *N,N*-di-isopropylbenzylamineboronic acid catalysts for direct amide formation between carboxylic acids and amines

Kenny Arnold, Andrei S. Batsanov, Bryan Davies and Andrew Whiting*

Three new derivatives of *N,N*-di-isopropylbenzylamine-2-boronic acid have been prepared and compared with other catalysed and thermal direct amide formation reactions in refluxing toluene and fluorobenzene.




AUTHOR INDEX

- | | | | |
|--------------------------------|-----------------------------|----------------------------|-------------------------|
| Alfonsi, Kim, 31 | Garcia-Verdugo, Eduardo, 98 | Lindner, Falk, 13 | Selva, Maurizio, 73 |
| Arning, Jürgen, 47, 117 | Hamley, Paul A., 98 | López-Martin, Ignacio, 67 | Silvero, Guadalupe, 87 |
| Arnold, Kenny, 124 | Han, Buxing, 59 | Ma, Xiumin, 59 | Stark, Annegret, 41 |
| Batsanov, Andrei S., 124 | Hayashi, Kensaku, 44 | Militello, Enrico, 73 | Stefaniak, Mark, 31 |
| Behr, Arno, 13 | Holbrey, John D., 87 | Nagy, Mark A., 31 | Stock, Frauke, 47 |
| Bösch, Andrea, 47 | Ion, Angelica, 111 | Neto, Carlos Pascoal, 93 | Stolte, Stefan, 47, 117 |
| Cho, Chul-Woong, 67 | Irawadi, Ken, 13 | Ohno, Hiroyuki, 44 | Struempel, Michael, 41 |
| Colberg, Juan, 31 | Jacobs, Pierre, 111 | Ondruschka, Bernd, 41 | Tee, Kang Lan, 117 |
| Coote, A. Stuart, 98 | Jastorff, Bernd, 47, 117 | Parvulescu, Vasile, 111 | Vos, Dirk De, 111 |
| Daute, Ralf, 41 | Jennings, Sandra, 31 | Pearson, Ian, 98 | Wada, Masahisa, 44 |
| Davies, Bryan, 124 | Jeon, You-Chul, 67 | Perry, David A., 31 | Welz-Biermann, Urs, 47 |
| Doorslaer, Charlie Van, 111 | Jiang, Tao, 59 | Phuong Thuy Pham, Thi, 67 | Whiting, Andrew, 124 |
| Dunn, Peter J., 31 | Jin, Myung-Jong, 37 | Pitner, William-Robert, 47 | Yan, Chong, 98 |
| Eilting, Jens, 13 | Johnson, Timothy A., 31 | Poliakoff, Martyn, 98 | Yun, Yeoung-Sang, 67 |
| Fabris, Massimo, 73 | Kleine, H. Peter, 31 | Qiu, Huili, 37 | Zhang, Jicheng, 59 |
| Fernandes, Susana, 93 | Knight, Craig, 31 | Ranke, Johannes, 47 | Zheng, Xi, 87 |
| Fevig, Thomas, 31 | Kobrak, Mark N., 80 | Roccatano, Danilo, 117 | Zhou, Yinxi, 59 |
| Fraga-Dubreuil, Joan, 98 | Kulacki, Konrad J., 104 | Rothenberg, Gadi, 87 | Zhu, Anlian, 59 |
| Freire, Carmen Sofia Rocha, 93 | Lamberti, Gary A., 104 | Sarkar, Shaheen M., 37 | |
| Fukaya, Yukinobu, 44 | Lee, Dong-Hwan, 37 | Schwaneberg, Ulrich, 117 | |
| Gandini, Alessandro, 93 | Leschinski, Julia, 13 | Seddon, Kenneth R., 87 | |

FREE E-MAIL ALERTS AND RSS FEEDS


Contents lists in advance of publication are available on the web *via* www.rsc.org/greenchem - or take advantage of our free e-mail alerting service (www.rsc.org/ej_alert) to receive notification each time a new list becomes available.

 Try our RSS feeds for up-to-the-minute news of the latest research. By setting up RSS feeds, preferably using feed reader software, you can be alerted to the latest Advance Articles published on the RSC web site. Visit www.rsc.org/publishing/technology/rss.asp for details.

ADVANCE ARTICLES AND ELECTRONIC JOURNAL

Free site-wide access to Advance Articles and the electronic form of this journal is provided with a full-rate institutional subscription. See www.rsc.org/ejs for more information.

* Indicates the author for correspondence: see article for details.

 Electronic supplementary information (ESI) is available *via* the online article (see <http://www.rsc.org/esi> for general information about ESI).

A new journal from RSC Publishing Launching summer 2008

Energy & Environmental Science

A new journal linking all aspects of the chemical sciences relating to energy conversion and storage, alternative fuel technologies and environmental science.

As well as research articles, *Energy & Environmental Science* will also publish communications and reviews. It will be supported by an international Editorial Board, chaired by Professor Nathan Lewis of Caltech.

Contact the Editor, Philip Earis, at ees@rsc.org or visit the website for more details.



The current issue of *Energy & Environmental Science* will be freely available to all. Free access to all 2008 and 2009 content of the journal will be available following registration.

RSC Publishing

www.rsc.org/ees

Registered Charity Number 207890

Chemical Technology

Thermoplastic polystyrene sheets turn into a device mould in a toaster oven

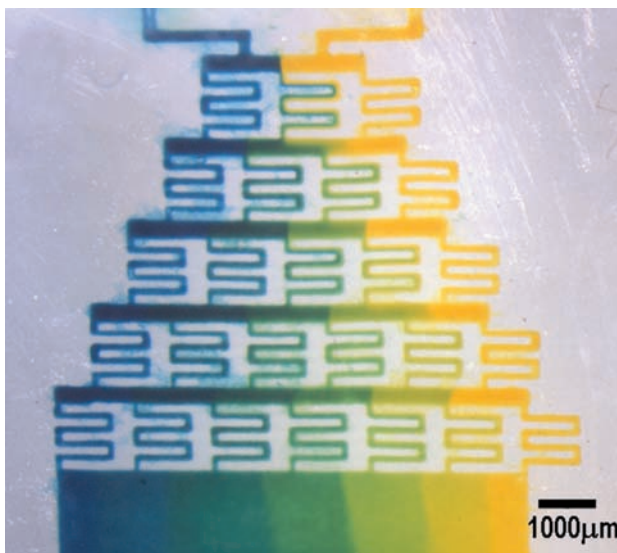
Shrinky Dink microfluidics

A children's toy has been turned into a microfluidic research tool in the hands of US engineers.

Michelle Khine's team from the University of California, Merced, printed microfluidic mould patterns onto Shrinky Dinks® and used them to make patterns of channels for mixing fluids and moving cells about. The technique allows the whole process – from device design conception to working device – to be completed with very simple tools within minutes.

Shrinky Dinks are thermoplastic sheets of polystyrene which have been pre-heated and stretched. When they are reheated they shrink to their original size, also shrinking anything drawn on them. The drawn features become narrower and more raised as the ink lines are compressed.

Using only a laserjet printer and a toaster oven, the team printed a device layout on a Shrinky Dink sheet and shrunk it down to make a mould. The ink lines printed on their Shrinky Dinks were raised by over 500% to form a series of



small walls with slightly rounded edges, ideal for making channels for use with microfluidic valves. The polydimethylsiloxane plastic used to make the devices could then be simply poured onto the mould, cured, and peeled off.

'Many researchers are excited

Moulds for channel patterns can be printed and shrunk quickly

about this, because it dramatically lowers the barrier to entry into the microfluidics field,' said Khine. 'There are no tooling costs – all you need is a printer and a toaster oven.'

'I am not a patient person,' explained Khine, 'and being a new faculty member at a brand new university, I did not have the cleanroom facilities I am accustomed to. As I was brainstorming solutions, I remembered my favourite childhood toy and decided to try it in my kitchen one night, and it worked amazingly well!' The Shrinky Dink moulds can be used more than ten times, and different heights of channel can be made by running the Shrinky Dink sheets through the printer more than once.

'We are using the microfluidic chips for chemotaxis experiments and cell culture experiments,' she added, 'and we definitely have a couple more projects based on this in the oven.'

Clare Boothby

Reference

A Grimes *et al*, *Lab Chip*, 2008, DOI: 10.1039/b711622e

In this issue

The holy grail of hydrogen storage

High surface area in porous polyaniline gives high affinity

Capped carbon nanotubes as chemical couriers

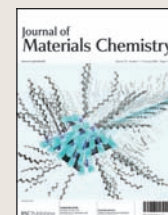
Polymers seal tube ends after being pulled into the cavity

Interview: Exciting materials

Seth Marder talks to Gavin Armstrong about organic electronics, two photon chemistry and surface patterning

Instant insight: Ionic liquids – instantly on site

Natalia Plechkov and Kenneth Seddon examine how ionic liquids are being applied in the real world



The latest applications and technological aspects of research across the chemical sciences

Application highlights

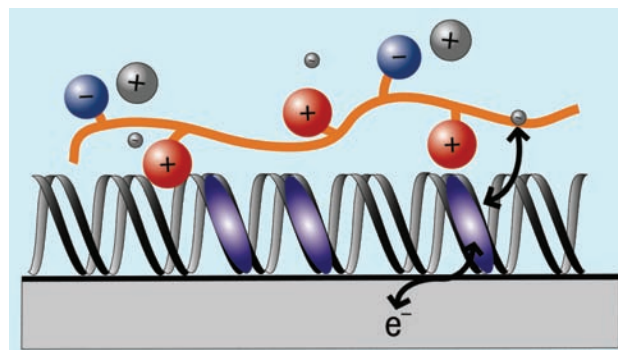
Electrochromic device uses biomolecule to stop dimerisation

Digital displays with better breeding

Mixing dyes with DNA could be the solution for bright, robust electronic displays and digital paper.

Japanese chemists have discovered that DNA strands make useful hosts for electrochemically-responsive dyes called viologens. These electrochromic molecules, which change colour from pale yellow to deep blue when triggered by a current, are promising candidates for display devices. However, bright displays require that the dye is used in high concentration, conditions under which viologens typically dimerise, and eventually stop working.

Hiroyuki Ohno and colleagues at the Tokyo University of Agriculture and Technology have successfully overcome viologen dimerisation by trapping



the dye within grooves in the DNA double helix. Ohno used a polymerised ionic liquid to act as the electrolyte. This mixture, held between two transparent glass electrodes, could be repeatedly cycled between coloured and bleached states without deterioration, said Ohno.

'It's not well known that DNA

A polymerised ionic liquid acts as an electrolyte

is a very cheap biopolymer, and a large amount of DNA is awaiting application,' said Ohno. And the technique isn't limited to viologens, Ohno added, 'DNA is expected to be a useful matrix for most dye molecules,' and 'may open new possibilities in display devices,' he said

Roger Mortimer, who researches electrochromism at Loughborough University, UK, agreed that the DNA host was an effective mechanism to stop dimerisation. 'A huge amount of electrochromics research is done on single electrodes, but in this case they have made a working device,' Mortimer added.

James Mitchell Crow

Reference

T Kakibe and H Ohno, *Chem. Commun.*, 2007, DOI: 10.1039/b713202f

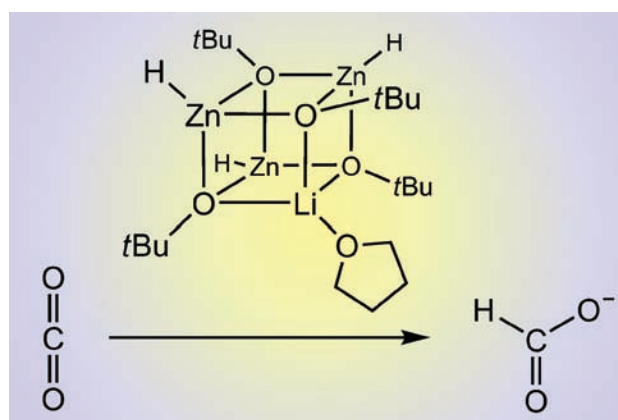
Zinc cluster compounds show promise for producing formic acid

Lithium livens up CO₂ conversion catalyst

Wouldn't it be good if we could make useful chemicals from carbon dioxide? German chemists are a step closer to making this goal a reality by greatly improving the reactivity of a catalyst to convert carbon dioxide into formic acid, an industrially important chemical.

Carbon dioxide could be a valuable precursor for the synthesis of organic chemicals, but there's a problem – it's just not very reactive. Processes have already been developed to convert carbon dioxide into methanol, but efficiently making formic acid from carbon dioxide has proved elusive. Matthias Driess and colleagues from the Technical University of Berlin have now found that incorporating lithium into a known zinc cluster compound greatly improves the rate of conversion of carbon dioxide into formate.

Zinc oxide is known to catalyse reactions of water–gas (an industrially available mixture of



carbon dioxide and hydrogen), but little is known about how it works at the molecular level. Therefore, Driess took zinc–oxygen cluster compounds known as cubanes, and used them as model compounds, studying their reactions with pure carbon dioxide by infra-red spectroscopy.

The simplest cubane they tested, with four zinc–hydride

The reaction speeds up from days to minutes by a simple change to the catalyst

groups, took three days to react with carbon dioxide. The same reaction was complete within minutes when one of the zinc hydride groups was replaced with a lithium–tetrahydrofuran unit, said Driess. His team are now hoping to use these cubanes to make heterogeneous catalysts capable of selectively converting water–gas to formic acid derivatives, he says.

The work is described as a 'milestone' by Hansjörg Grützmacher, an inorganic chemist at ETH Zürich, Switzerland, who said that the research 'gives insight at an unprecedented molecular level into the water–gas shift reaction promoted by zinc oxide – truly a reaction of immense importance.'

David Barden

Reference

K Merz *et al.*, *Chem. Commun.*, 2008, 73 (DOI: 10.1039/b714806b)

High surface area in porous polyaniline gives high affinity

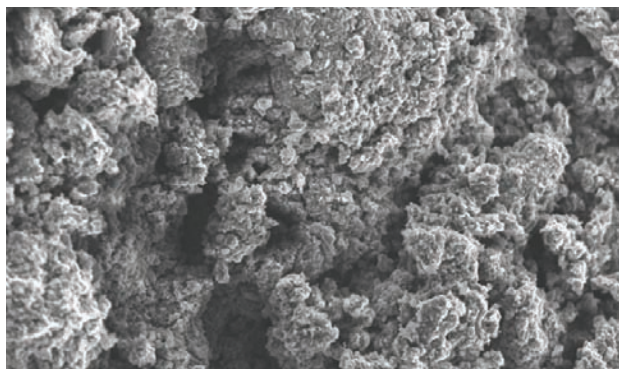
The holey grail of hydrogen storage

A polymer riddled with tiny pores could lead to a novel hydrogen fuel tank, say chemists in the US.

Frantisek Svec of the Lawrence Berkeley National Laboratory and colleagues at the University of California, Berkeley, made the highly porous materials from polyaniline. Svec used hypercrosslinking to give a mesh-like material with a strong affinity for hydrogen, and a high surface area.

'Using hydrogen as a CO₂-free fuel is a nice idea,' said Svec. But storing the gas is complicated as the gas is 'very difficult to compress or liquefy. One alternative is to store it in materials with a very high surface area.'

The Berkeley team made the new material by adding small molecular crosslinkers to polyaniline that had been swelled in solvent. These short, rigid crosslinks hold the



polymer chains apart even when the solvent is removed, leaving a material full of nanometre-scale pores. The resulting mesh had a surface area eight times higher than the best previous porous polyaniline, and a high affinity for hydrogen.

'The key advance with this work is the new approach to make

Molecular crosslinks keep the polymers apart to create pores

porous polymers,' said Andrew Cooper, who studies hydrogen storage polymers at the University of Liverpool, UK. The materials are still far from practical hydrogen stores, Cooper added: 'With what you'd have to change in structure to achieve room temperature hydrogen storage, it's arguable whether you could still call it the same material.'

Svec agreed there is still a lot of work ahead. 'We need polyanilines with a much higher surface area – we need small pores, and a lot of them,' he said. The Berkeley team is currently trying different crosslinkers, and different reaction conditions, to increase the material's proportion of 1–2 nm pores.

James Mitchell Crow

Reference

J Germain, J M J Fréchet and F Svec, *J. Mater. Chem.*, 2007, **17**, 4989 (DOI: 10.1039/b711509a)

Polymers seal tube ends after being pulled into the cavity

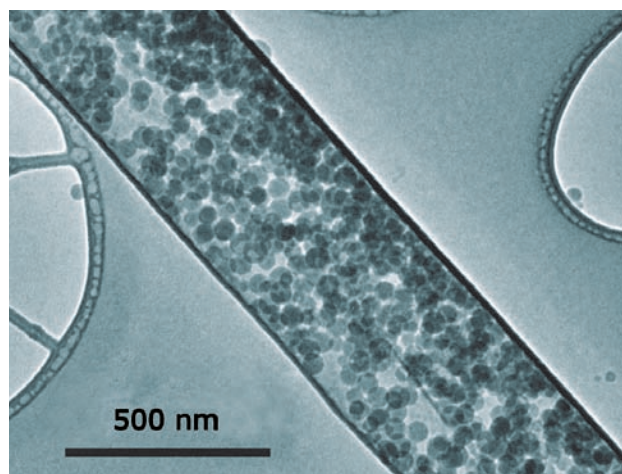
Capped nanotubes act as chemical couriers

US scientists have reported a mild method for trapping liquids and nanoparticles inside carbon nanotubes.

Alexander Yarin's team at the University of Illinois in Chicago, US, have developed a room-temperature method to fill carbon nanotubes with liquids.

The filling of carbon nanotubes with aqueous solutions can have biomedical uses, as Yarin explained. 'Nanotubes with diameters of the order of 100 nm are possible drug carriers, which can deliver biological payloads to a certain location, such as a tumour,' he said.

In Yarin's technique, water is dragged into nanotubes by a self-sustained diffusion mechanism. A toluene solution of a polymer, in this case polycaprolactone, is then pulled into the nanotubes. As the polymer is insoluble in the water already in the tubes, the polymer gathers at the ends and forms



caps. As a result, the water becomes trapped within the nanotubes. Crucially, this takes place under mild conditions, which is where this method holds its advantage according to Yarin: 'existing filling methods involve high pressures or temperatures, which are

This method fills nanotubes at room temperature

detrimental to biologically active materials'.

Marc in het Panhuis, a senior lecturer at the University of Wollongong, Australia, forecasted how this technique may avoid current problems involved with using nanotubes for drug delivery: 'This is an elegant way of tuning the properties of nanotubes from within, while the outer surface can be modified to render the nanotube biocompatible.'

Surfactants and particles, such as polystyrene nanospheres, have also been trapped inside carbon nanotubes using this method. This means that the technique could have multiple other future uses, Yarin suggested, such as in 'catalysis, supercoolants, optoelectronics and sensors'.

Jon Silversides

Reference

A V Bazilevsky, *J. Mater. Chem.*, 2008, DOI: 10.1039/b714541c

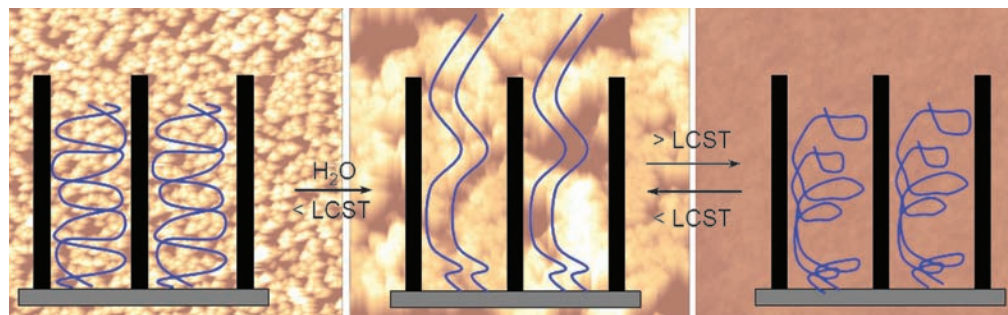
Vertically aligned carbon nanotube composite film could also clean itself

Protruding polymer offers release

Researchers from the US have created smart nanocomposite films whose potential applications range from self-cleaning sensors to fuel efficient transport.

Liming Dai at the University of Dayton, Ohio, and co-workers prepared composites of vertically aligned carbon nanotubes and a temperature responsive polymer. Above a critical temperature, the polymer chains exist in a collapsed conformation, and recede beneath the surface, then on cooling the chains expand and protrude from the surface.

Carbon nanotubes have been used in a variety of sensing applications and the ability of a sensor surface to clean itself – the expanding polymer chains push debris away from the surface – means that the useful lifetime of the sensor can be extended. But this is not the only potentially useful feature. If something is trapped in the polymer, the change in conformation can be used to release it in a controlled fashion.



‘Vertically aligned carbon nanotube composites are more difficult to prepare than the non-aligned versions that are often used,’ said Dai. ‘Some of our other research efforts have been directed to the problem of aligning nanotubes more efficiently as this will be an important step in achieving our long term goals for these materials.’

Dai and his colleagues have big plans for this technology. And by big, you need to think on the macro-scale. ‘What if we could keep a boat so clean that there was much less drag acting on it as it travels?’ asked Dai.

The chains expand on cooling and extend beyond the nanotubes

Reference
W Chen *et al.*, *Chem. Commun.*, 2008, DOI: 10.1039/b715079b

‘The multi-functionality of these composites is very impressive,’ said Christopher Li, a professor of materials science and engineering from Drexel University in Philadelphia, US. ‘The future holds many challenges that are dependant on the specific direction the research takes. For large scale applications, it will be important to develop methods to prepare these films on a very large scale. If controlled release is the goal, it would be nice to be able to release several different agents in a controlled way from one device.’
Stephen Davey

Samples tested within a quarter of an hour

Radioactive urine analysis

A system to detect plutonium in urine quickly in an emergency has been developed by Canadian scientists.

Dominic Larivière and colleagues at the Radiation Protection Bureau at Health Canada and Carleton University, Canada, used extraction chromatography with an automated flow injection system to analyse 10 ml samples of urine within 15 minutes. This small amount is representative of a typical sample that would be received from an individual following an emergency. This, together with the ability to process up to 80 samples per day per instrument, makes the technique suited for emergency situations, according to Larivière.

Other methods for detecting plutonium, which involve radiochemical separation followed



by alpha spectrometry, can take hours to days to process one sample, explained Larivière. In emergency situations, analysis has to be performed quickly to give a prognosis and determine treatment strategies. Personnel with minimal training need to be able to perform the analysis easily, and a high sample throughput would be needed to cope with the large

One instrument can analyse up to 80 samples a day

number of samples that would have to be tested following an event.

‘Following September 11, 2001, the government of Canada recognized a need for the development of rapid analytical methodologies to detect and quantify radioactive contamination,’ said Larivière. ‘This project was developed to fill a gap in emergency preparedness and response.’

Larivière is hoping to show the potential of this automated system to detect plutonium in other areas that are relevant to emergency response, such as milk, food and air particulates.

Caroline Moore

Reference
D Larivière *et al.*, *J. Anal. At. Spectrom.*, 2008, DOI: 10.1039/b714135a

Instant insight

Ionic liquids – instantly on site

Natalia Plechkova and Kenneth Seddon at the Queen's University Ionic Liquids (QUILL) Research Centre, Belfast, examine how ionic liquids are being applied in the real world

Ionic liquids are liquids composed solely of ions, in contrast to conventional solvents comprised of covalent molecules. Their properties mean they are intrinsically excellent candidates for industrial applications compared to volatile organic solvents. Organic solvents have been known for several centuries, and therefore occupy most of the solvent market in industry. If the properties of ionic liquids and organic solvents are to be compared, however, it could be anticipated that industry may be a natural environment for ionic liquids. At the current level of development, ionic liquids can nicely complement, and even sometimes work better than, organic solvents in a number of industrial processes. This statement should not diminish the fact that ionic liquids have plenty of academic applications.

The field of ionic liquids is growing at a rate that was unpredictable even five years ago – there were over 2000 papers published in 2006 – and the range of commercial applications is quite staggering; not just in the number, but in their wide diversity, arising from close cooperation between academia and industry. Of all the industrial giants, BASF have done the most publicly to implement ionic liquid technology. They possess the largest patent portfolio, have the broadest range of applications, and work openly with leading academics. Currently, the most successful example of an industrial process using ionic



liquid technology is the BASIL™ (biphasic acid scavenging utilising ionic liquids) process. This first commercial publicly-announced process was introduced to the BASF site in Ludwigshafen, Germany, in 2002. The BASIL™ process is used for the production of the generic photoinitiator precursor alkoxyphenylphosphines.

In the original process, triethylamine was used to scavenge the acid that was formed in the course of the reaction, but this made the reaction mixture difficult to handle as the waste by-product, trimethylammonium chloride, formed a dense insoluble paste. Replacing triethylamine with 1-methylimidazole results in the formation of 1-methylimidazolium chloride, an ionic liquid that separates out of the reaction mixture as a discrete phase. The new process uses a much smaller reactor than the initial process; the space–time yield increased from $8 \text{ g m}^{-3} \text{ h}^{-1}$ to $690\,000 \text{ kg m}^{-3} \text{ h}^{-1}$, and the

BASF's BASIL™ process results in the creation of an ionic liquid by-product, making it far easier to separate than the paste from an older process

yield from 50% to 98%. 1-Methylimidazole is recycled, via base decomposition of 1-*H*-3-methylimidazolium chloride, in a proprietary process. The reaction is now carried out at a multi-ton scale, proving that handling large quantities of ionic liquids is practical. BASF have also developed process for breaking azeotropes, dissolving and processing cellulose, replacing phosgene as a chlorinating agent with hydrochloric acid, and aluminium plating. And there are at least fifteen other companies with processes either operating or at pilot. Degussa, for example, have a hydrosilylation process, have developed ionic liquids as paint additives and have a programme for lithium ion batteries.

The concepts and paradigms of ionic liquids are new and still not fully accepted in the wider community: it is hard for conservative scientists to throw away thousands of years of concepts grown from the fertile ground (ocean?) of molecular solvents, and if chemists are conservative, then chemical engineers are even more so. But there is always a flipside or mirror image, and there are now many laboratories all over the world (and the growth in China is spectacular) that work with ionic liquids.

Read more in Natalia Plechkova and Ken Seddon's critical review 'Applications of ionic liquids in the chemical industry' in January's Chemical Society Reviews

Reference
N V Plechkova and K R Seddon, *Chem. Soc. Rev.*, 2008, DOI: 10.1039/b006677j

STOP!

searching...

Don't waste any more time searching for that elusive piece of vital chemical information.

Let us do it for you at the library and information centre of the RSC

We provide:

- Chemical enquiry helpdesk
- FREE remote access to full text books and journals for RSC members
- Expert chemical information specialist staff

So tap into the foremost source of chemical knowledge in Europe, send your enquiries to:

library@rsc.org

19070757

Interview

Exciting materials

Seth Marder talks to Gavin Armstrong about organic electronics, two-photon chemistry and surface patterning



Seth Marder

Seth Marder is professor of chemistry at the Georgia Institute of Technology, US, and director of the Center for Organic Photonics and Electronics. His research focuses on how the chemical structure of molecules and materials relates to their electronic and optical properties. Seth is on the advisory editorial board for *Chemical Communications* and *Journal of Materials Chemistry*.

You have a fundamental interest in how materials interact with light and electric fields. What prompted this interest?

While I was a postdoc at Oxford, I read an article on organic nonlinear optics. I realised I could make organometallic compounds that could expand upon what people were doing with organic compounds. I ended up trying to make a compound and isolating an unwanted side product. The side product had very interesting nonlinear optical properties that resulted in a paper in *Nature*. While I understood the basic design guidelines to make compounds that could work, I didn't really understand the underlying physics behind why they worked. Conversely, I realised that while physicists understood the physics of nonlinear optics, they didn't really understand how chemical structure intrinsically maps onto the nonlinear optical properties of materials. One thing led to another and 22 years later, I have a better understanding than I did when I submitted that first paper.

Some of your research involves two-photon chemistry. Can you explain what this is?

Two-photon absorption is a nonlinear optical effect in which a molecule simultaneously absorbs two photons of light. It's significant because the probability of this happening scales quadratically with the intensity of the light. Consider a beam of light that is focused to a point on a material: if the material is a good two-photon absorber, you can have efficient absorption right at the focus. The rate of absorption will fall off quadratically with distance from the focus. This means you can localise where you excite the material. This has important ramifications if you want to do three-dimensional fluorescence imaging or if you want to write three-dimensional structures.

My colleagues and I have spent many years trying to understand how to make two-photon absorption of light by molecules very efficient. We've also worked on coupling the efficient absorption of light with other properties, such as the ability to initiate chemical reactions. The structure–property relationships that our team have developed are now widely accepted as a standard paradigm.

What other projects are you working on?

Another area that I think is very important is interfacial chemistry. My collaborators and I recently reported a new kind of nanolithography called thermochemical nanolithography. We used a crosslinked, and therefore mechanically robust, polymer featuring esters with active leaving groups. We then took an atomic force microscopy tip over the polymer and heated it, converting the esters to carboxylic acids and thus changing the chemical reactivity of the surface. This allows you to use that surface for a subsequent chemical reaction or a molecular recognition event. I think that this is an exciting area and it will be a very complementary technique to dip-pen lithography.

What is the secret to being a successful scientist?

Much of our work is interdisciplinary and collaborative. For the collaborations to work, it is necessary to build strong human relationships along with the science. I have found that good relationships with good people typically result in good science. If you have bad relationships even with good scientists, I think one can find it very frustrating.

I also think an absolute desire to be a good teacher is essential. If you cannot explain to people what you're doing and why, I think you've not done your job as a scientist.

Which scientist do you admire?

Jacob Bronowski was a mathematician, a biologist and a philosopher. He wrote a book called 'The Ascent of Man,' which the BBC made into a TV series in the early 1970s. In one of the chapters, called 'Knowledge or Certainty,' he talked about the danger of arrogance as a scientist and thinking you have absolute knowledge when in reality you never can. The image of Bronowski standing in a pond at Auschwitz talking about how arrogance and dogma led to his family's ashes being in that pond was probably the single most influential event in my life as a scientist. It was a transformational point for me. It really emphasised the need for us to realise the humanity of what we do and our intrinsic fallibility.

Essential elements

A new journal for the new year

A new journal, *Energy & Environmental Science*, will be launched in summer 2008 by RSC Publishing. The announcement was made at the recent MRS Fall meeting in Boston, US, attended by RSC staff.

'The challenges relating to energy and environmental science that face the world today are complex,' said Robert Parker, managing director of RSC Publishing. 'From alternative fuels to environmental impacts, climate change to energy conversion and storage – research in the chemical sciences underpins all the work that is so important to the future of our world. RSC Publishing recognises the significance



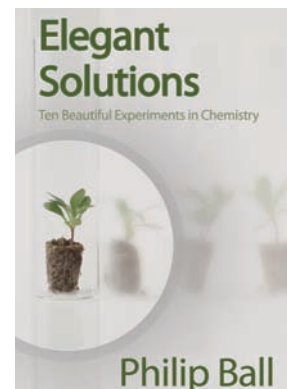
of this area by launching *Energy & Environmental Science*.'

The journal will link all aspects of the chemical sciences by publishing research

relating to energy conversion and storage, alternative fuel technologies, and environmental science. The monthly issues will contain topical reviews and original research as communications and full papers. Editor Philip Earis, announcing the appointment of Nathan Lewis of Caltech as editorial board chair, said: 'We're delighted to have such a prestigious scientist driving the journal forward.'

By recognising the complexity of issues and challenges relating to energy and environmental science, it is expected that the journal will provide a forum for work of an interdisciplinary nature across both the (bio)chemical sciences and chemical engineering disciplines. www.rsc.org/ees

And finally...



Elegant Solutions: Ten Beautiful Experiments in Chemistry has been awarded the 2007 Dingle Prize. The Dingle Prize, presented by The British Society for the History of Science Outreach and Education Committee, acknowledges the best recent book that communicates the history of science, technology and/or medicine to a wide audience of non-specialists.

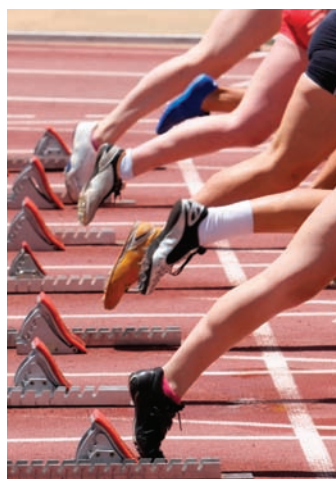
Published by RSC Publishing in 2005, *Elegant Solutions: Ten Beautiful Experiments in Chemistry* has received widespread critical acclaim. Philip Ball has won several awards himself, including the James T Grady–James H Stack Award for Interpreting Chemistry for the Public, awarded by the American Chemical Society in 2006. Philip is also a regular contributor to *Chemistry World*, with his column, 'The Crucible'.

For more information on this award-winning book, and many other international best sellers, visit www.rsc.org/books

It's off and running!

Less than three years after the first ever publication in 2005 – *Molecular BioSystems* is now officially off and running as a solo publication.

Molecular BioSystems' editorial board chair, Thomas Kodadek, commented: 'Biologists interested in systems-level phenomena can benefit greatly from tools being developed by chemists to monitor and manipulate cellular processes. Likewise, chemists will increasingly turn to -omics approaches to understand mechanism of action and specificity of bioactive molecules. *Molecular BioSystems* provides a



home for this rapidly developing interdisciplinary science.'

Successes since launch include being indexed in MEDLINE, its first impact factor of 2.45*, rapid publication times of around 80 days from receipt to publication of papers, and extra online features such as enhanced HTML articles via RSC Prospect and 3D visualisation of complex molecules.

From January 2008, *Molecular BioSystems* is available with a subscription or as part of RSC Journals Package A/A+. See www.molecularbiosystems.org

*2006 Thomson Scientific (ISI) Journal Citation Reports®

Chemical Technology (ISSN: 1744-1560) is published monthly by the Royal Society of Chemistry, Thomas Graham House, Science Park, Milton Road, Cambridge UK CB4 0WF. It is distributed free with *Chemical Communications*, *Journal of Materials Chemistry*, *The Analyst*, *Lab on a Chip*, *Journal of Atomic Absorption Spectrometry*, *Green Chemistry*, *CrystEngComm*, *Physical Chemistry Chemical Physics* and *Analytical Abstracts*.

Chemical Technology can also be purchased separately. 2008 annual subscription rate: £199; US \$396. All orders accompanied by payment should be sent to Sales and Customer Services, RSC (address above). Tel +44 (0) 1223 432360, Fax +44 (0) 1223 426017 Email: sales@rsc.org

Editor: Neil Withers

Associate editors: Nina Notman, Celia Clarke

Interviews editor: Joanne Thomson

Essential Elements: Daniel Bradnam, Rebecca Jeeves, and Valerie Simpson

Publishing assistant: Ruth Bircham

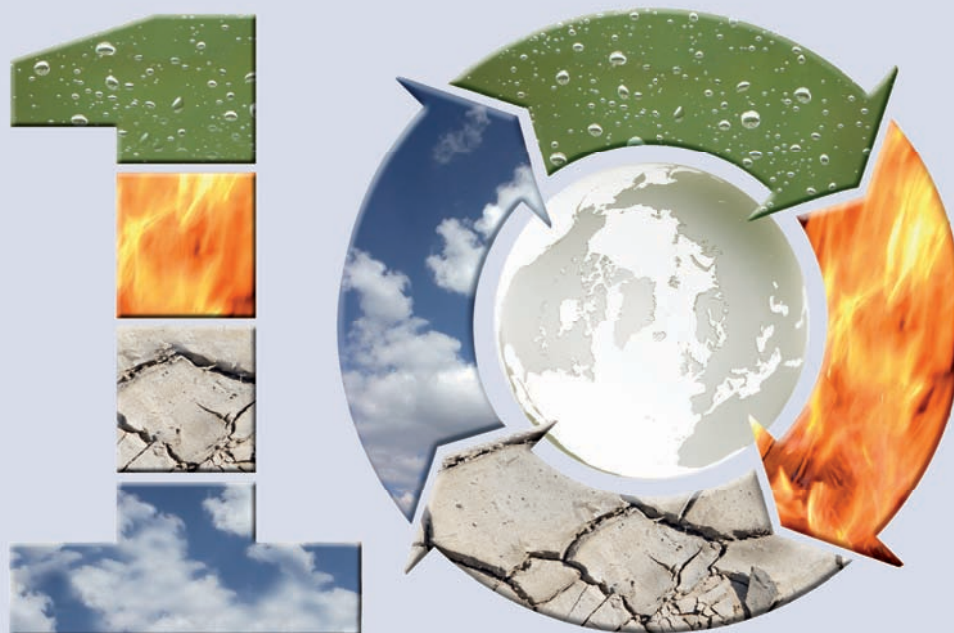
Publisher: Graham McCann

Apart from fair dealing for the purposes of research or private study for non-commercial purposes, or criticism or review, as permitted under the Copyright, Designs and Patents Act 1988 and the copyright and Related Rights Regulations 2003, this publication may only be reproduced, stored or transmitted, in any form or by any means, with the prior permission of the Publisher or in the case of reprographic reproduction in accordance with the terms of licences issued by the Copyright Licensing Agency in the UK. US copyright law is applicable to users in the USA.

The Royal Society of Chemistry takes reasonable care in the preparation of this publication but does not accept liability for the consequences of any errors or omissions.

Royal Society of Chemistry: Registered Charity No. 207890.

RSC Publishing



years of publishing!

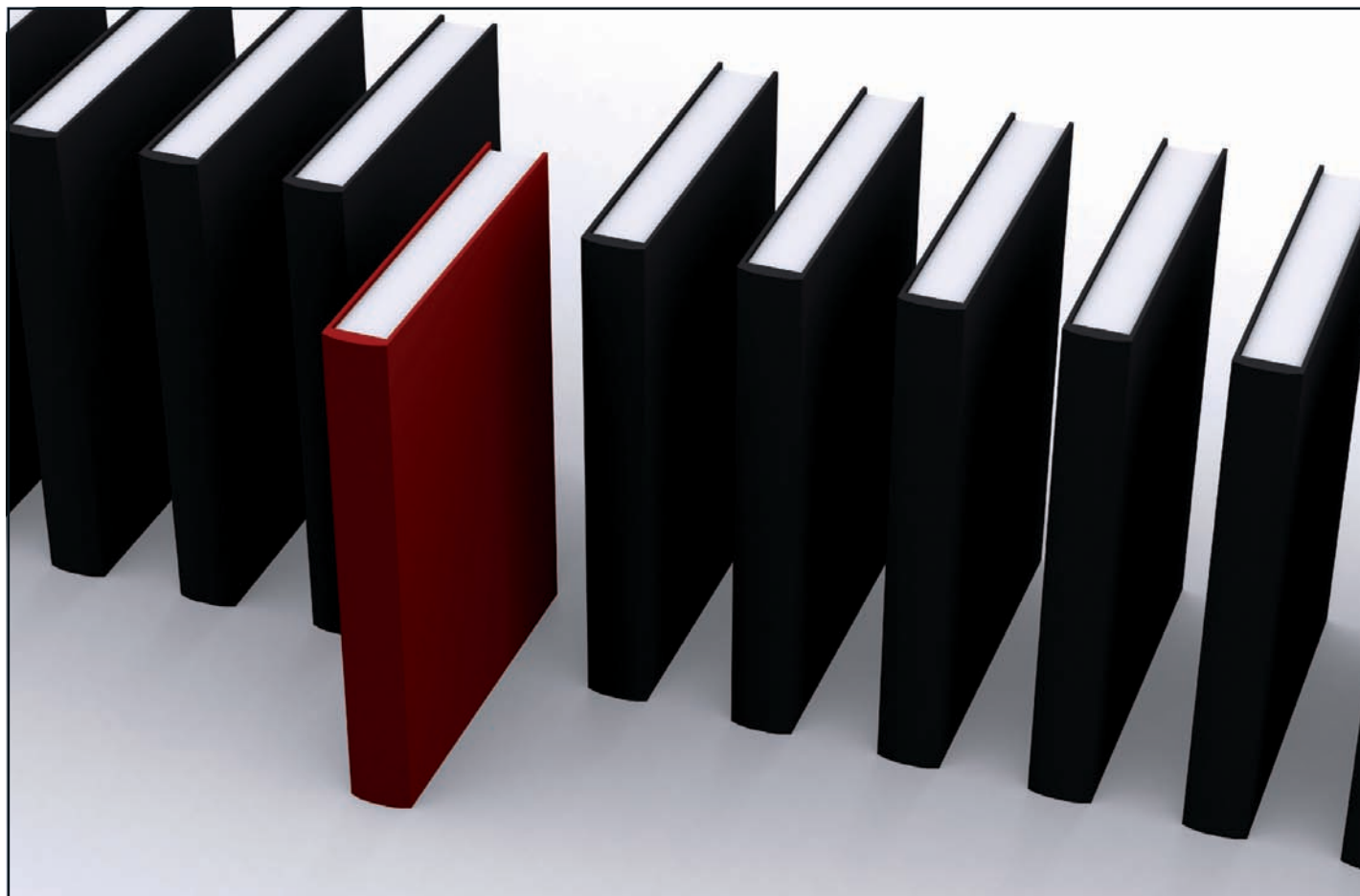
Journal of Environmental Monitoring...



- Highly visible and cited in MEDLINE
- Accelerated publication rates, typically around 80 days
- Dedicated to the measurement of natural and anthropogenic sources of pollution with a view to assessing environmental and human health effects

Celebrating 10 years of publishing, *Journal of Environmental Monitoring* offers comprehensive and high quality coverage of multidisciplinary, international research relating to the measurement, pathways, impact and management of contaminants in all environments.

...for environmental processes and impacts!



'Green Chemistry book of choice'



Why not take advantage of free book chapters from the RSC? Through our 'Green Chemistry book of choice' scheme *Green Chemistry* will regularly highlight a book from the RSC eBook Collection relevant to your research interests. Read the latest chapter today by visiting the *Green Chemistry* website.

The RSC eBook Collection offers:

- Over 900 new and existing books
- Fully searchable
- Unlimited access

Why not take a look today? Go online to find out more!

RSC Publishing

www.rsc.org/greenchem

Registered Charity Number 207890

Improved utilisation of renewable resources: New important derivatives of glycerol

Arno Behr,* Jens Eilting, Ken Irawadi, Julia Leschinski and Falk Lindner

Received 10th July 2007, Accepted 22nd October 2007

First published as an Advance Article on the web 12th November 2007

DOI: 10.1039/b710561d

Although glycerol has been a well-known renewable chemical for centuries, its commercial relevance has increased considerably in the last few years because of its rising inevitable formation as a by-product of biodiesel production. The present review gives a broad overview on the chemistry of glycerol starting from the classic esters and oligomers to new products like glycerol carbonate, telomers, branched alkyl ethers, propanediols and epoxides. In particular, the novel possibilities to control the numerous addition, reduction and oxidation reactions *via* heterogeneous, homogeneous and biocatalysis will be presented. A benchmark will be given to determine the products which will have the best chances of entering the market and which processes are currently most developed.

1. Introduction

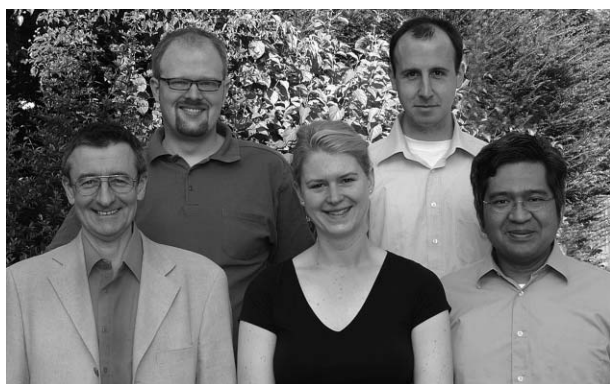
Glycerol, 1,2,3-propane triol, has been a well known chemical for more than two centuries. It was discovered in 1783 by the Swedish chemist Carl Wilhelm Scheele when treating natural oils with alkali materials. He noticed the formation of a liquid which he tasted, finding a very sweet flavour. He published his research results under the title "Experiment about a special sugar material coming from squeezed oils and fats". However, the discovery of "Scheele's sweet" had no further impact on scientific research or industrial usage for a long time. The name "glycerol" was given in 1811 by the chemist Michel

Eugene Chevreul, who deduced this name from the Greek word "glykos" (= sweet).

In 1866 the first technical usage of glycerol was the production of the trinitrate of glycerol, the so-called nitro glycerol. Dynamite is formed when nitro glycerol is adsorbed on diatomaceous earth, which can be used as an explosive, for instance, for the construction of tunnels, channels or railroad routes. Just for the construction of the Panama channel (started in 1879) 30 000 tons of dynamite were applied. At the end of the nineteenth century the processing of natural oils and fats and hence the production of glycerol increased continuously.

Nowadays the production of glycerol from fats and oils is carried out by saponification yielding glycerol and soaps (Scheme 1, $Y = \text{ONa}$), by hydrolysis yielding glycerol and fatty

Department of Biochemical and Chemical Engineering, Technical Chemistry A, Dortmund University, D-44227 Dortmund, Germany



From left: Arno Behr, Jens Eilting, Julia Leschinski, Falk Lindner and Ken Irawadi

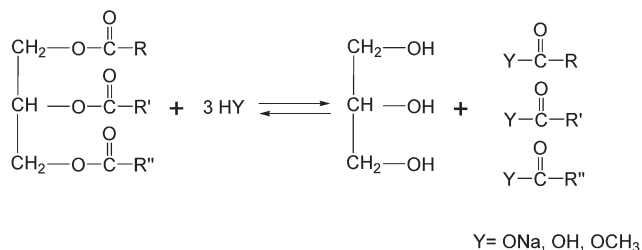
Arno Behr studied chemistry at Aachen University, Germany and did his PhD in 1979. After 10 years' work in industry he assumed a position at the Chair of Technical Chemistry, University of Dortmund, Germany, in 1996. One of his research interests is the chemistry of renewable resources.

Ken Irawadi earned his BSc in Agriculture Technology from Bogor Agricultural University, Indonesia and his MSc in Process Engineering at the TU Hamburg, Germany. He has been a lecturer and a researcher at Bogor Agricultural University. Since October 2006 he has been a PhD student under the supervision of Prof. Dr Arno Behr at the University of Dortmund, Germany.

Julia Leschinski studied chemical engineering at the University of Dortmund, Germany. She was awarded her Dipl.-Ing. in 2005 and has started her PhD studies in Dortmund at the division of Chemical Process Development under the supervision of Prof. Dr Arno Behr.

Jens Eilting studied chemical engineering at the University of Dortmund, Germany. He got his Dipl.-Ing. in September 2005. In November 2005 he started his PhD studies in Dortmund at the division of Chemical Process Development under the supervision of Prof. Dr Arno Behr.

Falk Lindner studied chemical engineering at the University of Dortmund, Germany. He received his diploma in 2005 and works now as a research assistant at the division of Chemical Process Development/Technical Chemistry A under the supervision of Prof. Dr Arno Behr.



Scheme 1 Synthesis of glycerol from fats and oils.

acids (Scheme 1, Y = OH) or by transesterification with methanol yielding glycerol and fatty acid methyl esters (Scheme 1, Y = OCH₃).

The commercial production of fats and oils has increased rapidly during the last century, especially in the last three decades. Whereas in 1970 the total production of fats and oils was only in the range of 40 million tons (Mt), this value climbed to about 144 Mt in 2005. A further considerable rise to about 200 Mt can be foreseen for the year 2015. However, it must be stressed that only a small part of this material is converted within the chemical industry: about 81% of the worldwide oil production is used for the food industry, 14% in the chemical industry and 7% for feed. Today more than 20 Mt annum⁻¹ of fats and oils are processed chemically, yielding large amounts of glycerol.

A new trend has overlapped with this increasing production of natural oils and fats: for several years, renewable oils have also been used for energy applications. The so-called "biodiesel" has been implemented as automotive fuels in the US and in Europe. Biodiesel is a popular term for the fatty acid methyl esters formed according to Scheme 1, for instance from the transesterification of rapeseed oil with methanol. Biodiesel production in the EU was estimated to be about 6 Mt in 2006 and is forecasted to increase to about 12 Mt in 2010.

These trends influence remarkably the glycerol market. Before starting biodiesel production, the European glycerol market was in the range of 250 000 to 400 000 t annum⁻¹. Now, additional glycerol stemming from biodiesel production is flooding the market. One ton of biodiesel yields about 110 kg of crude glycerol or about 100 kg of pure glycerol. Therefore, by 2010 about 1.2 Mt annum⁻¹ of additional glycerol will enter the European market. Of course this influences substantially the glycerol price; while the glycerol price moved in the range of 1000 to 1300 € t⁻¹ between 2000 and 2003, from 2004 to 2006 it decreased to 500 to 700 € t⁻¹. Besides the high quality glycerol, there is a large quantity of impure glycerol on the market available for very low prices.

Obviously the question arises how this additional glycerol can be used wisely. There is already a great number of common glycerol applications; for instance, glycerol is used in pharmaceuticals, cosmetics (hair and skin care), soaps and toothpastes. Also the direct use as sweetener in candies and cakes and as a wetting agent in tobacco is widespread. Some chemical functionalisation of glycerol is also carried out in industry, especially the synthesis of some esters, polyethers and alkyd resins. There seems to be little scope to extend the uses of glycerol in these areas. So the question arises whether there are any additional fields of application, where glycerol itself or

some of its derivatives can find new handlings in the chemical industry.¹ The present article will provide a broad review regarding the areas of opportunity where it would be possible to capitalize on the surplus chemical glycerol. Well known chemistry, as for instance the formation of esters or acetals, and especially catalytic routes to new derivatives, will be considered and discussed in detail. In the following, we will first examine the production of esters, ethers, acetals and ketals of glycerol. Subsequently, the conversion of glycerol to diols and epoxides will be treated, followed by a review of the different possibilities to oxidise and to dehydrate glycerol to aldehydes, ketones or carboxylic acids. We will conclude by discussing other feasible reactions, like for instance the conversion of glycerol to synthesis gas.

2. Glycerol esters

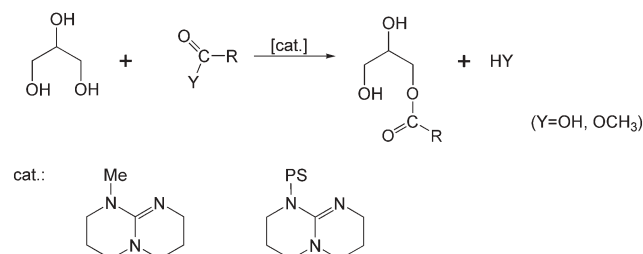
In this section we will consider mono-, di- and triesters of glycerol with carboxylic acids (section 2.1) as well as the cyclic ester of glycerol with carbonic acid, the glycerol carbonate (section 2.2).

2.1 Glycerol esters with carboxylic acids

Glycerol monoesters can be prepared by esterification of glycerol with carboxylic acids as well as by transesterification with their methyl esters (Scheme 2). They can be used as emulsifiers in the food industry, in cosmetics as well as in pharmaceuticals.

Barrault *et al.*² describe a relatively selective synthesis of monoglycerides in a "one pot" reaction by converting unprotected glycerol with different methyl esters which can vary in their chain length between 11 up to 17 carbon atoms. A guanidine catalyst is used as a homogeneous catalyst or as an immobilised catalyst fixed on crosslinked polystyrene (Scheme 2). The transesterification experiments with stoichiometric amounts of glycerol and methyl esters were performed at a temperature of 110 °C and with a relatively high catalyst concentration of 12.5 mol%. To achieve high yields between 96% and 100% a reaction time of 8 h was necessary when using the heterogeneous catalyst. With the homogeneous guanidine catalyst the reaction time increases from 2 to 3.5 h. The selectivity to monoesters reaches 65%, the selectivity to diesters 34% and the selectivity to triesters at most 5%.

The results are completely different when a heterogeneous catalyst is used. Here the selectivity to monoesters decreases from 62% for shorter methyl esters to 47% for longer methyl esters. For di- and triesters the situation is reversed: With



Scheme 2 Selective catalytic syntheses of monoglycerides (PS = crosslinked polystyrene).

Table 1 Synthesis of glycerol esters with basic oxide catalysts

Catalyst	Conversion (%)	Selectivity (%)		
		Monoesters	Diesters	Triesters
—	3	100	0	0
ZnO	18	80	20	0
MgO	80	38	50	12
CeO ₂	82	42	52	6
La ₂ O ₃	97	28	61	11

increasing chain length the selectivity also increases. This steering effect may be caused by the hydrophobicity of the esters which is rising with a longer alkyl chain. Due to the polystyrene chain the heterogeneous catalyst also has a high hydrophobicity, so that the interaction between the catalyst and the methyl ester is more intensive. In the end this leads to a higher selectivity to the di- and triesters.

The influence of solvents has also been investigated: The reaction rate is very low in solvents in which the methyl esters are only sparingly miscible. In solvents where good miscibility is achieved the reaction rate is as high as without a solvent.

Barrault *et al.* have also investigated basic oxides as possible catalysts for the synthesis of glycerides.³ All experiments have been performed at 220 °C, with an equimolar glycerol/methyl stearate mixture and a catalyst concentration of 2.7 wt.%. Experiments were performed with ZnO, MgO, CeO₂ and La₂O₃ (Table 1).

When La₂O₃ is used as catalyst the formation of the unwanted by-product acrolein is observed. Small conversions of glycerol lead to a high selectivity towards monoglycerides whereas at higher glycerol conversions the selectivity decreases dramatically. The highest conversion of glycerol could be achieved applying the catalyst with the lowest surface area.

Chang and Wu investigated the lipase-catalysed synthesis of triglycerides of phenylalkanoic acids.⁴ These esters act as pharmaceuticals which convert slowly into acids and glycerol inside the human body leading to a long residence time and a high concentration level of the active ingredient. The esterification to triglycerides could be performed in yields of 70% when the lipase Novozym 435 was used at a temperature of 60 °C. A solvent-free system leads to the best yields of triglycerides. Non-polar solvents only give very small yields whereas with increasing solvent polarity the yield to the products increases, too. By using 4-phenylbutyric acid an optimum temperature of 65 °C was found whereas higher temperatures lead to lower yields presumably because of deactivation of the enzymes. The water removal is a further very important aspect: *Via* removing the water—especially by the use of molecular sieves—the equilibrium of the reaction can be shifted towards the products. The use of saturated salt solutions or the removal of the water by pervaporation was not as effective.

Pérez-Pariente *et al.* investigated the synthesis of monoglycerides by converting glycerol with fatty acids using functionalised mesoporous materials as catalysts.⁵ The esterification of glycerol with oleic acid was performed with an equimolar ratio of the starting compounds at a temperature of 100 °C, a catalyst concentration of 5 wt.% and a reaction time of 24 h. The influence of the catalyst synthesis procedure, the effects of hydrophobicity and organosulfonic functional

groups and the impact of the catalyst structure were studied in detail. The catalyst synthesised by the so-called co-condensation method achieved a glycerol conversion of 24%, while the catalyst built by the post synthesis only led to conversions of 11%, each with a selectivity to the monoglycerides of about 69%. Hydrophobic catalysts lead to higher conversions of glycerol and to a higher selectivity of monoglycerides (75–95%). To create the acid sites of the catalyst two different sulfonation procedures were tested: The method with SO₃ proved to be more effective than the method with chlorosulfonic acid, because a higher acid content could be obtained. Concerning the catalyst structure the MCM-41 catalyst proved to be the best one, better than SBA-15, SBA-12 and SBA-2. MCM-41 led to the highest selectivity to monoglycerides (77%).

Corma *et al.*⁶ investigated Lewis basic hydrotalcites as catalysts for the conversion of methyl oleate with glycerol to esters which are valuable as surfactants and emulsifiers. In detail they compared Lewis- and Brønsted-basic materials. At a reaction temperature of 200 °C the Lewis-basic hydrotalcite led only to a yield of monoglycerides of about 60% while solid Brønsted-basic catalysts reached 80%. Water has an important influence on the catalytic performance of the hydrotalcites, because higher water amounts can block the catalytically active sites on the surface.

The conversion of glycerol with acetic acid leads to the glycerol mono-, di- and triacetins, which can be purchased for instance from Cognis.⁷ Bremus *et al.*⁸ invented a process to produce the triacetin continuously: In a first step the glycerol is converted only partly with acetic acid. In a second unit this reaction mixture is mixed with acetic acid anhydride to achieve a nearly complete conversion to triacetin. As a final step the triacetin is separated and purified by distillation. The non-toxic triacetin can be used for instance as a textile auxiliary.⁹

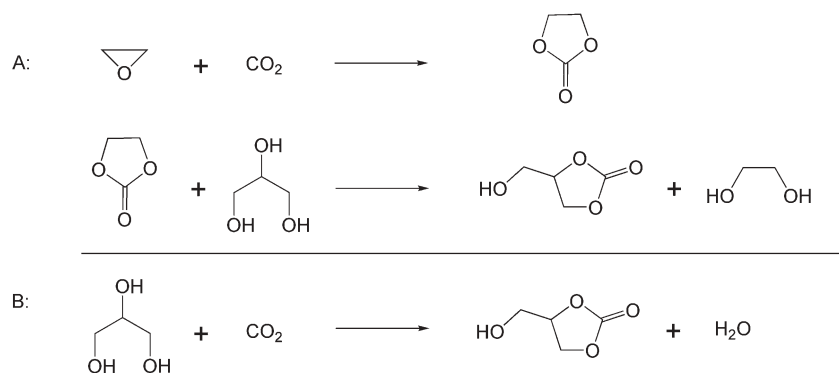
Roice *et al.* published a paper about the use of glycerol dimethacrylate as monomer. This diester can be used for the synthesis of copolymers with new interesting properties.¹⁰

2.2 Glycerol carbonate

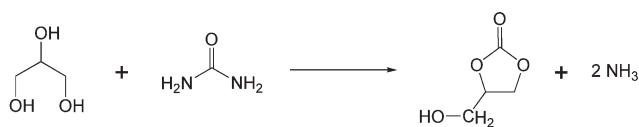
The technical synthesis of glycerol carbonate uses a multi-step reaction: First ethylene oxide reacts with carbon dioxide to yield the cyclic ethylene carbonate which then reacts further with glycerol to yield glycerol carbonate and ethylene glycol (Scheme 3, route A). Obviously, it would be more economic to convert glycerol and carbon dioxide directly into glycerol carbonate (Scheme 3, route B).

Glycerol carbonate and its esters are very interesting derivatives of glycerol, because they can be used as solvents for many applications, for instance in colours, varnishes, glues, cosmetics and pharmaceuticals.¹¹ The use as extraction medium or as monomer for the synthesis of new types of polymers may also become of interest.

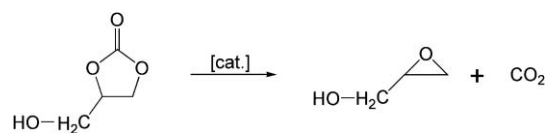
The direct synthesis of glycerol carbonate by the conversion of glycerol with carbon dioxide (route B) is therefore an interesting target of scientific research groups. Aresta *et al.*¹² have investigated this reaction using di(n-butyl)tin dimethoxide, di(n-butyl)tin oxide and tin dimethoxide as catalysts. Under the investigated reaction conditions (50 bar CO₂,



Scheme 3 Syntheses of glycerol carbonate.



Scheme 4 Synthesis of glycerol carbonate from glycerol and urea.



Scheme 5 Conversion of glycerol carbonate to glycidol.

180 °C) tin dimethoxide led only to traces of glycerol carbonate. However, di(*n*-butyl)tin dimethoxide led to a conversion of glycerol of maximum 7% depending on the reaction conditions. No solvent was used and molecular sieves were added in order to remove water from the gas phase. Using di(*n*-butyl)tin oxide as catalyst conversions of glycerol up to 2% were reported.

Similar tin catalysts were investigated successfully by Ballivet–Tkatchenko in the direct synthesis of dimethyl carbonate working in supercritical carbon dioxide.¹³ The reaction of glycerol and carbon dioxide has still to be further optimised to become a technical route to glycerol carbonate.

The catalytic conversion of glycerol with urea to glycerol carbonate has been investigated by Yoo and Mouloungui.¹⁴ Scheme 4 depicts the formal chemical equation.

Heterogeneous zinc catalysts were used to perform the reaction. At temperatures between 140–150 °C and a pressure of 40 mbar equimolar amounts of glycerol and urea react to glycerol carbonate. Table 2 shows the main results of the reaction optimisations.

In particular, the catalyst Zn(CH₃C₆H₄-SO₃)₂ leads to yields of more than 80% towards glycerol carbonate in a relative short reaction time of about 1 h. Similar high yields can be achieved by other catalysts, but only at longer reaction times.

Glycerol carbonate can split off carbon dioxide yielding glycidol.¹⁵ For this reaction (Scheme 5) zeolite A proved to be a very active catalyst. At a temperature of 180 °C and a

pressure of 35 mbar a yield of 86% and a purity of 99% could be attained.

Rokicki *et al.* investigated the use of glycerol carbonate as monomer to produce hyperbranched aliphatic polyethers (polyglycerols).¹⁶

3. Glycerol ethers

In the present section we will consider:

- The oligomers of glycerol in which the glycerol units are linked together *via* ether bondings to linear or cyclic compounds. When a higher number of glycerol molecules is linked together these compounds are also called polyglycerols. Both the oligoglycerols as well as their esters have already found important technical applications.

- The alkyl ethers of glycerol, for instance the glycerol tertiary butyl ethers.

- The alkenyl ethers of glycerol, for instance the telomers of glycerol with butadiene.

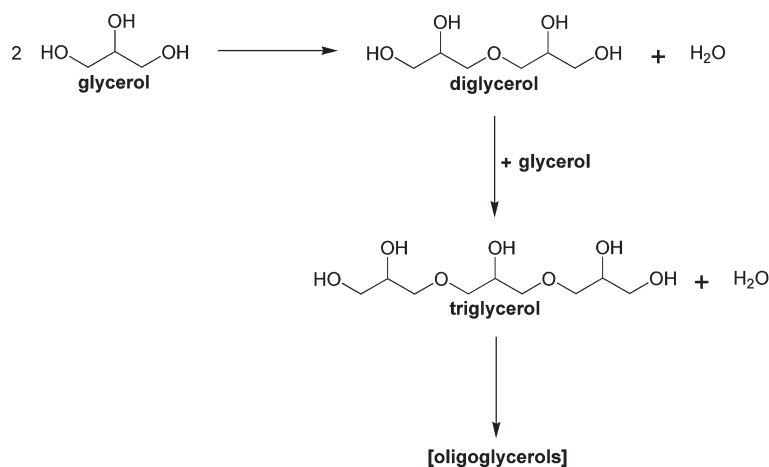
3.1 Glycerol oligomers/polymers (and their esters)

As an example Scheme 6 shows the synthesis of the linear diglycerol and triglycerol in which the glycerol units are linked together *via* their primary hydroxy groups. A great number of other linkages and of higher oligomers can be formed.

The oligoglycerols are gaining more and more interest as products used in cosmetics, food-additives or lubricants.¹⁷ Short overviews about the synthesis of glycerol oligomers from di- to pentaglycerol have been published by Rollin *et al.*¹⁸ and Pérez-Pariente *et al.*¹⁹ Generally oligoglycerols are produced using basic homogeneous catalysis, but lately increased attention has been paid towards heterogeneously catalysed processes.²⁰ Despite a lower activity heterogeneous catalysts reveal many advantages: Firstly, the separation of the catalyst does not cause any problems because the catalyst is a solid which is insoluble in the reaction medium. Secondly, a higher selectivity has been observed when heterogeneous catalysts such as

Table 2 Investigation of zinc catalysts for the synthesis of glycerol carbonate from glycerol and urea

Catalyst	Reaction time/h	Molar yield (%)
Zn(CH ₃ C ₆ H ₄ -SO ₃) ₂	1	81
Zn(CH ₃ C ₆ H ₄ -SO ₃) ₂	1.25	85
ZnSO ₄ ·H ₂ O	2	83
ZnSO ₄ (pre-treated for 3 h at 450 °C)	2	86



Scheme 6 Synthesis of oligoglycerols by intermolecular dehydration of glycerol units.

Table 3 Comparison of homogeneous and heterogeneous catalysts in glycerol oligomerisation

Catalyst	Na ₂ CO ₃	Cs-MCM-41	Amberlyst 16	Amberlyst 31
Conversion (%)	80 (8 h)	95 (24 h)	35–40	35–40
Selectivity (%)				
Diglycerol	31	59	85	75
Triglycerol	28	30	15	25
Tetraglycerol	17	11	<1	<1
Higher oligomers	24	<1	<1	<1

zeolites, ion exchangers or mesoporous molecular sieves of the type MCM-41 are used.^{17,21,22} However, it should be emphasised that so far the conversion of glycerol using heterogeneous catalysts is by far lower than using homogeneous catalysts.

A typical comparison is given in Table 3: The homogeneously catalysed oligomerisation of glycerol with the catalyst Na₂CO₃ leads to a conversion of 80% after a reaction time of 8 h, while with the heterogeneous catalyst Cs-MCM-41 the conversion reached 95% but only after 24 h. Both reactions were carried out at 260 °C under ambient pressure. The amount of catalyst used was 2 wt.%. The homogeneous catalyst yields a very broad product distribution from 31% diglycerol to 24% higher oligoglycerols. In contrast most heterogeneous catalysts yield relatively high amounts of diglycerol, for instance 59% with Cs-MCM-41, and only very low amounts of higher oligomers.¹⁷ Ion exchangers, for instance Amberlyst 16 and Amberlyst 31, are also very selective catalysts for the specific formation of the short chain oligomers and only a low reaction temperature of 140 °C is

needed. The amount of catalyst used in these reactions was in this case 5 wt.%. However, if these acidic catalysts are used, significant amounts of acrolein are formed.

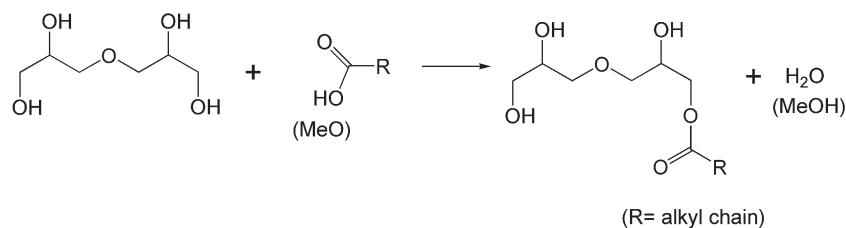
Moreover homogeneous catalysts lead to a different product distribution in contrast to heterogeneous catalysts: Homogeneous catalysts produce mostly linear oligomers whereas heterogeneous catalysts result predominantly in branched oligomers.¹⁷

Akzo Nobel reported a saponite catalyst for the synthesis of glycerol oligomers.²³ The catalyst is a Mg-rich clay which leads to a glycerol conversion of 56% after 40 h of reaction. In this case the selectivity to diglycerol is 30%.

Important derivatives of the oligoglycerols are the oligoglycerol esters. Starting from the oligomers described above, monoesters can be produced *via* esterification with carboxylic acids or transesterification with carboxylic acid methyl esters (Scheme 7). Di- or triesters of glycerol oligomers can be synthesised in a comparable way.

Plasman *et al.* discuss the applicability of these polyglycerol esters,²⁴ especially as antifogging and antistatic agents or as lubricants in the food industry. Only 0.5% of diglycerol monooleate are sufficient to achieve an antifogging effect in food packages. Polyglycerol esters are biodegradable and exhibit a high thermal stability as well as a colourless appearance even after thermal treatment in air at 250 °C.

Barrault *et al.* compared MgO and Cs-MCM-41 as heterogeneous catalysts for the selective synthesis of glycerol esters and diglycerol esters.¹⁷ Table 4 shows the results of the conversion of glycerol with methyl dodecanoate at 240 °C. At these conditions the glycerol is esterified to its mono-, di- and triesters and oligomerised to diglycerol followed by further



Scheme 7 Synthesis of monoesters of diglycerol.

Table 4 Conversion of glycerol with methyl dodecanoate using heterogeneous catalysts

Catalyst	Ester conversion (%)	Selectivity (%)					
		Glycerol			Diglycerol		
		Mono-	Di-	Tri-	Mono-	Di-	Tri-
MgO	98	10	45	34	1	5	5
Cs-MCM-41	89	7	2	38	17	18	19

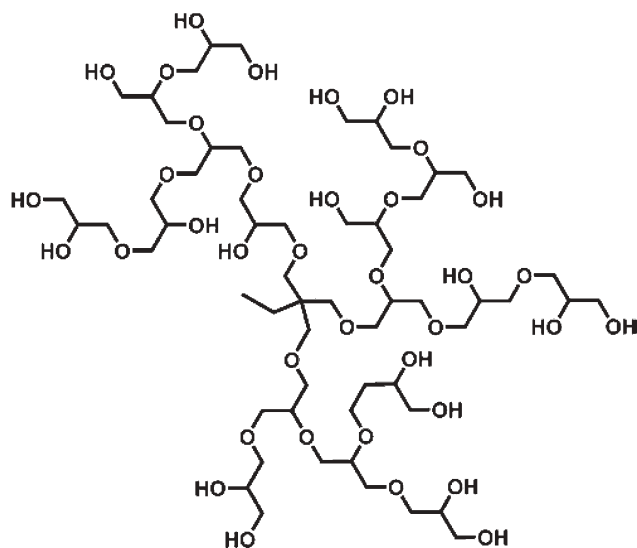
esterification. Whereas MgO leads to a high selectivity of glycerol esters (Σ 89%) the mesoporous catalyst Cs-MCM-41 leads to higher amounts of diglycerol esters (Σ 54%). The concentration of catalyst was 14 wt.% referring to glycerol and 6 wt.% referring to the ester.

Hao described polyglycerol esters which are used as stabilisation agents in water-in-gasoline microemulsions.²⁵ The addition of small amounts of water to gasoline reduces both NO_x emissions as well as soot formation. The water can be dissolved in gasoline by adding a mixture of a polyglycerol ester, a surfactant, and an alcohol thus yielding a microemulsion. The best system proved to be diglycerol diisostearate combined with sodium oleate in a ratio of 6 : 4, dissolved in 1-butanol. The highest water content in the microemulsion could be reached at a temperature of 16 °C.

Jérôme *et al.*²⁶ reported on a phosphazene catalyst for the synthesis of the mono- and diesters of glycerol derivatives. Using this catalyst, regioselective syntheses can be performed.

The last group of glycerol ethers to be presented are the hyperbranched polyglycerols. Scheme 8 depicts the general molecular structure of these compounds.

However, until now hyperbranched polyglycerols cannot be synthesised directly from glycerol as feedstock. The synthesis of such molecules, for instance *via* reaction of trimethylolpropane and glycidol, has been described in detail by Mülhaupt *et al.*^{27,28} Mecking *et al.* reported the incorporation of Pd-nanoclusters into polyglycerols to yield catalysts which are active in the hydrogenation of cyclohexene.²⁹ These palladium/polyglycerol catalysts can easily be recycled and

**Scheme 8** Hyperbranched polyglycerols.

show a constant activity. Haag *et al.* presented polyglycerols able to solubilise hydrophobic drugs.³⁰

The structure of the polyglycerols and polyglycerol esters were investigated by using small-angle neutron scattering (SANS).³¹

Further investigations have been performed by Dworak *et al.*³² They investigated the polymerisation of glycidol using Lewis and protonic acids. Moreover, they elucidated the structure of the polymer by NMR-measurements and suggested a reaction mechanism.

In 2001 a company was founded which deals with hyperbranched polymers commercially.³³

Glycidol has also been mentioned for the synthesis of modified epoxy resins. Those resins are produced by Evonik.³⁴

Furthermore, hyperbranched polymers have been described which have been obtained from glycerol carbonate, which has been synthesised previously from glycerol and dimethyl carbonate.¹⁶

Glycerol as a building block for polymers has also been previously described. The Konkuk University in Seoul has made a patent application in which glycerol and fatty acids are essentials for polyurethaneamide adhesives.³⁵

3.2 Glycerol alkyl ethers

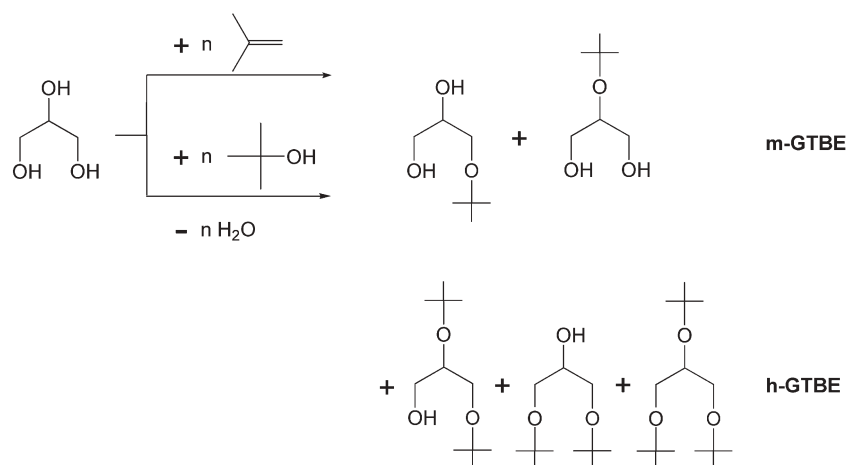
Alkyl ethers of glycerol can generally be synthesised *via* three different routes:

- The Williamson synthesis of sodium-glycerolate with an alkyl halide.
- The addition of an active alkene, especially a branched alkene, to glycerol.
- The condensation reaction between glycerol and an aliphatic alcohol under elimination of water.

Aubry *et al.* reported on the synthesis of glycerol 1-monoethers starting from 1,2-isopropylidene glycerol, potassium hydroxide and different bromoalkanes.³⁶ As these monoethers have the characteristics of solvents as well as of surfactants they are entitled “green solvo-surfactants”, which should be considered for the replacement of ethylene or propylene glycol ethers. However, their synthesis only proceeds with time-consuming protecting group chemistry and stoichiometric amounts of alkali bromides are formed as by-products.

The two other routes of ether synthesis will be demonstrated with the example of the glycerol tertiary-butyl ethers, the GTBE. They can be synthesised *via* the reaction of glycerol with isobutene or with tertiary butanol (Scheme 9).

The conversion of glycerol with isobutene yields the mono-, di- and tri-tertiary butyl ethers of glycerol. Due to the two remaining hydroxy groups the monoethers (m-GTBE) are still soluble in polar solvents, whereas a mixture of the di- and triethers, the so-called “higher ethers” (h-GTBE), are soluble in unpolar media, for instance in hydrocarbons. This property enables the application of the higher GTBE as fuel additives. Because of the glycerol content this additive can be assigned to the renewables and may help to meet the biocomponent target of the European Union. h-GTBE can be used as a diesel fuel additive, which reduces remarkably the emissions of particulate matter.^{37,38} However, because of the branched alkyl substituents the higher GTBE can also be used as potential



Scheme 9 Synthesis of GTBE via reaction of glycerol with isobutene or tertiary-butanol (m-GTBE = monoethers; h-GTBE = higher ethers).

components for the use in gasoline (“octane-boosters”) substituting the methyl tertiary butyl ether MTBE which is under discussion because of some environmental disadvantages.^{39,40}

The catalytic reaction of glycerol with isobutene was first investigated in 1992 by Behr and Lohr at the Henkel Company.⁴¹ They discovered some very active homogeneous and heterogeneous catalysts, for instance *p*-toluene sulfonic acid, acidic ion exchangers like Amberlyst 15 and several synthetic zeolites. In 1996 Behr and Obendorf^{42,43} continued these investigations and developed a technical process for the production of the higher GTBE. With *p*-toluene sulfonic acid (*p*-TSA) as the best catalyst the etherification of glycerol with isobutene was performed in a stirred batch reactor at 90 °C with a molar ratio of isobutene to glycerol of 2 : 1. At the beginning of the reaction the system consists of two immiscible phases, the polar glycerol and the unpolar isobutene phase. As the reaction proceeds, the mono-, di- and triethers are formed and after 40 min the reaction system becomes single-phased. After a total reaction time of about 3 h the reaction equilibrium is achieved yielding a mixture of about 45 wt.% diethers, 30 wt.% monoethers and 5 wt.% of unconverted glycerol.

Based on these laboratory investigations a continuous production process of the higher ethers was designed (Fig. 1), which enables the complete recycling of the homogeneous catalyst *p*-TSA and of the unwanted monoethers. The process consists of a reactor cascade operated at 20–30 bar followed by

an extraction at the same pressure conditions. Isobutene is fed directly to the reactor, whereas glycerol is fed to the extractor separating the catalyst and the monoethers from the reaction mixture. The polar glycerol/moethers-phase (R1) is run back to the reactor, whereas the unpolar phase is conducted to a flasher where the unreacted isobutene is stripped and then also recycled to the reaction unit. The bottom product of the flash passes a vacuum rectification column obtaining pure higher ethers overhead. The bottom product of the rectification which contains some traces of m-GTBE and the catalyst *p*-TSA is passed back to the reactor (R2). This process seems to be more economic than other processes proposed in some patents.^{44–50}

Karinen and Krause have investigated the same reaction system using Amberlyst 35WET as a heterogeneous catalyst.⁵¹ At a ratio of isobutene and glycerol of 2 : 1 the highest selectivity towards ethers of about 92% can be reached whereas a molar ratio of 4 : 1 leads to a selectivity of about 80%. 80 °C is described to be the best reaction temperature. High ratios of isobutene to glycerol lead to small fractions of monoethers, whereas small ratios lead to large amounts of monoethers, which, however, cannot be used as octane-boosters.⁴³

In 2003 Klepáčová *et al.* investigated the reaction of glycerol with *tert*-butanol in the presence of heterogeneous catalysts⁵² and compared Amberlyst 15 with the zeolites H-Y and H-Beta. By using Amberlyst 15 as catalyst the highest glycerol conversion is achieved at 90 °C after 3 h. A catalyst concentration

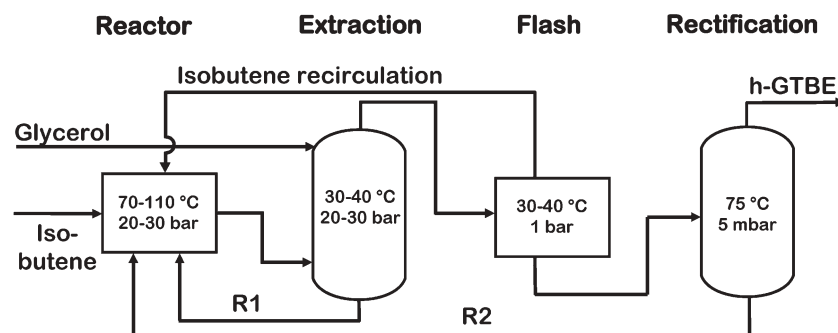


Fig. 1 Flow scheme for the technical process for the production of higher GTBE (R1 = recycle of glycerol, *p*-TSA and m-GTBE; R2 = recycle of traces of m-GTBE and *p*-TSA).

between 5 and 8 wt.% and an equimolar ratio between *tert*-butanol and glycerol gives optimum results.

In 2005 Klepáčová *et al.* published new investigations⁵³ where they compared experiments with isobutene as well as with *tert*-butanol. If the same temperature and catalyst is used isobutene always leads to higher conversions of glycerol than *tert*-butanol. This can be explained by the formation of the by-product water, which deactivates the catalyst. At 60 °C with the catalyst Amberlyst 35 in the dry form the conversion of glycerol with isobutene is almost quantitatively, whereas the conversion of glycerol with *tert*-butanol is only 86%.

3.3 Glycerol alkenyl ethers (telomers)

An atom-economic way to get unsaturated ethers of glycerol is the transition-metal catalysed telomerisation of butadiene with glycerol^{54–56} leading to the products shown in Scheme 10.

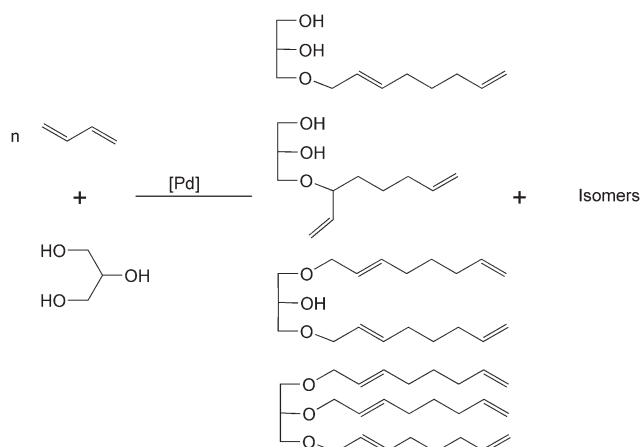
Like other ethers of glycerol they can be used as emulsifiers or surfactants due to their amphiphilic nature after hydrogenation of the remaining double bonds. Moreover, glycerol monoethers in particular have some special advantages regarding *e.g.* toxicity and biodegradability.⁵⁷

The telomerisation is catalysed homogeneously at temperatures around 80 °C by metal complexes of palladium or nickel containing suitable ligands, *e.g.* phosphines, leading to telomer selectivities > 95%.^{55,56,58,59} Because of the homogeneous catalyst, recycling of metal and ligands is necessary to make the reaction efficient. Some recycling concepts are already described in the literature.^{58,60}

4. Glycerol acetals and ketals

Various acetals and ketals can be used as ignition accelerators and antiknock additives in combustion engines either based on petrochemical fuel like diesel and Otto fuel or bio-fuels.

They can be added up to 10 vol% of the fuel used^{61,62} and one main advantage is—comparable to the GTBE—the reduction of particle emissions.⁶³ A second application of glycerol acetals is the use as scent or flavour, *e.g.* the acetalisation of phenylacetaldehyde or vanillin with glycerol leading to hyacinth or vanilla flavours.^{64,65} Glycerol acetals can also be used as the basis for surfactants.⁶⁶



Scheme 10 Telomerisation of butadiene with glycerol to glycerol alkenyl ethers.



Scheme 11 General structures of glycerol acetals and ketals (R = H, alkyl chain).

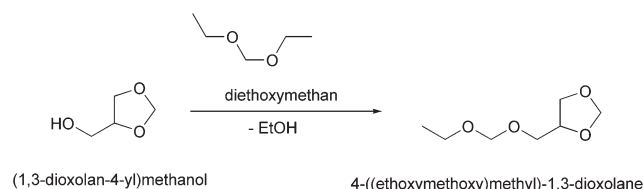
Acetals or ketals can be formed by reaction of glycerol with various aldehydes or ketones yielding five- or six-membered cycles (Scheme 11).

In the acetalisation reaction, the five- and six-ring compounds are usually formed in a ratio of 50 : 50. Some efforts have been made to change and control this ratio by varying the reaction parameters such as temperature, aldehyde or ketone to glycerol ratio and the choice of solvent. One example is the reaction of glycerol with acetone in dichloromethane at about 40 °C leading to a ratio of the five-membered to the six-membered ring as 99 : 1. In the case where the reaction is carried out with formaldehyde under the same conditions only a ratio of 22 : 78 is found.

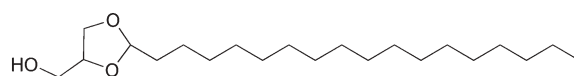
To perform an acetalisation, a catalyst is needed, which is mostly a solid acid catalyst. For example Amberlyst 15 catalyses the acetalisation of glycerol with various aldehydes or ketones *e.g.* butanal⁶¹ or acrolein⁶⁷ at temperatures below 70 °C leading to high selectivities. Also Amberlyst 36 is active in the acetalisation of glycerol, *e.g.* with formaldehyde at $T = 50\text{--}110$ °C with a yield of 77%. The glycerol formal can be used as disinfectant or solvent for medical or cosmetic applications.^{68,69} Furthermore, various zeolites catalyse the acetalisation reaction.⁶⁴ To modify the solubility and other physical properties, glycerol acetals can be varied by a further reaction of the remaining hydroxy group, which is shown in an example in Scheme 12.⁷⁰

Another standard way to change the polarity of glycerol acetals is the etherification of the remaining hydroxy group with tertiary alkenes.⁷¹

A further way to change the properties of given acetals or ketals is the transacetalisation by which *e.g.* long chained molecules (Scheme 13) can be obtained.^{72,73} Overall very polar (Scheme 12) as well as very unpolar acetals and ketals (Scheme 13) can be produced.



Scheme 12 Modification of the glycerol formal by etherification of the hydroxy group.



Scheme 13 Acetalisation of glycerol with octadecanal to 2-hepta-decyl-4-hydroxymethyl-1,3-dioxolan.

5. From glycerol to propanediols

Glycerol can be converted to 1,2-propanediol and 1,3-propanediol, which are useful final products, but also valuable starting compounds for the production of polymers. The world consumption of propylene glycols in 2003 was 1.2 million metric tons, the biggest producers being Dow and Lyondell with 35% and 25%, respectively, of the world production.⁷⁴ 1,3-Propanediol is an important diol in the production of polyesters, polycarbonates and polyurethanes. Three examples of large scale applications of 1,3-propanediol are SORONA and HYTREL made by DuPont and CORTERRA, trade mark of Shell.

While 1,3-propanediol is mainly used as a starting material for polymers, 1,2-propanediol is often used without further modification *e.g.* as an additive in nutrition products, solvent for colourings and flavours, wetting agent in tobaccos, additive in cosmetics, as component of break or hydraulic fluids, lubricants or anti-freezing agent. Furthermore, it can be used as a starting material for solvents, emulsifiers and plasticisers.

5.1 From glycerol to 1,2-propanediol

The present industrial way for manufacturing 1,2-propanediol (= propylene glycol) is the hydrolysis of propylene oxide with water at temperatures between 125 °C and 200 °C at a pressure of 20 bar (Scheme 14). After the reaction step, the mixture must be stripped and distilled to separate the product from water and the higher substituted polyols. Although there are further processes such as the acetoxidation of propene followed by hydrolysis or the direct hydroxylation catalysed by osmium compounds, the classical route based on propylene oxide is still widely used.⁷⁵

In particular, when 1,2-propanediol or its derivatives are applied in food, cosmetics or pharmaceutical products, the use of fossil raw materials is less favourable to the consumer acceptance, which leads to the demand of a renewable feedstock such as glycerol or sugars. Agribusiness companies such as Archer Daniels Midland (ADM) have developed processes based on these starting materials.⁷⁶ Glycerol can be converted to 1,2-propanediol using heterogeneous, homogeneous or biocatalysts, which are described in the following section.

(a) Heterogeneous catalysts. One possible way to obtain 1,2-propanediol from glycerol is the direct hydrogenation of glycerol by classical heterogeneous hydrogenation catalysts used in the production of fatty alcohols or in fat hardening. Moreover, catalysts containing an active copper compound such as Cu-chromite, Cu-ZnO₂ or Cu-Al₂O₃ are active in

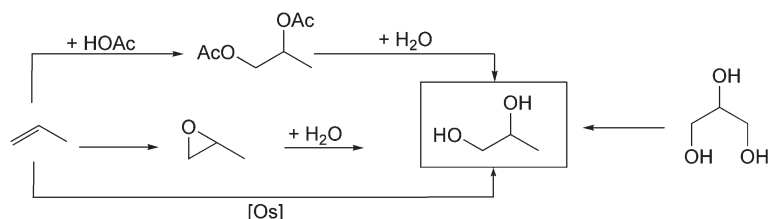
glycerol hydrogenation at temperatures between 150–320 °C and pressures between 100 and 250 bar.^{77–80} With similar reaction conditions, a catalyst system containing cobalt, copper, manganese and molybdenum as well as inorganic polyacids leads to nearly quantitative conversions with selectivities > 95%.⁸¹ Another way of converting glycerol to propylene glycol is the use of ruthenium in combination with acids or ion-exchange resins, which enables slightly milder reaction conditions, but also smaller conversions and selectivities.^{82–84}

Another approach is the use of Raney-nickel as hydrogenation catalyst. As in the case of Ru as a catalyst, reaction conditions are relatively mild.⁸⁵ The use of rhenium as catalyst metal in a multimetallic catalyst leads to conversions up to 80% with selectivities > 30% at temperatures > 120 °C and 80 bar hydrogen pressure.⁸⁶ Besides the influence of metal and support also the choice of solvent has a strong influence on the performance of the catalyst system, especially on the selectivity towards 1,2- or 1,3-propanediol.⁸⁷

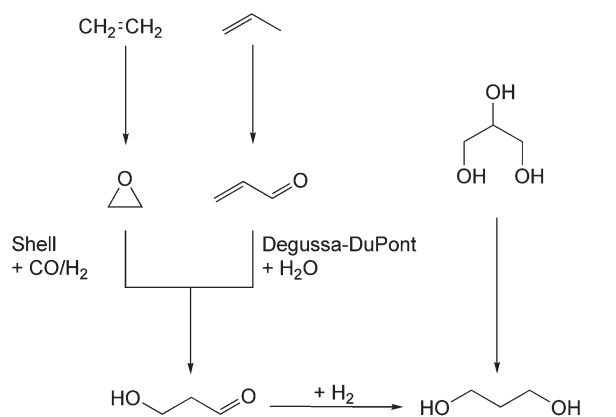
Not only the catalyst systems and solvents have been improved, but also completely new processes have been developed. One example will be described in section 5.2a.

(b) Homogeneous catalysts. In general the hydrogenolysis of glycerol by homogeneous catalysts leads to a variety of by-products such as propanol or ethers and to a mixture of 1,2- and 1,3-propanediol. The amount of different products depends on the mechanism of the product formation. Typical catalysts for this application are metals of the platinum group either in complexes with iodocarbonyl compounds⁸⁸ or phosphorous, arsenic or antimony ligands.⁸⁹ The selectivity for 1,2-propanediol of these processes is usually below 25%. These processes operate at conditions, which are comparable to the ones applied in heterogeneous systems, only the pressure range can be decreased ($T > 100$ °C, $p = 5$ –100 bar). There have also been process simulations to develop production routes leading from biomass such as glycerol or sugar to 1,2-PDO and ethylene glycol.⁹⁰

(c) Biocatalysts. A typical commercial example of a technology switch with respect to catalyst and feedstock was demonstrated by a joint venture of the chemical company Ashland Inc. and the food processor Cargill. The aim of this project was the production of propylene glycol out of glycerol from the biodiesel industry at a factory in Europe with an initial capital investment of \$80–\$100 million and a capacity of 65 000 t year⁻¹.^{91–93} Cargill has already presented a process to obtain propylene glycol out of carbohydrates with *Escherichia coli* or *Thermoanaerobacterium thermo-saccharolyticum* HG-8.^{94,95}



Scheme 14 Comparison of the reaction routes to 1,2-propanediol starting from propene or glycerol.



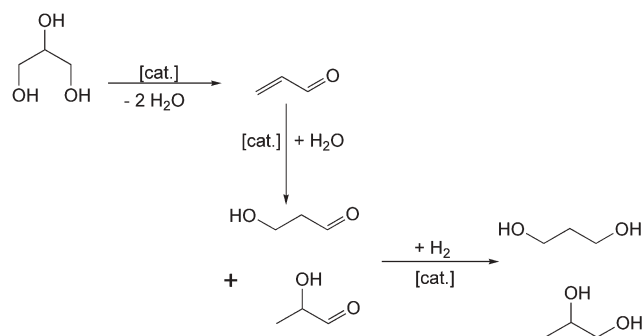
Scheme 15 Different routes to 1,3-propanediol starting from ethene, propene or glycerol.

5. 2 From glycerol to 1,3-propanediol

As mentioned above, 1,3-propanediol is an important compound in polymer production and is therefore much more valuable than 1,2-propanediol. There are two examples for the synthesis of 1,3-propanediol based on petrochemicals: the first one is the Shell process^{96–99} consisting of the hydroformylation of ethylene oxide to 3-hydroxypropanal followed by hydrogenation to 1,3-propanediol. The second is the Degussa–DuPont process^{100–103} based on the hydration of acrolein to 3-hydroxypropanal and further hydrogenation analogue to the Shell process (Scheme 15).

Problems in the conventional processes are the high pressure applied in the hydroformylation and hydrogenation steps as well as the use of aromatic solvents in the first and loss of acrolein due to extraction processes in the second example. The yields are around 80% in the first and about 40% in the second process, so besides the demand of renewable sources like glycerol, there is also a huge interest in improving yields and overall selectivity of the processes applied. Therefore, the reaction from glycerol to 1,3-propanediol *via* heterogeneous, homogeneous or biocatalytic processes may become an attractive alternative.

(a) Heterogeneous catalysts. Heterogeneous catalysts are not selective in the formation of 3-hydroxypropanal out of glycerol. That is why mainly mixtures of 1,2- and 1,3-propanediol are obtained with heterogeneous catalyst systems (*e.g.* yield, $Y(1,3\text{-PD}) = 12\%$, $Y(1,2\text{-PD}) = 6\%$ described in ref. 87. Using the present known heterogeneous catalysts an improvement of the existing production routes cannot be achieved. What can be improved, besides the catalyst, is the reaction engineering as described in ref. 104. In this process, the yield of 1,3-propanediol is 60% (1,2-propanediol 10%), which is comparable to the processes based on petrochemicals. Glycerol is dehydrated to acrolein in the first step at 250 °C–340 °C with acid catalysts such as zeolites, inorganic acids or metal oxides (Al_2O_3 or TiO_2), followed by the acid-catalysed hydration of the acrolein at 20 °C–120 °C to the hydroxypropyl aldehydes and further hydrogenation to a mixture of 1,2- and 1,3-propanediol catalysed by Raney-nickel, platinum or ruthenium on a support or nickel on Al_2O_3 ¹⁰⁴ (Scheme 16).

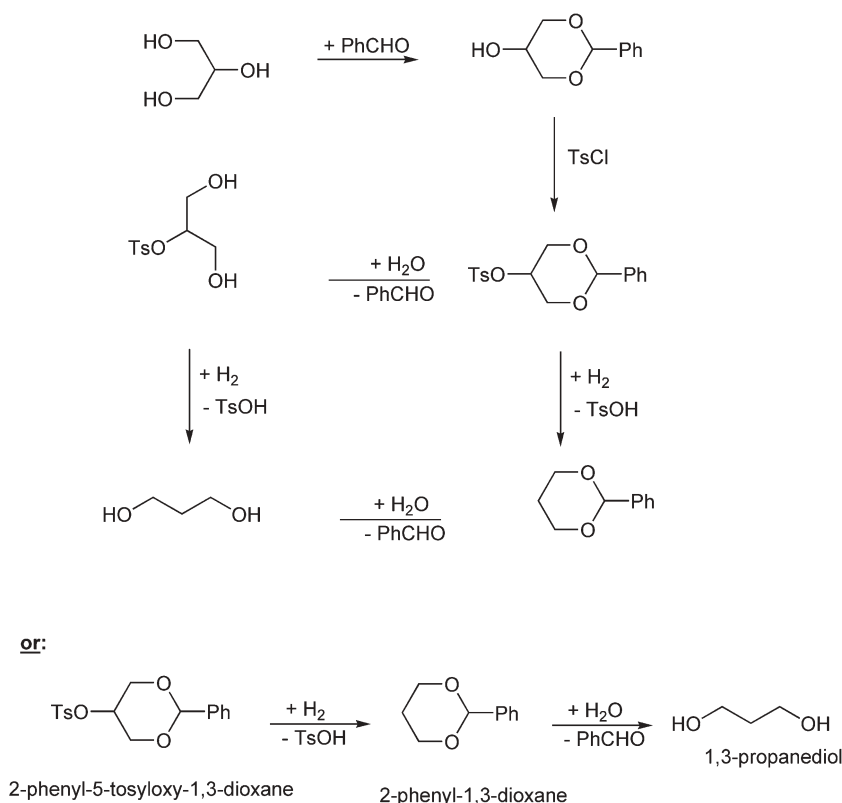


Scheme 16 Stepwise conversion of glycerol to propanediols.

(b) Homogeneous catalysts. A typical advantage of homogeneous catalysts is their high selectivity, which can be explained by the well known mechanisms *via* organometallic species. Successful systems to convert glycerol to 1,3-propanediol are *e.g.* rhodium carbonyl catalysts such as $\text{Rh}(\text{CO})_2(\text{acac})$, which lead to a 21% selective conversion to 1,3-propanediol at room temperature and ambient pressure, which is a remarkable advantage compared to the reaction conditions used in the petrochemical routes.¹⁰⁵ Analogous to the heterogeneous systems, mixtures of different alcohols are obtained *e.g.* by using group VIII metals and/or tungsten as described in ref. 106 (yield, $Y(1,2\text{-PD}) = 26\%$; $Y(1,3\text{-PD}) = 24\%$). Moreover, process development can improve the results too, *e.g.* the process described in ref. 107 where the catalyst *p*-toluenesulfonic acid is used (Scheme 17). The process works with protection groups and consists of four steps, namely acetalisation of glycerol with benzaldehyde, tosylation of the resulting 5-hydroxy-2-phenyl-1,3-dioxane and further hydrolysis and hydrogenolysis which leads to 1,3-propanediol with an overall yield of 72%.

(c) Biocatalysts. Some enzymes and microorganisms possess a very high selectivity to convert several carbon sources to 1,3-propanediol. For instance glycerol can be converted to 3-hydroxypropanal in a one-step enzymatic reaction in an aqueous solution at room temperature and ambient pressure with yields > 85%. Six genera of bacteria are able to ferment glycerol with sufficient results, namely *Bacillus*, *Klebsiella*, *Citrobacter*, *Enterobacter*, *Clostridium* and *Lactobacillus*.^{108–114} Furthermore, some thermophilic strains have been developed to convert hot effluents from the fat industry.¹¹⁵

Besides glycerol, other polyols, like starch or glucose, can be used in the production of 1,3-propanediol by fermentation with the bacteria mentioned above. One example of a technology switch from petrochemicals to renewable sources is the fibre SORONA made by DuPont. Genencor International and DuPont have developed in conjunction a process for producing 1,3-propanediol by fermentation with recombinant *Escherichia coli*. The genome with the information about the conversion of glycerol to 1,3-propanediol has been isolated from a donor organism and transferred to *E. coli*. This modified organism is 500 times more effective than the original one.^{114,116–120} The process can convert glycerol but was afterwards switched to the cheaper glucose, now a fundamental technique for DuPont to produce 1,3-propanediol. In



Scheme 17 Alternative process from glycerol to 1,3-propanediol using protection groups.

the first plant in Loudon, Tennessee, 500 t year⁻¹ of 1,3-propanediol can be produced starting from glucose obtained from corn.^{121–124} According to DuPont the process saves 40% of the energy consumed by its petrochemical counterpart.

6. From glycerol to epoxides

In the past glycerol was made out of epichlorohydrine, but—as mentioned earlier—there is no further need for a specific synthesis of glycerol nowadays. Therefore Solvay came up with the idea to reverse the classic synthesis route and to produce epichlorohydrine from glycerol (Scheme 18). This process is divided into two main steps: The first step is the chlorination of glycerol with anhydrous hydrogen chloride to 1,3-dichloropropan-2-ol at moderate temperatures of about 110 °C.^{125,126} The second step is the formation of the epoxide by addition of sodium hydroxide. Thus the desired epichlorohydrine, the so-called Epicerol, is obtained. The preparation of epichlorohydrine on the basis of glycerol shows significant advantages compared to the present process based on propene: First of all the feedstock is renewable and the water

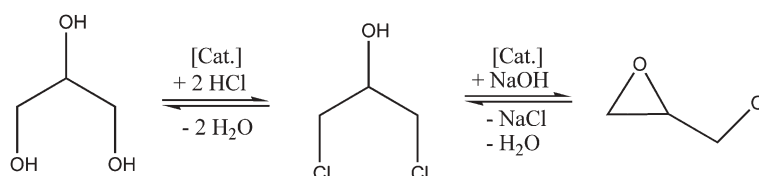
consumption is lower. In addition the chlorinated residues are reduced and the chlorination agent is hydrochloric acid instead of the more expensive chlorine.¹²⁷

Another epoxide with the glycerol structure is the glycidol whose synthesis has already been described in Scheme 5 in section 2.2.

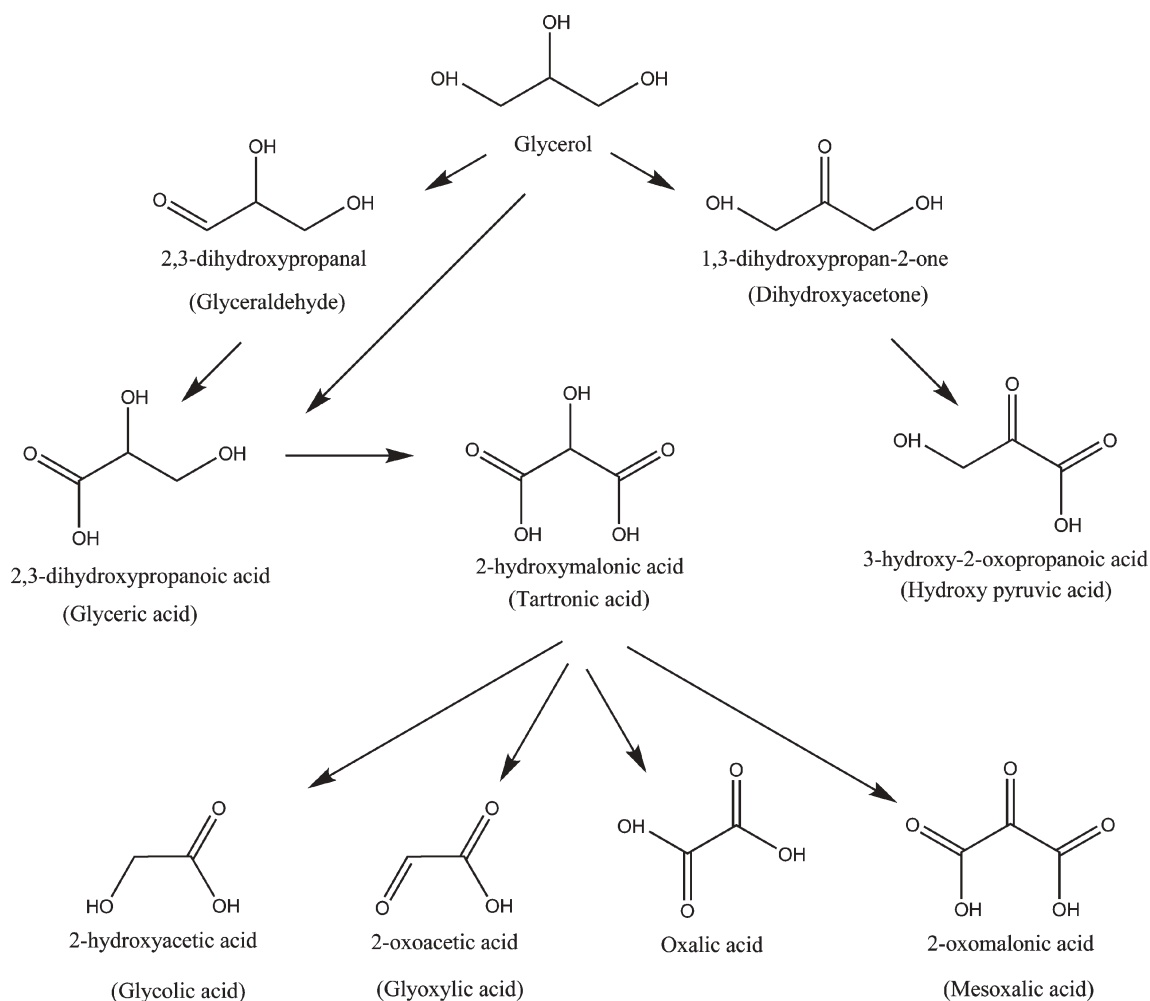
7. Glycerol oxidation and dehydration

Glycerol oxidation is a complex pathway of reactions that can lead to a large number of products (Scheme 19). Many of these products are useful intermediate substances or valuable fine chemicals. However, until now they are being produced by expensive processes and therefore their utilisation on an industrial scale is still low.

In the following section (section 7.1) some valuable glycerol oxidation products are presented together with their main application fields. Secondly, the most important catalytic oxidation processes of glycerol are discussed (section 7.2). In the last section (section 7.3) the dehydration of glycerol to acrolein is presented.



Scheme 18 Conversion of glycerol to epichlorohydrine.



Scheme 19 Oxidation products of glycerol.¹²⁸

7.1 Glycerol oxidation products

If the secondary hydroxy group of glycerol is oxidised selectively, dihydroxyacetone (DHA) is formed (Scheme 19). Conventionally, this can be done by a fermentation process, for example *via* the microorganism *Gluconobacter oxydans* in a fed batch reactor.¹²⁹ DHA has been used for years as an active substance in sunless tanning lotions. A combination of DHA incorporated in lamellar structures, *e.g.* phospholipids, and free DHA particles has resulted in a even more intensive and longer tanning effect.¹³⁰ Beside its main utilization in cosmetics, DHA has also other applications, for instance as a monomer in polymeric biomaterials.¹³¹

The oxidation of the primary hydroxy groups of glycerol produces glyceraldehyde, an intermediate in the carbohydrate metabolism. Glyceraldehyde is also used as a standard by which chiral molecules of the D- or L-series are compared. Further oxidation of glyceraldehyde produces carboxylic acids, like glyceric acid, tartronic acid and mesoxalic acid (Scheme 19). These acids are mainly converted into various market products, *e.g.* polymers or biodegradable emulsifiers. In addition to these applications, glyceric acid can be used for treatment of skin disorders,^{132,133} or as an anionic monomer of packaging material for exothermic and volatile agents.¹³⁴ In its

ester form, glyceric acid can act together with a quaternary ammonium salt as an effective and biodegradable fabric softener.¹³⁵ Tartronic acid can be used as a potentiating agent or adjuvant to increase the blood absorption of a tetracycline antibiotic.¹³⁶ Moreover, it can be used to scavenge dissolved oxygen in alkaline water.¹³⁷

7.2 Glycerol oxidation processes

Depending on the reaction conditions (pH, temperature, substrate to metal ratio) and the noble metal employed, the reaction pathway can be directed either to the oxidation of the primary or the secondary hydroxy group. Aerobic catalytic oxidations of glycerol have already been investigated with metal catalysts of platinum, palladium and recently of gold. In addition, non-aerobic electrocatalytic oxidations of glycerol using tetramethyl piperidine-1-oxyl (TEMPO) as oxidation agent and Ag/AgCl as catalyst have also been introduced.¹³⁸

Platinum metal catalysts are more selective for the oxidation of primary than for secondary alcohols. The main product of glycerol oxidation using platinum supported on active charcoal is glyceric acid (selectivity 55% at 90% conversion) with a small amount of DHA (selectivity 12%).¹³⁹ The selectivity towards the secondary alcohol can be increased by

association of the platinum with p-electron metals, especially lead and bismuth.^{140,141} These metal promoters can be added to the platinum-metals by co-impregnation, impregnation or redox surface reaction.¹⁴² In batch reactions the aerobic glycerol oxidation with Pt–Bi catalysts, prepared by means of the co-impregnation method, has a selectivity of 37% towards DHA at a 75% conversion of glycerol.¹³⁹ A still better result of the Pt–Bi catalysts could be achieved in catalytic glycerol oxidation by using a fixed-bed reactor, producing DHA with 80% selectivity at 40% conversion.^{143,144}

The utilizations of palladium catalysts for catalytic glycerol oxidations have been initiated by the group of Hutchings and the group of Kimura.^{145,146} Palladium catalysts at basic conditions have a high selectivity towards glyceric acid (77% at 90% conversion), whereas the selectivities to the other reaction products (DHA, tartronic and oxalic acids) are always lower than 10%.¹³⁹ However, palladium shows a weaker catalytic activity compared to platinum for the oxidation of the secondary hydroxy group of tartronic acid to produce mesoxalic acid.¹⁴⁷

Despite its successful application in aerobic glycerol oxidation processes, platinum suffers strongly from oxygen poisoning at high oxygen partial pressures. Therefore, this system can only be utilised at low oxygen partial pressures or by using air at atmospheric pressure, in order to limit the oxygen dissolution.¹⁴⁸ On the other hand, gold has a better resistance to oxygen poisoning compared to platinum.¹⁴⁹ Catalytic glycerol oxidation using gold catalysts have demonstrated a high selectivity to glyceric acid (more than 90% selectivity at 90% conversion), depending on the catalysts preparation methods used.¹⁴⁸

To evaluate the effect of preparation methods on glycerol oxidation, gold catalysts were prepared by different methods, e.g. by sol–gel, incipient wetness and impregnation. In the sol–gel method, the effect of protection agents, for instance polyvinyl alcohol (PVA), sodium citrate and tetrakis(hydroxypropyl)phosphonium chloride (THPC) has been investigated, and it was shown that the gold catalysts prepared by the sol–gel method have a higher activity than the catalysts prepared by the two other methods.^{148,150}

The increase in activity can also be caused by smaller catalyst particles. For gold it has been shown that the activity is highly dependent upon the particle size.^{150,151} If THPC or PVA are used to stabilise the colloid gold solutions, particles smaller than 10 nm were formed.^{148,150} However, if glyceric acid is the desired main product, the sol–gel method (Table 5, entries 3 and 4) is not the suitable method, since the selectivities are lower compared to the impregnation and incipient wetness methods (Table 5, entries 1 and 2).¹⁴⁸

Table 5 Glycerol oxidation with Au (1%) on activated carbon at 60 °C: Effect of the preparation method.¹⁴⁸

Entry	Preparation method	Glyceric acid selectivity at	
		50% conversion	90% conversion
1	Impregnation	71	70
2	Incipient wetness	80	78
3	Sol–gel (PVA)	47	35
4	Sol–gel (THPC)	52	45
5	Sol–gel (sodium citrate)	75	75

Table 6 Comparisons between monometallic and bimetallic catalysts for the glycerol oxidation at 50 °C¹⁵³

Catalyst	Conversion (%)	Selectivity (%)				TOF/h ⁻¹ ^a
		Glyceric acid	Glycolic acid	Oxalic acid	Tartronic acid	
Pt/C	50	42	31	8	6	532
Pd/C	50	81	3	0	14	1151
	100	21	27	12	39	ns
Au/C	50	65	12	10	9	1090
	100	45	24	19	10	ns
Au–Pt/C	50	72	18	1	8	1987
	100	31	35	5	28	ns
Au–Pd/C	50	77	5	0	18	1775
	100	49	25	2	25	ns

^a Calculation of TOF/h⁻¹ after 0.25 h of reaction. TOF members were calculated on the basis of total loading of metals. ^b ns = not specified.

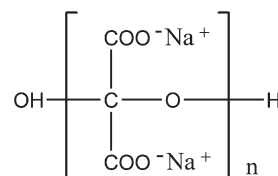
Basic reaction conditions are essential for the gold catalysis, since the initial step of the oxidation and the dehydrogenation of glycerol cannot proceed in the absence of a base. In the presence of a base, the H⁺ is readily abstracted from one of the primary hydroxy groups to form glyceric acid.^{145,152}

To improve the rate and selectivity of glycerol oxidation processes bimetallic catalysts were used. The comparisons between monometallic Au, Pd, or Pt and bimetallic Au–Pd¹⁵³ or Au–Pt^{154,155} catalysts proved that in many cases bimetallic catalysts have higher activity and resistance to deactivation (Table 6).^{141,142,153}

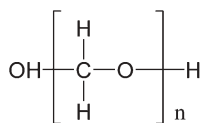
Monometallic Pd/C catalysts exhibit the highest activity with 50 °C, compared to the other metals. Under these conditions, Pd/C shows a better performance than Pt/C which cannot even reach 100% conversion because of the oxygen poisoning. However, if Pt is combined with Au, this bimetallic catalyst has the highest activity compared to all other catalyst systems. The bimetallic Au–Pd catalyst also provides an increase in activity.

The alloyed phase of the bimetallic Au–Pd system is much more active than the same system with segregated metals. The key to avoiding palladium segregation is by slowing down the reduction rate of the palladium salt. This can be achieved *via* two consecutive preparation steps: First the gold sol is immobilised on carbon using sodium boranate as reducing agent and then the palladium sol is precipitated on the Au/C surface using hydrogen as reducing agent. Applying NaBH₄ in the second step would result the unwanted palladium segregation.¹⁵⁶

One example of a three-metal catalyst in glycerol oxidation is Pd–Bi–Ce supported on charcoal. This catalyst has a multifunctional role, *i.e.* to oxidise glycerol to tartronic and mesoxalic acid and then to carry out the polymerisation of the mesoxalic acid into poly(ketomalonate) (Scheme 20).¹⁴⁷



Scheme 20 Structure of poly(ketomalonate).



Scheme 21 Structure of poly(oxymethylene).

Furthermore, in the case of excessive oxidation, a decarboxylation process takes time and results in the conversion of poly(ketomalonate) to poly(oxymethylene) (Scheme 21).¹⁵⁷ The poly(oxymethylene) is an engineering plastic which is also known as polyacetal, acetal resin, polytrioxane, polyformaldehyde, and paraformaldehyde.

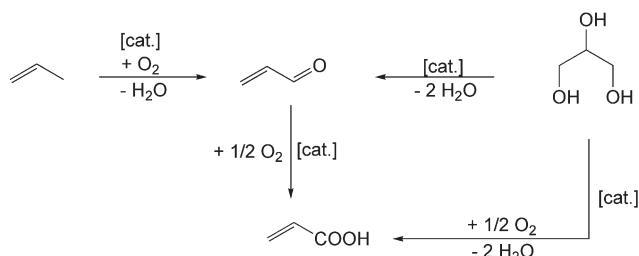
7.3 Glycerol dehydration

Acrolein is a valuable intermediate in the production of acrylic acid, glutaraldehyde and methionine. In particular, acrylic acid can be converted to water absorbing polymers, which can be used *e.g.* in diapers, as retention agents in paper production¹⁵⁸ or to remove water from hydraulic oil or fuel systems. It can also be used as an herbicide without further modification. The usual path to obtain acrolein is based on propene which is oxidised at heterogeneous catalysts containing metals such as bismuth and molybdenum at high temperatures (>300 °C) with yields $Y > 90\%$ (Scheme 22).^{159–162} Some efforts have been made to switch the feedstock from propene to the cheaper propane by using catalysts based on Mo, V and Te.¹⁶³

Additional to this petrochemical route, acrolein can also be obtained from glycerol by dehydration in the liquid or in the gas phase on heterogeneous catalysts. Typical catalysts are for instance zeolites, Nafion composites, aluminas, phosphor- or silicotungstic acids or acid salts which should all have an Hammet acidity of less than + 2 leading to a yield of greater 70% at $T = 250\text{--}350$ °C.^{164–166} A further approach is the direct reaction to acrylic acid, starting from glycerol to avoid separation problems (Scheme 22).¹⁶⁷

Heterogeneous catalysis is not the only appropriate route for the dehydration of glycerol, but also homogeneous systems or even systems without catalyst can lead to acrolein. One approach is the reaction in near supercritical or supercritical water ($T > 300$ °C, $p > 300$ bar), using either no catalyst or different additives (Table 7).

Besides using chemical pathways, acrolein can also be produced by biocatalysis. Glycerol can be fermented to 3-hydroxypropanal *e.g.* by *Lactobacillus reuteri* and subsequent thermal dehydration leads to acrolein.¹⁰⁸ The catalysts



Scheme 22 Production of acrolein and acrylic acid based on propene or glycerol.

Table 7 Yields of acrolein in supercritical water

Catalyst/additive	Yield (%)	Literature
None	12	168
Sulfuric acid (1–5 mmol l ⁻¹)	74	169,170
Zinc sulfate (0–790 ppm)	>40	171,172

and reaction systems used are the same as in the production of 1,3-propanediol with 3-hydroxypropanal as an intermediate step (section 5.2).

8. From glycerol to synthesis gas

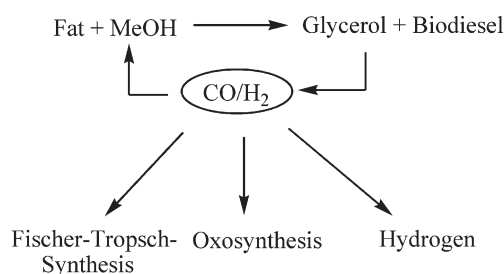
A further potential application of glycerol is its conversion to synthesis gas by enabling the production of a large variety of important chemicals: For instance methanol, a component of biodiesel, can be obtained from synthesis gas and thus a real biodiesel on the exclusive basis of renewable feedstocks can be produced (Scheme 23). In current biodiesel plants the methanol used for the transesterification step is still synthesised on the basis of petroleum.

The synthesis gas can also be utilised in Fischer–Tropsch reactions with the great advantage that the CO/H₂-mixture does not contain any oxygen impurities, making the reaction much easier to handle.

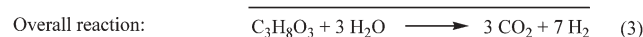
There are several processes to prepare synthesis gas from glycerol. These alternatives, the steam reforming, the aqueous phase reforming and the gasification in supercritical water, are discussed in the following sections.

8.1 Steam reforming

The steam reforming of glycerol yielding a synthesis gas of carbon monoxide and hydrogen is performed in the gas phase usually at atmospheric pressure and temperatures higher than 400 °C. The conversion of glycerol takes place according to eqn (1) in Scheme 24, resulting in a molar H₂/CO ratio of about 1.33. This ratio can be increased by the water–gas shift (WGS) reaction, shown in eqn (2), which converts carbon



Scheme 23 Production of synthesis gas from triglycerides via glycerol.



Scheme 24 Main reactions in the steam reforming of glycerol.

Table 8 Steam reforming of glycerol: Typical reaction conditions and results

Temperature/°C	Catalyst	S/C ^a	C/O ^b	Y H ₂ (%) ^c	S _{CO} (%) ^d	Lit.
1055	RhCeWc ^e	0	1.2	56	79	174
825	RhCeWc ^e	2	1.2	75	58	174
862	RhCeWc ^e	4.5	1.2	79	27	174
400	Pt/C	2.3	1	—	80	175
500–600	Ru/Y ₂ O ₃	3.3	1	82	20	173

^a Steam to carbon ratio. ^b Carbon to oxygen ratio in feed. ^c Yield H₂ according to eqn (3). ^d Selectivity from carbon to CO. ^e Rhodium–ceria washcoat. All experiments were carried out at atmospheric pressure.

monoxide into carbon dioxide. Overall, glycerol can be converted to carbon dioxide and hydrogen (eqn (3)).¹⁷³

Typical catalysts are platinum, ruthenium or rhenium applied on a carrier like carbon, yttrium oxide or ceria washcoat. Some characteristic results are listed in Table 8. Platinum is a very effective steam reforming metal because it is already active at very mild conditions (400 °C) and yields great amounts of carbon monoxide.

8.2 Aqueous phase reforming (APR)

A variation of the steam reforming described above is the aqueous phase reforming (APR). This reaction follows the same equations as shown in Scheme 24, however, in this process the glycerol is kept in the liquid phase. Much higher pressures (25–35 bar) are needed, whereas the reaction

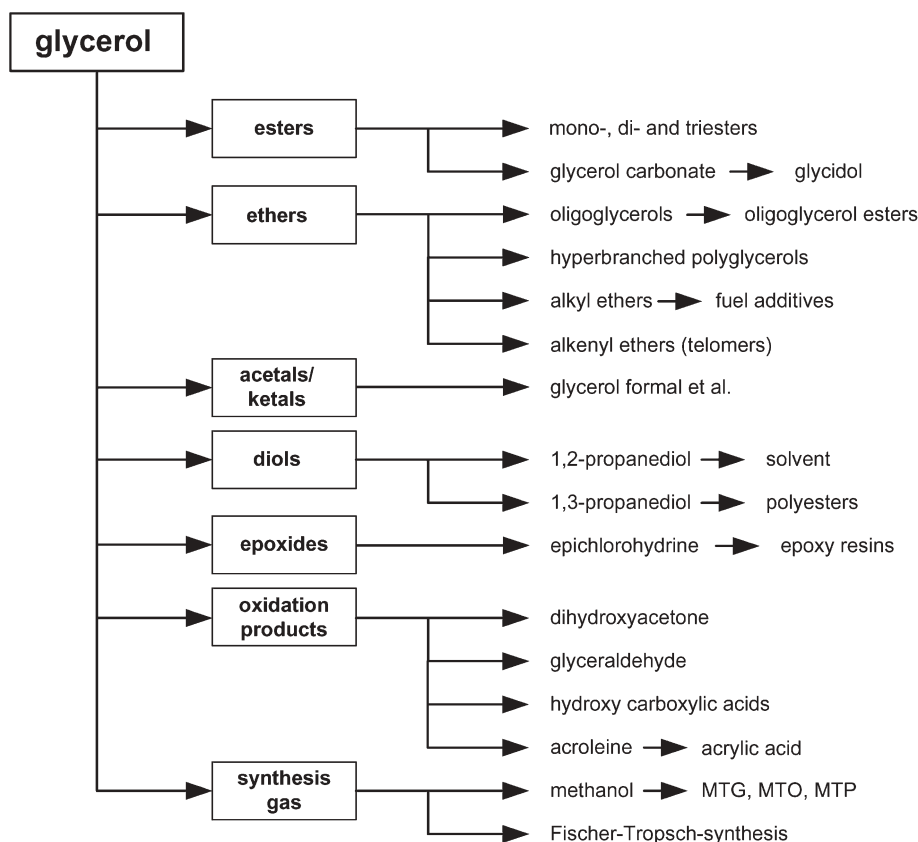
temperature can be slightly lower ($T = 125$ °C). Under these conditions the water–gas shift reaction is thermodynamically much more favourable.

The aqueous phase reforming metals such as platinum, palladium or Ni–Sn alloys show high selectivity for hydrogen production, whereas supported nickel catalysts tend to deactivate with time, which may be due to sintering of the metal particles. Also the support plays an important role in the selectivity of the APR process: Basic or neutral supports, e.g. alumina, favour the formation of hydrogen and carbon dioxide. Since the separation of H₂ and CO₂ is relatively easy, aqueous phase reforming can be used to produce pure hydrogen.¹⁷⁶

8.3 Supercritical water gasification (SCWG)

The gasification in supercritical water is a new technology to convert wet biomass to hydrogen or synthesis gas. Also glycerol can be used as feedstock in supercritical water gasification (SCWG). This reaction can already be carried out without any catalyst, whether very diluted feed solutions (<2 wt.%) are applied. However, better results are obtained if transition metal catalysts are used. A ruthenium catalyst with 3% Ru on a titanium dioxide support yields a quantitative gasification also at higher concentrated (5–17 wt.%) feed solutions.

The conversion of glycerol increases with temperatures from 20% (at 450 °C) up to 90% (at 700 °C); a further increase does not lead to higher conversions. The composition of the gas



Scheme 25 Compilation of the main glycerol derivatisation routes.

slightly changes with the temperature: at higher temperatures a larger amount of hydrogen can be obtained. Experimental results from capillary reactors showed that the pressure has no influence on the carbon efficiency and the product gas yield.¹⁷⁷

9. Conclusions

In the present review on glycerol derivatisation a great number of recently published articles and patents have been cited, thus proving the immense activity in this field. All main subjects are compiled once again in Scheme 25:

- An important aim is the selective synthesis of glycerol monoesters with both homogeneous and heterogeneous catalysts. The direct catalytic reaction of glycerol and carbon dioxide to glycerol carbonate still remains a great scientific challenge.

- The formation of glycerol ethers has been carried out via different routes using alkyl halides, alkenes and dienes as reaction partners. The application of the ethers as fuel additives would consume a great amount of the glycerol surplus formed in the biodiesel production.

- Glycerol acetals and ketals can also be considered as potential fuel additives. A great advantage of these derivatives is the broad range of polarity which can be tuned in a few reaction steps.

- The production of the two propanediols on the basis of glycerol has already been started. In particular, 1,3-propanediol seems to have become a new platform chemical in polyester chemistry.

- The two-step reaction of glycerol to epichlorohydrin, which was developed and implemented by Solvay, is a typical example for the partial change from petrochemical to renewable starting materials.

- The oxidation and dehydration chemistry of glycerol is still in its infancy and further investigations are needed to find better catalysts and reaction performance. However, the possible target molecules of glycerol oxidation may become interesting building blocks in fine and polymer chemistry.

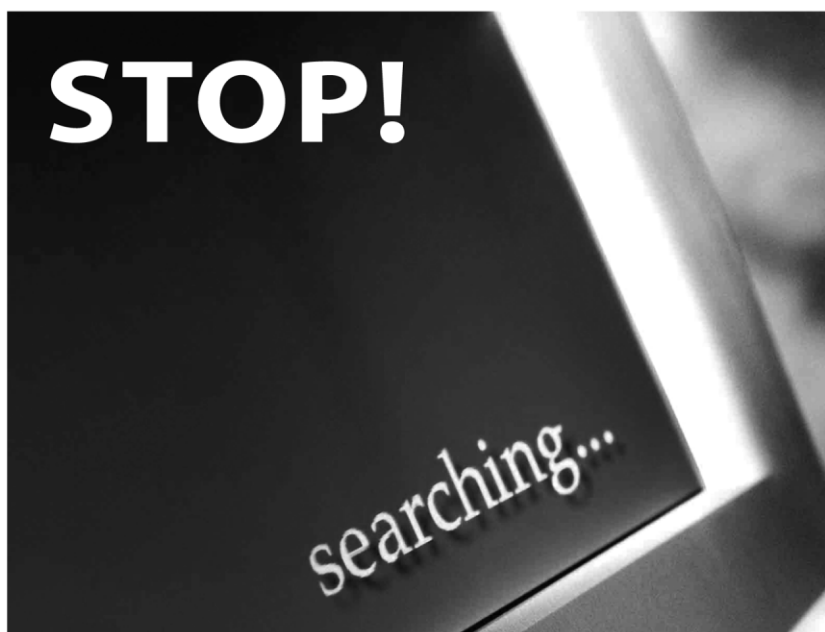
- Finally, the conversion from glycerol to synthesis gas or pure hydrogen, respectively, has to be mentioned which may become an alternative to the traditional synthesis routes based on raw fossil materials.

References

- 1 T. Werpy and G. Petersen, *Top Value Added Chemicals From Biomass*, U.S. Department of Energy, Oak Ridge, TN, USA, 2004.
- 2 F. Jérôme, G. Kharchafi, I. Adam and J. Barrault, *Green Chem.*, 2004, **6**, 72–74.
- 3 J. Barrault, Y. Pouilloux, J. M. Clacens, C. Vanhove and S. Bancquart, *Catal. Today*, 2002, **75**, 177–181.
- 4 C.-S. Chang and P.-L. Wu, *J. Biotechnol.*, 2007, **127**, 694–702.
- 5 J. Pérez-Pariente, I. Diaz, F. Mohino and E. Sastre, *Appl. Catal., A*, 2003, **254**, 173–188.
- 6 A. Corma, S. B. Abd Hamid, S. Iborra and A. Velty, *J. Catal.*, 2005, **234**, 340–347.
- 7 <http://www.de.cognis.com/framescout.html?/ProductCatalog/FindYourProduct.html>, 2007.
- 8 *US Pat.*, 4 381 407, 1983.
- 9 *Ger. Pat.*, 3 913 692 A1, 1989.
- 10 M. Roice, K. P. Subhashchandran, A. Gean, J. Franklin and V. N. R. Pillai, *Polymer*, 2003, **44**, 911–922.
- 11 *Ger. Pat.*, 10 110 855 A1, 2001.
- 12 M. Aresta, A. Dibenedetto, F. Nocito and C. Pastore, *J. Mol. Catal. A: Chem.*, 2006, **257**, 149–153.
- 13 D. Ballivet-Tkatchenko, S. Chambrey, R. Keiski, R. Ligabue, L. Plasseraud, P. Richard and H. Turunen, *Catal. Today*, 2006, **115**, 80–87.
- 14 J.-W. Yoo and Z. Mouloungui, *Stud. Surf. Sci. Catal.*, 2003, **146**, 757–760.
- 15 M. Pagliaro, R. Ciriminna, H. Kimura, M. Rossi and C. Della Pina, *Angew. Chem., Int. Ed.*, 2007, **46**, 4434–4440.
- 16 G. Rokicki, P. Rakoczy, P. Parzuchowski and M. Sobiecki, *Green Chem.*, 2005, **7**, 529–539.
- 17 J. Barrault, F. Jerome and Y. Pouilloux, *Lipid Technol.*, 2005, **17**, 131–135.
- 18 S. Cassel, C. Debaig, T. Benvegnu, P. Chaimbault, M. Lafosse, D. Plusquellec and P. Rollin, *Eur. J. Org. Chem.*, 2001, 875–896.
- 19 C. Márquez-Alvarez, E. Sastre and J. Pérez-Pariente, *Top. Catal.*, 2004, **27**, 105–117.
- 20 J.-M. Clacens, Y. Pouilloux and J. Barrault, *Appl. Catal., A*, 2002, **227**, 181–190.
- 21 J. Barrault, Y. Pouilloux, C. Vanhove, K. Cottin, S. Abro and J.-M. Clacens, in *Catalysis in organic reactions*, ed. F. E. Herkes, Marcel Dekker, New Orleans, LA, USA, 1998, pp. 13–23.
- 22 J. Barrault, J.-M. Clacens and Y. Pouilloux, *Top. Catal.*, 2004, **27**, 137–142.
- 23 *Eur. Pat.*, 1 316 577 A1, 2002.
- 24 V. Plasman, T. Caulier and N. Boulos, *Plastics Additives & Compounding*, March/April 2005, 30–33.
- 25 Z. Y. Ding, A. Y. Hao and Z. N. Wang, *Fuel*, 2007, **86**, 597–602.
- 26 G. Kharchafi, F. Jérôme, J. P. Douliez and J. Barrault, *Green Chem.*, 2006, **8**, 710–716.
- 27 A. Sunder, R. Hanselmann, H. Frey and R. Mülhaupt, *Macromolecules*, 1999, **32**, 4240–4246.
- 28 A. Sunder, M. Krämer, R. Hanselmann, R. Mülhaupt and H. Frey, *Angew. Chem., Int. Ed.*, 1999, **38**, 3552–3555.
- 29 S. Mecking, R. Thomann, H. Frey and A. Sunder, *Macromolecules*, 2000, **33**, 3958–3960.
- 30 H. Türk, A. Shukla, P. C. A. Rodrigues, H. Rehage and R. Haag, *Chem.-Eur. J.*, 2007, **13**, 4187–4196.
- 31 V. M. Garamus, T. V. Maksimova, H. Kautz, E. Barriau, H. Frey, U. Schlotterbeck, S. Mecking and W. Richtering, *Macromolecules*, 2004, **37**, 8394–8399.
- 32 A. Dworak, W. Walach and B. Trzebiecka, *Macromol. Chem. Phys.*, 1995, **196**, 1963–1970.
- 33 <http://www.hyperpolymers.com>, 2007.
- 34 http://www.degussa-bk.de/asp/documents/21_Document.pdf, 2007.
- 35 *Int. Pat.*, 2004/053 012, 2004.
- 36 S. Queste, P. Bauduin, D. Touraud, W. Kunz and J. M. Aubry, *Green Chem.*, 2006, **8**, 822–830.
- 37 J. K. Spooner-Wyman, D. B. Appleby and D. M. Yost, *SAE Spec. Publ.*, 2003, **SP-1791**, 1–14.
- 38 *US Pat.*, 5 308 365, 1993.
- 39 R. Wessendorf, *Erdoel Kohle, Erdgas, Petrochem.*, 1995, **48**, 138–143.
- 40 K. Gottlieb, H. Neitsch and R. Wessendorf, *Chem.-Ing.-Tech.*, 1994, **66**, 64–66.
- 41 *Ger. Pat.*, 4 222 183 A1, 1992.
- 42 A. Behr and L. Obendorf, *Eng. Life Sci.*, 2003, **2**, 185–189.
- 43 A. Behr and L. Obendorf, *Chem.-Ing.-Tech.*, 2001, **73**, 1463–1467.
- 44 *Ger. Pat.*, 19 544 413 A1, 1995.
- 45 *Eur. Pat.*, 0 718 270 A2, 1995.
- 46 *US Pat.*, 5 476 971, 1995.
- 47 *US Pat.*, 5 731 476, 1995.
- 48 *Ger. Pat.*, 4 445 635 A1, 1994.
- 49 *Eur. Pat.*, 0 649 829 A1, 1994.
- 50 *Fr. Pat.*, 2 866 653 A1, 2004.
- 51 R. S. Karinen and A. O. I. Krause, *Appl. Catal., A*, 2006, **306**, 128–133.
- 52 K. Klepáčová, D. Mravec, E. Hájeková and M. Bajus, *Pet. Coal*, 2003, **45**, 54–57.
- 53 K. Klepáčová, D. Mravec and M. Bajus, *Appl. Catal., A*, 2005, **294**, 141–147.
- 54 *Int. Pat.*, 93/02 032, 1993.

- 55 A. Behr and M. Urschey, *Adv. Synth. Catal.*, 2003, **345**, 1242–1246.
- 56 M. Urschey, PhD thesis, Universität Dortmund, Germany, 2004.
- 57 S. Queste, Y. Michina, A. Dewilde, R. Neueder, W. Kunz and J. M. Aubry, *Green Chem.*, 2007, **9**, 491–499.
- 58 A. Behr, M. Urschey and V. A. Brehme, *Green Chem.*, 2003, **5**, 198–204.
- 59 *US Pat.*, 6 504 063 B2, 2003.
- 60 A. Behr and J. Seuster, in *Multiphase homogeneous catalysis*, ed. B. Cornils, Wiley-VCH, Weinheim, 2005, pp. 114–122.
- 61 *Fr. Pat.*, 2 833 607 A1, 2003.
- 62 *Int. Pat.*, 2005/093 015 A1, 2005.
- 63 *US Pat.*, 2004/0 025 417 A1, 2004.
- 64 M. J. Climent, A. Corma and A. Velty, *Appl. Catal., A*, 2004, **263**, 155–161.
- 65 M. J. Climent, A. Velty and A. Corma, *Green Chem.*, 2002, **4**, 565–569.
- 66 A. Piasecki, A. Sokolowski, B. Burczyk and U. Kotlewska, *J. Am. Oil Chem. Soc.*, 1997, **74**, 33–37.
- 67 *Ger. Pat.*, DE 4 040 362 A1, 1992.
- 68 P. Sari, M. Razzak and I. G. Tucker, *Pharm. Dev. Technol.*, 2004, **9**, 97–106.
- 69 *Global Cosmetic Ind.*, 2001, **169**, 16.
- 70 J. Deutsch, A. Martin and H. Lieske, *J. Catal.*, 2007, **245**, 428–435.
- 71 *Int. Pat.*, 2005/010 131 A1, 2005.
- 72 C. Piantadosi, C. E. Anderson, E. A. Brecht and C. L. Yarbro, *J. Am. Chem. Soc.*, 1959, **80**, 6613–6617.
- 73 A. J. Showler and P. A. Darley, *Chem. Rev.*, 1967, **67**, 427–440.
- 74 <http://www.sriconsulting.com>, 2007.
- 75 C. J. Sullivan, in *Ullmann's Encyclopedia of Industrial Chemistry*, Wiley-VCH, Weinheim, 7th edn, 2005.
- 76 M. McCoy, *Chem. Eng. News*, 2006, **84**, 32–33.
- 77 *Ger. Pat.*, 4 302 464 A1, 1994.
- 78 *US Pat.*, 5 214 219, 1993.
- 79 *US Pat.*, 5 276 181, 1994.
- 80 M. A. Dasari, P. P. Kiatsimkul, W. R. Sutterlin and G. J. Suppes, *Appl. Catal., A*, 2005, **281**, 225–231.
- 81 *US Pat.*, 5 616 817, 1997.
- 82 Y. Kusunoki, T. Miyazawa, K. Kunimori and K. Tomishige, *Catal. Commun.*, 2005, **6**, 645–649.
- 83 D. G. Lahr and B. H. Shanks, *J. Catal.*, 2005, **232**, 386–394.
- 84 T. Miyazawa, Y. Kusunoki, K. Kunimori and K. Tomishige, *J. Catal.*, 2006, **240**, 213–221.
- 85 A. Perosa and P. Tundo, *Ind. Eng. Chem. Res.*, 2005, **44**, 8535–8537.
- 86 *Int. Pat.*, 03/035 582 A1, 2003.
- 87 J. Chaminand, L. Djakovitch, P. Gallezot, P. Marion, C. Pinel and C. Rosier, *Green Chem.*, 2004, **6**, 359–361.
- 88 G. Braca, A. M. Raspolli Galletti and G. Sbrana, *J. Organomet. Chem.*, 1991, **417**, 41–49.
- 89 *US Pat.*, 6 080 898, 2000.
- 90 S. P. Crabtree, R. C. Lawrence, M. W. Tuck and D. V. Tyers, *Hydrocarbon Process.*, 2006, **85**, 87–92.
- 91 <http://www.chemietechnik.de/news/2cfbab18ac2.html>, 2007.
- 92 http://www.ashland.com/press_room/news_detail.asp?s=1524, 2007.
- 93 http://www.cargill.com/news/news_releases/070508_ashlandjv.htm, 2007.
- 94 N. E. Altaras and D. C. Cameron, *Appl. Environ. Microbiol.*, 1999, **65**, 1180–1185.
- 95 N. E. Altaras, M. R. Etzel and D. C. Cameron, *Biotechnol. Prog.*, 2001, **17**, 52–56.
- 96 *Int. Pat.*, 97/16 250, 1997.
- 97 *US Pat.*, 2003/0 153 796 A1, 2003.
- 98 *US Pat.*, 3 350 871, 1967.
- 99 *Int. Pat.*, 00/25 914, 2000.
- 100 D. Arntz, T. Haas, A. Müller and N. Wiegand, *Chem.-Ing.-Tech.*, 1991, **63**, 733–735.
- 101 *Ger. Pat.*, 3 926 136 A1, 1991.
- 102 *Ger. Pat.*, 19 703 383 A1, 1998.
- 103 *US Pat.*, 3 814 725, 1974.
- 104 *Ger. Pat.*, 4 238 492 A1, 1994.
- 105 M. Schlaf, *Dalton Trans.*, 2006, 4645–4653.
- 106 *US Pat.*, 4 642 394, 1987.
- 107 K. Y. Wang, M. C. Hawley and S. J. DeAthos, *Ind. Eng. Chem. Res.*, 2003, **42**, 2913–2923.
- 108 S. Vollenweider and C. Lacroix, *Appl. Microbiol. Biotechnol.*, 2004, **64**, 16–27.
- 109 D. C. Cameron, N. E. Altaras, M. L. Hoffman and A. J. Shaw, *Biotechnol. Prog.*, 1998, **14**, 116–125.
- 110 M. Hartlep and A.-P. Zeng, *Chem.-Ing.-Tech.*, 2002, **74**, 663–664.
- 111 C. Ulmer, W.-D. Deckwer and A.-P. Zeng, *Chem.-Ing.-Tech.*, 2002, **74**, 674.
- 112 R. Bock, PhD thesis, Universität Braunschweig, Germany, 2004.
- 113 R. H. Lin, H. J. Liu, J. Hao, K. Cheng and D. H. Liu, *Biotechnol. Lett.*, 2005, **27**, 1755–1759.
- 114 *Int. Pat.*, 01/11 070 A2, 2001.
- 115 P. Wittlich, A. Themann and K.-D. Vorlop, *Biotechnol. Lett.*, 2001, **23**, 463–466.
- 116 *Int. Pat.*, 98/21 341, 1998.
- 117 *Aust. Pat.*, 2003 266 472 A1, 2003.
- 118 *Int. Pat.*, 01/21 825 A2, 2001.
- 119 *US Pat.*, 2007/0 048 849 A1, 2007.
- 120 *US Pat.*, 7 005 291 B1, 2006.
- 121 http://www2.dupont.com/Sorona/en_US/home/bio_pdo_home.html, 2007.
- 122 *Chem. Eng.*, 2007, **114**, 10.
- 123 *Ind. Environ.*, 2007, **18**, 2–5.
- 124 E. Chynoweth, *ICIS Chem. Bus.*, 2006, **1**, 45.
- 125 *Int. Pat.*, 2007/054 505 A2, 2007.
- 126 *Int. Pat.*, 2005/054 167 A1, 2005.
- 127 M. Klumpe, presented in part at the DGF-meeting “Oleochemicals under Changing Global Conditions”, Hamburg, Germany, 2007.
- 128 S. Demirel-Gülen, M. Lucas and P. Claus, *Catal. Today*, 2005, **102–103**, 166–172.
- 129 D. Hekmat, R. Bauer and V. Neff, *Process Biochem.*, 2007, **42**, 71–76.
- 130 *US Pat.*, 2007/009 452 A1, 2007.
- 131 *Int. Pat.*, 2005/108 457 A1, 2005.
- 132 *US Pat.*, 2007/086 977 A1, 2007.
- 133 *US Pat.*, 2007/092 461 A1, 2007.
- 134 *US Pat.*, 2007/0 003 675 A1, 2007.
- 135 *Can. Pat.*, 2 151 319, 1995.
- 136 *US Pat.*, 3 080 288, 1963.
- 137 *Int. Pat.*, 98/16 475, 1998.
- 138 R. Ciriminna, G. Palmisano, C. Della Pina, M. Rossi and M. Pagliaro, *Tetrahedron Lett.*, 2006, **47**, 6993–6995.
- 139 R. Garcia, M. Besson and P. Gallezot, *Appl. Catal., A*, 1995, **127**, 165–176.
- 140 P. Fordham, M. Besson and P. Gallezot, *Appl. Catal., A*, 1995, **133**, L179–L184.
- 141 T. Mallat and A. Baiker, *Catal. Today*, 1994, **19**, 247–284.
- 142 M. Besson and P. Gallezot, *Catal. Today*, 2000, **57**, 127–141.
- 143 H. Kimura, *Appl. Catal., A*, 1993, **105**, 147–158.
- 144 H. Kimura, K. Tsuto, T. Wakisaka, Y. Kazumi and Y. Inaya, *Appl. Catal., A*, 1993, **96**, 217–228.
- 145 S. Carrettin, P. McMorn, P. Johnston, K. Griffin, C. J. Kiely and G. J. Hutchings, *Phys. Chem. Chem. Phys.*, 2003, **5**, 1329–1336.
- 146 H. Kimura, *J. Polym. Sci., Part A: Polym. Chem.*, 1998, **36**, 195–205.
- 147 H. Kimura, *Polym. Adv. Technol.*, 2001, **12**, 697–710.
- 148 F. Porta and L. Prati, *J. Catal.*, 2004, **224**, 397–403.
- 149 L. Prati and M. Rossi, *J. Catal.*, 1998, **176**, 552–560.
- 150 S. Demirel, K. Lehnert, M. Lucas and P. Claus, *Appl. Catal., B*, 2007, **70**, 637–643.
- 151 S. Carrettin, P. McMorn, P. Johnston, K. Griffin and G. J. Hutchings, *Chem. Commun.*, 2002, 696–697.
- 152 S. Carrettin, P. McMorn, P. Johnston, K. Griffin, C. J. Kiely, G. A. Attard and G. J. Hutchings, *Top. Catal.*, 2004, **27**, 131–136.
- 153 C. L. Bianchi, P. Canton, N. Dimitratos, F. Porta and L. Prati, *Catal. Today*, 2005, **102–103**, 203–212.
- 154 N. Dimitratos, C. Messi, F. Porta, L. Prati and A. Villa, *J. Mol. Catal. A: Chem.*, 2006, **256**, 21–28.
- 155 *Int. Pat.*, 2007/033 807 A2, 2007.
- 156 D. Wang, A. Villa, F. Porta, D. S. Su and L. Prati, *Chem. Commun.*, 2006, 1956–1958.

- 157 H. Kimura, *Recent Res. Dev. Polym. Sci.*, 1999, **3**, 327–354.
 158 *Pap. Tech.*, 2006, 11, www.papierundtechnik.de/pt/live/archiv/artikel/detail/30818710.html.
 159 *US Pat.*, 625 330, 1949.
 160 *Int. Pat.*, 2005/047 224 A1, 2005.
 161 S. R. G. Carrazán, C. Martín, R. Mateos and V. Rives, *Catal. Today*, 2006, **112**, 121–125.
 162 *Eur. Pat.*, 0 959 062 A1, 1999.
 163 L. Q. Chen, J. Liang, H. Lin, W. Z. Weng, H. L. Wan and J. C. Védrine, *Appl. Catal., A*, 2005, **293**, 49–55.
 164 *Ger. Pat.*, 4 238 493 C1, 1994.
 165 *Fr. Pat.*, 2 882 053 A1, 2005.
 166 *Int. Pat.*, 2006/087 083 A2, 2006.
 167 *Int. Pat.*, 2006/092 272 A2, 2006.
 168 W. Bühler, E. Dinjus, H. J. Ederer, A. Kruse and C. Mas, *J. Supercrit. Fluids*, 2002, **22**, 37–53.
- 169 M. J. Antal, W. S. L. Mok, J. C. Roy, A. T. Raissi and D. G. M. Anderson, *J. Anal. Appl. Pyrol.*, 1985, **8**, 291–303.
 170 M. Watanabe, T. Iida, Y. Aizawa, T. M. Aida and H. Inomata, *Bioresour. Technol.*, 2007, **98**, 1285–1290.
 171 L. Ott, M. Bicker and H. Vogel, *Chem.-Ing.-Tech.*, 2004, **76**, 1292.
 172 L. Ott, M. Bicker and H. Vogel, *Green Chem.*, 2006, **8**, 214–220.
 173 T. Hirai, N. Ikenaga, T. Miyake and T. Suzuki, *Energy Fuels*, 2005, **19**, 1761–1762.
 174 P. J. Dauenhauer, J. R. Salge and L. D. Schmidt, *J. Catal.*, 2006, **244**, 238–247.
 175 R. R. Soares, D. A. Simonetti and J. A. Dumesic, *Angew. Chem., Int. Ed.*, 2006, **45**, 3982–3985.
 176 R. R. Davda, J. W. Shabaker, G. W. Huber, R. D. Cortright and J. A. Dumesic, *Appl. Catal., B*, 2005, **56**, 171–186.
 177 S. R. A. Kersten, B. Potic, W. Prins and W. P. M. Van Swaaij, *Ind. Eng. Chem. Res.*, 2006, **45**, 4169–4177.



Save valuable time searching for that elusive piece of vital chemical information.

Let us do it for you at the Library and Information Centre of the RSC.

We are your chemical information support, providing:

- Chemical enquiry helpdesk
- Remote access chemical information resources
- Speedy response
- Expert chemical information specialist staff

Tap into the foremost source of chemical knowledge in Europe and send your enquiries to

library@rsc.org

Green chemistry tools to influence a medicinal chemistry and research chemistry based organisation†

Kim Alfonsi,^a Juan Colberg,^b Peter J. Dunn,^{*c} Thomas Fevig,^d Sandra Jennings,^a Timothy A. Johnson,^b H. Peter Kleine,^d Craig Knight,^c Mark A. Nagy,^d David A. Perry^{*b} and Mark Stefaniak^c

Received 1st August 2007, Accepted 30th October 2007

First published as an Advance Article on the web 16th November 2007

DOI: 10.1039/b711717e

Influencing and improving the environmental performance of a large multi-national pharmaceutical company can be achieved with the help of electronic education tools, backed up by site champions and strong site teams. This paper describes the development of two of those education tools.

Introduction

The success of the pharmaceutical industry is, in large part, built on the towering achievements of organic chemistry, a mature science which emerged as a distinct discipline well over 150 years ago. This long history is both a blessing and a curse. Many of our most reliable strategies for assembling target molecules employ reactions which are fifty to one hundred years old and often named in honour of their discoverer. During these early years, the chronic toxicological properties of chemicals were often completely unknown and many unwittingly became indispensable tools of the trade. Infamously, benzene was widely employed as a solvent, a hand-cleaner and even as an aftershave, decades before its carcinogenicity became appreciated.¹ Today chemists are still taught the efficacy of chromium, osmium and lead compounds as oxidants, the virtues of chlorinated solvents and the use of atom-inefficient methodologies, while the curricula in most undergraduate chemistry programs provide little or no training in toxicology,² environmental science³ or sustainable technology.⁴

Early pioneers in green chemistry included Trost (who developed the atom economy principle)⁵ and Sheldon (who developed the E-Factor).⁶ These measures were introduced to encourage the use of more sustainable chemistry and provide some benchmarking data to encourage scientists to aspire to more benign synthesis. Later, green chemistry became formalised by the publication by Warner and Anastas⁷ of a holistic set of principles designed to raise awareness of the safe, environmentally sensitive and sustainable practice of chemistry. While many of these principles were second nature to process development chemists and their manufacturing

colleagues in the wake of the pollution control legislation over the last 30 years, the same cannot be said of their medicinal chemistry colleagues. The modern practice of drug discovery relies heavily on speed of execution, which in turn relies on robust methodologies emphasising reliability rather than environmental impact. While the scale of the reactions conducted at the early stages of a program is usually small, the cumulative footprint generated by tens or hundreds of laboratories in a pharmaceutical company becomes significant. Moreover, the delay that may be incurred by the necessity to reengineer a 'discovery route' to achieve a scaleable process impacts the development timeline, as well as its cost. This paper describes ongoing initiatives in Pfizer to equip its medicinal chemists with a working knowledge of the principles of green chemistry, favouring restraint over constraint, and providing access to tools which guide the selection of greener solvents and reagents. We believe the success of these initiatives will reduce our environmental impact, improve worker safety and reduce the time taken to deliver important new medicines addressing major unmet medical needs.

Development of the solvent selection tool

A number of companies have previously published solvent selection guides,⁸ more recently Fischer *et al.*⁹ published a detailed and comprehensive approach to the environmental selection of solvents, though in our view this assessment is too generous to volatile solvents. Volatile solvents have more potential for environmental release and may also have more flammability issues (*e.g.*, pentane or diethyl ether). In reviewing previous work, we felt that because of the challenges and time pressures associated with the medicinal chemistry job, any tool needed to be extremely simple for the end user scientist. However, this does not mean that the information behind the tool is simple. The work to produce a tool was initiated in our environment, health and safety (EHS) group, and solvents were assessed in a thorough and systematic way in three general areas.

(i) **Worker safety**¹⁰ – including carcinogenicity, mutagenicity, reprotoxicity, skin absorption/sensitisation, and toxicity

(ii) **Process safety** – including flammability, potential for high emissions through high vapour pressure, static charge, potential for peroxide formation and odour issues.

^aPfizer Global Research and Development, Ann Arbor, Michigan, MI-48105, USA

^bPfizer Global Research and Development, Groton, Connecticut, CT-06340, USA

^cPfizer Global Research and Development, Sandwich, Kent, CT139NJ, UK

^dPfizer Global Research and Development, Chesterfield, Missouri, MO63017, USA

† Electronic supplementary information (ESI) available: Grid 3 – oxidation of secondary alcohols to ketones. Grid 4 – amide formation from acids (prone to racemisation) and amines. See DOI: 10.1039/b711717e

Preferred	Usable	Undesirable
Water	Cyclohexane	Pentane
Acetone	Heptane	Hexane(s)
Ethanol	Toluene	Di-isopropyl ether
2-Propanol	Methylcyclohexane	Diethyl ether
1-Propanol	Methyl <i>t</i> -butyl ether	Dichloromethane
Ethyl acetate	Isooctane	Dichloroethane
Isopropyl acetate	Acetonitrile	Chloroform
Methanol	2-MethylTHF	Dimethyl formamide
Methyl ethyl ketone	Tetrahydrofuran	<i>N</i> -Methylpyrrolidinone
1-Butanol	Xylenes	Pyridine
<i>t</i> -Butanol	Dimethyl sulfoxide	Dimethyl acetate
	Acetic acid	Dioxane
	Ethylene glycol	Dimethoxyethane
		Benzene
		Carbon tetrachloride

Fig. 1 Pfizer solvent selection guide for medicinal chemistry.

(iii) **Environmental and regulatory considerations**¹¹ - including ecotoxicity and ground water contamination, potential EHS regulatory restrictions, ozone depletion potential, photo-reactive potential. Of course compliance with regulations and company guidelines provide the baseline of Pfizer's environmental policy.

This detailed assessment was then translated into a simple 1 page guide which is shown in Fig. 1.¹²

A summary of why each solvent is placed in the red category is provided in Table 1.

The list of solvents covered in Fig. 1 is not extensive but covers solvents commonly used in medicinal chemistry.

Table 1 Red category solvents

Red solvent	Flash point	Reason
Pentane	-49 °C	Very low flash point, good alternative available.
Hexane(s)	-23 °C	More toxic than the alternative heptane, classified as a hazardous airborne pollutant (HAP) in the US.
Diisopropyl ether	-12 °C	Very powerful peroxide former, good alternative ethers available.
Diether ether	-40 °C	Very low flash point, good alternative ethers available.
Chloroform	N/A	Carcinogen, classified as a HAP in the US.
Dichloroethane	15 °C	Carcinogen, classified as a HAP in the US.
Dimethyl formamide	57 °C	Toxicity, strongly regulated by EU Solvent Directive, classified as a HAP in the US.
Dimethyl acetamide	70 °C	Toxicity, strongly regulated by EU Solvent Directive.
<i>N</i> -Methyl pyrrolidinone	86 °C	Toxicity, strongly regulated by EU Solvent Directive.
Pyridine	20 °C	Carinogenic/mutagenic/reprotoxic (CMR) category 3 carcinogen, toxicity, very low threshold limit value TLV for worker exposures.
Dioxane	12 °C	CMR category 3 carcinogen, classified as HAP in US.
Dichloromethane	N/A	High volume use, regulated by EU solvent directive, classified as HAP in the US.
Dimethoxyethane	0 °C	CMR category 2 carcinogen, toxicity.
Benzene	-11 °C	Avoid use : CMR category 1 carcinogen, toxic to humans and environment, very low TLV (0.5 ppm), strongly regulated in the EU and the US (HAP).
Carbon tetrachloride	N/A	Avoid use : CMR category 3 carcinogen, toxic, ozone depleter, banned under the Montreal protocol, not available for large-scale use, strongly regulated in the EU and US (HAP).

Table 2 Solvent replacement table

Undesirable solvents	Alternative
Pentane	Heptane
Hexane(s)	Heptane
Di-isopropyl ether or diethyl ether	2-MeTHF or <i>tert</i> -butyl methyl ether
Dioxane or dimethoxyethane	2-MeTHF or <i>tert</i> -butyl methyl ether
Chloroform, dichloroethane or carbon tetrachloride	Dichloromethane
Dimethyl formamide, dimethyl acetamide or <i>N</i> -methylpyrrolidinone	Acetonitrile
Pyridine	Et ₃ N (if pyridine used as base)
Dichloromethane (extractions)	EtOAc, MTBE, toluene, 2-MeTHF
Dichloromethane (chromatography)	EtOAc/heptane
Benzene	Toluene

Solvents, such as benzene and carbon tetrachloride, were included to reinforce the avoidance of their use.

In addition, the scientists in our green chemistry teams produced a simple solvent replacement table for each of the solvents in the red/undesirable category, with the philosophy of adopting a "use this instead" policy rather than a "don't use" policy. This replacement table is shown in Table 2. The replacements are either chemically similar (*e.g.*, heptane as a replacement for the high flammable pentane) or functionally equivalent (*e.g.*, ethyl acetate, methyl *tert*-butyl ether (MTBE) or 2-methyltetrahydrofuran (2-MeTHF) as alternative extraction solvents to dichloromethane).

There are a number of points that need further comment. Many of our scientists are surprised that dichloromethane is the recommended alternative to other chlorinated solvents, such as chloroform. All that Table 2 is indicating is that if a chlorinated solvent needs to be used, dichloromethane is the best choice out of the four.

All of the solvents have good replacements, with the exception of one group, which is the dipolar aprotic solvents dimethyl formamide, dimethyl acetamide and *N*-methylpyrrolidinone. For this group of solvents, acetonitrile is a relatively poor substitute, especially for reactions involving a strong base. Due to the lack of good alternatives, Pfizer, with a group of other pharmaceutical companies, has identified finding replacements for these solvents as a key target in green chemistry research.¹³

The guide and replacement table seem almost ridiculously simple but when used by our enthusiastic site teams they led to amazing results, including a 50% reduction in chlorinated solvent use across the whole of our research division (more than 1600 lab based synthetic organic chemists, and four scale-up facilities) during the time period 2004–2006. Even sites that had an increase in the number of chemists during that period were able to report a 50% reduction in chlorinated solvent use. In addition, we were able to reduce the use of an undesirable ether by 97% over the same two year period and substantially promote the use of heptane compared with hexane (more toxic) and pentane (much more flammable).

The development of a reagent guide

This was much more challenging than the solvent guide because of the wide variety of reagents and by the fact that reagents by their very nature are designed to be reactive (whereas solvents are ideally inert), potentially causing additional safety and environmental issues. To our knowledge, no other company has tried to develop a guide of this nature. We wanted the guide to achieve three purposes.

- To provide a balanced assessment of chemical methodologies, taking into account the many constraints that scientists have to take into account when making decisions in their work. To our mind the ideal reagent would have three ideal characteristics:

- (i) The ability to work in good yield in a wide variety of “drug like molecules” —this is a characteristic highly valued by medicinal chemists.

- (ii) The ability of a reagent to be used for scale-up to prepare multi-kilogram batches—a characteristic valued by our Chemical R and D, Kilo Lab and Pilot Plant chemists and engineers.

- (iii) To be as green as possible. Our green chemistry teams would like to introduce the greenest possible reagent as early as possible in the discovery/development process. The assessment of greenness included worker safety, ecotoxicity and atom economy.

- To provide easy access to the chemical literature or procedures for reagents that score well in the assessment. In the on-line Pfizer version of the guide, reagents that score well are linked directly through electronic links to key literature papers, internal procedures or both.

- To raise awareness of newer emerging green methodologies.

We decided to map the reagents onto a series of grids (or Venn diagrams), with each grid representing a commonly used chemical transformation. Each Venn diagram indicates which of the three ideal characteristics each reagent met. A breakdown of the grids and a discussion of the zones in the grid are shown in Fig. 2.

Zone 1: reagents in this zone have all three desirable characteristics. These are reagents we would like our scientists in medicinal chemistry and chemical research and development to try first.

Zone 2: the reagents in this zone meet the wide applicability and scalability criteria but do not meet our greenness criterion. Reagents in this zone are still fully acceptable for use in late discovery/early development. Note that reagents with gross

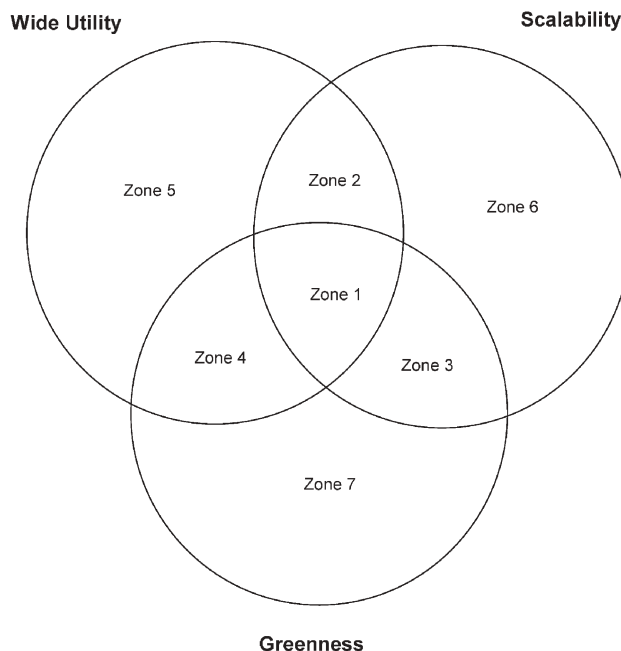


Fig. 2 The zones in the Venn diagram (or grid) that form the basis of the reagent guide.

environmental issues, such as a thallium or tin reagent, would not be in this zone as they would fail the scalability criterion, but reagents with a slightly higher molecular weight and poor atom economy, such as EDCI for amide coupling, would make this zone.

Zone 3: this zone retains the positive attributes of scalability and greenness and reagents in this zone are good for our chemical research and development groups.

Zone 4: this zone has positive attributes for greenness and wide applicability but fails the scalability criterion, an example might be an electrolysis reaction where the company does not have access to large-scale electrolysis equipment.

Reagents in zones 5, 6 and 7 only meet one positive attribute and are less favoured. In the Pfizer electronic version of the guide, only reagents that fall in zones one to four are hypertext linked to in-house procedures or key references.

Two sample grids are shown to illustrate the reagent guide with a further two available in the electronic supplementary information.†

Fig. 3^{14,15} shows the grid for the oxidation of alcohols to aldehydes.

The three most common oxidants used by Pfizer’s medicinal chemists for this transformation are Dess–Martin periodinane¹⁶ or its precursor IBX, tetrapropylammonium perruthenate (TPAP)¹⁷ and the Swern oxidation.¹⁸ All of these methods have significant scale-up issues, for example Dess–Martin periodinane is a high energy molecule¹⁴ that has poor atom economy and is prohibitively expensive for use on a multi-kilogram scale. The use of stoichiometric TPAP again has very poor atom economy and is also prohibitively expensive for large-scale use. A review of large-scale oxidations since 1980 revealed only one large-scale use of TPAP to catalyse an oxidation with a co-oxidant and no examples of stoichiometric use.¹⁵ The Swern oxidation is used at Pilot Plant scale but

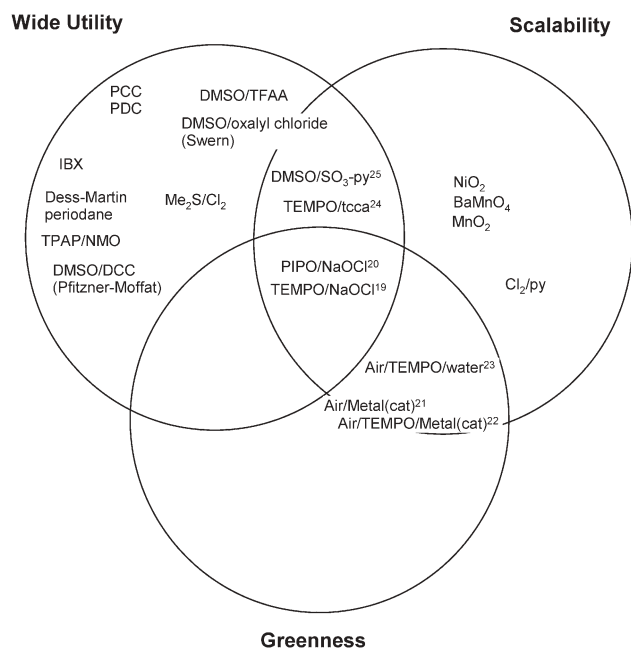


Fig. 3 Oxidation of primary alcohol to aldehyde.

generates toxic by-products and the stench of dimethylsulfide. Hence, the purpose of the reagent guide is to influence the medicinal chemist away from the reliable but environmentally unfriendly methods to more friendly methods, such as the oxidation with bleach (NaOCl) catalysed by nitroxyl radicals, such as TEMPO¹⁹ and PIPO.²⁰ In addition, there has been an explosion in the chemical literature of methods that use molecular oxygen as an oxidant, with more than 150 papers in the last 3 years. These methods carry some challenges on scale-up, as the use of molecular oxygen to aerate flammable solvents is a significant safety concern. These concerns can be reduced by using oxygen diluted with large volumes of nitrogen but still these methods^{21,22} lie on the edge of acceptability when judged against the scalability criteria. An improved safety profile and more acceptable scalability is obtained if the oxidation is performed in water.²³ Again, the purpose of the reagent guide is to provide scientists with easy up-to-date access to developments in this exciting area of green oxidation. Other methods shown in Fig. 3 can be found in the following publications.^{24,25}

A similar Venn diagram covering the oxidation of secondary alcohols to ketones can be found in the electronic supplementary information.†

Fig. 4 shows the grid for amide formation from acids (not prone to racemisation) and amines.

For the oxidation grids we were able to set strict criteria for greenness (reaction by-products should be either water or sodium chloride and there should be no major process safety issues). For amide formation, the majority of literature methods had very poor atom economy. We decided to set the greenness criteria for this transformation as the following.

- Side products should have a molecular weight less than 200.
- No major process safety issues.
- No major environmental issues.

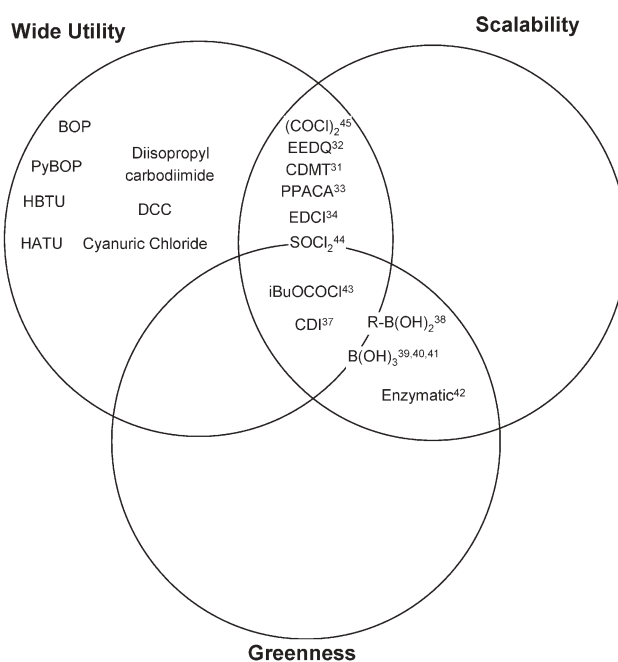


Fig. 4 Amide formation from acids (not prone to racemisation) and amines.

The first of these criteria, based on atom economy, might seem overly generous but in fact 50% of the reagents in Fig. 4 fail this criterion.

Uronium salts, such as HATU²⁶ and HBTU,²⁷ have become widely used in research laboratories but have many green chemistry issues. Their by-products have molecular weights of 398 and 397, respectively, for accomplishing a dehydration reaction (removing a molecule of water with a molecular weight of 18). They are both highly energetic molecules and HATU is shock sensitive.²⁸ The phosphorus based reagent BOP²⁹ and PyBOP³⁰ are again energetic molecules and have even worse atom economy. BOP has the further major disadvantage that its manufacture and use involve HMPA (a class I carcinogen).

Dicyclohexyl carbodiimide (DCC) and di-isopropyl carbodiimide fail our green criteria because of their very strong sensitisation properties and hence in recent years have become rarely used for scale-up in the pharmaceutical industry. Cyanuric chloride is similarly a very strong sensitiser. Oxalyl chloride does not meet our greenness criteria on account of its poisonous by-product carbon monoxide. 1-Chloro-4,6-dimethoxy-1,3,5-triazine (CDMT) is a sensitiser but has been used by some process groups for scale-up.³¹ EEDQ,³² PPACA,³³ and EDCI³⁴ do not meet our greenness criteria on the basis of atom economy but are widely used for scale-up chemistry. Thionyl chloride and chloroformates are the most common reagents for this transformation used by the pharmaceutical industry,³⁵ *N,N'*-carbonyldiimidazole (CDI) is growing in popularity and was used in the commercial synthesis of sildenafil³⁶ and sunitinib.³⁷ We judged that thionyl chloride did not fully meet our greenness criteria because of its worker safety issues but was preferred to oxalyl chloride for acid chloride formation. Although reagents such as CDI and isobutyl chloroformate are described as green, they are not

without issue, for example, the synthesis of CDI uses highly poisonous phosgene, our assessment simply says they are greener than some of the alternatives available at this time.

All of the reagents discussed so far are stoichiometric reagents but the real opportunity is in the development of catalytic reagents where the only by-product would be water. The use of boronic acids,³⁸ and in particular boric acid,³⁹ to catalyse amide formation is very exciting and works well in some substrates.⁴⁰ In reality, boric acid is a poor catalyst for amide formation but it does help drive the reaction of acids and amines that undergo substantial uncatalysed reaction over to completion.⁴¹ For these substrates, boric acid catalysis represents a very green methodology. Enzymatic methods are another catalytic method where the only by-product is water.⁴²

The boric acid and enzymatic methodology are active research areas and the regularly updated Pfizer reagent guide gives Pfizer scientists easy access to the latest green advances in these areas. The grid also gives references to other reagents that meet two out of the three criteria.^{43–45}

A Venn diagram covering amide formation from acids, prone to racemisation, and amines can be found in the electronic supplementary information.†

Conclusions

The experience within Pfizer has demonstrated that the medicinal chemistry population is very receptive to changing work habits in response to our green chemistry outreach initiatives. Particularly encouraging has been the remarkable response to two separate solvent reduction campaigns targeting chlorinated solvents and selected ethers. In addition, the replacement of hexane and pentane in our stockrooms with the less toxic and less volatile heptane has been extraordinarily well received. Key to these successes has been the philosophy of encouragement and education rather than obligation and scrutiny. The advantage of this Pfizer solvent tool over previous work is its simplicity, in many ways the replacements given in Table 2 are obvious. Nevertheless, the results are outstanding and we wonder if a similar approach could also work in academic laboratories and make a huge environmental difference. Chemists are highly creative individuals and when provided with the new guidance they have proved willing to adopt or invent new, greener practices. We are now moving forward with a new suite of on-line tools designed to promote greener synthetic reagents. These tools provide simple access to a diverse range of documentation and literature, which can rapidly provide the working chemist with the information they need to try new procedures. We are optimistic that this guide will share the success of our solvent initiatives and will influence our scientists to adopt safer and greener syntheses.

Acknowledgements

We would like to thank the following chemistry and EHS colleagues who helped us develop the solvent and reagent tools: Jerry Clark, Robert Dugger, David Ellis, Elizabeth Girardi Schoen, Laurence Harris, Catherine Kostlan, James Long, Frank Mastrocco, Thomas Mannsbart, Andrew Mansfield, Julie Newman, Stuart Rozze, Christopher Smith,

Chuck Schwartz, Brian Swierenga, Richard Webster, Christine Visnic and Ji Zhang. We also thank Steve Groombridge and Donna Medley for IT support, especially for the in-house Pfizer version of the reagent guide which provides rapid access to literature and in-house procedures.

References

- 1 P. Harremoës, *The Precautionary Principle in the 20th Century: late lessons from early warnings*, James & James/Earthscan, London, 2002, pp. 35–48.
- 2 J. H. Duffus and H. G. J. Worth, *Fundamental Toxicology for Chemists*, The Royal Society of Chemistry, London 1996, p. vi.
- 3 *Precaution, Environmental Science, and Preventive Public Policy*, ed. J. Tickner, Island Press, Washington DC, 2002, p. 297.
- 4 *Beyond the Molecular Frontier: Challenges for Chemistry and Chemical Engineering*, National Academy Press, Washington DC, 2003, p. 181.
- 5 B. Trost, *Science*, 1991, **254**, 1471–1477.
- 6 R. A. Sheldon, *Chem. and Ind.*, 1992, 903–906.
- 7 *Green Chemistry Theory and Practice*, ed P. T. Anastas and J. C. Warner, Oxford University Press, Oxford, 1998.
- 8 A. D. Curzons, D. C. Constable and V. L. Cunningham, *Clean Prod. Process.*, 1999, **1**, 82–90; C. Jimenez-Gonzalez, A. D. Curzons, D. J. C. Constable and V. L. Cunningham, *Clean Technol. Environ. Pol.*, 2005, **7**, 42–50.
- 9 C. Capello, U. Fischer and K. Hungerbuhler, *Green Chem.*, 2007, **9**, 917–934.
- 10 The highest priority for the solvent evaluations was given to worker safety issues as handling of large quantities of solvents in manufacturing facilities bears the highest potential health and safety risk to our workforce. Within this group of solvents, the Carcinogenicity, Mutagenicity, Reprotoxicity as indicated from the CMR classification are rated as highest concern due to the potential for chronic effects on human health. Sensitisation and toxicity were also given a very high priority in the evaluation. Skin absorption properties increase the likelihood for sensitisation due to the potential carrier effects of these solvents. Toxicity (mainly assessed through literature LD₅₀ figures) has the potential for acute and direct impact on the health and safety of our workforce.
- 11 Environmental and regulatory considerations were considered next. Regulatory considerations vary globally so this work incorporated both major EU and US classifications such as the EU risk phrases and the US hazardous air pollutant and toxic chemical lists. Solvents with ecotoxic properties such as those designated by the EU R50, R51 and R53 risk phrases, are difficult to treat in wastewater facilities or very expensive to dispose of. There is increased public attention to potential environmental impact of facility operations which is supported by publicly available polluter registers in some countries such as the Toxic Release Inventory in the United States. Some solvents with ozone depleting and photoreactive potential are getting more public and government attention as they are regularly discussed at profession forums and regulated under various country permitting or use restriction regulations. Solvents classified as very toxic and/or classified with CMR properties or as potentially environmentally difficult materials (e.g. with the potential for persistence and bioaccumulation) are subject to increasing regulatory attention. This may include, restricted or prohibited use and/or increased requirements increased requirements to control and report use. Certain regulated compounds such as US HAPs and chemicals subject to EU Integrated Pollution Prevention and Control (IPPC) can trigger expensive and technically challenging control requirements. In summary, the use and handling of such substances is monitored very tightly by the Environmental Protection Agencies worldwide.
- 12 The detailed information on these 39 solvents and a further 45 solvents are held in a more detailed Pfizer solvent selection tool, called the bundle book (solvents are classified into bundles). This more detailed tool is available to all Pfizer scientists through various internal websites.
- 13 D. J. C. Constable, P. J. Dunn, J. D. Hayler, G. R. Humphrey, J. Leazer, Jr., R. J. Linderman, K. Lorenz, J. Manley,

- B. A. Pearlman, A. Wells, A. Zaks and T. Y. Zhang, *Green Chem.*, 2007, **9**, 411–420.
- 14 For a review covering the green and sustainable aspects of oxidation reactions see D. Lenoir, *Angew. Chem., Int. Ed.*, 2006, **45**, 3206–3210.
- 15 For a review covering large-scale oxidations in the Pharmaceutical Industry see S. Caron, R. W. Dugger, S. Gut Ruggeri, J. A. Ragan and D. H. B. Ripin, *Chem. Rev.*, 2006, **106**, 2943–2989.
- 16 D. B. Dess and J. C. Martin, *J. Org. Chem.*, 1983, **48**, 4155–4156.
- 17 S. V. Ley, J. Norman, W. P. Griffith and S. P. Marsden, *Synthesis*, 1994, 639–666.
- 18 A. J. Mancuso, S.-L. Huang and D. Swern, *J. Org. Chem.*, 1978, **12**, 2480–2482; A. J. Mancuso and D. Swern, *Synthesis*, 1981, 165–185.
- 19 M. R. Leanna, T. J. Sowin and H. E. Morton, *Tetrahedron Lett.*, 1992, **33**, 5029–5032; A. E. J. de Nooy, A. C. Besemer and H. van Bekkum, *Synthesis*, 1996, 1153–1174.
- 20 A. Dijkman, I. W. C. E. Arends and R. A. Sheldon, *Chem. Commun.*, 2000, 271–272; A. Dijkman, I. W. C. E. Arends and R. A. Sheldon, *Synlett*, 2001, 102–104; R. A. Sheldon, I. W. C. E. Arends, G.-J. ten Brink and A. Dijkman, *Acc. Chem. Res.*, 2002, **35**, 774–781; S. Grimaldi, *Speciality Chem.*, 2006, 32–33.
- 21 For aerobic oxidations catalysed by copper reagents see I. E. Marko, A. Gautier, R. Dumeunier, K. Doda, F. Philippart, S. M. Brown and C. J. Urch, *Angew. Chem., Int. Ed.*, 2004, **43**, 1588 and references therein. For aerobic oxidations by palladium reagents see G.-J. ten Brink, I. W. C. E. Arends and R. A. Sheldon, *Science*, 2000, **287**, 1636–1639 and S. S. Stahl, *Angew. Chem., Int. Ed.*, 2004, **43**, 3400 and references therein. For aerobic oxidations catalysed by ruthenium reagents see B.-Z. Zhan, M. A. White, T.-K. Sham, J. A. Pincock, R. J. Doucet, K. V. Ramano Rao, K. N. Robertson and T. S. Cameron, *J. Am. Chem. Soc.*, 2003, **124**, 2195–2199 and references therein.
- 22 P. Gamez, I. W. C. E. Arends, J. Reedijk and R. A. Sheldon, *Chem. Commun.*, 2003, 2414–2415.
- 23 R. Liu, C. Dong, X. Liang, X. Wang and X. Hu, *J. Org. Chem.*, 2005, **70**, 729–731. Note this reference also gives a very logical breakdown of the recent literature involving air oxidations of alcohols.
- 24 J. De Luca, G. Giacomelli and A. Porcheddu, *Org. Lett.*, 2001, **3**, 3041–3043.
- 25 J. R. Parikh and W. v. E. Doering, *J. Am. Chem. Soc.*, 1967, **89**, 5505–5507.
- 26 F. Albericio, M. Cases, J. Alsina, S. A. Triolo, L. A. Carpino and S. A. Yates, *Tetrahedron Lett.*, 1997, **38**, 4853–4856.
- 27 R. Knorr, A. Trzeciak, W. Bannwarth and D. Gillissen, *Tetrahedron Lett.*, 1989, **30**, 1927–1930; V. Dourtoglou, J.-C. Ziegler and B. Gross, *Tetrahedron Lett.*, 1978, **15**, 1269–1272.
- 28 D. J. Dale, unpublished results.
- 29 B. Castro, J. R. Dormoy, G. Evin and C. Selve, *Tetrahedron Lett.*, 1975, **16**, 1219–1222.
- 30 W. Weng and J. S. McMurray, *Tetrahedron Lett.*, 1999, **40**, 2501–2504.
- 31 C. E. Garrett, X. Jiang, K. Prasad and O. Repic, *Tetrahedron Lett.*, 2002, **43**, 4161–4165; C. J. Barnett, T. M. Wilson and M. E. Kobierski, *Org. Process Res. Dev.*, 1999, **3**, 184–188.
- 32 B. Belleau and G. Malek, *J. Am. Chem. Soc.*, 1968, **90**, 1651–1652; N. Izumiya and M. Muraoka, *J. Am. Chem. Soc.*, 1969, **91**, 2391–2392.
- 33 For an example of the large scale use of PPACA see P. J. Dunn, M. L. Hughes, P. M. Searle and A. S. Wood, *Org. Process Res. Dev.*, 2003, **7**, 244–253.
- 34 For an example of the large scale use of EDCI see ref. 33.
- 35 J. S. Carey, D. Laffan, C. Thomson and M. T. Williams, *Org. Biomol. Chem.*, 2006, **4**, 2337–2347.
- 36 P. J. Dunn, S. Galvin and K. Hettenbach, *Green Chem.*, 2004, **6**, 43–48.
- 37 R. Vaidyanathan, V. G. Kalthod, N. P. Ngo, J. M. Manley and S. P. Lapekas, *J. Org. Chem.*, 2004, **69**, 2565–2568.
- 38 K. Ishihara, S. Ohara and H. Yamamoto, *J. Org. Chem.*, 1996, **61**, 4196–4197.
- 39 J. E. Anderson, R. Davies, R. N. Fitzgerald and J. M. Haberman, *Synth. Commun.*, 2006, **36**, 2129–2133.
- 40 P. Tang, *Org. Synth.*, 2005, **81**, 262.
- 41 K. Arnold, B. Davies, R. L. Giles, C. Grosjean, G. E. Smith and A. Whiting, *Adv. Synth. Catal.*, 2006, **348**, 813–820.
- 42 V. Schellenberger and H.-D. Jakubke, *Angew. Chem., Int. Ed.*, 1991, **30**, 1437–1449.
- 43 For an example of the large scale use of *i*BuOCOCl see M. Prashad, D. Har, B. Hu, H.-Y. Kim, M. J. Girgis, A. Chaudhary, O. Repic, T. J. Blacklock and W. Marterer, *Org. Process Res. Dev.*, 2004, **8**, 330–340.
- 44 For an example of the large scale use of thionyl chloride see S. Cai, M. Dimitroff, T. McKennon, M. Reider, L. Robarge, D. Ryckman, X. Shang and J. Therrien, *Org. Process Res. Dev.*, 2004, **8**, 353–359 and M. Allegretti, R. Anacardio, M. C. Cesta, R. Curti, M. Mantovanini and G. Nano, *Org. Process Res. Dev.*, 2003, **7**, 209–213.
- 45 For an example of the large scale use of oxalyl chloride see I. H. Smith, A. Alorati, G. Frampton, S. Jones, J. O'Rourke and M. W. Woods, *Org. Process Res. Dev.*, 2003, **7**, 1034–1039.

Highly effective silica gel-supported *N*-heterocyclic carbene–Pd catalyst for Suzuki–Miyaura coupling reaction

Huili Qiu, Shaheen M. Sarkar, Dong-Hwan Lee and Myung-Jong Jin*

Received 16th August 2007, Accepted 29th October 2007

First published as an Advance Article on the web 2nd November 2007

DOI: 10.1039/b712624g

The immobilized *N*-heterocyclic carbene–Pd complex was readily prepared by reaction of silica gel-supported imidazolium chloride with Pd(OAc)₂. The Pd complex exhibited excellent catalytic activity in the coupling reaction of aryl halides with arylboronic acid. The heterogeneous Pd catalyst was reusable as well as air-stable to allow easy use.

Introduction

Metal-catalyzed coupling reactions have been recognized as convenient one-step methods for assembling complex structures.¹ Among them, Suzuki–Miyaura coupling reaction of aryl halides with arylboronic acids is one of the most powerful tools for the synthesis of biaryl derivatives.² Palladium catalysts are known to possess high activity for the coupling reaction.³ However, the traditional homogeneous catalysis causes major problems in purification of product and separation of expensive palladium catalyst that leads to toxic wastes. These problems are of environmental and economic concern in large scale-synthesis. Immobilized Pd catalysts have been developed in order to overcome these problems facing green chemistry.^{4,5} The search for an effective and recyclable catalyst is still a major challenge. Recently, *N*-heterocyclic carbene (NHC)–Pd complexes were found to act as efficient catalysts in coupling reactions.^{6,7} Our interest in this area led us to explore the NHC–Pd complex immobilized onto the surface of amorphous silica gel, which can be easily separated from the reaction mixture. Silica gel as an inorganic support has some advantageous properties such as excellent stability, good accessibility, and the fact that organic groups can be robustly anchored to the surface.⁸ Herein, we wish to describe the synthesis of reusable silica-supported NHC–Pd complex **3** and its catalytic activity in the Suzuki–Miyaura coupling reaction.

Experimental

Immobilization of ionic liquid **1** onto the surface of silica gel

To a solution of triethoxysilylpropylimidazolium chloride ionic liquid **1** (0.70 g, 2.2 mmol) in toluene was added commercially available silica gel (2.0 g, Merck® 9385, particle size 230–400 mesh, surface area 550 m² g⁻¹). The mixture was stirred at 105 °C for 12 h. After cooling, the reaction mixture was filtered and washed

with CH₂Cl₂ (10 mL × 3), and dried at 60 °C under vacuum to yield silica-supported ionic liquid **2** (2.39 g). Elemental analysis and weight gain showed that 0.89 mmol of ionic liquid **1** was anchored on 1.0 g of **2**.

Preparation of silica-supported NHC–Pd complex **3**

To a solution of silica-supported ionic liquid **2** (1.0 g, 0.89 mmol g⁻¹) in DMSO (4.5 mL) was added Pd(OAc)₂ (101 mg, 0.45 mmol). The mixture was stirred for 4 h at 60 °C. The reaction was then allowed to proceed for an additional 30 min at 100 °C. Silica-supported NHC–Pd complex **3** was collected on a glass frit and washed with CH₂Cl₂ (10 mL × 3) to remove unreacted Pd(OAc)₂, and dried at 50 °C under vacuum. ICP analysis (atomic %): Pd 3.65.

The ICP analysis showed that 0.34 mmol of Pd was anchored on 1.0 g of **3**. The IR spectrum of **3** showed an absorption band at 1575 cm⁻¹ which is attributed to the C=C stretching vibration of the imidazolium group.

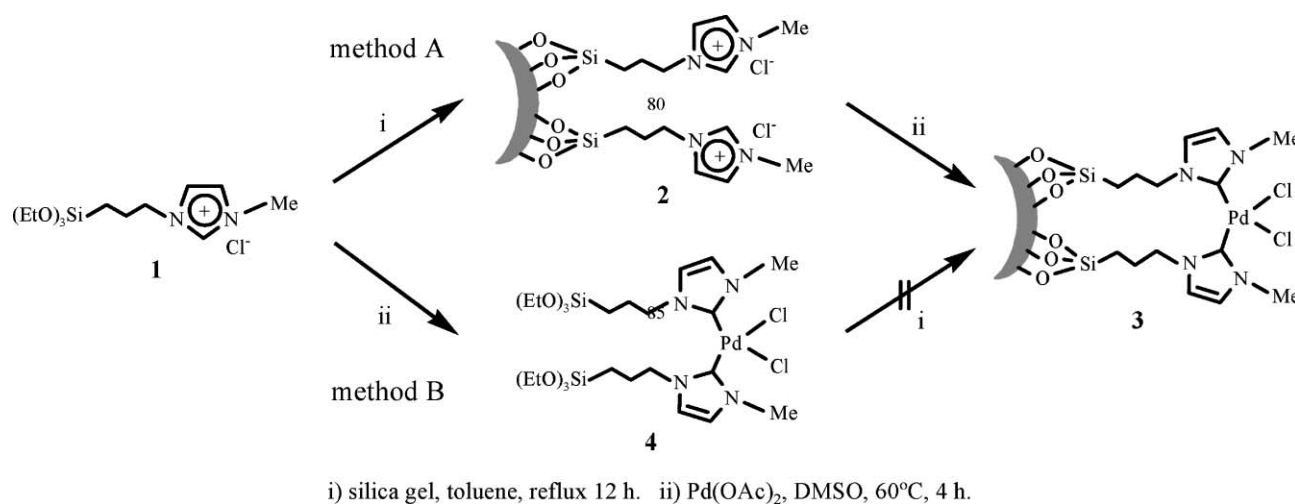
General procedure for heterogeneous Suzuki reaction

Aryl halide (1.0 mmol), phenylboronic acid (134 mg, 1.1 mmol), Na₂CO₃ (212 mg, 2.0 mmol), dodecane (40 mg, internal standard) and catalyst **3** (3 mg, 0.34 mmol g⁻¹, 0.1 mol%) were mixed in DMF–H₂O (3.6 mL, 1 : 1, v/v). The mixture was stirred at 65 °C in an air atmosphere. The samples were withdrawn periodically and analysed by GC/GC-MS. The reaction mixture was filtered and washed with H₂O and Et₂O. The organic phase was separated and dried over MgSO₄, and the solvent was evaporated under reduced pressure. The product was isolated by column chromatography on silica gel. GC/GC-MS analyses were performed on an Agilent 6890N GC (He carrier gas, HP-5MS column, 30 m × 0.25 m × 0.25 μm) coupled to an Agilent 5975 Network Mass Selective Detector (electron impact ionization at 70 eV). The initial temperature of the column was set at 80 °C for 5 min, and ramped at 10 °C min⁻¹ to a final temperature of 240 °C. The carrier gas was set at a constant velocity of 40 cm s⁻¹.

The reuse of silica-supported Pd catalyst **3**

In the recycling experiment, the reaction was performed by using a mixture of iodobenzene or 1-bromo-4-nitrobenzene (4.0 mmol), phenylboronic acid (4.4 mmol), Na₂CO₃ (8.0 mmol), and catalyst **3** (0.2 mol%) at 65 °C. After completion of the reaction, the reaction mixture was worked up as described above. The filtered catalyst was successively reused in the same reaction.

School of Chemical Science and Engineering, Inha University, Incheon 402-751, South Korea. E-mail: mjjin@inha.ac.kr; Fax: +82 32-872-0959; Tel: +82 32-860-7469



Scheme 1

Results and discussion

As shown in Scheme 1, the immobilization of the NHC–Pd complex onto the surface of amorphous silica gel was attempted through two methods: (A) immobilization of triethoxysilylated ionic liquid **1**⁹ onto silica gel, followed by reaction with Pd(OAc)₂ and (B) preparation of triethoxysilylated NHC–Pd complex **4**, followed by the immobilization onto the silica gel. Method A was chosen as a better strategy for the immobilization of the NHC–Pd complex because it is difficult to immobilize complex **4** which has very low solubility in most organic solvents. A similar procedure was previously used in the conversion of **2** to **3**.¹⁰

With the heterogeneous catalyst **3** in hand, we first tested Suzuki coupling of iodobenzene with phenylboronic acid in DMF–H₂O (1 : 1, v/v) as a model reaction. The reaction was initially performed in the presence of 1 mol% of **3** and Na₂CO₃ as a base. High conversion was obtained at 50–65 °C within 0.5 h (entries 1 and 2). It is noteworthy that the catalyst **3** shows outstanding performance even at a low temperature of 40 °C (entry 3). When the loading of **3** was decreased from 1 mol% to 0.01 mol%, reactivity was slightly influenced (entries 4–7). Surprisingly, high conversion could be still maintained at 0.01 mol% of very low catalyst loading, in which high TOF of 9100 h^{−1} was obtained for the coupling (entry 7). The results are summarized in Table 1. Further optimization of the reaction conditions was not attempted to obtain higher TOF. Solvent effect on the activity of **3** was surveyed with different polar solvents. When the reaction was conducted in aqueous DMSO, DMA, ethanol and methanol instead of aqueous DMF, similar results were obtained under the same conditions (entries 8–18). It is interesting that the reactions in aqueous ethanol and methanol gave excellent results. Aqueous solvent appears to be necessary for mild conditions because of low solubility of Na₂CO₃ in organic solvents. The complex is very stable to oxygen and moisture. Less change of its activity was observed when the Pd complex was exposed to air and water in the Suzuki reaction.

We next examined the catalytic activity of **3** for reaction of aryl halides with arylboronic acid. As shown in Table 2, high catalytic activity was observed in the coupling of deactivated aryl iodides such as 2-iodoanisole, 4-iodo-anisole, 2-iodotoluene and

4-iodophenol (entries 1–4) as well as activated 1-iodo-4-nitrobenzene and 1-iodo-3-nitrobenzene (entries 5 and 6). Deactivated aryl iodides possessing an electron-donating group showed a slight drop in reactivity compared to those possessing an electron-withdrawing group. However, only a little longer reaction time was required to reach almost quantitative conversion. In order to investigate the scope on aryl halides in the coupling with phenylboronic acid, different aryl bromides were employed in the reaction (entries 7–13). Electron-rich, electron-neutral, and electron-poor aryl bromides were readily coupled in the presence of catalyst **3**. The catalytic system was further extended to the coupling reactions with arylboronic acids containing electron-donating and electron-withdrawing substituents (entries 14–19). Most of the reactions could be also conducted with high yields.

Table 1 Suzuki coupling of iodobenzene with phenylboronic acid^a

Entry	Solvent (1 : 1)	3 (mol%)	Temp./°C	Time/h	Yield ^b (%)
1	DMF–H ₂ O	1	65	0.3	100
2	DMF–H ₂ O	1	50	0.5	93
3	DMF–H ₂ O	1	40	1.0	90
4	DMF–H ₂ O	0.5	65	0.4	100
5	DMF–H ₂ O	0.1	65	0.5	100 (96)
6	DMF–H ₂ O	0.05	75	0.5	95 (90)
7	DMF–H ₂ O	0.01	85	1.0	91
8	DMA–H ₂ O	1	65	0.3	100
9	DMA–H ₂ O	0.5	65	0.3	100
10	DMA–H ₂ O	0.1	65	0.4	100
11	DMA–H ₂ O	0.05	75	0.5	96
12	DMSO–H ₂ O	1	65	0.3	100
13	DMSO–H ₂ O	0.5	65	0.4	99
14	DMSO–H ₂ O	0.1	65	0.5	99
15	EtOH–H ₂ O	1	65	0.4	98
16	EtOH–H ₂ O	0.5	65	0.5	96
17	MeOH–H ₂ O	1	65	0.4	98
18	MeOH–H ₂ O	0.5	65	0.5	97

^a Molar ratio: iodobenzene (1.0 equiv.), phenylboronic acid (1.1 equiv.), Pd complex **3** (1–0.01 mol%, Pd loading ratio = 0.34 mmol g^{−1}), and Na₂CO₃ (2.0 equiv.). ^b GC yield determined using *n*-dodecane as an internal standard and based on the amount of iodobenzene employed. Isolated yield is given in parenthesis.

Table 2 Suzuki coupling of various aryl halides with arylboronic acid^a

		Substrate	ArB(OH) ₂	Time/h	Yield ^b (%)
1			0.6	92	
2			0.5	95 (91)	
3			0.8	90	
4			0.4	100	
5			0.3	100	
6			0.3	100	
7			0.5	95 (90)	
8			0.8	91	
9			0.7	92	
10			0.6	95	
11			1.0	96	
12			0.4	100	
13			0.4	100	
14			1.0	95	
15			0.7	92	
16			3	83	
17			3	91	

Table 2 Suzuki coupling of various aryl halides with arylboronic acid^a (Continued)

		Substrate	ArB(OH) ₂	Time/h	Yield ^b (%)
18			0.7	100	
19			0.8	99	
20			3	46	
21			12	99 (92)	
22			12	66/23 ^c	
23			20	50/29 ^c	

^a Molar ratio: aryl halide (1.0 equiv.), arylboronic acid (1.1 equiv.), Pd complex **3** (0.1 mol%), Pd loading ratio = 0.34 mmol g⁻¹, and Na₂CO₃ (2.0 equiv.). ^b GC yield determined using *n*-dodecane as an internal standard and based on the amount of iodobenzene employed. Isolated yield is given in parenthesis. ^c The GC yield of biphenyl. Entries 21–23: reactions were performed in the presence of 1 mol% of catalyst **3** at 85 °C.

However, catalyst **3** showed low activity in the reaction of deactivated 2-bromoanisole with electron-rich 2-methoxyphenylboronic acid (entry 20). A trace amount of biphenyl was detected as a by-product in the reactions of aryl iodides and aryl bromides.

Encouraged by these results, we tested the coupling of several aryl chlorides in the presence of 1 mol% of **3** at 85 °C. The reaction of chlorobenzene with phenylboronic acid proceeded smoothly to afford biphenyl product with high yield (entry 21). However, low yields were observed in the coupling of substituted aryl chlorides (entries 22 and 23). In addition, biphenyl by-product from homo-coupling of phenylboronic acid was remarkably formed with the increase of temperature and the prolongation of reaction time.

The recycling of the catalyst is an important issue in the heterogeneous reaction. We turn our attention to reusability of our Pd catalyst. As shown in Table 3, the catalyst **3** was recycled in the

Table 3 Reusability of Pd complex **3** in Suzuki coupling^a

Aryl halide	Cycle	Yield ^b (%)	Cycle	Yield ^b (%)
	1	100	4	100
	2	100	5	98
	3	100	6	96
	1	100	4	100
	2	100	5	99
	3	100	6	98

^a Molar ratio: aryl halide (1.0 equiv.), phenylboronic acid (1.1 equiv.), **3** (0.2 mol%), and Na₂CO₃ (2.0 equiv.). ^b GC yield determined using *n*-dodecane as an internal standard and based on the amount of aryl halide employed.

reactions of iodobenzene and 1-bromo-4-nitrobenzene with phenylboronic acid. We have observed that the catalyst could be reused six times without significant loss of activity. Furthermore, analysis of the solution by atomic absorption indicated that no Pd species leached into the reaction solution. This excellent reusability and high stability of the catalyst would be explained by strong binding of the NHC to palladium and site isolation, that is, the absence of interactions between catalytic sites, which are followed by aggregation of the Pd complex and formation of less active Pd catalyst.

Conclusions

In conclusion, we have easily prepared a silica-supported NHC–Pd complex **3** from triethoxysilylated ionic liquid **1**. The heterogeneous complex showed high catalytic activity for Suzuki coupling reaction in an aqueous medium. Furthermore, this catalyst could be simply recovered and reused without a significant loss of catalytic activity. Further studies of other coupling reactions catalyzed by this system are currently in progress.

Notes and references

- For reviews of metal-catalyzed cross-couplings, see: (a) F. Diederich and P. J. Stang, *Metal-Catalyzed Cross-Coupling Reactions*, Wiley-VCH, New York, 1998; (b) M. Beller and C. Bolm, *Transition Metals for Organic Synthesis*, Wiley-VCH, Weinheim, 2nd edn, 2004.
- For reviews, see: (a) N. Miyaura and A. Suzuki, *Chem. Rev.*, 1995, **95**, 2457–2483; (b) A. F. Littke and G. C. Fu, *Angew. Chem., Int. Ed.*, 2002, **41**, 4176–4211; (c) S. Kotha, K. Lahiri and D. Kashinath, *Tetrahedron*, 2002, **58**, 9633–9695; (d) L. A. Agrofoglio, I. Gillaizeau and Y. Saito, *Chem. Rev.*, 2003, **103**, 1875–1916.
- (a) J. P. Wolfe, R. A. Singer, B. H. Yang and S. L. Buchwald, *J. Am. Chem. Soc.*, 1999, **121**, 9550–9561; (b) A. D. Littke, C. Dai and G. C. Fu, *J. Am. Chem. Soc.*, 2000, **122**, 4020–4028; (c) M. R. Netherton, C. Dai, K. Neuschütz and G. C. Fu, *J. Am. Chem. Soc.*, 2001, **123**, 10099–10100; (d) J. Yin, M. P. Rainka, X.-X. Zhang and S. L. Buchwald, *J. Am. Chem. Soc.*, 2002, **24**, 1162–1163; (e) R. B. Bedford, C. S. J. Cazin and S. L. Hazelwood, *Angew. Chem., Int. Ed.*, 2002, **41**, 4120–4122; (f) F. Churrua, R. SanMartin, B. Inés, I. Tellitu and E. Dominguez, *Adv. Synth. Catal.*, 2006, **348**, 1836–1840.
- For reviews, see: (a) N. E. Leadbeater and M. Marco, *Chem. Rev.*, 2002, **102**, 3217–3274; (b) L. Yin and J. Liebscher, *Chem. Rev.*, 2007, **107**, 133–173.
- (a) L. Djakovitch and K. Koehler, *J. Am. Chem. Soc.*, 2001, **123**, 5990–5999; (b) Y. M. A. Yoichi, K. Takeda, H. Takahashi and S. Ikegami, *Org. Lett.*, 2002, **20**, 3371–3374; (c) S. Paul and J. H. Clark, *Green Chem.*, 2003, **5**, 635–638; (d) A. Corma, H. Garcia, A. Leiva and A. Primo, *Appl. Catal., A*, 2003, **247**, 41–49; (e) A. Corma, H. Garcia, A. Leiva and A. Primo, *Appl. Catal., A*, 2004, **257**, 77–83; (f) J. J. E. Hardy, S. Hubert, D. J. Macquarrie and A. J. Wilson, *Green Chem.*, 2004, **6**, 53–56.
- For review, see: W. A. Herrmann, *Angew. Chem., Int. Ed.*, 2002, **41**, 1290–1390.
- (a) W. A. Herrmann, C.-P. Reisinger and M. Spiegler, *J. Organomet. Chem.*, 1998, **557**, 93–96; (b) W. A. Herrmann, V. P. W. Bohm, C. W. K. Gstottmayr, M. Grosche, C. P. Reisinger and T. J. Wskamp, *J. Organomet. Chem.*, 2001, **617**, 616–628; (c) O. Navarro, R. A. III. Kelly and S. P. Nolan, *J. Am. Chem. Soc.*, 2003, **125**, 16194–16195; (d) O. Navarro, H. Kaur, P. Mahjoor and S. P. Nolan, *J. Org. Chem.*, 2003, **69**, 3173–3180; (e) G. Altenhoff, R. Goddard, C. W. Lehmann and F. Glorius, *J. Am. Chem. Soc.*, 2004, **126**, 15195–15201; (f) F. B. Barrett, J. L. Chaytor and M. E. A. Heska, *Org. Lett.*, 2004, **6**, 3641–3644; (g) A. E. Wang, J. H. Xie, L. X. Wang and Q. L. Zhou, *Tetrahedron*, 2005, **61**, 259–266.
- (a) M. K. Richmond, S. L. Scott and H. Alper, *J. Am. Chem. Soc.*, 2001, **123**, 10521–10525; (b) C. Baleizao, A. Corma, H. Garcia and A. Leyva, *Chem. Commun.*, 2003, 606–607; (c) P.-H. Li and L. Wang, *Adv. Synth. Catal.*, 2006, **348**, 681–685.
- (a) C. P. Mehnert, R. A. Cook, N. C. Dispenziere and M. Afeworki, *J. Am. Chem. Soc.*, 2002, **124**, 12932–12933; (b) S. Brenna, T. Posset, J. Furrer and J. Blumel, *Chem.–Eur. J.*, 2006, **12**, 2880–2888; (c) B. Gadenne, P. Hesemann and J. J. E. Moreau, *Chem. Commun.*, 2004, 1768–1769.
- J. Schwarz, V. P. W. Bohm, M. G. Gardiner, M. Grosche, W. A. Herrmann, W. Hieringer and G. R. Sieber, *Chem.–Eur. J.*, 2000, **6**, 1773–1780.

Making diazomethane accessible for R&D and industry: generation and direct conversion in a continuous micro-reactor set-up†

Michael Struempel,^a Bernd Ondruschka,^a Ralf Daute^b and Annegret Stark^{*a}

Received 10th July 2007, Accepted 30th October 2007

First published as an Advance Article on the web 9th November 2007

DOI: 10.1039/b710554a

Micro-reaction technology offers a safe way to deliver diazomethane on demand both on the R&D and the industrially relevant scale, including *in situ* conversion to the desired product to avoid handling and storage of explosive diazomethane solutions, thus making this potent compound accessible for the pharmaceutical and fine chemical sector.

Diazomethane, which is generally liberated from the more stable^{1,2} and commercially available precursor *N*-methyl-*N*-nitroso-*p*-toluenesulfonamide (Diazald[®]) by treatment with a strong base, is an extremely reactive substance. Although it features interesting and versatile chemistries under mild conditions,^{3–10} and can perform as methylating agent, 1,3-dipolar compound or carbene source (Scheme 1), its industrial relevance, for example in the derivatisation of labile biogenic substances and complex pharmaceutical compounds,^{5,11} is nil. In the laboratory, its use is mostly avoided, as the hazardous properties of diazomethane, such as explosiveness, toxicity, and carcinogenicity,^{12–14} make special techniques and safety precautions necessary during its preparation and handling, such as explosion protection and fire-polished glassware.¹

In order to spur diazomethane chemistry for both laboratory and industrial applications, especially for fine chemicals,

^aFriedrich-Schiller University of Jena, Institute for Technical Chemistry and Environmental Chemistry, Lessingstr. 12, 07743 Jena, Germany. E-mail: annegret.stark@uni-jena.de; Fax: +49 3641 948402; Tel: +49 3641 948413

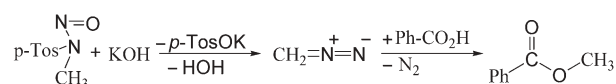
^bCHEMTEC LEUNA, Gesellschaft für Chemie und Technologie mbH, Am Haupttor, 06237 Leuna, Germany

† Electronic supplementary information (ESI) available: experimental and analytical details, and graphs detailing both the dependence of yield on reaction temperature and the stability of the set-up during continuous operation. See DOI: 10.1039/b710554a.

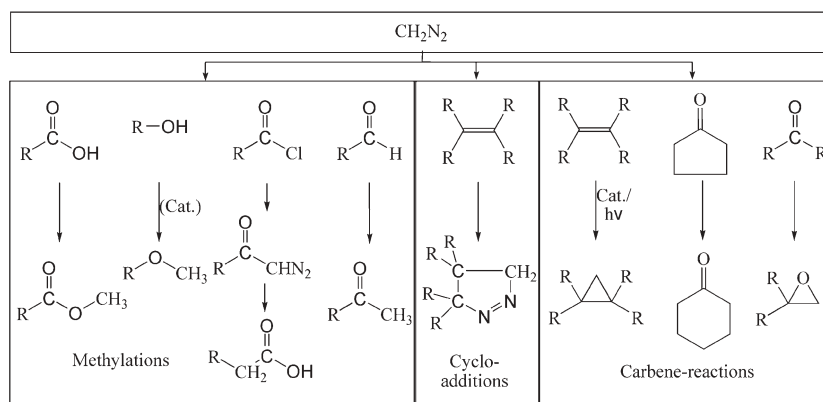
specialities and pharmaceutical products, the use of micro-reaction technology^{15–18} was envisaged as a consummate tool to overcome any safety issues: micro-reactor technology features extremely small internal volumes, resulting in uncritically low spatiotemporal concentrations of diazomethane. The concise arrangement of the reactor and peripheral equipment allows for the installation of additional safety equipment, such as a surrounding acid bath, and temperature and pressure sensors. Thus, the customarily hazardous batch distillation for the generation of diazomethane from the precursor Diazald[®], and successive conversion with a reactant to the desired product, was replaced by a safe two-stage continuous micro-reaction process in which the diazomethane is produced on demand only.¹⁹

In addition to the advantages relating to process safety, another benefit arises in the context of effective process development: due to the optimisation of the continuous production at an early R&D stage, the scale-up to relevant (and flexible) product quantities is achieved by simple numbering-up to multiple manufacturing lines running in parallel.

As a model reaction to demonstrate the practicability of this concept, the generation of diazomethane from Diazald[®], and its rapid, direct conversion with benzoic acid⁵ to benzoic acid methyl ester (Scheme 2), was chosen. For a micro-reaction process, it is of crucial importance to ensure particle-free conditions to avoid clogging due to precipitation from feeds with high saline load.



Scheme 2 Generation of diazomethane from the precursor Diazald[®] with KOH, and its reaction with benzoic acid to benzoic acid methyl ester.



Scheme 1 Overview of the reaction types of diazomethane.

Table 1 Solvent study: selected experimental conditions and results of batch experiments

Entry	Diazald [®]	KOH	Benzoic acid	No. liquid phases	Precipitate	Yield (%) ^a
1	Diethyl ether	Water : carbitol (2 : 1) ^b	Diethyl ether	2	No	21
2	Diethyl ether : carbitol (1 : 1)	Water	Diethyl ether	2	No	30
3	Diethyl ether	Water : carbitol (2 : 1)	Carbitol	1	No	20
4	Carbitol	Water : carbitol (2 : 1)	Diethyl ether	2	No	23
5	Diethyldiglycol	2-Propanol	2-Propanol : water (1 : 1)	1	No	75
6	Carbitol	2-Propanol	Diethyl ether	1	Yes ^c	72
7	Tetrahydrofuran	2-Propanol	Tetrahydrofuran	1	Yes ^{c,d}	58
8	Toluene	2-Propanol	Toluene	1	Yes ^{c,d}	42
9	Carbitol	2-Propanol	Carbitol	1	No	58

^a Yield of benzoic acid methyl ester. ^b Carbitol = di(ethylene glycol) ethyl ether. ^c After addition of benzoic acid. ^d Before addition of benzoic acid.

Therefore, before studying the influence of residence times, flow rate and temperature, a thorough solvent study was carried out. Finally, a long-term test of the optimised system was carried out to demonstrate the stability of the process for industrial applications.

Table 1 shows selected results of the preliminary solvent study, which was carried out in batch experiments, see Electronic Supplementary Information (ESI)[†], to determine potential solvents from which precipitation of salts does not occur, while giving maximum yields of benzoic acid methyl ester. The relative concentrations of the reactants in the respective solvent was chosen based on the reagent with the lowest solubility, which was used as a concentrated solution. The other feed solutions were prepared in relation to allow for the quantitative conversion of Diazald[®] to diazomethane, while also providing sufficient benzoic acid for both the neutralisation of any unconverted KOH and the complete conversion of diazomethane to benzoic acid methyl ester. This ratio was found to be Diazald[®] : KOH : benzoic acid = 1.0 : 1.5 : 4.0.

Depending on the choice of solvent, a mono- or biphasic liquid–liquid system was obtained. In most instances (except entry 9), the precipitation of solids (either during the liberation of diazomethane, or during its reaction with benzoic acid) was prevented only if at least one feed solvent contained water. The major effect with respect to yield was observed for the solvent selection of the base KOH: if it contained water, yields below 30% were obtained (entries 1–4), whereas for non-aqueous base feeds, *e.g.*, with 2-propanol, yields were increased up to 75% (entries 5–9). On the other hand, the solvents of the organic feeds (Diazald[®], benzoic acid) did not crucially influence the product yield. However, they determine the solubility of starting material and products, and their choice is therefore important for both minimising the formation of particles and achieving economically high concentrations of reactants. Thus, diethyldiglycol and carbitol show optimal solubility and minimal formation of particles in combination with high yields (entries 5 and 9), which are comparable to those described previously in the batch synthesis.¹

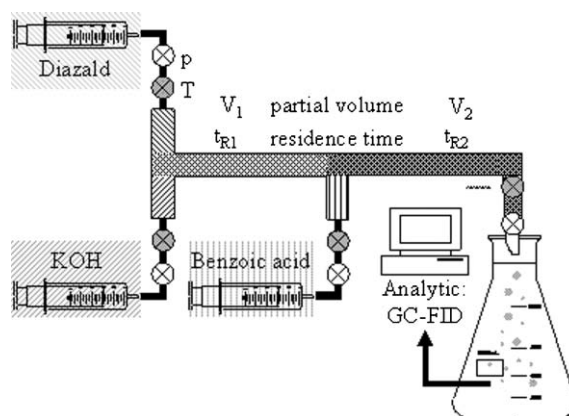
In a first attempt to transpose the reaction into continuous mode, the solvent combination of entry 5 was adopted, as it promises the highest yields. Surprisingly, unlike in batch mode, precipitation did occur in the micro-reactor as a result of locally exceeding the maximum solubility. Therefore, the second favourite alternative, *i.e.*, carbitol–2-propanol (entry 9) was investigated in the micro-reaction set-up (Scheme 3), giving a yield of 60%, which corresponds well with the result in batch mode[†]. Additionally, it was found that similar to the batch experiments, the process results in low yields when the base is dissolved in water or an aqueous

solvent mixture, so that only 5% of benzoic acid methyl ester was obtained when the organic (Diazald[®], benzoic acid) and KOH feeds were provided in dichloromethane and water, respectively.

In order to further optimise the process conditions, the influence of the parameters residence time, flow rate and reaction temperature were investigated. Using the optimised solvent system, *i.e.*, 2-propanol for the base and carbitol for the organic feeds, the effect of the first residence time for the generation of diazomethane from the precursor by treatment with the base (t_{R1}) was investigated, and compared with a capillary reactor without mixing elements. Different residence times were achieved by adjustment of the feed flows. The results show a clear dependency of the yield of benzoic acid methyl ester (relative to Diazald[®]) on t_{R1} for the use of a capillary as reaction device (Fig. 1). The maximum yield can only be reached at residence times >50 s, whereas the micro-reactor does not show any dependence of the maximum yield with $t_{R1} > 5$ s. These results indicate that the mixing efficiency in the micro-reactor is greater than in the capillary, probably due to the mixing elements of the former.

In contrast to t_{R1} , variation of the second residence time (10 s < $t_{R2} < 70$ s) for the reaction of the generated diazomethane with benzoic acid did not exhibit any effect on the yield, and no differences between micro-reactor and capillary became apparent. Likewise, neither the micro-reactor nor the capillary set-up showed an effect on the total flow rate[‡] as long as the residence time t_{R1} was sufficient (micro-reactor > 5 s, capillary > 50 s; Fig. 2).

With the inherent safety of the micro-reactor set-up, it was for the first time possible to investigate the dependence of the



Scheme 3 Flow scheme of the experimental set-up for the continuous experiments.

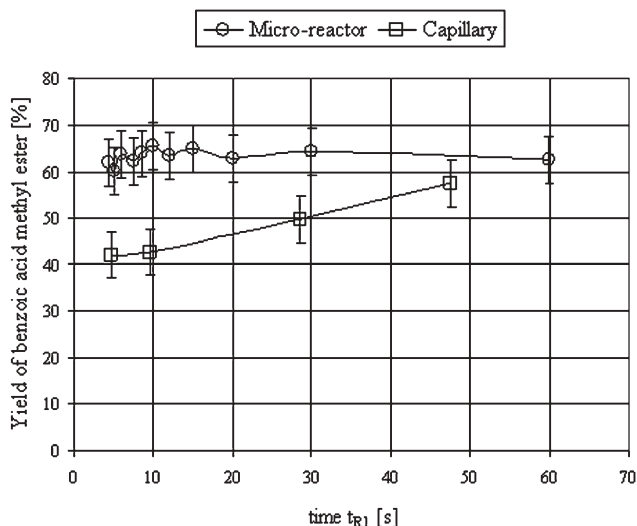


Fig. 1 Dependence of the yield of benzoic acid methyl ester (relative to Diazald[®]) on the residence time t_{R1} ; formation of diazomethane, in the micro-reactor and capillary. For experimental conditions, see ESI†.

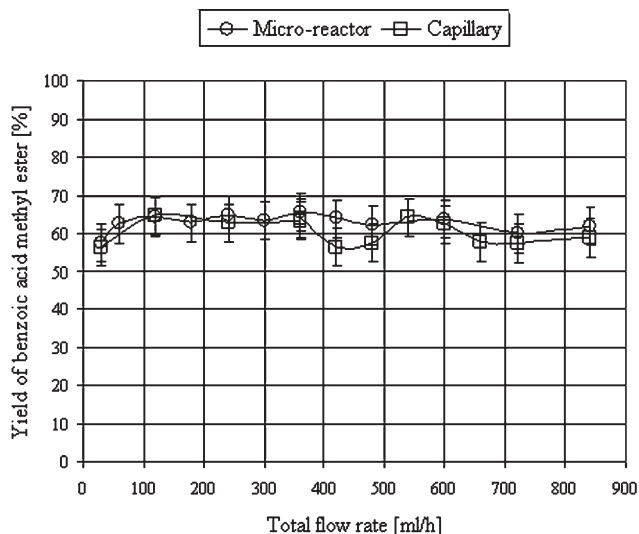


Fig. 2 Dependence of the yield of benzoic acid methyl ester on the total flow rate in the micro-reactor in comparison to the capillary. For experimental conditions, see ESI†.

temperature on diazomethane formation. Under optimised conditions†, a constant yield of >65% of benzoic acid methyl ester is achieved between temperatures of 0 and 50 °C. At temperatures of about 50–85 °C, the yield appears to decrease slightly. This may be due to a starting decomposition.^{6,12,14} Although the yields of this particular reaction cannot be optimised by adjustment of the temperature, the set-up demonstrates an inherent process safety, even at high temperatures up to 85 °C. Therefore, its application is extendable to both reactions of diazomethane with other, less reactive, substrates (Scheme 1) and to other highly hazardous reactants with potential synthetic relevance.

The final aim to show that the method and technique are suitable for industrial application was achieved by a continuous stability test, which indicated a stable micro-reaction process under

optimised conditions: a constant yield of 75% of benzoic acid methyl ester is generated over a period of at least 1 hour, and longer production periods appear feasible without the risk of clogging†. Therefore, it should be possible to produce and directly convert about 2.5 mol d⁻¹ of diazomethane with a single micro-reactor, at a total flow rate of 840 ml h⁻¹. These calculations show that through its continuity and the inherent safety, the process fulfils the requirements for industrial applications. Micro-reaction technology also allows for fast and easy scaling up to flexibly adapt product quantities to market demands (the numbering-up principle).

In conclusion, this study has shown the potential of micro-reactor technology to make previously hazardous chemistries available for the pharmaceutical, fine chemical and speciality sectors, while providing yields which compare well with the classic batch synthesis. As shown for the example of diazomethane, its high reactivity and tolerance to functional groups can be used under mild conditions. Nevertheless, where required, the set-up presented herein may also be used at elevated temperatures. As opposed to when scaling up batch equipments, the micro-reactor can simply be numbered up to produce the required quantities, and is thus highly flexible to the demands of the market.

Chemtec Leuna provided financial support for this project. M.S. would like to acknowledge a fellowship from Deutsche Bundesstiftung Umwelt (DBU), and Dr. Ferstl (Fraunhofer Institut Chemische Technologie Pfinztal) for helpful information given in private correspondence (2006).

Notes and references

† The total flow rate is defined as the sum of the three inlet flow rates. The relative ratio of feeds, and the reactant ratios, were kept constant.

- Th. J. de Boer and H. J. Backer, *Org. Synth.*, 1963, **Coll. Vol. 4**, 250.
- F. Arndt, *Org. Synth.*, 1943, **Coll. Vol. 2**, 165.
- H. v. Pechmann, *Chem. Ber.*, 1894, **27**, 1888.
- H. B. Hopps, *Aldrichim. Acta*, 1970, **3**, 9.
- T. H. Black, *Aldrichim. Acta*, 1983, **16**, 3.
- J. A. Moore and D. E. Reed, *Org. Synth.*, 1961, **41**, 16.
- H. Meerwein and G. Hintz, *Liebigs Ann. Chem.*, 1930, **484**, 1.
- F. Schlotterbeck, *Chem. Ber.*, 1907, **40**, 479.
- H. E. Simmons and R. D. Smith, *J. Am. Chem. Soc.*, 1958, **80**, 5323.
- W. E. Bachmann and W. S. Struve, *Org. Reactions*, 1942, **1**, 50.
- T. Archibald, Diazomethane, www.thomasarchibald.com/adobe/diazomethane.pdf, 28.03.2007.
- Occupational Safety and Health Administration, www.osha.gov/SLTC/healthguidelines/diazomethane/recognition.html, 17.02.00; www.gifte.de/chemikalien/diazomethan.htm, 17.08.05; International Occupational Safety and Health Information Centre, ICSC 1256, www.ilo.org/public/english/protection/safework/cis/products/icsc/dtasht/_icsc1256.htm, 03.95.
- C. D. Gutsche, *Org. Reactions*, 1954, **8**, 391.
- E. B. LeWinn, *Am. J. Med. Sci.*, 1949, **218**, 556.
- E. Klemm, M. Rudek, G. Markowz and R. Schütte, 'Mikroverfahrenstechnik', in *Chemische Technik—Prozesse und Produkte*, eds. Winnacker, Küchler, Wiley-VCH, Weinheim, 2004.
- K. Jähnisch, V. Hessel, H. Löwe and M. Baerns, *Angew. Chem., Int. Ed.*, 2004, **43**, 406.
- W. Ehrfeld, V. Hessel and H. Löwe, *Microreactors—New Technology for Modern Chemistry*, Wiley-VCH, Weinheim, 2005.
- Micro Process Engineering—Fundamentals, Devices, Fabrication, and Applications*, ed. N. Kockmann, Wiley-VCH, Weinheim, 2006.
- W. F. Ferstl, M. S. Schwarzer and S. L. Lötbecke, *Chem.-Ing.-Tech.*, 2004, **76**, 1326.

Cellulose dissolution with polar ionic liquids under mild conditions: required factors for anions†

Yukinobu Fukaya,^a Kensaku Hayashi,^a Masahisa Wada^b and Hiroyuki Ohno^{*a}

Received 29th August 2007, Accepted 24th October 2007

First published as an Advance Article on the web 12th November 2007

DOI: 10.1039/b713289a

A series of alkylimidazolium salts containing dimethyl phosphate, methyl methylphosphonate, or methyl phosphonate prepared by a facile, one-pot procedure were obtained as room temperature ionic liquids, which have the potential to solubilize cellulose under mild conditions. Especially, *N*-ethyl-*N'*-methylimidazolium methylphosphonate enables the preparation of 10 wt% cellulose solution by keeping it at 45 °C for 30 min with stirring and rendered soluble 2–4 wt% cellulose without pretreatments and heating.

Cellulose is the major carbohydrate produced by plant photosynthesis, and is therefore the most abundant organic polymer produced on Earth. Cellulose can be used as a 'green' polymer for fabricating new and attractive materials, by chemical modification or mixing with other components.¹ Cellulose consists of linear chains of 1,4-linked β -D-glucose units, so that its biodegradation has a great impact on the recovery of natural resources, as well as the production of electrochemical energy by bio-fuel cells. It should be noted here that the total energy needed to produce useful energy from biomass is very important. Accordingly, its treatment with low energy should be important. Cellulose is hardly soluble in conventional solvents because of its many intermolecular hydrogen bonds. Solvent systems² currently used for cellulose suffer drawbacks such as volatility or generation of poisonous gas. Furthermore, to fully dissolve cellulose, multi-step pretreatments are needed, followed by prolonged stirring.

The low melting point organic salts known as ionic liquids (ILs) are attracting increasing attention as a new class of solvents.³ Because of the diversity of their component organic ions, it is possible to tune their physico-chemical properties, including polarity, viscosity and melting point. This promising diversity suggests that appropriate ILs would be non-volatile polar solvents for cellulose. ILs such as *N,N'*-dialkylimidazolium chloride salts ([RR'im][Cl]) dissolve cellulose⁴ and other biomacromolecules.⁵ However, most [RR'im][Cl] salts are solid or a sticky paste at room temperature,⁶ and it is necessary to handle them at high temperatures. For more efficient energy production from biomass, heating should be avoided to reduce the energy cost.

^aDepartment of Biotechnology, Tokyo University of Agriculture & Technology, 2-24-16 Naka-cho, Koganei, Tokyo, 184-8588, Japan. E-mail: ohnoh@cc.tuat.ac.jp; Fax: +81-42-388-7024; Tel: +81-42-388-7024

^bDepartment of Biomaterials Science, Graduate School of Agricultural and Life Sciences, The University of Tokyo, Yayoi 1-1-1, Bunkyo-ku, Tokyo, 113-8657, Japan

† Electronic supplementary information (ESI) available: experimental details as well as ¹H and ¹³C-NMR charts of ILs. See DOI: 10.1039/b713289a

Recently, we have reported the *N,N'*-dialkylimidazolium formates ([RR'im][HCOO]) as new solvents for cellulose.⁷ These [RR'im][HCOO] ILs were obtained as low viscosity liquids at room temperature, but they showed relatively poor thermal stability because of decarboxylation. Moreover, [RR'im][HCOO] IL is prepared by a two step reaction, in which the halide counter anion of the imidazolium cation is first converted to hydroxide, then coupled with the desired HCOO anion. To overcome the above drawbacks, we need a new class of easily-preparable ILs with sufficient ability to dissolve cellulose. Previous studies of the solubilization of cellulose indicate the choice and design of anions are important for preparation of polar ILs to solubilize cellulose. Accordingly, in this study, we prepared a series of ILs with a fixed cation, *N*-ethyl-*N'*-methylimidazolium ([C2mim]) with a variety of anions by one-pot procedure. Here, we focused on the effect of the anion structure of ILs on the solubilization of cellulose under mild conditions.

Since many kinds of acid esters are commercially available, we prepared a series of IL candidates by the one step quarternization of tertiary amines with acid esters. While there are several alkylimidazolium salts having alkylsulfate,⁸ alkylsulfonate,⁹ and alkylphosphate¹⁰ anion derivatives prepared by one step quarternization, there has been no evaluation of these ionic liquids as solvents for cellulose. As model experiments, we thus prepared [C2mim] salts with methanesulfonate ([MeSO₃]), methylsulfate ([MeOSO₃]), ethylsulfate ([EtOSO₃]), and dimethylphosphate ([C2mim][(MeO)₂PO₂]). Microcrystalline cellulose (MCC; DP = 200–250) was added to them to a final concentration of 2.0 wt%. Only [C2mim][(MeO)₂PO₂] dissolved MCC at 45 °C. In the ¹H and ¹³C NMR spectra of neat [C2mim][(MeO)₂PO₂]/MCC solution, all chemical shifts and the integrated peak ratios were in good agreement with those of the neat IL, implying that no decomposition of the IL occurred during the dissolution process. Moreover, cellobiose, a model compound of cellulose, exhibited identical ¹H and ¹³C NMR spectra even after regenerating from IL solution, suggesting that [C2mim][(MeO)₂PO₂] solubilized cellobiose without derivatization (see Electronic Supplementary Information†). We then analyzed other [C2mim][RR'PO₂] salts (Chart 1) in an attempt to improve the solubilizing ability.

Both **1**¹¹ and **2** were readily prepared by the reaction of *N*-ethylimidazole with the corresponding acid esters. These ILs were all found to be room temperature ILs (RTILs). Differential

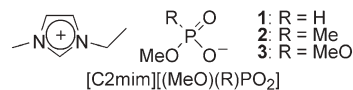


Chart 1 Chemical structure of ionic liquids examined.

Table 1 Physico-chemical properties of **1**, **2** and **3**

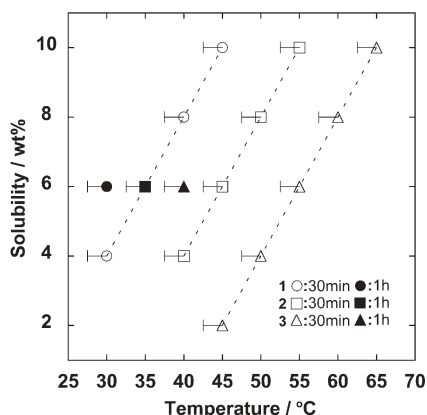
ILs	T_g^a	T_m^a	T_{dec}^b	η/cP^c	Kamlet–Taft parameters ^c		
					α	β	π^*
1	−86	^d	275	107	0.52	1.00	1.06
2	−66	^d	262	510	0.50	1.07	1.04
3	−74	21	289	265	0.51	1.00	1.06

^a Temperature (°C) at signal peak. ^b Temperature (°C) at 10% weight loss. ^c Measured at 25 °C. ^d Not detected.

scanning calorimetry (DSC) found that the melting temperature (T_m) of [C2mim][(MeO)₂PO₂] (*i.e.*, **3**) was 21 °C, whereas the others had only the low glass transition temperature (T_g) of −66 °C (**2**) and −86 °C (**1**) (Table 1). Melting and freezing behaviour could not be detected, even when these ILs were slowly cooled or heated at 1 °C min^{−1} in the DSC measurements; this suggests that they were in stable molten or supercooled states. The asymmetric structure of the anions for **1** and **2** might give rise to poor packing of ions. The thermal stability of [C2mim][(MeO)(R)PO₂] was generally better than that for previously reported polar ILs. In particular, the temperature at 10% weight loss (T_{dec}) of [RR'im][HCOO] was approximately 210 °C, whereas that of [C2mim][(MeO)(R)PO₂] was above 260 °C. This might be due to the thermal stability of phosphorus containing ILs.¹²

Table 1 also shows the Kamlet–Taft parameters¹³ (α : hydrogen bond acidity, β : hydrogen bond basicity, and π^* : dipolarity) for [C2mim][(MeO)(R)PO₂]. The ILs prepared here displayed high β values (above 1.0): in particular, the β value of **2** was 1.07, whereas the β value of [RR'im][Cl] ILs and [RR'im][HCOO] ILs was around 0.84 to 0.99, respectively.⁷ The ILs were revealed to have moderate or low viscosity in spite of their greater hydrogen bonding ability. *N*-Allyl-*N'*-methylimidazolium chloride, which is sufficiently polar to solubilize MCC, has lower viscosity than any previously discovered chloride salt known to date. The viscosity at 25 °C of [C2mim][(MeO)(R)PO₂] is in the range 100–500 cP, which is lower than that for polar chloride salts. This low viscosity can be attributable to small ion size, low T_g value, and the flat shape of the cation.

We first determined the solubility of MCC in these ILs using stirring for 30 min. As shown in Fig. 1, each IL successfully solubilized MCC under mild conditions. The temperature needed to solubilize the same concentration of MCC depends strongly on

**Fig. 1** Solubility of cellulose in **1**, **2** and **3**.

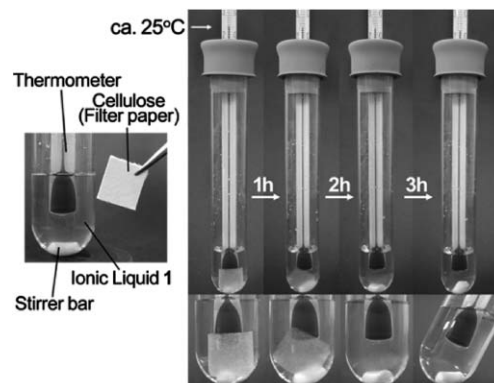
the anion structure of the ILs. For example, **2** required heating to 55 °C to solubilize 10 wt% of MCC, whereas the corresponding temperature for **3** was 65 °C. Recent NMR studies on the dissolution mechanism of cellulose in [C4mim][Cl] indicates that the anion of ILs acts as a hydrogen bond acceptor which interacts with the hydroxyl group of cellulose.¹⁴ Since **2** has stronger hydrogen bond basicity (β value = 1.07) than **3** (β value = 1.00), the greater ability to dissolve MCC of **2** compared with **3** is easily comprehended. Unexpectedly, we found that **1** dissolved MCC better at lower temperatures than any other of the ILs prepared in this study. The polarity parameters of **1** are similar to those of **3**. Also, since **1** had lower viscosity than **3**, MCC was more easily dispersed in **1** than in **3**. Hence, MCC can be solubilized in **1** more readily than in **2** or **3**. To minimize the effect of viscosity on the solubilization, we examined the solubilization of MCC with stirring for 60 min. As is shown in Fig. 1, the sample of [C2mim][(MeO)(R)PO₂] required heating at 35–55 °C with stirring for 30 min to solubilize 6 wt% MCC, whereas only 30–40 °C was enough to solubilize the same amount of MCC when they were mixed for 60 min. The temperature of the mixed solution was maintained and there was no additional heat effect generated by mechanical stirring.

These findings were promising enough for us to examine the solubilization of MCC without heating. We found that 2 wt% MCC dissolved completely in these ILs at room temperature (25 °C) within 3 hr, and 4 wt% within 5 hr. Fig. 2 shows the solubilization of filter paper (1.0 wt%) into IL **1** without heating. From this figure, it is clear that the paper was dissolved in it within 3 hr. Again, no rise in temperature of the solution was found during mixing.

While ILs prepared here are potential candidates for low energy solubilization of cellulose, further investigations on the degradation of cellulose during the solubilization and toxicology of the precursors and the resulting ILs should be addressed. These topics are now being investigated and will be reported elsewhere.

In conclusion, a [C2mim][(MeO)(R)PO₂] series was prepared by an easy one-pot procedure. These were polar RTILs with relatively low viscosity and good thermal stability. These polar ILs successfully solubilized cellulose at high concentrations and can dissolve cellulose at room temperature.‡

This study was supported by a Grant-in-Aid for Scientific Research from the Ministry of Education, Culture, Sports, Science and Technology, Japan (No. 17205020 and 17073005), and the

**Fig. 2** Solubilization of cellulose (filter paper: 1 wt%) in IL **1** at room temperature.

21st Century COE program of "Future Nano-Materials" in Tokyo University of Agriculture & Technology.

Notes and references

† (1) **Synthesis and characterization of ionic liquids.** As the general preparation procedure of [C2mim][(MeO)(R)PO₂], synthesis of IL 1 is mentioned as follows. To a THF solution of *N*-ethylimidazole, dimethyl phosphite in THF was added dropwise under argon gas atmosphere at room temperature. The reaction mixture was stirred with reflux at 90 °C for 2 days. After removal of THF under reduced pressure, the resulting liquid was washed with an excess amount of diethyl ether repeatedly. The residual liquid was dissolved in dichloromethane, and the resulting solution was passed through a column filled with neutral activated alumina. After removal of dichloromethane, residual liquid was dried *in vacuo* at 80 °C for 24 h to give 1 as a colourless liquid in 95% yield. ¹H-NMR (400 MHz; CDCl₃; Me₄Si) δ = 1.58 (3H, t, *J* = 7.3 Hz, NCH₃), 3.55 (3H, d, *J* = 11.9 Hz, POCH₃), 4.06 (3H, s, NCH₃), 4.36 (2H, q, *J* = 7.3 Hz, NCH₂CH₃), 6.92 (1H, d, *J* = 588.5 Hz, PH), 7.58 (2H, d, *J* = 11.3 Hz, NCHCHN), 10.66 (1H, s, NCHN). ¹³C-NMR (100 MHz; CDCl₃; Me₄Si) δ = 15.22 (NCH₂CH₃), 35.87 (NCH₃), 44.57 (NCH₂CH₃), 50.05 (POCH₃), 121.35, 123.17 (NCHCHN), 138.40 (NCHN). ESI-TOF-MS: calcd for C₇H₁₅N₂O₃P [M]⁺: *m/z* = 111.17; found: 111.37. Elemental analysis: calcd for C₇H₁₅N₂O₃P: C, 40.78; H, 7.33; N, 13.59; found: C, 40.72; H, 7.47; N, 13.72. Ion chromatography: cation 99.98 (area%), anion 99.65 (area%). IL 2 (in 96% yield): ¹H-NMR (400 MHz; CDCl₃; Me₄Si) δ = 1.28 (3H, d, *J* = 16.0 Hz, PCH₃), 1.57 (3H, t, *J* = 7.3 Hz, NCH₂CH₃), 3.58 (3H, d, *J* = 10.1 Hz, POCH₃), 4.08 (3H, s, NCH₃), 4.38 (2H, q, *J* = 7.3 Hz, NCH₂CH₃), 7.47 (2H, d, *J* = 14.2 Hz, NCHCHN), 10.92 (1H, s, NCHN). ¹³C-NMR (100 MHz; CDCl₃; Me₄Si) δ = 11.24, 12.56 (PCH₃), 15.31 (NCH₂CH₃), 35.92 (NCH₃), 44.60 (NCH₂CH₃), 50.05 (POCH₃), 121.00, 121.96 (NCHCHN), 139.28 (NCHN). ESI-TOF-MS: calcd for C₈H₁₇N₂O₃P [M]⁺: *m/z* = 111.17; found: 111.37, [M]⁻: *m/z* = 109.04; found: 108.91. Elemental analysis: calcd for C₈H₁₇N₂O₃P: C, 43.63; H, 7.78; N, 12.72. Found: C, 43.56; H, 7.91; N, 12.95. Ion chromatography: cation 99.99 (area%), anion 99.98 (area%). IL 3 (in 94% yield): ¹H-NMR (400 MHz; CDCl₃; Me₄Si) δ = 1.57 (3H, t, *J* = 12.0 Hz, NCH₂CH₃), 3.59 (6H, d, *J* = 8 Hz, POCH₃), 4.06 (3H, s, NCH₃), 4.36 (2H, q, *J* = 24 Hz, NCH₂CH₃), 7.52 (2H, d, *J* = 24 Hz, NCHCHN), 10.57 (1H, s, NCHN). ¹³C-NMR (100 MHz; CDCl₃; Me₄Si) δ = 15.28 (NCH₂CH₃), 35.93 (NCH₃), 44.61 (NCH₂CH₃), 52.10 (POCH₃), 121.40, 123.36 (NCHCHN), 138.20 (NCHN). ESI-TOF-MS: calcd for C₈H₁₇N₂O₄P [M]⁺: *m/z* = 111.17; found: 111.37, [M]⁻: *m/z* = 124.89; found: 125.04. Elemental analysis: calcd for C₈H₁₇N₂O₄P: C, 40.68; H, 7.25; N, 11.86. Found: C, 40.65; H, 7.86; N, 11.69. Ion chromatography: cation 99.97 (area%), anion 100 (area%). The amount of water for all ILs prepared in this study was confirmed at less than 1000 ppm.

(2) **Measurement of the Kamlet-Taft parameters of ionic liquids.** Measurement of the Kamlet-Taft parameters of a series of ionic liquids was carried out as follows. The solvatochromic dyes, (2,6-dichloro-4-(2,4,6-triphenyl-1-pyridinio)phenolate (Reichardt's dye 33) (from Fluka), 4-nitroaniline (from Tokyo Chemical Industries Co., Ltd), and *N,N*-diethyl-4-nitroaniline (from Kanto Chem.), were used as received. To 0.2 ml of ionic liquid, the dye was added as a concentrated dry methanol solution. The methanol was then carefully removed by vacuum drying at 40 °C for 6 h. To avoid dye aggregation, the dye concentration in a series of ionic liquids was such that it had an absorbance between 0.15 and 0.30. These ionic liquid solutions were placed into quartz cells with 1 mm light-path length. Temperature of the quartz sample cell was maintained at 25 °C by water circulation. From the wavelength at the maximum absorption (λ_{\max}) determined, the α , β and π^* values were calculated by use of the following equations:

$$v_{(\text{dye})} = 1/(\lambda_{\max(\text{dye})} \times 10^{-4})$$

$$E_T(30) = 0.9986 (28\,592/\lambda_{\max}(\text{Reichardt's dye 33})) - 8.6878$$

$$\pi^* = 0.314(27.52 - v_{(N,N\text{-diethyl-4-nitroaniline})})$$

$$\alpha = 0.0649 E_T(30) - 2.03 - 0.72\pi^*$$

$$\beta = (1.035v_{(N,N\text{-diethyl-4-nitroaniline})} + 2.64 - v_{(4\text{-nitroaniline})})/2.80$$

(3) **Dissolution of cellulose.** Suspensions of microcrystalline cellulose (Aldrich; DP = *ca.* 250) (2.0, 4.0, 6.0, 8.0, and 10.0 wt%) in dried ionic liquids were prepared under dry nitrogen gas atmosphere. The mixtures were heated from 25 °C to 100 °C in 5 °C increments under nitrogen gas in a temperature controlled oil bath, and were stirred for 30 (or 60) min at each temperature. The lowest temperature to give a clear solution was recorded as the dissolution temperature.

- 1 *Cellulose Derivatives Modification, Characterization, and Nanostructures*, ACS Symposium Series 688, eds. T. H. Heinze and W. G. Glasser, American Chemical Society, Washington, DC, 1997.
- 2 (a) C. L. McCormick, P. A. Callais and B. H. Hutchinson, Jr., *Macromolecules*, 1985, **18**, 2394–2401; (b) H. Chanzy, A. Peguy, S. Chaunis and P. Monzie, *J. Polym. Sci., Polym. Phys. Ed*, 1980, **18**, 1137–1144; (c) J. Cai and L. Zhang, *Macromol. Biosci.*, 2005, **5**, 539–548; (d) M. Yanagisawa, I. Shibata and A. Isogai, *Cellulose*, 2004, **11**, 169–176.
- 3 *Ionic Liquids in Synthesis*, eds. P. Wasserscheid and T. Welton, Wiley-VCH, Weinheim, Germany, 2003.
- 4 (a) R. P. Swatloski, S. K. Spear, J. D. Holbrey and R. D. Rogers, *J. Am. Chem. Soc.*, 2002, **124**, 4974–4975; (b) H. Zhang, W. J. Zhang and J. He, *Macromolecules*, 2005, **38**, 8272–8277; (c) M. B. Turner, S. K. Spear, J. D. Holbrey and R. D. Rogers, *Biomacromolecules*, 2004, **5**, 1379–1384.
- 5 (a) D. M. Phillips, L. F. Drummy, D. G. Conrady, D. M. Fox, R. R. Naik, M. O. Stone, P. C. Trulove, H. C. De Long and R. A. Mantz, *J. Am. Chem. Soc.*, 2004, **126**, 14350–14351; (b) H. Xie, S. Li and S. Zhang, *Green Chem.*, 2005, **7**, 606–608; (c) K. Fujita, Y. Fukaya, N. Nishimura and H. Ohno, in *Electrochemical Aspects of Ionic Liquids*, ed. H. Ohno, Wiley-Interscience, New York, 2005, pp 157–167; (d) S. A. Forsyth, D. R. MacFarlane, R. J. Thomson and M. V. Itzstein, *Chem. Commun.*, 2002, 714–715; D. W. Armstrong, L. He and Y.-S. Liu, *Anal. Chem.*, 1999, **71**, 3873–3876.
- 6 T. Mizumo, E. Marwanta, N. Matsumi and H. Ohno, *Chem. Lett.*, 2004, **33**, 1360–1361.
- 7 Y. Fukaya, A. Sugimoto and H. Ohno, *Biomacromolecules*, 2006, **7**, 3295–3298.
- 8 A. J. Carmichael, M. Deetlefs, M. J. Earle, U. Frohlich and K. Seddon, in *Ionic Liquids as Green Solvents, Progress and Prospects*, ACS Symposium Series 856, eds. R. D. Rogers and K. R. Seddon, American Chemical Society, Washington, 2003, pp 14–31.
- 9 S. Himmler, S. Hörmann, R. V. Hal, P. S. Schulz and P. Wasserscheid, *Green Chem.*, 2006, **10**, 887–894.
- 10 E. Kuhlmann, S. Himmler, H. Giebelhaus and P. Wasserscheid, *Green Chem.*, 2007, **3**, 233–242.
- 11 C. Anding, S. Trinh and J.-M. Gaulliard, *French Patent*, vol. 80, p. 15323.
- 12 R. E. Del Sesto, C. Corley, A. Robertson and J. S. Wilkes, *J. Organomet. Chem.*, 2005, **690**, 2536–2542.
- 13 (a) L. Crowhurst, P. R. Mawdsley, J. M. Perez-Arlandis, P. A. Salter and T. Welton, *Phys. Chem. Chem. Phys.*, 2003, **5**, 2790–2794; (b) S. N. Baker, G. A. Baker and F. V. Bright, *Green Chem.*, 2002, **4**, 165–169.
- 14 (a) R. C. Remsing, R. P. Swatloski, R. D. Rogers and G. Moyna, *Chem. Commun.*, 2006, 1271–1273; (b) J. S. Moulthrop, R. P. Swatloski, G. Moyna and R. D. Rogers, *Chem. Commun.*, 2005, 1557–1559.

Qualitative and quantitative structure activity relationships for the inhibitory effects of cationic head groups, functionalised side chains and anions of ionic liquids on acetylcholinesterase

Jürgen Arning,^{*a} Stefan Stolte,^a Andrea Bösch,^a Frauke Stock,^b William-Robert Pitner,^c Urs Welz-Biermann,^c Bernd Jastorff^a and Johannes Ranke^a

Received 7th August 2007, Accepted 28th September 2007

First published as an Advance Article on the web 19th October 2007

DOI: 10.1039/b712109a

To contribute to a deeper insight into the hazard potential of ionic liquids to humans and the environment, an acetylcholinesterase (AChE) inhibition screening assay was used to identify toxicophore substructures and interaction potentials mediating enzyme inhibition.

The positively charged nitrogen atom, a widely delocalised aromatic system, and the lipophilicity of the side chains connected to the cationic head groups can be identified as the key structural elements in binding to the enzymes active site. With respect to this, the dimethylaminopyridinium, the quinolinium and the pyridinium head groups exhibit a very strong inhibitory potential to the enzyme with IC₅₀ values around 10 μM. In contrast, the polar and non-aromatic morpholinium head group is found to be only weakly inhibiting to the enzyme activity, with IC₅₀ values > 500 μM.

The introduction of polar hydroxy, ether or nitrile functions into the alkyl side chain is shown to be a potent structural alteration to shift the corresponding ionic liquids to a lower inhibitory potential. Supporting this fact, for a series of imidazolium cations, a QSAR correlation was set up by the linear regression of the log IC₅₀ versus the logarithm of the HPLC-derived lipophilicity parameter *k*₀.

Additionally, a broad set of anion species (inorganic, organic and complex borate anions), commonly used as ionic liquid counterions, was tested and the vast majority exhibited no effect on AChE. Only the fluoride and fluoride containing anion species which readily undergo hydrolytic cleavage can be identified to act as AChE inhibitors.

Introduction

Especially since the imminent intensification of the new EU chemicals legislation REACH (which was put into force in June 2006),¹ the knowledge of (eco)toxicological hazard potentials of chemical substances is attached to increasing importance.

This requires efficient testing strategies, similar to those applied in the field of pharmacological drug design, to generate valid datasets for the registration procedure under REACH, and to get a profound insight into mode of toxic action and possible target sites of industrial chemicals. Regarding this issue, we trace a T-SAR^{2,3} (thinking in terms of structure activity relationships) guided and tiered strategy to:

- Systematically select test compounds and structural elements according to the “testkit concept”.^{3,4}
- Test the selected substances in a flexible (eco)toxicological test battery at different levels of biological complexity (*e.g.* enzymes, cells, microorganisms and organisms).⁵
- Improve the molecular understanding of (eco)toxicological results by relating them to physicochemical properties.⁶

- Identify toxicophore substructures in chemicals and to use this knowledge in the prospective design of inherently safer chemical products.

Following this concept, we are aiming to assess the hazard potential for a set of 79 ionic liquids at the molecular level using an enzyme inhibition test.

The interest in ionic liquids and in their promising physical and chemical properties is still growing rapidly. Diverse applications of this heterogeneous substance class in different fields have been recently described.^{7–12}

Regarding toxicological issues, they are predominantly discussed as “green” or “sustainable” chemicals, just based on their negligible vapour pressure, resulting in reduced inhalatory exposure and the absence of flammability.

However, the knowledge about their (eco)toxicological impacts on humans and the environment is still very basic and restricted to only a few chemical entities out of the enormous pool of available ionic liquids.⁴ Our attempt to fill this gap of information is to test the ionic liquids systematically in different test systems out of our flexible test battery.^{13–16}

By applying the above mentioned T-SAR based strategy, we subdivide ionic liquids into the cationic head group, the side chain, and the corresponding anion to handle this structural variability and to identify how these individual structural

^aUFT - Centre for Environmental Research and Technology, University of Bremen, Leobener Straße, D-28359, Bremen, Germany.

E-mail: jarning@uni-bremen.de

^bUmweltbundesamt, Postfach 1406, D-06813, Dessau, Germany

^cMerck KGaA, Frankfurter Straße 250, D-64293, Darmstadt, Germany

variables may evoke inhibitory effects on the enzyme acetylcholinesterase (AChE).

The enzyme acetylcholinesterase catalyses the rapid degradation of the neurotransmitter acetylcholine in the synaptic cleft—one of the key mechanisms in neurotransmission in nearly all higher organisms, including humans.^{17,18} Thus, an inhibition of acetylcholinesterase leads to various adverse effects in neuronal processes, such as heart diseases or myasthenia in humans.^{19,20} Furthermore, acetylcholinesterase represented the main target in the development of potent insecticides based on phosphoric acid esters (*e.g.* Parathione[®]) and carbamates (*e.g.* Carbendazim[®]) and therefore the activity pattern of this enzyme in different biological matrices and tissues is used as an established biomarker to monitor the pesticide burden in non-target species.^{17,21,22}

We considered the enzyme acetylcholinesterase to be an (eco)toxicologically relevant molecular target for a broad toxicity screening assay with ionic liquids based on several considerations.

i. The acetylcholinesterase can be found in nearly all higher organisms with a highly conserved and well known active site region, which allows for detailed structure activity analysis.^{18,23}

ii. The enzyme is a crucial target in the development of insecticides and in human drug design and thus the structure activity relationships leading to enzyme inhibition have been intensively studied for a variety of chemical entities.^{24–26}

iii. The amino acid residues with their specific interaction potentials building up the catalytic site and the substrate binding pocket are well known from detailed X-ray studies.²⁷

iv. As key features for the inhibitory potential, a positively charged quaternary nitrogen atom, an electron-deficient aromatic system, as well as a certain lipophilicity could be identified in all potent reversibly acting inhibitors of the enzyme.²⁴

v. The inhibition assay can be performed in a microtiter plate format and thus represents a fast and cost effective screening tool for early toxicity testing of industrial chemicals.

With respect to this, we could recently show that the nitrogen containing imidazolium and pyridinium head groups in ionic liquids act as potent inhibitors of electric eel acetylcholinesterase. In addition, a correlation between an increasing chain length of the side chains connected to the cationic head groups and an enhanced inhibitory potential of the ionic liquids was found.²⁸

The testkits presented here, consisting of a larger variety of head groups, functionalised side chains, anions and substitution patterns, are combined to identify the acetylcholinesterase inhibitory potential of ionic liquids in more detail. Furthermore, the necessity of certain molecular interaction potentials in the tested substances to interact specifically with the enzyme is demonstrated by comparing a potent imidazolium based inhibitor ionic liquid with structural analogues lacking the positively charged nitrogen moiety. And finally, the previously described side chain effect^{14,28} could be confirmed in the enzymatic test system with a quantitative structure activity correlation.

Characterising such structural features responsible for the toxic mode of action of chemical substances, the so called

toxicophores, can help to achieve the goal of a sustainable design of new chemical products by reducing or eliminating toxic or harmful structural elements of an industrial chemical. Additionally, such structural insights provide useful knowledge to concurrently maintain or even to improve the desired technical features of a substance, described by the so called technicophores, and to reduce the toxicity of the resulting product.

The testkit compounds

To investigate the influence of the cationic head groups on the inhibitory potential of the corresponding ionic liquid, thirteen different commonly used aromatic, heterocyclic and non-cyclic quaternary nitrogen containing structures were selected (Fig. 1). Additionally, the results for a quaternary phosphonium head group is presented for comparison.

To test whether the anion species frequently used in ionic liquids exhibit any intrinsic inhibitory effect on the acetylcholinesterase, a selection of the sodium or lithium salts (depending on their availability) of different anions (Fig. 2) was investigated in the enzyme assay and the results are presented.

Additionally, a testkit comprising five cationic head groups and eleven alkyl and functionalised alkyl side chains containing ether (in varying positions), terminal hydroxy and nitrile functions (Table 3) was set up to demonstrate the impact of the side chain on the enzyme inhibitory potential of the ionic liquids.

For a series of 1-butylpyridinium ionic liquids the side chain was kept constant and the methyl substitution pattern at the aromatic core structure was altered to elucidate regioselective impacts on the inhibitory potential of the pyridinium containing ionic liquids (see Table 4a).

To demonstrate the need of certain molecular interaction potentials to bind to the active site of electric eel acetylcholinesterase, a testkit of three substances was arranged containing the potent inhibitor 1-methyl-3-octylimidazolium and two uncharged structurally related octyl compounds (see Table 4b).

Acronyms for the ionic liquids

The following system of acronyms is used to facilitate the notation of the ionic liquids. The cation is abbreviated according to the type of the head group; “Py-4NMe₂” (dimethylamino)pyridinium, “Py” (pyridinium), “IM” (imidazolium), “Mor” (morpholinium), “Pip” (piperidinium), “Pyr” (pyrrolidinium) and “N” (quaternary ammonium). The substituents at the nitrogen atom(s) of the head group are given as numbers corresponding to their alkyl chain length. For example, the 1-butyl-3-methylimidazolium cation has the shorthand notation IM14. Ether containing side chains are indicated by splitting the chain in alkyl units with the symbol “O” for the oxygen in between (*e.g.* IM11O2 for 1-(ethoxymethyl)-3-methylimidazolium). Terminal hydroxy or nitrile groups are shortened as OH (*e.g.* IM14OH is 1-(4-hydroxybutyl)-3-methyl-imidazolium) or CN (*e.g.* IM11CN is 1-cyanomethyl-3-methylimidazolium, see also Table 3). The acronyms used for the halides are as in the periodic table.

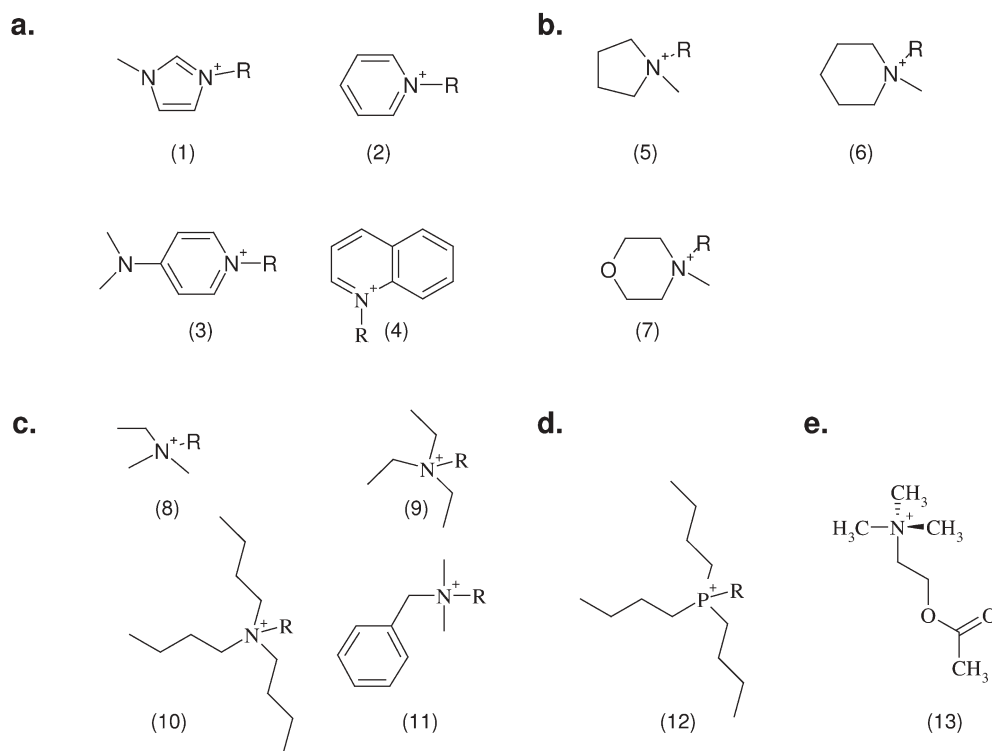


Fig. 1 All tested cationic head group structures of ionic liquids and the natural substrate of the enzyme are presented, grouped by their specific core elements. The side chain is replaced by the “R” marker. (a) Aromatic quaternary ammonium compounds: (1) imidazolium, (2) pyridinium, (3) dimethylaminopyridinium and (4) quinolinium. (b) Heterocyclic quaternary ammonium compounds: (5) pyrrolidinium, (6) piperidinium and (7) morpholinium. (c) Non-cyclic quaternary ammonium compounds: (8) ethyl-dimethyl-ammonium, (9) triethylammonium, (10) tributylammonium and (11) dimethylbenzylammonium. (d) Quaternary phosphonium compounds: (12) tributylphosphonium. (e) The natural substrate of acetylcholinesterase: (13) acetylcholine.

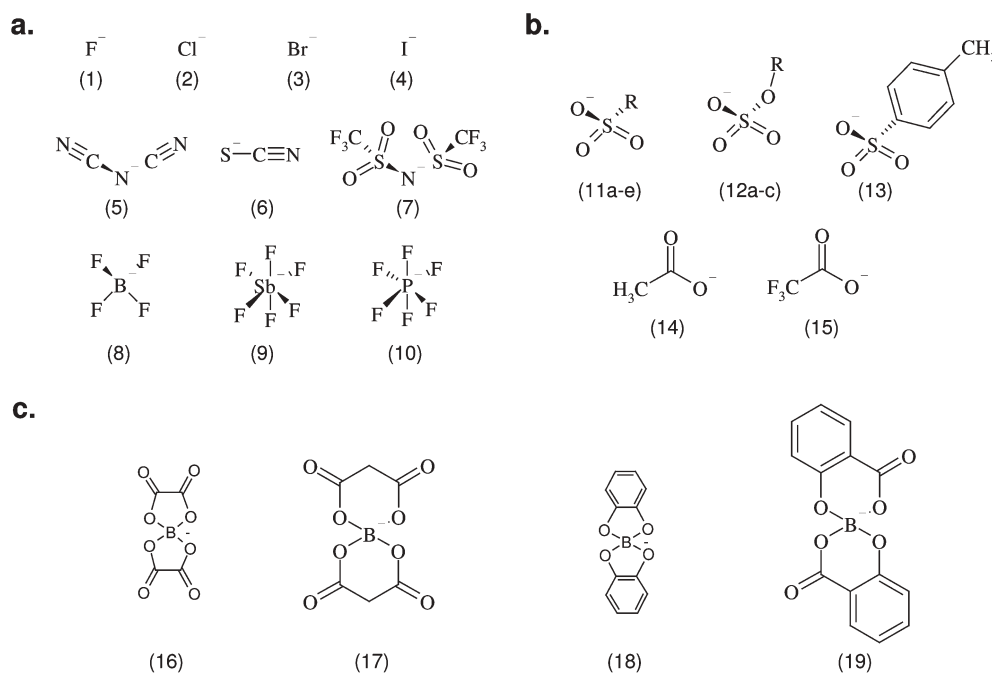


Fig. 2 The structures or element symbols of all investigated anion species are shown grouped into inorganic (a), organic (b) and complex borate (c) anions. The “R” marker replaces different side chains. The names and the corresponding $\log IC_{50}$ (μM) values of the tested sodium or lithium salts of the anion species, together with the 95% confidence intervals in parentheses, are listed in Table 1.

Table 1 The anion species are listed due to their numbers referring to Fig. 2. The decadic logarithm of the IC_{50} values in μM is presented with the 95% confidence interval in parenthesis. If no complete concentration response curve was obtained in the enzyme inhibition assay, the IC_{50} (μM) value is indicated to be higher than the decadic logarithm of the maximum test concentration (e.g. >3)

Number	Name	Log IC_{50} AChE/ μM
1	Fluoride	2.76 (2.69–2.82)
2	Chloride	>3
3	Bromide	>3
4	Iodide	>3
5	Dicyanamide	>3
6	Thiocyanate	>3
7	Bis(trifluoromethylsulfonyl)amide	>3
8	Tetrafluoroborate	>3
9	Hexafluoroantimonate	2.34 (2.28–2.39)
10	Hexafluorophosphate	2.16 (2.12–2.19)
11a	1-Methanesulfonate	>3
11b	Trifluoromethanesulfonate	>3
11c	1-Butanesulfonate	>3
11d	1-Hexanesulfonate	>3
11e	1-Octanesulfonate	>3
12a	1-Methylsulfate	>3
12b	1-Octylsulfate	>3
12c	1-Dodecylsulfate	2.96 (2.91–3.00)
13	Toluene-4-sulfonate	>3
14	Acetate	>3
15	Trifluoroacetate	>3
16	Bis[oxalato(2-)]-borate	>3
17	Bis[malonato(2-)]-borate	>3
18	Bis[1,2-benzenediolato(2-)-O1,O2]borate	>3
19	Bis[2-hydroxybenzoato(2-)-O1,O2]borate	>3

The identifiers for the cation and for the anion separated by a white space represent the complete acronym for an ionic liquid.

Statistics and effect data modelling

All enzyme inhibition experiments were carried out at least in triplicates, with three replicates in each. The normalised (0 to 100% enzyme activity) concentration response curves were fitted to the multinomial data with the R language and the environment for statistic computing using the probit model for the relation of enzyme activity to the decadic logarithm of the tested concentrations.²⁹ Confidence intervals ($\alpha = 0.05$) of the calculated IC_{50} values and the linear regression parameters of the logarithm of the IC_{50} values *versus* the logarithm of the lipophilicity parameter k_0 were calculated with the R language as well.

Results

The data for the tested anion species are summarised in Table 1. All calculated IC_{50} values for the ionic liquids and the corresponding confidence intervals are presented in Table 2. In the following subsections the results obtained for the influence of anions, head groups, side chains and regioselective effects on the enzyme inhibitory potential of ionic liquids are systematically presented.

A summary of all acetylcholinesterase inhibition data of ionic liquids generated in our test battery has recently been published in Ranke *et al.*³⁰ All relevant results discussed in the following sections are summarised in Table 2.

Influence of the anion species

For the vast majority of the tested anion species, no influence on the activity of the acetylcholinesterase was detectable up to the highest tested concentration range of 1000 μM . Only for fluoride and the fluoride containing hexafluoroantimonate and hexafluorophosphate, was a significant inhibition found, with IC_{50} values of 575 μM (F^-), 219 μM (SbF_6^-) and 145 μM (PF_6^-), respectively (Table 1). The concentration response curves demonstrate the range of the inhibitory potential of the three substances, with the PF_6^- anion acting as the strongest inhibitor and the fluoride ion at the upper end of the scale (Fig. 3).

Additionally, the 1-dodecylsulfate anion was found to be a weak ($IC_{50} = 912 \mu M$) inhibitor of the enzymes activity. Since all cationic head groups discussed in the following sections were exclusively tested with either halides (chloride, bromide or iodide) or with the non-inhibiting tetrafluoroborate as counterions, it was concluded that all observed inhibitory effects on the enzyme can be exclusively attributed to the cationic moiety.

Influence of the head group

In general, it could be shown that all investigated cationic head groups containing the butyl side chain affected the activity of electric eel acetylcholinesterase in an inhibitory manner. Furthermore, the two ammonium based cations tetraethylammonium and decylbenzyltrimethylammonium were found to inhibit the enzyme's activity (Table 2). To investigate this influence of the cations on the enzyme inhibitory potential of ionic liquids in more detail, a subset of different core structures (Fig. 4) was combined, all carrying the butyl side chain as a reference standard.

Comparing all these tested butyl-containing head groups, the range of the measured IC_{50} values spans nearly three orders of magnitude (Fig. 4), within which the most striking inhibitory effect could be detected for the *N*-dimethylamminopyridinium and the quinolinium head groups, where IC_{50} values of 4 μM and 6 μM , respectively, were calculated from the concentration response data. These values are in the same range as the IC_{50} of the strong and specific carbamate-type acetylcholinesterase inhibitor Aldicarb[®] ($IC_{50} = 5 \mu M$), which was used as a positive standard in our assay. Thus, the *N*-dimethylamminopyridinium and the quinolinium moiety exhibited an inhibitory potential one or even two orders of magnitude higher than that for all other tested butyl-containing ionic liquid head groups in this study.

Looking at the other end of the scale, one could find that the polar and non-aromatic morpholinium head group, as well as the sterically bulky tetrabutylammonium cation, exhibited the lowest inhibitory potential to the enzyme, corresponding to IC_{50} values of 513 μM and 197 μM , respectively.

Grouping the remaining cations into that range of enzyme inhibition potential, one could find the aromatic pyridinium and imidazolium head groups, as well as the heterocyclic but non-aromatic piperidinium and pyrrolidinium moieties, to show lower IC_{50} values lying closely together in the range from 50 μM ("Py") to 83 μM ("Pyr"). The butylethyltrimethylammonium head group, which is structurally closely related to

Table 2 All tested and discussed ionic liquids are listed in alphabetical order. The decadic logarithm of the IC_{50} (μM) is given with the 95% confidence interval in parenthesis. For the substances where no complete concentration response curve was obtained in the enzyme inhibition assay, the decadic logarithm of the highest tested concentration is shown (*e.g.* >3). The decadic logarithm of the k_0 values are presented for all imidazolium compounds building up the correlation in Fig. 6

Name	Log IC_{50} AchE/ μM	Log k_0
1-(2-Ethoxyethyl)-1-methylpiperidinium bromide	2.6 (2.58–2.63)	
1-(2-Ethoxyethyl)-1-methylpyrrolidinium bromide	2.6 (2.58–2.63)	
1-(2-Ethoxyethyl)-3-methylimidazolium bromide	2.27 (2.25–2.29)	0.45
1-(2-Ethoxyethyl)pyridinium bromide	1.55 (1.53–1.57)	
1-(2-Hydroxyethyl)-1-methylpiperidinium iodide	2.34 (2.31–2.38)	
1-(2-Hydroxyethyl)-1-methylpyrrolidinium iodide	2.63 (2.61–2.65)	
1-(2-Hydroxyethyl)-3-methylimidazolium iodide	2.96 (2.93–2.99)	–0.28
1-(2-Hydroxyethyl)pyridinium iodide	2.69 (2.67–2.71)	
1-(2-Methoxyethyl)-1-methylpiperidinium bromide	2.06 (2.03–2.09)	
1-(2-Methoxyethyl)-1-methylpyrrolidinium chloride	2.38 (2.36–2.39)	
1-(2-Methoxyethyl)-3-methylimidazolium chloride	2.58 (2.58–2.61)	–0.02
1-(2-Methoxyethyl)pyridinium chloride	2.07 (2.05–2.09)	
1-(3-Hydroxypropyl)-1-methylpiperidinium chloride	2.53 (2.51–2.56)	
1-(3-Hydroxypropyl)-1-methylpyrrolidinium chloride	2.86 (2.84–2.89)	
1-(3-Hydroxypropyl)-3-methylimidazolium chloride	2.99 (2.94–3.04)	–0.23
1-(3-Hydroxypropyl)pyridinium chloride	2.65 (2.62–2.68)	
1-(3-Methoxypropyl)-1-methylpiperidinium chloride	2.2 (2.17–2.23)	
1-(3-Methoxypropyl)-1-methylpyrrolidinium chloride	2.74 (2.71–2.77)	
1-(3-Methoxypropyl)-3-methylimidazolium chloride	2.61 (2.58–2.64)	
1-(3-Methoxypropyl)pyridinium chloride	2.15 (2.11–2.18)	
1-(4-Hydroxybutyl)-3-methylimidazolium chloride	2.74 (2.69–2.8)	–0.06
1-(8-Hydroxyoctyl)-3-methylimidazolium bromide	1.28 (1.22–1.33)	0.90
1-(Cyanomethyl)-1-methylpiperidinium chloride	2.43 (2.4–2.46)	
1-(Cyanomethyl)-1-methylpyrrolidinium chloride	2.88 (2.86–2.91)	
1-(Cyanomethyl)-3-methylimidazolium chloride	2.89 (2.86–2.92)	–0.29
1-(Cyanomethyl)pyridinium chloride	2.47 (2.45–2.49)	
1-(Ethoxymethyl)-1-methylpiperidinium chloride	2.14 (2.12–2.17)	
1-(Ethoxymethyl)-1-methylpyrrolidinium chloride	1.86 (1.84–1.87)	
1-(Ethoxymethyl)-3-methylimidazolium chloride	2.61 (2.59–2.63)	0.21
1-(Ethoxymethyl)pyridinium chloride	2.06 (2.02–2.11)	
1,3-Diethylimidazolium bromide	2.08 (2.02–2.13)	0.09
1-Butyl-1-methylpiperidinium bromide	1.83 (1.81–1.85)	
1-Butyl-1-methylpyrrolidinium chloride	1.92 (1.87–1.96)	
1-Butyl-2-methylpyridinium chloride	0.7 (0.66–0.75)	
1-Butyl-3-methylimidazolium chloride	1.91 (1.88–1.95)	0.63
1-Butyl-3-methylpyridinium chloride	1.15 (1.13–1.17)	
1-Butyl-4-methylpyridinium chloride	1.44 (1.42–1.46)	
1-Butylpyridinium chloride	1.7 (1.68–1.71)	
1-Butylquinolinium bromide	0.79 (0.77–0.82)	
1-Decyl-3-methylimidazolium chloride	1.09 (1.04–1.13)	2.37
1-Ethyl-3-methylimidazolium chloride	2.06 (2.02–2.1)	
1-Ethyl-3-propylimidazolium bromide	2.21 (2.17–2.25)	0.56
1-Ethylpyridinium chloride	2.1 (2.08–2.11)	
1-Heptyl-3-methylimidazolium chloride	2.07 (2.04–2.11)	1.57
1-Hexadecyl-3-methylimidazolium chloride	0.68 (0.66–0.71)	
1-Hexyl-3-methylimidazolium chloride	1.92 (1.88–1.96)	1.24
1-Hexylpyridinium chloride	1.72 (1.7–1.74)	
1-Hexylquinolinium tetrafluoroborate	0.48 (0.46–0.5)	
1-Methyl-1-octylpyrrolidinium chloride	2.36 (2.32–2.4)	
1-Methyl-3-(2-phenylethyl)imidazolium chloride	1.91 (1.88–1.94)	1.01
1-Methyl-3-(3-oxobutyl)imidazolium bromide	2.79 (2.75–2.84)	0.00
1-Methyl-3-(phenylmethyl)imidazolium chloride	2.04 (1.97–2.11)	0.83
1-Methyl-3-[(4-methylphenyl)methyl]imidazolium chloride	1.86 (1.81–1.91)	1.12
1-Methyl-3-nonylimidazolium chloride	1.36 (1.31–1.42)	2.10
1-Methyl-3-octadecylimidazolium chloride	0.96 (0.85–1.07)	
1-Methyl-3-octylimidazolium chloride	1.6 (1.56–1.63)	1.85
1-Methyl-3-pentylimidazolium chloride	1.96 (1.94–1.99)	0.92
1-Methyl-3-propylimidazolium chloride	2.27 (2.24–2.3)	0.42

the quaternary ammonium moiety in the natural substrate acetylcholine (see Fig. 1), exhibited a middle inhibitory potential ($IC_{50} = 115 \mu M$) ranging significantly lower than those of the pyridinium ($IC_{50} = 50 \mu M$) and imidazolium ($IC_{50} = 82 \mu M$) cations. Looking at the solely tested phosphonium based head group, one could observe that the

tetrabutylphosphonium cation was significantly less active, with an IC_{50} of $411 \mu M$, than its structural quaternary nitrogen analogue, the tetrabutylammonium head group (Table 2).

Comparing the tetraethylammonium cation ($IC_{50} = 637 \mu M$) with the imidazolium, pyridinium and dimethylaminopyridinium head groups carrying the ethyl side chain (see Table 2), it

Table 2 All tested and discussed ionic liquids are listed in alphabetical order. The decadic logarithm of the IC_{50} (μM) is given with the 95% confidence interval in parenthesis. For the substances where no complete concentration response curve was obtained in the enzyme inhibition assay, the decadic logarithm of the highest tested concentration is shown (*e.g.* >3). The decadic logarithm of the k_0 values are presented for all imidazolium compounds building up the correlation in Fig. 6 (*Continued*)

Name	Log IC_{50} AchE/ μM	Log k_0
1-Octylimidazol	>3	
1-Octylpyridinium chloride	1.6 (1.57–1.64)	
1-Octylquinolinium bromide	<0	
1-Pentylpyridinium bromide	1.52 (1.5–1.54)	
1-Propylpyridinium bromide	2.22 (2.19–2.24)	
4-(2-Ethoxyethyl)-4-methylmorpholinium bromide	>3	
4-(2-Hydroxyethyl)-4-methylmorpholinium iodide	2.96 (2.93–3)	
4-(2-Methoxyethyl)-4-methylmorpholinium chloride	2.98 (2.95–3.02)	
4-(3-Hydroxypropyl)-4-methylmorpholinium chloride	>3	
4-(3-Methoxypropyl)-4-methylmorpholinium chloride	>3	
4-(Cyanomethyl)-4-methylmorpholinium chloride	>3	
4-(Dimethylamino)-1-butylpyridinium chloride	0.6 (0.57–0.62)	
4-(Dimethylamino)-1-ethylpyridinium bromide	0.99 (0.97–1.01)	
4-(Dimethylamino)-1-hexylpyridinium chloride	0.5 (0.48–0.52)	
4-(Ethoxymethyl)-4-methylmorpholinium chloride	2.96 (2.93–3)	
4-Butyl-4-methylmorpholinium bromide	2.71 (2.69–2.73)	
Aldicarb [®] (2-methyl-2-(methylthio)propionaldehyde-O-methylcarbamoyloxime)	0.69 (0.63–0.75)	
Butylethyldimethylammonium chloride	2.06 (2.04–2.08)	
Decylbenzyltrimethylammonium chloride	0.73 (0.68–0.77)	
Tetrabutylammonium bromide	2.3 (2.25–2.35)	
Tetrabutylphosphonium bromide	2.61 (2.58–2.64)	
Tetraethylammonium chloride	2.8 (2.74–2.87)	

is noticeable that the relatively small non-cyclic quaternary ammonium cation exhibited a very weak inhibitory potential towards the acetylcholinesterase.

In contrast, the decylbenzyltrimethylammonium cation ($IC_{50} = 5 \mu M$) exhibited a slightly stronger effect on the enzyme activity, compared to the aromatic imidazolium cation IM1-10 ($IC_{50} = 12 \mu M$).

Influence of the side chain

When first looking at the alkyl side chains, the previously reported side chain effect could generally be confirmed for the imidazolium cations (IM12–IM1-18) and for the pyridinium moiety (Py2–Py8, see Table 2). Remarkably, the butyl side

chain seemed to represent a local minimum in the series of the IC_{50} values. The side chain effect for the imidazolium cations is analysed in more detail in the following.

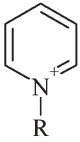
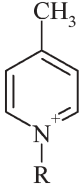
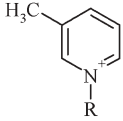
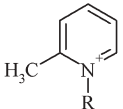
Furthermore, it could be demonstrated that for the strong inhibiting dimethylaminopyridinium (Py2-4NMe2–Py6-4NMe2) and quinolinium (Quin4–Quin8) head groups, the side chain effect was only marginal compared to the less inhibitory imidazolium (IM12–IM18) and pyridinium (Py2–Py8, see Table 2) cations. This means that the strong effect on the enzyme activity for the dimethylaminopyridinium and the quinolinium cations is mainly dominated by the cationic core structure, whereas for the less active head groups the lipophilicity of the side chain is the dominating factor mediating the inhibitory potential.

Table 3 The IC_{50} values in μM for a selection of different cationic head groups (see Fig. 1) combined with varying alkyl side chains and their functionalised analogues (R) are presented to demonstrate the influence of a side chain modification on the enzyme inhibitory potential of the corresponding ionic liquid (for confidence intervals see Table 2). The abbreviations of the sidechains and headgroups are indicated. If no IC_{50} value could be calculated the highest tested concentration is given (*e.g.* >1000 μM) in the table. The alkyl side chains and the corresponding IC_{50} (μM) values are marked in bold, serving as benchmark for the modified analogues with the same atom number in the chain. For all presented cations, the halides chloride, bromide or iodide served as counterions

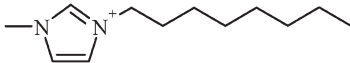
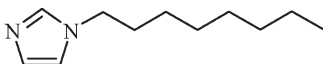
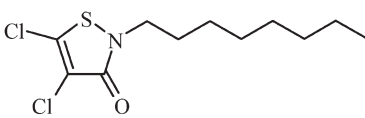
R	IC_{50} AchE/ μM					
Structure	Abbreviations	“Py”	“IM1”	“Mor1”	“Pip1”	“Pyr1”
–C ₂ H ₅	2	125	115			
–C ₃ H ₇	3	164	185			
–CH ₂ CH ₂ –OH	2OH		913	919	221	430
–CH ₂ CN	1CN		776	>1000	267	767
–C ₄ H ₉	4		82	513	68	83
–CH ₂ CH ₂ CH ₂ –OH	3OH		990	>1000	342	731
–CH ₂ –O–CH ₂ CH ₃	1O2		407	920	139	72
–CH ₂ CH ₂ –O–CH ₃	2O1		379	999	114	239
–C ₅ H ₁₁	5		92			
–CH ₂ CH ₂ –O–CH ₂ CH ₃	2O2		187	>1000	401	400
–CH ₂ CH ₂ CH ₂ –O–CH ₃	3O1		405	>1000	158	545

Table 4 The IC₅₀ values for a series of 1-butylmethylpyridinium cations

(a) To demonstrate regioselective impacts on the enzyme inhibitory potential, three methyl substituted 1-butylpyridinium cations with their corresponding IC₅₀ values in μM are presented. The unsubstituted 1-butylpyridinium serves as reference. The 95% confidence intervals are given in parenthesis and for all cations the chloride serves as the counterion

Structure	Name	IC ₅₀ AchE/μM
	1-Butylpyridinium	50.0 (48.3–51.5)
	1-Butyl-4-methylpyridinium	27.4 (26.3–28.6)
	1-Butyl-3-methylpyridinium	14.1 (13.5–14.8)
	1-Butyl-2-methylpyridinium	5.1 (4.55–5.59)

(b) To show the necessity of certain molecular interaction potentials of a substance to interfere with the active site of the AchE, the potent inhibitor 1-methyl-3-octylimidazolium chloride is compared with its mainly uncharged (pKs ~ 6 and pH 8.0 of the test buffer) analogue 1-octylimidazol and with an aromatic, heterocyclic and highly reactive 2-octyl-isothiazol-3-one biocide. The IC₅₀ value in μM of the imidazolium compound is given with the 95% confidence interval in parenthesis. For the two remaining substances, the highest tested concentration in the enzyme inhibition assay is presented

Structure	Name	IC ₅₀ AchE/μM
	1-Methyl-3-octylimidazolium	39.4 (36.7–42.3)
	1-Octylimidazol	>2000
	4,5-Dichloro-2-octylisothiazol-3-one	>1000

Focusing now on the influence of functionalised side chains on the enzyme activity, the results for the ethyl, propyl, butyl and pentyl side chains are presented together with their structurally related (with respect to the chain length) terminal hydroxy, ether and nitrile analogues (Table 3).

In general, one could find a consistent pattern in which the more polar functionalised side chains exhibited a lower inhibitory potential than their lipophilic alkyl references. The hydroxy-functionalised side chains, which provide a donor and an acceptor potential for hydrogen bonding—and thus are the most polar derivatives tested—showed the weakest inhibitory potential compared to the less polar (only hydrogen bonding acceptor potential) ether analogues. The short and polar nitrile side chain showed for all tested head groups, relatively high IC₅₀ values comparable

to those for the other polar oxygen containing ether and hydroxy residues.

For the imidazolium head group connected to a four atom containing side chain, it could be shown that the introduction of a hydroxy function into the alkyl side chain was able to shift the IC₅₀ one order of magnitude to the side of lower enzyme inhibition. The ether-containing side chains are lying in between the highly polar hydroxy side chain and the butyl reference and no significant regioselective effect with respect to the position of the ether bridge was observable (Fig. 5).

The above presented results for the alkyl and functionalised side chains reinforce the assumption that the lipophilicity of the side chain for one cationic head group is a key parameter in predicting the acetylcholinesterase inhibitory potential of the corresponding ionic liquid when looking at a relatively weak

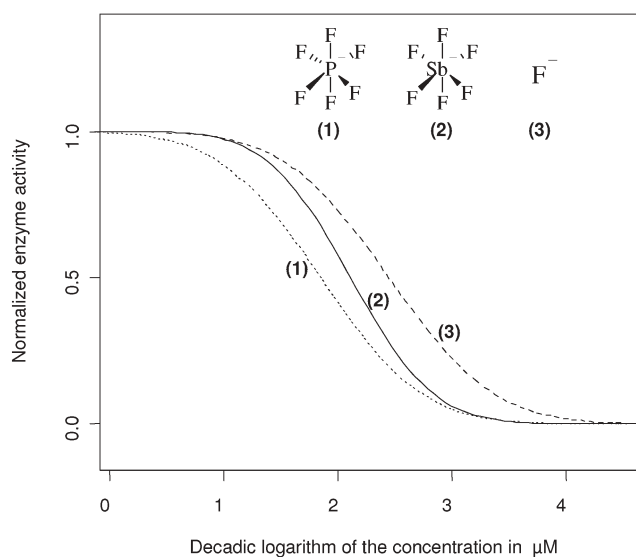


Fig. 3 The fitted concentration response curves for the fluoride and two fluoride containing anion species exhibiting an inhibitory effect on the acetylcholinesterase are shown. The exact $\log IC_{50}$ (μM) values and the corresponding 95% confidence intervals are given in Table 1.

inhibiting head group (e.g. imidazolium, pyrrolidinium or morpholinium). With respect to this, for a series of imidazolium head groups connected to different alkyl and functionalised side chains, a quantitative structure activity relationship

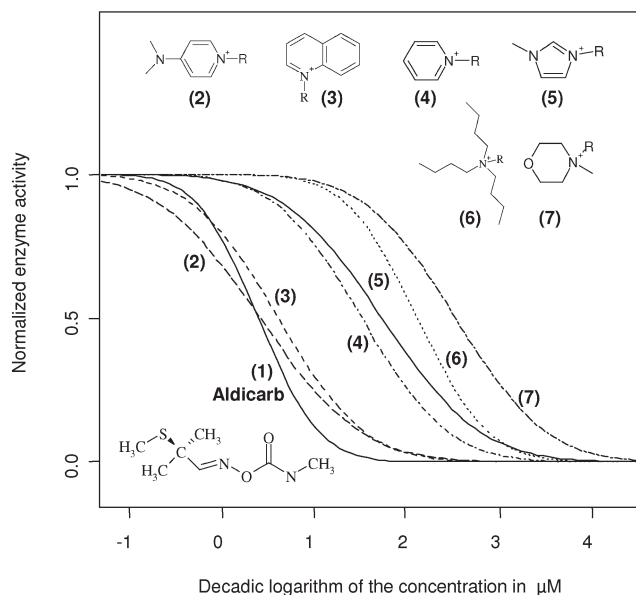


Fig. 4 To demonstrate that the cationic head group acts as a key structural element in the interaction with the active site of the acetylcholinesterase, the fitted concentration response curves of some butyl ("R" = C_4H_9) cations are presented. For comparison, the concentration response curve for the strong carbamate type acetylcholinesterase inhibitor Aldicarb[®] (2-methyl-2-(methylthio)propionaldehyde-O-methylcarbamoyloxime) was added. As counterions for the cationic head groups, the halides chloride, bromide and iodide were used. The exact $\log IC_{50}$ (μM) data with the corresponding confidence intervals are listed in Table 2.

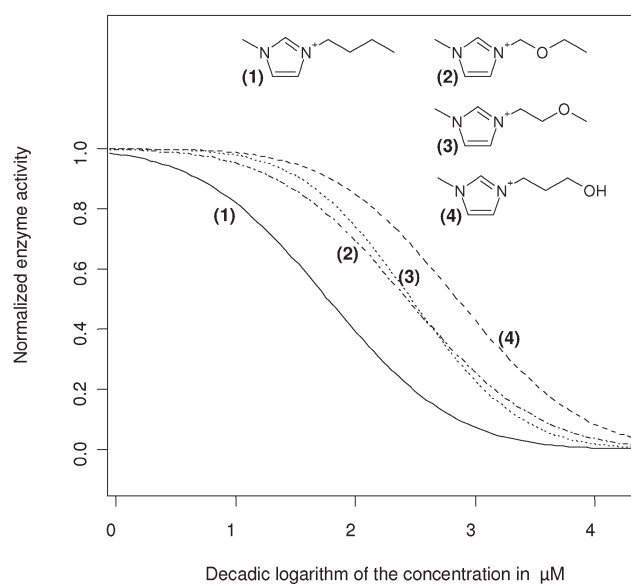


Fig. 5 Fitted concentration response curves for 1-butyl-3-methylimidazolium and three 3-methylimidazolium headgroups containing functionalised butyl side chain analogues (ether (2),(3) and hydroxy (4) functions). The chloride serves as a counterion for all shown cations. For the exact IC_{50} values in μM , see Table 3.

was derived by the linear regression of the $\log IC_{50}$ values versus the logarithm of the HPLC-derived lipophilicity parameter k_0 of the ionic liquids cations (Fig. 6). A good correlation ($r^2 = 0.79$) with three outliers could be found for a decrease in the IC_{50} values, with increasing lipophilicity of the side chain.

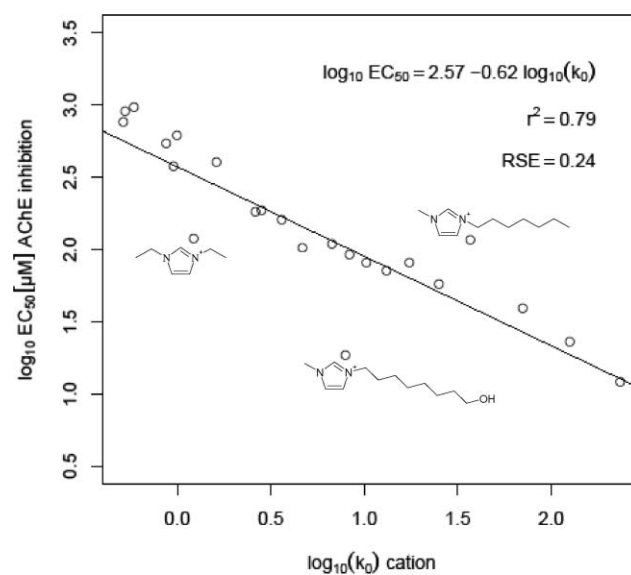


Fig. 6 Quantitative structure activity relationship between the decadic logarithm of the lipophilicity parameter k_0 and the $\log IC_{50}$ values (μM) of a series of imidazolium headgroups (see Table 2). The three prominent outliers are indicated by their structural formula. The calculated regression function is specified together with the corresponding quadratic correlation coefficient (r^2) and the residual standard error (RSE).

Regioselective and general structural considerations

To demonstrate the strong influence a simple structural alteration in a chemical entity can exert on the interaction with a biomolecule, the IC_{50} values for a series of 1-butylmethylpyridinium cations are presented (Table 4a). The introduction of a methyl substituent at the aromatic core structure significantly increased the inhibitory potential of the 1-butylpyridinium cation. Additionally, it could be observed that the IC_{50} values decreased when going from the linear 1-butyl-4-methylpyridinium to the angled 1-butyl-2-methylpyridinium configuration, showing more structural analogy to the natural substrate acetylcholine. Looking at the toxicity range of the substituted pyridinium type ionic liquids, one could state that they all exhibited a rather high acetylcholinesterase inhibitory potential with a subtle regioselective influence.

However, comparing the observed IC_{50} values for the positively charged aromatic 1-methyl-3-octylimidazolium, the uncharged (under the assay conditions) 1-octylimidazol and the aromatic, electron-deficient and highly reactive 4,5-dichloro-2-octylisothiazol-3-one, the necessity of certain molecular interaction potentials for the binding to the active site of acetylcholinesterase becomes obvious (Table 4b). Neither the structurally closely related 1-octylimidazol, nor the also octyl-substituted isothiazol-3-one structure exhibited any inhibitory effect on AchE up to the highest concentration tested. Thus, for a strong specific interaction of a compound with the active site of acetylcholinesterase, the positively charged nitrogen atom could be identified to act as the key molecular interaction potential. The lipophilicity of the side chain and the presence or absence of an aromatic ring system modulated the strength of the resulting inhibitory potential.

Discussion

It is the aim of this study to get a deeper insight into the (eco)toxicological impacts of structural variations in ionic liquid substructural elements, built up by the positively charged head group, substituted with one or more different side chains, and the corresponding anionic species, in an (eco)toxicologically relevant molecular test system.

To discuss the above presented results, the catalytic cycle of the enzyme and the essential amino acid residues involved in substrate binding are presented. The active site of acetylcholinesterase is located at the bottom of a narrow gorge. The gorge is lined with lipophilic aromatic amino acid residues and the entrance is built up with negatively charged residues. The active centre can be divided into the catalytic esteratic site where the acetyl group of the substrate is bound, and the anionic site where the quaternary ammonium moiety of the acetylcholine is stabilised *via* a cation- π interaction with the essential tryptophane residue Trp 84.³¹ Additionally, a peripheral anionic site (PAS) could be identified at the entrance of the narrow gorge, where the substrate acetylcholine is bound to Trp 279, again *via* cation- π interactions, and is thereby orientated towards the active centre.³² The catalytic cycle of the enzyme can be described in three steps. At first, the substrate is attracted by the negative potential surrounding the entrance of the gorge and binds to Trp 279. The so orientated substrate molecule is subsequently

transferred through the lipophilic gorge and bound to the active centre with the positively charged nitrogen moiety interacting with the Trp 84 and the acetyl group lying at the esteratic site. The ester bond is hydrolysed and the resulting choline moiety leaves the catalytic site *via* the gorge. In the last step, a water molecule regenerates the acetylated enzyme and the acetate anion is expelled *via* the channel formed by the lipophilic gorge.³³

Thus, competitive inhibitors of acetylcholinesterase can act *via* two distinct mechanisms. They can either bind directly to the active site and thereby inhibit the cleavage of the natural substrate or inhibitors can bind to the PAS and block substrate traffic into and out of the catalytic centre by steric interference or allosteric alteration of the enzymes active centre.³²

With respect to this, the identified molecular interaction potentials found for the inhibiting ionic liquids can be interpreted. The cationic head groups are attracted by the negative surface potential of the enzyme and bind *via* the positively charged nitrogen atom, in a competitive manner, to the essential tryptophane residues at the catalytic site or the PAS. Especially, the quinolinium and dimethylaminopyridinium head groups can bind strongly *via* π - π interactions to the Trp 279 at the PAS, due to their large aromatic systems. The natural substrate acetylcholine or the acetylthiocholine used in our assay are only weakly bound to the PAS, which explains the strong inhibiting effect of these two aromatic ionic liquid head groups. The aromatic stacking interactions for the quinolinium and the dimethylaminopyridinium head groups are that strong that the side chain effect is negligible.

For the remaining aromatic head groups—the pyridinium and imidazolium cations—the side chain enforces the weaker π - π interactions of the smaller aromatic systems by lipophilic interactions with the amino acid residues lining the narrow gorge. Thus, the correlation of increasing side chain lipophilicity and decreasing IC_{50} values for the different head groups can be explained and even quantified in a QSAR correlation in the case of the imidazolium cations. The most prominent outlier in the linear regression, the IM18OH, may be explained by an additional interaction at an allosteric subsite, far away from the active site.

The morpholinium head group is lacking the aromatic π - π interaction potential and provides the lowest lipophilic interaction potential compared to all other tested cations and therefore exhibits the observed low inhibitory potential. The introduced free electron pairs at the oxygen atom of the morpholinium head group are only weak donors or acceptors for π - π interactions. It is more likely that they are involved in strong hydrogen bonding interactions to water molecules, making the morpholinium head group even more hydrophilic.

The quaternary ammonium head groups, as well as the remaining heterocyclic cations, are also able to bind only *via* cation- π and lipophilic interactions to the tryptophane residues and the aromatic gorge. The significance of a π - π interaction for a tight binding to the enzyme can also be demonstrated when comparing the non-aromatic quaternary ammonium compound decylbenzyltrimethylammonium with the 1-decyl-3-methylimidazolium cation. The benzyl residue connected to the ammonium moiety interacts slightly stronger with the

tryptophane ring system than the smaller aromatic imidazolium system.

The tested phosphonium head group is more bulky and subsequently the positive charge density is decreased compared to its nitrogen containing analogue. Thus, the interactions with the tryptophane residues in the enzyme are smaller, resulting in a higher IC_{50} for the tetrabutylphosphonium cation.

The local maximum in the inhibitory potential for the butyl side chain observed within the series of imidazolium and pyridinium ionic liquids may be explained by a strong interaction at the catalytic site in addition to the binding at the PAS. The butyl side chain is short enough to fit in the active centre, whereas the longer side chains only allow for binding at the PAS.

Additionally, the observed regioselective effects can be interpreted by the fact that the 1-butylpyridinium compounds can bind directly at the active site. The angled configuration is able to interact stronger with the Trp 84 than the more stretched isomers, due to its structural homology to the choline moiety. This angled configuration allows for an optimised orientation of the 2-methylpyridinium moiety towards the anionic subsite in the active centre of the AchE.

Considering the negative surface potential at the entrance to the catalytic centre, one would expect all anion species to exert no effect on the enzyme activity. Our results confirm this presumption, with the only exception of the fluoride anion and the fluoride containing SbF_6^- and PF_6^- species. Both species are known to readily undergo hydrolysis in aqueous media^{34–36} and thus the fluoride seems to be the active compound and acetylcholinesterase inhibition by F^- has already been described in the literature.^{37,38} The relatively low IC_{50} values for the SbF_6^- and PF_6^- anions compared to the fluoride are due to the fact that per mole SbF_6^- or PF_6^- , six moles of fluoride may theoretically be released.

The very weak inhibitory potential observed for the 1-dodecylsulfate anion is presumably due to non-specific detergent like inactivation of the acetylcholinesterase.

Conclusion

Using different testkits of anion species, cationic head groups and functionalised side chains connected to these head groups, we were able to identify three molecular key interaction potentials for the inhibitory effect of a broad variety of ionic liquid species on the enzyme acetylcholinesterase. Considering these interaction potentials and the molecular interaction potentials provided by the catalytic centre of the enzyme, the observed structure activity relationships of the tested substances can qualitatively and quantitatively be described. Thus, the applied enzyme inhibition screening assay with the electric eel acetylcholinesterase seems to be a valid and useful tool in a flexible (eco)toxicological test battery to analyse the impact of structural elements on the toxic mode of action of chemical substances. This implies that the AchE inhibition assay can be used to identify toxicophore substructures in a chemical entity, and thereby is able to support the design of new inherently safer and hence sustainable chemical products.

In detail, for the ionic liquids the positively charged nitrogen atom, a broad delocalised aromatic ring system and a certain

lipophilicity could be shown to be the mediators for the acetylcholinesterase inhibition potential. With respect to this, the dimethylaminopyridinium and the quinolinium head groups were identified to be very strong inhibitors of the enzyme. This trend has also been recently described for the cytotoxicity of these two head groups^{6,14} and thus the dimethylaminopyridinium and the quinolinium cations should be avoided when aiming at the design of non-toxic ionic liquids. The results obtained for the pyridinium and methylated pyridinium head groups confirm our previous results,²⁸ marking these cations also as strong AchE inhibitors. In contrast, the morpholinium head group was found to be only weakly inhibiting or even inactive, depending on the connected side chain. Again, this is well in accordance with recently published cytotoxicity data generated in our flexible test battery.¹⁴

Furthermore, the well known side chain effect²⁸ is confirmed for the imidazolium and pyridinium cations and could even be described by a QSAR correlation for a series of imidazolium ionic liquids. Additionally, the lipophilicity of the side chain was identified to be a potent structural element to alter the enzyme inhibitory potential of a broad spectrum of ionic liquid head groups. For example, the IC_{50} of IM14 is decreased one order of magnitude by the introduction of a hydroxy function into the side chain, resulting in the IM13OH cation.

Since the vast majority of the tested anion species exhibited no inhibiting effect to the enzyme, this structural element can be used to tune and improve the technicophore properties of the ionic liquids. Only fluoride or fluoride containing anions, which readily undergo hydrolytic cleavage, should be avoided.

Putting together our results, we have found a set of structural elements which allows for the rough and fine tuning of the molecular toxicity towards the electric eel acetylcholinesterase. The inherent head group effect can be modulated to lower inhibitory potentials by choosing polar, non-aromatic head groups or incorporating polar hydroxy, ether or nitrile functions into the side chains connected to the cationic core structure. The anion species represents the most promising structural element to tune the technical properties of the ionic liquids because a big pool of different anions (inorganic, organic and complex borate species) was shown to be inactive in the AchE inhibition assay.

However, it should be mentioned that the design of inherently safer chemical products with optimised technological and economical features is not an easy task and often leads to goal conflicts. These conflicts can only be overcome in close cooperation between industry and academic research groups.

Experimental

Chemicals

All tested ionic liquids, the 1-octylimidazol and the sodium or lithium salts of the investigated anion species were received by the Merck KGaA (Darmstadt, Germany), with the exception of 1-octyl-quinolinium bromide, which was prepared at the ITUC in Jena, Germany.

The 4,5-dichloro-2-octylisothiazol-3-one was donated by Rohm and Haas (Philadelphia, USA). Stock solutions of all

test substances were prepared in methanol or dimethylsulfoxide, depending on their solubility.

2-methyl-2-(methylthio)propionaldehyde-O-methylcarbamoyloxime (Aldicarb[®]), acetic acid, acetonitrile, methanol and dimethylsulfoxide, as well as bovine serum albumin, and sodium hydrogen phosphate, were purchased from the Sigma–Aldrich Cooperation (Steinheim, Germany).

Sodium hydrogen carbonate was purchased from GIBCO BRL Life technologies (Eggenstein, Germany) and acetylthiocholine iodide was provided by Fluka (Buchs, Switzerland).

Acetylcholinesterase (AChE, EC 3.1.1.7) from the electric organ of the electric eel (*Electrophorus electricus*) type VI-S was purchased from Sigma–Aldrich (Steinheim, Germany). The activity was determined to be 463 U mg protein⁻¹.

Acetylcholinesterase inhibition assay

The inhibition of the acetylcholinesterase was measured using a colorimetric assay based on the reduction of the dye 5,5'-dithio-bis-(2-nitrobenzoic acid) (DTNB) by the enzymatically formed thiocholine moiety from the AChE substrate acetylthiocholine iodide. The assay is described in detail in Stock *et al.*²⁸ Briefly, a dilution series of the test substances in phosphate buffer (0.02 M, pH 8.0) containing max. 1% methanol was prepared directly in the wells of a 96-well microtiter plate. DTNB (2 mM, 0.185 mg mL⁻¹ NaHCO₃ in phosphate buffer pH 8.0) and the enzyme (0.2 U mL⁻¹, 0.25 mg mL⁻¹ bovine serum albumin in phosphate buffer pH 8.0) were added to each well. The reaction was started by the addition of acetylthiocholine iodide (2 mM in phosphate buffer). The final test concentrations were 0.5 mM of DTNB and acetylthiocholine iodide, and 0.05 U mL⁻¹ acetylcholinesterase, respectively.

Enzyme kinetics were measured at 405 nm in 30 s intervals in a microplate-reader (MRX Dynatech) for a time period of 5 min. The enzyme activity was expressed as OD min⁻¹ from a linear regression. To avoid false positive results in preliminary tests, it was shown that none of the test substances interacts with the formed thiocholine during the assay (data not shown).

Determination of the lipophilicity parameter k_0

The lipophilicity parameter k_0 of the ionic liquids was derived using a gradient run HPLC method. The method, the theoretical background and the calculation of the log k_0 values were recently described in Ranke *et al.*⁶ Briefly, the HPLC system used for deriving the lipophilicity parameters was a Hewlett Packard system Series 1100, with gradient pump, online degasser, autosampler and a Bruker esquire ESI-MS ion trap detector. The column used was a MetaChem Polaris Ether bridged RP-18 column with 150 mm length, 3 mm inner diameter and 3 μ m particle size. A guard column with octadecylsilica material was also used (both Varian, Inc.). The eluent was composed of 0.25% acetic acid (*p.a.*) in Milipore (TM) water (pH = 3.2), mixed with gradient grade acetonitrile. The column dead time t_0 was calculated from retention time difference of thiourea with and without column. The equipment dwell volume t_D was quantified by switching from water to 0.1 mM NaNO₃ in 10 min. Cation retention times from a single gradient run with a gradient time t_G of 10 min were obtained for all substances listed in Table 2.

Acknowledgements

The authors gratefully thank Marianne Matzke, Tanja Juffernholz and Karen Thiele for helpful discussions. Furthermore, thanks are given to the Merck KgaA for their cooperation in a strategic partnership. Annegret Stark is acknowledged for providing the 1-octyl-quinolinium bromide as well as the Rohm and Haas company for donating the 4,5-dichloro-2-octylisothiazol-3-one.

The first author gratefully thanks the Deutsche Bundesstiftung Umwelt for funding the work with a PhD scholarship.

References

- 1 http://ec.europa.eu/environment/chemicals/reach/reach_intro.htm, 2007.
- 2 B. Jastorff, R. Störmann and U. Wölke, *Struktur-Wirkungs-Denken in der Chemie*, Universitätsverlag Aschenbeck & Isensee, Bremen, Oldenburg, 2004, pp. 15–150.
- 3 B. Jastorff, K. Mölter, P. Behrend, U. Bottin-Weber, J. Filser, A. Heimers, B. Ondruschka, J. Ranke, M. Schaefer, H. Schröder, A. Stark, P. Stepnowski, F. Stock, R. Störmann, S. Stolte, U. Welz-Biermann, S. Ziegert and J. Thöming, *Green Chem.*, 2005, **7**, 362–372.
- 4 B. Jastorff, R. Störmann, J. Ranke, K. Molter, F. Stock, B. Oberheitmann, W. Hoffmann, J. Hoffmann, M. Nuchter, B. Ondruschka and J. Filser, *Green Chem.*, 2003, **5**(2), 136–142.
- 5 M. Matzke, S. Stolte, K. Thiele, T. Juffernholz, J. Ranke, U. Welz-Biermann and B. Jastorff, *Green Chem.*, 2007, DOI: 10.1039/b705795d.
- 6 J. Ranke, F. Stock, A. Müller, S. Stolte, R. Störmann, U. Bottin-Weber and B. Jastorff, *Ecotoxicol. Environ. Saf.*, 2006, **107**, 2183–2206.
- 7 J. L. Anderson, D. W. Armstrong and G. T. Wei, *Anal. Chem.*, 2006, **78**(9), 2892–2902.
- 8 F. Endres, *Eur. J. Chem. Phys. Phys. Chem.*, 2002, **3**(2), 144–154.
- 9 W. M. Liu, C. F. Ye, Q. Y. Gong, H. Z. Wang and P. Wang, *Tribol. Lett.*, 2002, **13**(2), 81–85.
- 10 T. Welton, *Coord. Chem. Rev.*, 2004, **248**(21–24), 2459–2477.
- 11 H. Zhang, J. Wu, J. Zhang and J. S. He, *Macromolecules*, 2005, **38**(20), 8272–8277.
- 12 H. Zhao, *J. Mol. Cat. B: Enzym.*, 2005, **37**, 16–25.
- 13 J. Ranke, M. Cox, A. Müller, C. Schmidt and D. Beyersmann, *Toxicol. Environ. Chem.*, 2006, **88**(2), 273–285.
- 14 S. Stolte, J. Arning, U. Bottin-Weber, A. Müller, W. R. Pitner, U. Welz-Biermann, B. Jastorff and J. Ranke, *Green Chem.*, 2007, **9**(8), 760–767.
- 15 S. Stolte, M. Matzke, J. Arning, A. Böschen, W. R. Pitner, U. Welz-Biermann, B. Jastorff and J. Ranke, *Green Chem.*, 2007, DOI: 10.1039/b711119c.
- 16 S. Stolte, J. Arning, U. Bottin-Weber, M. Matzke, F. Stock, K. Thiele, M. Uerdingen, U. Welz-Biermann, B. Jastorff and J. Ranke, *Green Chem.*, 2006, **8**(7), 621–629.
- 17 M. H. Fulton and P. B. Key, *Environ. Toxicol. Chem.*, 2001, **20**(1), 37–45.
- 18 J. Massoulie, L. Pezzementi, S. Bon, E. Krejci and F. M. Vallette, *Prog. Neurobiol.*, 1993, **41**(1), 31–91.
- 19 J. M. Chemnitz, R. Sadowski, H. Winkel and R. Zech, *Chem.-Biol. Interact.*, 1999, **120**, 183–192.
- 20 C. Pope, S. Karanth and J. Liu, *Environ. Toxicol. Pharmacol.*, 2005, **19**(3), 433–446.
- 21 K. J. Eder, C. M. Leutenegger, B. W. Wilson and I. Werner, *Mar. Environ. Res.*, 2004, **58**(2–5), 809–813.
- 22 C. J. Rickwood and T. S. Galloway, *Aquat. Toxicol.*, 2004, **67**(1), 45–56.
- 23 J. Keizer, G. Dagostino, R. Nagel, T. Volpe, P. Gnemi and L. Vittozzi, *Sci. Total Environ.*, 1995, **171**(1–3), 213–220.
- 24 J. Kaur and M. Q. Zhang, *Curr. Med. Chem.*, 2000, **7**(3), 273–294.
- 25 M. Harel, D. M. Quinn, H. K. Nair, I. Silman and J. L. Sussman, *J. Am. Chem. Soc.*, 1996, **118**(10), 2340–2346.

- 26 M. Harel, J. L. Hyatt, B. Brumshtein, C. L. Morton, R. M. Wadkins, I. Silman, J. L. Sussman and P. M. Potter, *Chem.-Biol. Interact.*, 2005, **157–158**, 153–157.
- 27 J. L. Sussman, M. Harel, F. Frolow, C. Oefner, A. Goldman, L. Toker and I. Silman, *Science*, 1991, **253**(5022), 872–879.
- 28 F. Stock, J. Hoffmann, J. Ranke, R. Stormann, B. Ondruschka and B. Jastorff, *Green Chem.*, 2004, **6**(6), 286–290.
- 29 J. Ranke, *R News*, 2006, **3**, 7–12.
- 30 J. Ranke, S. Stolte, R. Störmann, J. Arning and B. Jastorff, *Chem. Rev.*, 2007, **107**(6), 2183–2206.
- 31 M. Harel, I. Schalk, L. Ehret-Sabatier, F. Bouet, M. Goeldner, C. Hirth, P. H. Axelsen, I. Silman and J. L. Sussman, *Proc. Natl. Acad. Sci. U. S. A.*, 1993, **90**(19), 9031–9035.
- 32 Y. Bourne, P. Taylor, Z. Radic and P. Marchot, *EMBO J.*, 2003, **22**(1), 1–12.
- 33 J. P. Colletier, D. Fournier, H. M. Greenblatt, J. Stojan, J. L. Sussman, G. Zaccai, I. Silman and M. Weik, *EMBO J.*, 2006, **25**(12), 2746–2756.
- 34 A. V. Plakhotnyk, L. Ernst and R. Schmutzler, *J. Fluorine Chem.*, 2005, **126**(1), 27–31.
- 35 M. Ponikvar, B. Zemva and J. F. Liebman, *J. Fluorine Chem.*, 2003, **123**(2), 217–220.
- 36 R. P. Swatloski, J. D. Holbrey and R. D. Rogers, *Green Chem.*, 2003, **5**(4), 361–363.
- 37 E. Heilbron, *Acta Chem., Scand.*, 1965, **19**(6), 1333–1346.
- 38 R. M. Krupka, *Mol. Pharmacol.*, 1966, **2**(6), 558–569.

Textbooks from the RSC

The RSC publishes a wide selection of textbooks for chemical science students. From the bestselling *Crime Scene to Court*, 2nd edition to groundbreaking books such as *Nanochemistry: A Chemical Approach to Nanomaterials*, to primers on individual topics from our successful *Tutorial Chemistry Texts series*, we can cater for all of your study needs.

Find out more at www.rsc.org/books

Lecturers can request inspection copies – please contact sales@rsc.org for further information.



Registered Charity No. 207890

RSC Publishing

www.rsc.org/books

Solvent-free Heck reaction catalyzed by a recyclable Pd catalyst supported on SBA-15 *via* an ionic liquid

Xiumin Ma, Yinxi Zhou, Jicheng Zhang, Anlian Zhu, Tao Jiang* and Buxing Han*

Received 16th August 2007, Accepted 2nd October 2007

First published as an Advance Article on the web 19th October 2007

DOI: 10.1039/b712627a

Heck arylation of olefins with aryl halides was carried out in solvent-free conditions with a Pd catalyst supported on 1,1,3,3-tetramethylguanidinium (TMG)-modified molecular sieve SBA-15 (designated as SBA-TMG-Pd). SBA-TMG-Pd was much more active and stable than a Pd catalyst supported on pristine SBA-15 (designated as SBA-Pd). The catalysts were characterized by Fourier transform infrared spectroscopy (FT-IR), X-ray photoelectron spectroscopy (XPS), and transmission electron microscopy (TEM), and the reasons for the excellent performance of catalyst SBA-TMG-Pd were also discussed.

Introduction

The palladium-catalyzed coupling of olefins with aryl or vinyl halides, known as the Heck reaction, is one of the most powerful methods to form a new carbon-carbon (Csp²-Csp²) bond in modern synthetic chemistry. The Heck reaction provides a direct route to assemble important arylated and vinylated olefins, and its wide functional group tolerance on both reactants allows the convenient application at a late stage of total synthesis without protecting groups. Since its discovery¹ by Heck and Mizoroki *et al.* in the late 1960s, the reaction has been extensively studied² and applied to a wide variety of fields, such as natural product synthesis,³ material science,⁴ and bioorganic chemistry.⁵ A major transformation in the Heck reaction is the synthesis of cinnamic acid and its derivatives, which are important intermediates in the synthesis of medical products and commonly used as flavor substances and UV absorbents. The reaction is usually catalyzed by palladium complexes in a homogeneous mode of operation and shares common drawbacks, *i.e.*, catalyst recovery and recycling is difficult. In addition, expensive, generally unstable and toxic ligands, such as phosphine, are required to activate and stabilize Pd against agglomeration and formation of Pd black.⁶ Therefore, cheaper and environmentally benign heterogeneous catalytic systems are attractive, and notable progress has been made in this area. Palladium supported on a diverse array of organic and inorganic materials, such as polymers,⁷ carbon,⁸ metal oxides,⁹ clay,¹⁰ ordered¹¹ or amorphous silicates,¹² and zeolites,¹³ have been developed and used to catalyze the Heck reaction.

Mesoporous SiO₂ are attractive supports due to their advantageous properties, such as excellent chemical and thermal stability, high porosity, large surface area, and high surface concentration of silanols. Ying *et al.*^{11d} reported Pd-grafted molecular sieves MCM-41 that effectively catalyzed heterogeneous Heck reactions. More recently, Crudden *et al.*^{11c}

demonstrated that thiol-modified mesoporous materials (SBA-15-SH) are excellent scavengers for Pd and the Mizoroki-Heck reaction was successfully catalyzed without leaching Pd into the solution.

In recent years, ionic liquids (ILs) have attracted much attention due to their special properties, such as negligible vapor pressure, wide liquid range, excellent chemical stability, high thermal stability, and the strong solvent power for a wide range of organic, inorganic, and polymeric molecules. Many reactions have been carried out in ILs,¹⁴ including the Heck reaction in 1,1,3,3-tetramethylguanidinium IL, without using additional base.^{14c} Recently, ILs immobilized onto solid supports have been used to prepare catalysts. For example, 1-butyl-3-methylimidazolium hexafluorophosphate ([bmim][PF₆]) and 1-butyl-3-methylimidazolium tetrafluoroborate ([bmim][BF₄]) dispersed on silica gel can provide a solvent environment for a Rh complex, resulting in the excellent catalytic activity and stability for hydrogenation.¹⁵ Some functional ILs exhibit a strong ability to stabilize nanoparticles. By immobilizing Pd and Ru nanoparticles on different supports with the assistance of 1,1,3,3-tetramethylguanidinium-based IL, different catalysts have been prepared, which also showed outstanding catalytic performance for the hydrogenation of benzene and olefins.¹⁶ More recently, a series of very effective supported catalysts for different organic reactions have been prepared using different ILs and solid supports.¹⁷

The Heck reaction can be performed in organic solvents, ionic liquids, and CO₂. However, less attention has been paid on the Heck reaction in a solvent-free condition,¹⁸ although it is environmentally benign and economically profitable. Based on the consideration of minimizing the amount of ILs used, avoiding the use of organic solvents, easy recovery of catalyst, in this work, Pd nanoparticles were immobilized on molecular sieves SBA-15 using IL 1,1,3,3-tetramethylguanidinium lactate (TMGL). The Heck reaction was performed in solvent-free conditions with the immobilized Pd catalyst (designated as SBA-TMG-Pd). It is shown that the catalyst has an excellent activity and reusability for the Heck reaction.

Beijing National Laboratory for Molecular Sciences, Institute of Chemistry, Chinese Academy of Sciences, Beijing, 100080, China.
E-mail: Jiangt@iccas.ac.cn; Hanbx@iccas.ac.cn; Fax: +86-10-62562821

Results and discussion

The coupling reaction of iodobenzene with methyl acrylate was used as a model reaction to investigate the catalytic performance of catalyst SBA-TMG-Pd. The influences of bases, solvents, reaction temperature and the catalyst loading on the yield were first investigated. The results are summarized in Table 1. Among the bases examined, Et₃N (Table 1, entry 1) showed the best coupling with the catalyst. Other bases, such as CH₃COONa (Table 1, entry 2), Na₂CO₃ (Table 1, entry 3) and NaOH (Table 1, entry 4) gave moderate yields, probably due to the poor solubility of these solid bases in the reaction system. When NaOH (Table 1, entry 4) was used, cinnamic acid was formed. The possible reason is that the product methyl cinnamate reacted with a trace of H₂O in the reaction system in the presence of the strong base NaOH. The influence of solvents on the reaction was also investigated (Table 1, entries 5 and 6). It can be seen from Table 1 that the solvent-free condition gave the best result. However, the reaction in *N*-methylpyrrolidone (NMP), which is one of the commonly used solvents for the Heck reaction, had a lower yield. When H₂O was used as the solvent, a high total yield was achieved. However, the main product was cinnamic acid, probably due to the reaction of methyl cinnamate with the reaction medium. Results obtained at other conditions also demonstrated that the catalyst is highly efficient for the Heck reaction. The model reaction proceeded smoothly and the yield of (*E*)-methyl cinnamate was 93%, even when the amount of Pd was 0.001 mol% (Table 1, entry 7). As expected, when the reaction temperature was reduced from 140 °C to 120 °C, the reaction time was prolonged from 65 min to 3 h to achieve a high yield (Table 1, entry 8).

The Heck arylation reaction of a variety of vinylic substrates with different functional groups was also investigated using SBA-TMG-Pd as the catalyst in solvent-free conditions, and the results are illustrated in Table 2. It is known that the catalyst is very effective for the reactions with iodobenzene as the arylating agent. For all the olefins examined, moderate to excellent yields were achieved. When monosubstituted vinylic substrates, such as acrylic acid and different acrylate esters, were employed (Table 2, entries 1, 2, 3 and 4), high yields and only *E*-isomers were obtained, which was confirmed by ³J(H-H) = 16 Hz. However, when styrene and acrylonitrile were used, except for the main product, a little of 1,1-diphenyl

ethylene and *Z*-isomer were detected, respectively (Table 2, entries 5 and 9). As for the bulky substrates, such as disubstituted olefins (Table 2, entries 6, 7 and 8), the yields were moderate. When 1-iodonaphthalene and 1-fluoro-4-iodobenzene were used as arylating agents (Table 2, entries 10, 11, 12, 13 and 14), the reaction could also proceed smoothly with high yields. For aryl bromides, the catalyst showed lower activity (Table 2, entries 15 and 16).

Experiments were also conducted to examine the recyclability of SBA-TMG-Pd. As can be seen from Fig. 1, after six repeated catalytic coupling reactions of iodobenzene with methyl acrylate, no obvious deactivation of the catalyst was observed, and the catalyst still remained as a grey powder. For comparison, we examined the reusability of the Pd catalyst supported on SBA-15 in the absence of the IL (designated as SBA-Pd). The results in Fig. 1 indicated that the deactivation of SBA-Pd was obvious. The catalyst was observed to become a white powder after 2 recycles. In other words, SBA-TMG-Pd had a much higher stability, although the catalytic activity of the two catalysts was similar in the first run.

The catalysts were characterized by X-ray photoelectron spectroscopy (XPS). Fig. 2 shows the Pd 3d spectrum of the catalyst. It can be seen that the deconvoluted spectrum showed a doublet for two chemically different Pd entities, with peak binding energies of 335.0 eV (Pd 3d_{5/2}) and 340.25 eV (Pd 3d_{3/2}), which confirmed the presence of Pd⁰ in the catalyst. Moreover, the peak at 336.1 eV suggests the presence of a Pd–O component, which probably resulted from the oxidation of the Pd nanoparticles upon exposure to air.

Fig. 3 shows the transmission electron microscope (TEM) images of the two catalysts. For SBA-TMG-Pd (Fig. 3a), most of Pd nanoparticles existed in the channels of SBA-15, and the diameters of Pd nanoparticles were in the range of 3–6 nm before use. However, for the catalyst SBA-Pd (Fig. 3b), the diameters of most Pd nanoparticles were in the range of 9–12 nm, which is bigger than the pore diameter of SBA-15, resulting in their existence on the outside surface of SBA-15. After six recycles, most Pd nanoparticles on SBA-TMG-Pd still existed in the channel of SBA-15, although some bigger Pd particles were formed (Fig. 3c). For SBA-Pd, after 2 recycles, most of Pd disappeared and few Pd nanoparticles existed on the surface of the support, as can be seen from the micrograph (Fig. 3d). The change of color of the two catalysts further

Table 1 Catalytic results for the Heck reaction between iodobenzene and methyl acrylate

Entry	Bases	Solvents	Temperature/°C	Pd (mol%)	Reaction time	Isolated yields (%)
1	Et ₃ N	—	140	0.01	65 min	91
2	CH ₃ COONa	—	140	0.01	65 min	64
3	Na ₂ CO ₃	—	140	0.01	65 min	60
4 ^a	NaOH	—	140	0.01	65 min	68
5	Et ₃ N	NMP	140	0.01	65 min	82
6 ^b	Et ₃ N	H ₂ O	140	0.01	65 min	92
7	Et ₃ N	—	140	0.001	2 h	93
8	Et ₃ N	—	120	0.01	3 h	92

^a The molar ratio of methyl cinnamate to cinnamic acid is 60 : 40; ^b The molar ratio of methyl cinnamate to cinnamic acid is 38 : 62.

Table 2 Heck reactions of aryl halides with olefins^a

Entry	Aryl halides	Alkenes	Products	Reaction time	Isolated yields (%) (a/b)
1				65 min	91
2				1.5 h	92
3				2 h	93
4 ^b				45 min	94
5			 + (a) + (b)	4 h	90 (95/5)
6 ^c				1.5 h	67
7				3 h	72
8				4.5 h	60
9			 + (a) + (b)	1.5 h	89 (88/12)
10				3.5 h	88
11				1.5 h	90

Table 2 Heck reactions of aryl halides with olefins^a (Continued)

Entry	Aryl halides	Alkenes	Products	Reaction time	Isolated yields (%) (a/b)
12			 + 	4.5 h	85 (80/20)
13				7 h	92
14				60 min	92
15 ^d				15 h	33
16 ^e				8 h	54

^a Reaction conditions: ArI (2 mmol), alkene (2.2 mmol), Et₃N (2.4 mmol), the amount of Pd is (0.01 mol%); ^b ArI (2 mmol), acrylic acid (2.2 mmol), Et₃N (4.4 mmol); ^c ArI (2 mmol), methacrylic acid (2.2 mmol), Et₃N (4.4 mmol); ^d The amount of Pd is 0.05 mol%; ^e The amount of Pd is 0.05 mol%.

confirmed this. The catalyst SBA-TMG-Pd still remained as a grey powder after six recycles. However, SBA-Pd became white powder after 2 recycles.

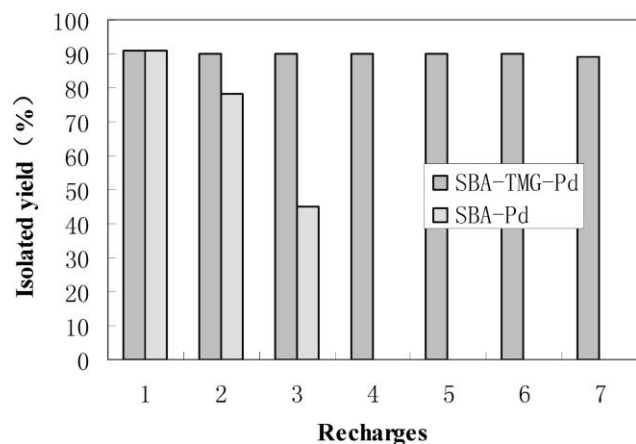


Fig. 1 Recycling of SBA-TMG-Pd and SBA-Pd for the Heck reaction of iodobenzene with methyl acrylate at 140 °C with a reaction time of 50 min each time (the amount of Pd is 0.05 mol%).

The difference of the two catalysts was that ionic liquid TMGL was utilized when preparing SBA-TMG-Pd. The presence of the cation of the ionic liquid in the catalyst

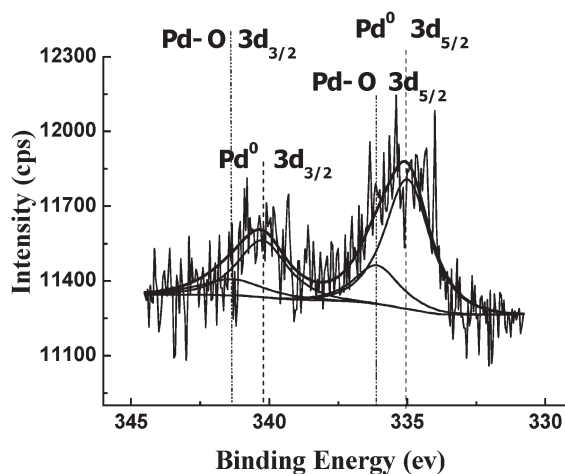


Fig. 2 XPS spectrum of the Pd 3d edge of the SBA-TMG-Pd sample. The vertical lines indicate the peak positions of the binding energies of Pd-O, and Pd.

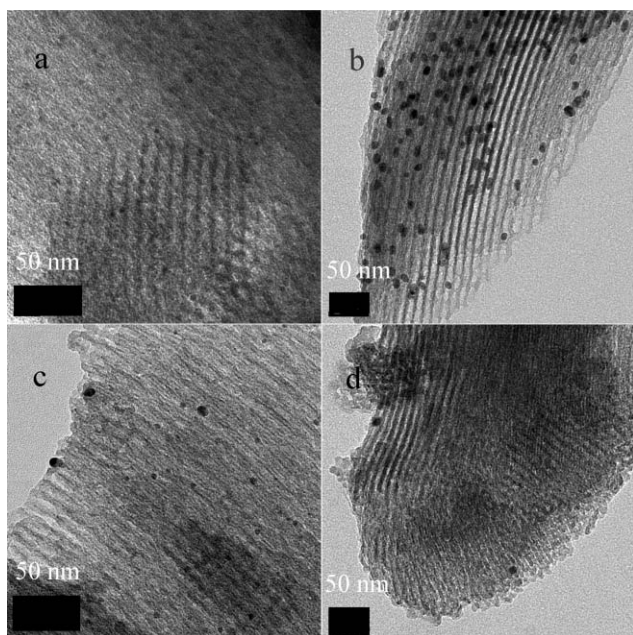


Fig. 3 TEM images of the catalysts (a) SBA-TMG-Pd; (b) SBA-Pd; (c) SBA-TMG-Pd after 6 recycles; (d) SBA-Pd after 2 recycles.

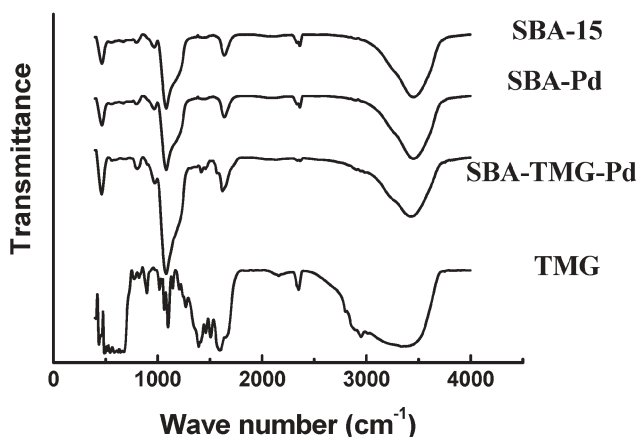
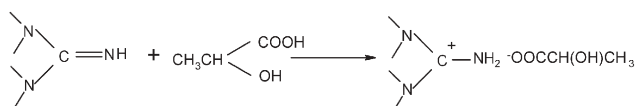


Fig. 4 The FT-IR of SBA-15, 1,1,3,3-tetramethylguanidine (TMG) and the as prepared catalysts.

SBA-TMG-Pd is supported by the fact that the catalyst contained 10 wt% organic compound, as determined by TGA. The existence of the TMG cations was also supported by the FT-IR spectrum (Fig. 4). The characteristic peaks of CH_3 group at 1412 cm^{-1} , 1455 cm^{-1} , and 2944 cm^{-1} , and the peak of the $\text{C}=\text{N}$ bond at 1612 cm^{-1} can be observed in the spectrum of SBA-TMG-Pd. TMG group played an important role in stabilizing the catalyst SBA-TMG-Pd. It is known that guanidine has considerable coordination ability.¹⁹ The reason for the better reusability of SBA-TMG-Pd than SBA-Pd was



Scheme 1 The synthesis of TMGL.

that TMG-modified SBA-15 was a better scavenger for Pd than the pristine SBA-15. After the aryl halides were completely consumed, palladium redeposited on the support with the help of TMG. But for SBA-Pd, most Pd was lost in the reaction solution.

Recently, the mechanism of the catalytic processes of the Heck reaction employing a supported palladium source as the catalyst has been intensely disputed in literature. Some researchers deduced that the catalyst was working in a heterogeneous manner,^{11b,11c,11d,20} while others reported that the support acted merely as a reservoir for a more active soluble form of Pd.^{9,21} In order to study the behavior of the Pd in our catalytic system, a filtration test was carried out using Pd-TMG-SBA as the catalyst in this work. After 25 min (the reaction was completed in 65 min), the reaction mixture was taken out from the autoclave. To ensure that all solid catalyst was separated, the reaction mixture was centrifuged at 16 000 rpm for 30 min. Then, the solid-free filtrate was allowed to continue to react under the same conditions for another 1 h. The results indicated that the reaction continued and iodobenzene was completely consumed. This suggests that the leaching of active palladium species from the solid support occurred during the reaction. However, Pd redeposited back onto the support after the completion of the reaction.^{9,20} This argument was supported by the AAS analysis of the reaction samples. After reaction, SBA-TMG-Pd was separated from the ethanol solution of the reaction mixture, and the solution was collected and analysed by AAS method for Pd metal. Only less than 0.3% Pd of the initially added catalyst was detected. From the whole catalytic process, the catalyst apparently behaved just like a heterogeneous catalyst, which could be recovered and reused facily.

Conclusion

The Pd catalyst immobilized onto SBA-15 by the cations of IL TMGL is a very active and stable catalyst for the Heck coupling reaction. The Heck reaction can be carried out smoothly in solvent-free conditions using the supported Pd catalyst. The yields for the arylated olefins, with respect to reaction time and amount of catalyst, show that the catalyst has excellent activity. It is easy to separate the supported catalyst from the reaction mixture and this catalyst can be reused at least 6 times without considerable deactivation. The cations of the IL is necessary for the excellent stability of the catalyst.

Experimental

Chemicals

1,1,3,3-tetramethylguanidine, lactic acid, tetraethyl orthosilicate, methyl acrylate, ethyl acrylate, *n*-butyl acrylate, acrylic acid, methacrylic acid, methyl methacrylate, ethyl methacrylate, acrylonitrile, styrene, bromobenzene, 1-iodonaphalene, ethyl ether, petroleum ether (with a boiling point range of 60–90 °C) were supplied by Beijing Chemical Reagent Factory. Pluronic P123, iodobenzene, 4'-bromoacetophenone, 1-fluoro-4-iodobenzene were purchased from ACROS organics. 1,1,3,3-tetramethylguanidine was distilled before use. All other chemicals (A. R. grade) were used without further purification.

Apparatus

All the experiments were conducted in a 7 mL stainless steel reactor with a magnetic stirrer in a batch mode. A constant temperature air bath was employed to heat the reactor and its temperature was controlled by a PID temperature controller (model SX/A-1, Beijing Tianchen Electronic Company). The temperature fluctuation of the air bath was ± 0.1 °C. The reactions were monitored by TLC. ^1H NMR spectra were determined in CDCl_3 or $\text{DMSO}-d_6$ on a Bruker 400 MHz spectrometer at room temperature. The morphology of the catalysts was investigated with a transmission electron microscope (TEM, JEOL, JEM-2010). The X-ray photoelectron spectrum of the catalyst was collected on an ESCALab220i-XL spectrometer. The FT-IR spectrum was determined by a Bruker Tensor 27 infrared spectrometer.

Synthesis of ionic liquid TMGL

TMGL was prepared directly by neutralization of 1,1,3,3-tetramethylguanidine with lactic acid at room temperature (Scheme 1).¹⁹

Synthesis of SBA-15

The SBA-15 silica was synthesized using the procedures reported by Zhao *et al.*²² In the experiment, 4.0 g Pluronic P123 was dissolved in 150 g of 1.6 M HCl solution. Then, 8.50 g of tetraethyl orthosilicate (TEOS) was added. The resulting mixture was stirred for 5 min and kept at 35 °C for 24 h without stirring, and then aged for 48 h at 80 °C. The solid product was filtered, and dried in an oven for 4 h at 140 °C. To completely remove organic materials, the as-synthesized product was subsequently calcined at 550 °C for 6 h in the air. The surface area, pore diameter, and pore volume were $750 \text{ m}^2 \text{ g}^{-1}$, 6.3 nm, and $1.1 \text{ cm}^3 \text{ g}^{-1}$, respectively.

Typical procedure to prepare SBA-TMG-Pd or SBA-Pd

The procedures were similar to those for preparing the TMG stabilized Ru catalyst for hydrogenation of benzene.^{16c} In a typical experiment, 21 mg of $\text{Pd}(\text{OAc})_2$ and 0.25 g of TMGL were dissolved in a mixture of THF and methanol (5 mL : 25 mL). Then 1.0 g of SBA-15 was added, and a slurry was obtained. The slurry was dried at 50 °C under vacuum for 2 h to obtain the powder catalytic precursor. The Pd(II) in the powder was reduced by H_2 at 180 °C for 2 h and then heated up to 220 °C for 3 h to remove the anion of the IL. The Pd catalyst designed as SBA-TMG-Pd was obtained as gray powders. The preparation of the catalyst designed as SBA-Pd was similar to that of SBA-TMG-Pd. The only difference was that TMGL was not employed to functionalize the SBA-15 silica for SBA-Pd.

General procedures for Heck reaction

The Heck reaction was carried out in a 7 mL stainless steel autoclave with a magnetic stirrer. In a typical experiment, aryl halide (2 mmol), vinylic substrate (2.2 mmol), triethylamine (2.4 mmol) and 2 mg of Pd catalyst were added into the

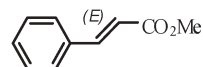
stainless steel autoclave. Then the reactor was sealed and placed in the constant temperature air bath under vigorous stirring. After a desired time, the autoclave was cooled by ice water. Workup was accomplished by adding the reaction mixture into 2 N HCl, followed by extraction with ethyl ether and TLC analysis. After drying and removal of the volatiles from the organic layer, the product was purified by column chromatography on silica gel with ethyl ether, petroleum ether or their mixtures as the eluent, depending on the structure of the products.

Recycling procedure of SBA-TMG-Pd or SBA-Pd

In the recycling experiment, iodobenzene (10 mmol), methyl acrylate (11 mmol), triethylamine (12 mmol) and 50 mg of Pd catalyst (the mole ratio of Pd to iodobenzene was 0.05%) were added into the reactor. After 50 min, the reaction was completed. The catalyst was separated by filtration and washed with ethanol several times. Then the catalyst was dried at 50 °C under vacuum for 3 h. The catalyst was reused in the next run without any regeneration.

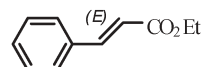
The ^1H NMR datum of the products are presented below

1



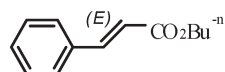
(E) - methyl cinnamate (CDCl_3 , 400 MHz, ppm): 7.70 (d, J = 16.0 Hz, 1H), 7.54–7.52 (m, 2H), 7.40–7.38 (m, 3H), 6.45 (d, J = 16.1 Hz, 1H), 3.81 (s, 3H);

2



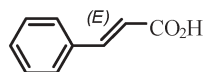
(E) - ethyl cinnamate (CDCl_3 , 400 MHz, ppm): 7.69 (d, J = 16.0 Hz, 1H), 7.53–7.51 (m, 2H), 7.39–7.37 (m, 3H), 6.44 (d, J = 16.0 Hz), 4.27 (q, J = 7.1 Hz, 2H), 1.33 (t, J = 7.1 Hz, 3H);

3



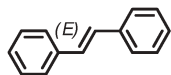
(E) - n-butyl cinnamate (CDCl_3 , 400 MHz, ppm): 7.68 (d, J = 16.0 Hz, 1H), 7.53–7.50 (m, 2H), 7.38–7.36 (m, 3H), 6.44 (d, J = 16.0 Hz, 1H), 4.20 (t, J = 6.7 Hz, 2H), 1.68 (m, 2H), 1.43 (m, 2H), 0.96 (t, J = 7.4 Hz, 3H);

4



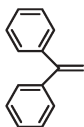
(E) - cinnamate acid (CDCl_3 , 400 MHz, ppm): 7.80 (d, J = 16.0 Hz, 1H), 7.58–7.55 (m, 2H), 7.44–7.40 (m, 3H), 6.47 (d, J = 16.0 Hz, 1H);

5



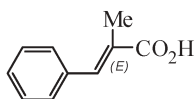
(E) - Trans-stilbene (CDCl₃, 400 MHz, ppm): 7.52 (d, 4H), 7.39–7.34 (t, 4H), 7.29–7.24(m, 2H), 7.12 (s, 2H);

6



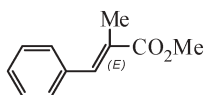
1, 1-Diphenylethylene (CDCl₃, 400 MHz, ppm): 7.34–7.20 (m, 10H), 5.46 (s, 2H);

7



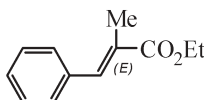
(E) - α -methylcinnamic acid (CDCl₃, 400 MHz, ppm): 11.80 (s, 1H), 7.82 (s, 1H), 7.43–7.21 (m, 5H), 2.14 (s, 3H);

8



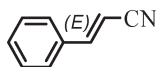
(E) - Methyl α -methylcinnamate (CDCl₃, 400 MHz, ppm): 7.70 (s, 1H), 7.40–7.21 (m, 5H), 3.82 (s, 3H), 2.11 (s, 3H);

9



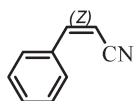
(E) - Ethyl α -methylcinnamate (CDCl₃, 400 MHz, ppm): 7.69 (s, 1H), 7.40–7.21 (m, 5H), 4.21 (q, J = 7.1 Hz, 2H), 2.12 (s, 3H), 1.35 (t, J = 7.1 Hz, 3H);

10



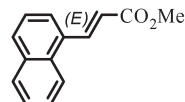
(E) - cinnamionitrile (CDCl₃, 400 MHz, ppm): 7.44–7.40 (m, 5H), 7.38 (d, J = 16.6 Hz, 1H), 5.87 (d, J = 16.6 Hz, 1H);

11



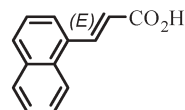
(Z) - cinnamionitrile (CDCl₃, 400 MHz, ppm): 7.43–7.40 (m, 5H), 7.13 (d, J = 12.1 Hz, 1H), 5.44 (d, J = 12.1 Hz, 1H);

12



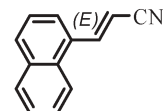
(E) - methyl 3-(1-naphthyl) acrylate (CDCl₃, 400 MHz, ppm): 8.53 (d, J = 15.7 Hz, 1H), 8.19 (d, J = 8.3 Hz, 1H), 7.90–7.83 (m, 2H), 7.74 (d, J = 7.2 Hz, 1H), 7.60–7.45 (m, 3H), 6.53 (d, J = 15.7 Hz, 1H), 3.84 (s, 3H);

13



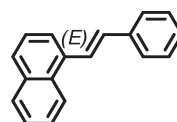
(E) - 3-(1-naphthyl) acrylic acid (d₆-DMSO, 400 MHz, ppm): 12.55 (s, 1H), 8.39 (d, J = 15.7 Hz, 1H), 8.21–7.55(m, 7H), 6.60 (d, J = 15.7 Hz, 1H);

14



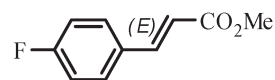
(E) - 3-(1-naphthyl) acrylonitrile (CDCl₃, 400 MHz, ppm): 8.35 (d, J = 16.4 Hz, 1H), 8.10–7.36 (m, 7H), 6.08 (d, J = 16.4 Hz, 1H);

15



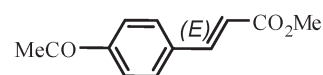
(E) - 1-styrylnaphthalene (CDCl₃, 400 MHz, ppm): 8.21 (d, J = 8.0 Hz, 1H), 7.91 (d, J = 16.0 Hz, 1H), 7.89–7.11 (m, 11H), 7.09 (d, J = 16.0 Hz, 1H);

16



(E) - methyl 3-(4-fluorophenyl) acrylate (CDCl₃, 400 MHz, ppm): 7.65 (d, J = 16.0 Hz, 1H), 7.51 (m, 2H), 7.07 (t, J = 8.4 Hz, 2H), 6.36 (d, J = 16.0 Hz, 1H), 3.80 (s, 3H);

17



(E) - methyl 3-(4-acetophenonyl) acrylate (CDCl₃, 400 MHz, ppm): 7.98 (d, J = 8.0 Hz, 2H), 7.72 (d, J = 16.0 Hz, 1H), 7.62 (d, J = 8.0 Hz, 2H), 6.53 (d, J = 16.0 Hz, 1H), 3.83 (s, 3H), 2.64 (s, 3H).

Acknowledgements

We sincerely acknowledge the financial supports from National Natural Science Foundation of China (20332030, 20473105) and State Key Laboratory of Coal Conversion (06-905).

References

- (a) R. F. Heck, *J. Am. Chem. Soc.*, 1969, **91**, 6707–6714; (b) Y. Fujiwara, I. Moritani, S. Danno, R. Asano and S. Teranishi, *J. Am. Chem. Soc.*, 1969, **91**, 7166–7169.
- (a) A. M. Trzeciak and J. J. Ziółkowski, *Coordin. Chem. Rev.*, 2007, **251**, 1281–1293; (b) A. Biffis, M. Zecca and M. Basato, *J. Mol. Catal. A: Chem.*, 2001, **173**, 249–274; (c) I. P. Beletskaya and A. V. Cheprakov, *Chem. Rev.*, 2000, **100**, 3009–3066; (d) R. F. Heck, in *Comprehensive Organic Synthesis*, ed. B. M. Trost, Pergamon, New York, 1991, vol. 4, ch. 4.3, pp. 833–863.
- (a) T. Mizutani, S. Honzawa, S. Tosaki and M. Shibasaki, *Angew. Chem., Int. Ed.*, 2002, **41**, 4680–4682; (b) J. T. Link and L. E. Overman, in *Metal-Catalyzed Cross-Coupling Reaction*, ed. F. Diederich and P. J. Stang, Wiley-VCH, Weinheim, Germany, 1998, ch. 6, pp. 231–269.
- (a) L. F. Tietze, G. Ketschau, U. Heuschert and G. Nordmann, *Chem. Eur. J.*, 2001, **7**, 368–373; (b) *Step-Growth Polymers for High-Performance Materials*, ed. J. K. Hedrick and J. W. Labadie, ACS Symposium Series 624, American Chemical Society, Washington, DC, 1996, ch. 1, pp. 29–31; ch. 2, pp. 58–62; ch. 4, pp. 90–91.
- (a) A. Haberli and C. J. Leumann, *Org. Lett.*, 2001, **3**, 489–492; (b) T. R. Burke, Jr., D. G. Liu and Y. Gao, *J. Org. Chem.*, 2000, **65**, 6288–6291.
- (a) C. Amatore, B. Godin, A. Jutand and F. Lemaître, *Chem. Eur. J.*, 2007, **13**, 2002–2011; (b) A. F. Littke and G. C. Fu, *J. Am. Chem. Soc.*, 2001, **123**, 6989–7000.
- (a) N. Panziera, P. Pertici, L. Barazzzone, A. M. Caporusso, G. Vitulli, P. Salvadori, S. Borsacchi, M. Geppi, C. A. Veracini, G. Martra and L. Bertineti, *J. Catal.*, 2007, **246**, 351–361; (b) C. A. Lin and F. T. Luo, *Tetrahedron Lett.*, 2003, **44**, 7565–7568.
- (a) F. Y. Zhao, M. Shirai, Y. Ikushima and M. Arai, *J. Mol. Catal. A: Chem.*, 2002, **180**, 211–219; (b) R. G. Heidenreich, K. Köhler, J. G. E. Krauter and J. Pietsch, *Synlett*, 2002, 1118–1122; (c) H. Yoon, S. Ko and J. Jang, *Chem. Commun.*, 2007, 1468–1470.
- S. S. Pröckl, W. Kleist, M. A. Gruber and K. Köhler, *Angew. Chem., Int. Ed.*, 2004, **43**, 1881–1882.
- (a) Z. H. Zhang and Z. Y. Wang, *J. Org. Chem.*, 2006, **71**, 7485–7487; (b) H. Zhou, G. L. Zhuo and X. Z. Jiang, *J. Mol. Catal. A: Chem.*, 2006, **248**, 26–31.
- (a) A. Papp, G. Galbacs and R. Molnar, *Tetrahedron Lett.*, 2005, **46**, 7725–7728; (b) L. Li, J. L. Shi and J. N. Yan, *Chem. Commun.*, 2004, 1990–1991; (c) C. M. Crudden, M. Sateesh and R. Lewis, *J. Am. Chem. Soc.*, 2005, **127**, 10045–10050; (d) C. P. Mehnert, D. W. Weaver and J. Y. Ying, *J. Am. Chem. Soc.*, 1998, **120**, 12289–12296; (e) M. Z. Cai, Q. H. Xu and J. W. Jiang, *J. Mol. Catal. A: Chem.*, 2006, **260**, 190–196.
- (a) L. Huang, Z. Wang, T. P. Ang, J. Tan and P. K. Wong, *Catal. Lett.*, 2006, **112**, 219–225; (b) K. Okubo, M. Shirai and C. Yokoyama, *Tetrahedron Lett.*, 2002, **43**, 7115–7118.
- (a) N. Ren, Y. H. Yang, Y. H. Zhang, Q. R. Wang and Y. Tang, *J. Catal.*, 2007, **246**, 215–222; (b) L. Djakovitch and K. Koehler, *J. Am. Chem. Soc.*, 2001, **123**, 5990–5999.
- (a) T. Welton, *Coordin. Chem. Rev.*, 2004, **248**, 2459–2477; (b) J. Dupont, R. F. de Souza and P. A. Z. Suarez, *Chem. Rev.*, 2002, **102**, 3667–3692; (c) S. Li, Y. Lin, H. Xie, S. Zhang and J. Xu, *Org. Lett.*, 2006, **8**(3), 391–394.
- C. P. Mehnert, E. J. Mozeleski and R. A. Cook, *Chem. Commun.*, 2002, 3010–3011.
- (a) J. Huang, T. Jiang, H. X. Gao, B. X. Han, Z. M. Liu, W. Z. Wu, Y. H. Chang and G. Y. Zhao, *Angew. Chem., Int. Ed.*, 2004, **43**, 1397–1399; (b) S. D. Miao, Z. M. Liu, B. X. Han, J. Huang, Z. Y. Sun, J. L. Zhang and T. Jiang, *Angew. Chem., Int. Ed.*, 2006, **45**, 266–269; (c) J. Huang, T. Jiang, B. X. Han, W. Z. Wu, Z. M. Liu, Z. L. Xie and J. L. Zhang, *Catal. Lett.*, 2005, **103**, 59–62.
- (a) Y. L. Gu, C. Ogawa, J. Kobayashi, Y. Mori and S. Kobayashi, *Angew. Chem., Int. Ed.*, 2006, **45**, 7217–7220; (b) M. R. Castillo, L. Fousse, J. M. Fraile, J. I. García and J. A. Mayoral, *Chem. Eur. J.*, 2006, **13**, 287–291.
- (a) N. E. Leadbeater, V. A. Williams, T. M. Barnard and M. J. Collins, *Synlett*, 2006, 2953–2958; (b) A. DiazOrtiz, P. Prieto and E. Vazquez, *Synlett*, 1997, 269–270.
- H. X. Gao, B. X. Han, J. C. Li, T. Jiang, Z. M. Liu, W. Z. Wu, Y. H. Chang and J. M. Zhang, *Synth. Commun.*, 2004, **34**, 3083–3089.
- (a) N. T. S. Phan, D. H. Brown, H. Adams, S. E. Spey and P. Styring, *Dalton Trans.*, 2004, 1348–1357; (b) M. T. Reetz and G. Lohmer, *Chem. Commun.*, 1996, 1921–1922; (c) A. Papp, K. Miklós, P. Forgo and A. Molnár, *J. Mol. Catal. A: Chem.*, 2005, **229**, 107–116.
- (a) M. Weck and C. W. Jones, *Inorg. Chem.*, 2007, **46**, 1865–1875; (b) K. Köhler, W. Kleist and S. S. Prockl, *Inorg. Chem.*, 2007, **46**, 1876–1883; (c) C. C. Cassol, A. P. Umpierre, G. Machado, S. I. Wolke and J. Dupont, *J. Am. Chem. Soc.*, 2005, **127**, 3298–3299.
- D. Y. Zhao, J. L. Feng, Q. S. Huo, N. Melosh, G. H. Fredrickson, B. F. Chmelka and G. D. Stucky, *Science*, 1998, **278**, 548–552.

Influence of anions on the toxic effects of ionic liquids to a phytoplankton *Selenastrum capricornutum*

Chul-Woong Cho,^a Thi Phuong Thuy Pham,^a You-Chul Jeon^b and Yeung-Sang Yun^{*ac}

Received 12th April 2007, Accepted 8th October 2007

First published as an Advance Article on the web 26th October 2007

DOI: 10.1039/b705520j

Investigations on the influence of anions of ionic liquids, with respect to toxicity and ecotoxicity, have been reported; however, no consistent conclusion has been drawn. The aim of this study was to elucidate the influence of the anionic component, using the alga *Selenastrum capricornutum*, by assessing the toxicity of various anions associated with imidazolium-based ionic liquids as well as alkali salts. Additionally, the hydrolysis of fluoride-containing ionic liquids, *i.e.*, 1-butyl-3-methylimidazolium [BMIM], incorporated with tetrafluoroborate, hexafluorophosphate and hexafluoroantimonate, was also estimated. The results obtained revealed that imidazolium-based ionic liquids were more toxic than their corresponding alkali salts. In both cases, SbF_6^- and PF_6^- were identified as the most toxic anions. In general, *Selenastrum capricornutum* was sensitive to the anion moieties in the order: $\text{SbF}_6^- > \text{PF}_6^- > \text{BF}_4^- > \text{CF}_3\text{SO}_3^- > \text{C}_8\text{H}_{17}\text{OSO}_3^- > \text{Br}^- \approx \text{Cl}^-$. With regard to the hydrolytic effect, [BMIM][SbF_6] generated a greater amount of fluoride compared with [BMIM][BF_4], but no fluoride formation occurred with the hexafluorophosphate.

Introduction

Room temperature ionic liquids are a class of non-molecular ionic solvents with low melting points. They are usually composed of asymmetrically substituted nitrogen-containing cations (*e.g.*, imidazole, pyridine, pyrrolidine and ammonium) or a phosphorus-containing cation (*e.g.*, phosphonium) with organic or inorganic anions. The physicochemical properties of ionic liquids (ILs) include non-volatility, non-flammability, high thermal, chemical and electrochemical stability, and the ability to be easily recycled, with favourable solvation behaviour (many organic, organometallic and inorganic compounds can be dissolved in ILs).^{1–4} Furthermore, it is possible to tune the physical and chemical properties of ILs by varying the nature of the anions and cations;⁵ in this way, they can be made task-specific.

Recently, ILs have gained considerable attention in several branches of the chemical industry as potential “green” substitutes for conventional organic solvents.^{6,7} The “green” aspect of ILs is mainly derived from their undetectable vapour pressure, as this decreases the risk of exposure and loss of solvent by evaporation, thereby reducing air pollution. However, these green credentials are currently unproven in aquatic environments, since the water solubility of many ILs is not negligible.⁸ As their popularity with industrial chemists increases, the probability that ILs will find their way into

watercourses through effluent discharges or accidental spills will also increase and they may affect the aquatic environment for a long time because of their poor biodegradability. According to Jastorff *et al.*,⁹ the toxicity of ILs is roughly driven by the head group, the side chain, and the anion. Currently, the biological effects of ILs have attracted considerable attention, resulting in increasing reports which have dealt mainly with the influence of the alkyl side chain length of various ILs head groups. Pernak *et al.* pointed out that their antimicrobial activity increased with increasing alkyl chain length on pyridinium, imidazolium and quaternary ammonium salts.^{10–14} Similar phenomena were also observed for enzyme acetylcholinesterase,¹⁵ the marine bacterium *Vibrio fischeri*,^{16,17} mammalian cells,¹⁶ human cell HeLa¹⁸ and higher organisms, including the soil nematode *Caenorhabditis elegans*,¹⁹ as well as the freshwater snail *Physa acuta*.²⁰ However, with respect to the influence of anions, no consistent conclusion has been obtained from previous investigations. Some studies have reported that varying the anion had minimal effects on the toxicities of several pyridinium and imidazolium compounds, and indicated that the toxicity of IL was largely driven by the alkyl chain branching and hydrophobicity of the cation.^{12,16,21,22} In the meantime, others have suggested that the counter-anion contributed significantly to their toxicity.^{18,23,24} In particular, some ILs with fluoride-containing anions were suggested to be relatively toxic because the anions were hydrolysed to fluoride in the aqueous solution and the fluoride had a toxic effect.^{18,23} However, in-depth studies on this hydrolysis of fluoride-containing anions and their effect on the toxicity were insufficient to explain the inhibitory effect of ILs.

The toxicity of ILs towards aquatic organisms, such as fish and invertebrates, has been extensively studied,^{9,21,24,25} but the influence of ILs on freshwater green algae has rarely been

^aDepartment of Bioprocess Engineering, Chonbuk National University, Chonbuk 561-756, Korea. E-mail: ysyun@chonbuk.ac.kr (Y.-S. Yun); Fax: +82-63-270-2306; Tel: +82-63-270-2308

^bCentral Research Institute of HYOSUNG Group, Kyeounggi 431-080, Korea

^cDivision of Environmental and Chemical Engineering and Research Institute of Industrial Technology, Chonbuk National University, Chonbuk 561-756, Korea. E-mail: ysyun@chonbuk.ac.kr (Y.-S. Yun); Fax: +82-63-270-2306; Tel: +82-63-270-2308

investigated and remains largely unknown. As algae are primary producers, either directly or indirectly, of organic matter required by small consumers in freshwater food chains, their ecology is crucial in providing the energy for sustaining other higher trophic levels. The widespread distribution of algae makes these organisms ideal for toxicological studies and, because they have a short life cycle, they can respond quickly to environmental change.^{26,27} In addition, algal assays are relatively simple, quick and inexpensive compared with bioassays using other organisms.²⁸ Thus, test procedures using algae are of advantage when used as biological assay tools for environmental impact studies.

In this paper, the influence of anions on the toxicity of ILs towards the freshwater green alga *Selenastrum capricornutum* (recently changed to *Pseudokirchneriella subcapitata*) was investigated based on the US Environmental Protection Agency (US EPA) standard²⁹ and Organization for Economic Cooperation and Development (OECD)³⁰ protocols. The hydrolytic effects of typical anions, BF_4^- , PF_6^- and SbF_6^- , were also assessed using ion chromatography.

Results and discussion

Influence of anions on toxicity of ionic liquid entities

The influence of ILs on the growth of *S. capricornutum* was estimated in relation to the toxic effect, with the relative activity defined as the ratio of the cell concentration of the treatment sample to that of the control. Fig. 1 demonstrates the growth inhibition of *S. capricornutum* during 96 h exposure to different concentrations of ILs added to the media. The pattern of algal cell inhibition was similar for all the ILs tested, regardless of the compound used. As is summarized in Table 1, the EC50 values obtained ranged from 135 to 2884 μM , indicating that the most toxic compound was [BMIM][SbF₆]. Fig. 1 reveals that the inhibitory effect on the algal growth rate became stronger with increasing IL concentration. Additionally, the entire dose-response curve of [BMIM][SbF₆]

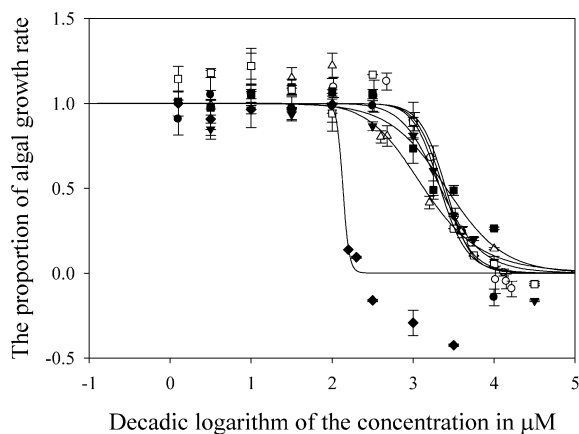


Fig. 1 Influence of anions with respect to 1-butyl-3-methylimidazolium-based ionic liquids on the alga *Selenastrum capricornutum*. [BMIM][BF₄] (●), [BMIM][Cl] (○), [BMIM][C₈H₁₇OSO₃] (▼), [BMIM][PF₆] (▽), [BMIM][CF₃SO₃] (■), [BMIM][Br] (□) and [BMIM][SbF₆] (◆). Error bars correspond to standard deviations of the experimental data.

Table 1 The effective concentrations of various ionic liquids and alkali salts to the alga, *Selenastrum capricornutum*, in 96-h chronic toxicity tests

Chemicals	EC50/ μM	Standard deviation/ μM
[BMIM][Br]	2137	1621–2818
[BMIM][Cl]	2884	2529–3289
[BMIM][BF ₄]	2512	2018–3126
[BMIM][PF ₆]	1318	954–1819
[BMIM][CF ₃ SO ₃]	2188	1828–2618
[BMIM][C ₈ H ₁₇ SO ₄]	2239	1914–2618
[BMIM][SbF ₆]	135	102–178
[NaCl]	125 892	84 723–187 068
[NaBr]	91 201	51 168–162 555
[NaBF ₄]	4466	4037–4943
[NaPF ₆]	1698	1189–2427
[KSBF ₆]	162	88.3–297.9
[KF]	40 738	35 810–46 345
[NaCF ₃ SO ₃]	5248	1047–26 303
[NaC ₈ H ₁₇ OSO ₃]	10 889	9016–13 152
Methanol	707 945	588 843–851 138
DMF	23 442	17 378–31 622
2-Propanol	194 984	147 253–269 153

was observed to shift to the left compared with those of the other ILs. Therefore, the imidazolium-based ILs, with SbF_6^- as the counter-anion, obviously drastically reduced the algal cell density, resulting in low EC50 values. In addition to [BMIM][SbF₆], [BMIM][PF₆] also exhibited slightly enhanced inhibition of the algal cell proliferation at an effective concentration of 1318 μM . With respect to the other ILs, the concentration-response curves showed no remarkable differences, but for those associated with chloride, bromide and hexafluorophosphate, at low concentrations, the *S. capricornutum* culture was recovered to attain a final density close to, or even higher than, the initial value. The aforementioned hormetic effect (*i.e.*, stimulatory effects occurring in response to low levels of exposure to agents harmful at high levels of exposure) depends both on the nature of the organism and the duration of exposure. Similar phenomena were also observed by Ranke *et al.* and Stepnowski *et al.*^{16,18} during their investigations on the toxicity of ILs towards IPC-81 leukaemia cells and HeLa cells, respectively. Considering [BMIM][CF₃SO₃] and [BMIM][C₈H₁₇OSO₃], their effective concentrations were identical and not significantly different from those of ILs combined with bromide, chloride as well as tetrafluoroborate.

In the toxicity experiment using imidazolium-based ILs the toxicity of the ILs containing halide anions was not remarkable, except for the cases of [BMIM][SbF₆] and [BMIM][PF₆]. This also accords with the earlier observation by Garcia *et al.*, and Zhao *et al.*,^{31,32} which showed that the nature of the inorganic anion has only a little effect. The toxicity of common organic solvents (methanol, dimethylformamide and 2-propanol) that have been widely used was explored for comparison with that of ILs on same alga. The toxicities of these solvents were estimated to be two to five orders of magnitude less than those of ILs (Table 1). Of the tested solvents, dimethylformamide was the most toxic compound with an effective concentration ranging between 17.4 and 31.6 mM, which was approximately 8 times higher compared with that of the least toxic IL ([BMIM][Cl]) in this study.

Influence of anions on toxicity of alkali salts

In order to explore the influence of the anionic compartment of the ILs, a reference group of sodium and potassium salts, with various anions, was also subjected to the toxicity assay, the results of which are presented in Table 1. As is shown in Fig. 2, the influence of anions was apparently easier to recognize compared with that obtained for ILs. From the results, SbF_6^- and PF_6^- were observed to be responsible for the strongest inhibition to alga growth, with effective concentrations of 162 and 1698 μM , respectively. These findings were in line with the IL data mentioned above, where SbF_6^- and PF_6^- as the counter-anions evidently caused serious algal growth inhibition after 96 h of exposure. With respect to BF_4^- and CF_3SO_3^- , their EC_{50} values were not significantly different in respect of the inhibitory effects towards the algal cell density. However, as can be deduced from the graph pattern, BF_4^- dramatically inhibited the algal growth at concentrations between 2511 and 5011 μM , while the toxic influence of CF_3SO_3^- gradually increased with increasing concentration and remained unchanged at concentrations above 10 mM. In the case of typical halogen atoms, Br^- was found to affect the algal growth at concentrations between 1 and 10 mM. However, both Br^- and Cl^- exhibited similar toxic effects, with EC_{50} values around 0.1 M. Additionally, Br^- and Cl^- were identified as the least toxic of the anions of the compounds tested on the growth rate of *S. capricornutum*. Especially in our study on Na^+ or K^+ -based salts, the results demonstrated that $\text{C}_8\text{H}_{17}\text{SO}_4^-$ exhibited higher toxicity towards freshwater green algae than the corrosive F^- and Cl^- . This was contrary to results found by Wasserscheid *et al.*,³³ who suggested that the imidazolium cation incorporated with octyl sulfate was “greener” than typical ILs consisting of halogen containing anions, as the presence of halogen atoms may be the cause of serious concerns. In detail, it was approximately 10 times more toxic than the halide anions, Br^- and Cl^- , but less toxic than the other anions.

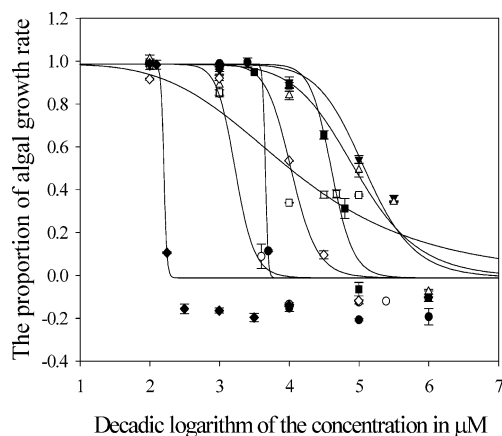
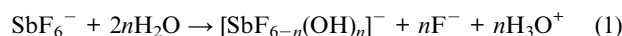


Fig. 2 Influence of anions with respect to sodium and potassium salts on the alga *Selenastrum capricornutum*. $[\text{NaBF}_4]$ (\bullet), $[\text{NaPF}_6]$ (\circ), $[\text{NaCl}]$ (\blacktriangledown), $[\text{NaBr}]$ (\triangledown), $[\text{KF}]$ (\blacksquare), $[\text{NaCF}_3\text{SO}_3]$ (\square), $[\text{NaC}_8\text{H}_{17}\text{OSO}_3]$ (\diamond) and $[\text{KSbF}_6]$ (\blacklozenge). Error bars correspond to standard deviations of the experimental data.

Hydrolysis of SbF_6^- , BF_4^- and PF_6^- associated with [BMIM] cations and fluoride effect on algal growth

In order to assess the hydrolysis of ILs leading to fluoride formation, ion chromatography analysis was performed on imidazolium salts combined with fluoride-containing anions, such as BF_4^- , PF_6^- and SbF_6^- . The experiments were conducted continuously for a 9-day period. Each IL compound was prepared by dissolving in a sufficient amount of distilled water to yield a concentration of 7 mM; the experimental data obtained are shown in Fig. 3. Additionally, $[\text{KF}]$ was also tested to find the toxic effect of fluoride on algal growth. As is illustrated in Fig. 3, fluoride was rapidly generated from $[\text{BMIM}][\text{SbF}_6]$ during the first 2 days, but the formation was retarded during the following days. This was in accordance with results found by Griffiths and Walrafen³⁴, who reported that the first step of SbF_6^- hydrolysis was virtually instantaneous. In principle, the extent of the hydrolysis reaction can be followed as a function of time by determining the fluoride ions formed in the reaction outlined in eqn. (1):



With regard to hexafluorophosphate, several researchers^{18,35,36} have dealt with the instability of PF_6^- containing ILs. In this study, however, an equivocal outcome was observed for the fluoride formation during the hydrolysis of PF_6^- moiety at ambient temperature, which was totally in agreement with results found by Villagrán *et al.*³⁷ However, considerable care should be taken when hexafluorophosphate-containing compounds are applied to industrial processes, as significant potential problems might occur due to their decomposition at high temperature.³⁸ In the case of $[\text{BMIM}][\text{BF}_4]$, the formation of fluoride was easy to observe, but the reaction rate as well as the amount of fluoride generated were less than those with $[\text{BMIM}][\text{SbF}_6]$. Considering the biological impact of fluoride ions, it was evident that F^- , with an effective concentration of 40.7 mM (Table 1), was a more toxic halide ion than the other halides examined.

In order to investigate the effect of the generated fluoride, the amount of fluoride formed by the hydrolysis of

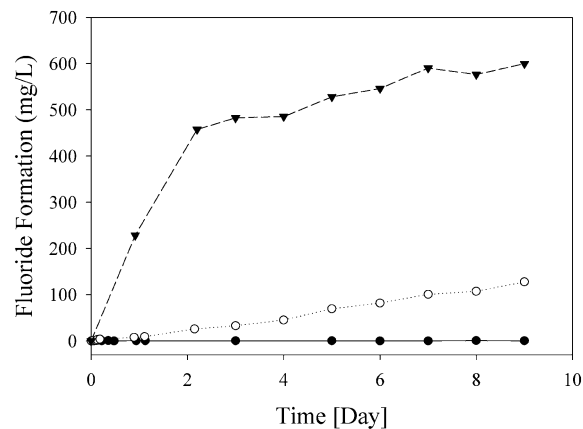


Fig. 3 Time variation of the formation of fluoride ions during the hydrolysis of $[\text{BMIM}][\text{SbF}_6]$ (\blacktriangledown), $[\text{BMIM}][\text{BF}_4]$ (\circ), and $[\text{BMIM}][\text{PF}_6]$ (\bullet) in water.

[BMIM][SbF₆] after 96 h was compared with the EC₅₀ value of [KF]. The fluoride concentration formed from the EC₅₀ concentration of [BMIM][SbF₆], and that proportionally calculated for [KSbF₆], were less than the EC₅₀ value of [KF]. Therefore, the fluoride formed by hydrolysis of [BMIM][BF₄] and [BMIM][SbF₆] might not affect the algal proliferation for 96 hours. However, because with increasing time, the formation of fluoride was observed to steadily increase, a re-experiment on the toxicity of [BMIM][BF₄] was performed on stock solution prepared 6 months before. The re-experiment was performed on 6-month old stock solution, not simply the exact same experiment re-done six months later. As a result, the toxicity was observed to have further increased, as shown in Fig. 4, with a log₁₀EC₅₀ value of [BMIM][BF₄] of 2.11 ± 0.042 , and a hormetic effect also occurred. The estimated EC₅₀ value using the incubated stock solution of [BMIM][BF₄] prepared 6 months earlier was similar with that of [BMIM][SbF₆].

Conclusions

This study has demonstrated the effects of several typical anions on the toxicity of imidazolium-based ILs toward *S. capricornutum*, which lives in surface waters, using a testing method based on algal growth. The present study identified that imidazolium-based ILs were more toxic to algae than Na⁺ or K⁺-based compounds. Of the imidazolium-based ILs, [BMIM][SbF₆] and [BMIM][PF₆] affected the algal growth rate much more than remaining compounds and the difference of EC₅₀ values of these compounds was not significant. Conversely, in the toxicity experiment on the anions combined with Na⁺ or K⁺, the influence of anions was clearly observed.

Also, in order to examine the hydrolysis of fluoride-containing anions, fluoride was detected using ion chromatography. Of the ILs analysed, fluoride ions were formed from [BMIM][SbF₆] and [BMIM][BF₄], but not from [BMIM][PF₆]. When only small amounts of fluoride ions were formed from [BMIM][SbF₆] and [BMIM][BF₄] within 96 h, the fluoride ion formed did not affect the algal growth rate. Nevertheless, the

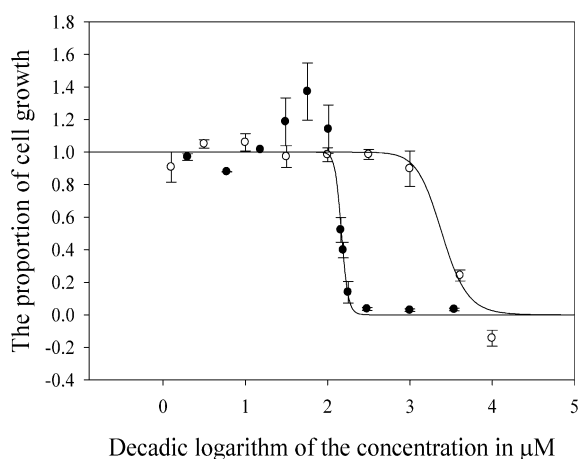


Fig. 4 Toxic effect of [BMIM][BF₄] according to storage time. Stock solution freshly prepared at the onset of testing experiment (-○-), Stock solution prepared 6 months earlier (-●-). Error bars correspond to standard deviations of the experimental data.

fluoride ion formation from [BMIM][BF₄] increased with incubating time of the stock solution, thus resulting in slightly higher toxicity of the 6 month old stock.

Anions are important, as they can decide the properties of ILs for their suitable use in several industrial applications. At the same time, an anionic component can, in part, determine the toxicity of ILs. Thus, further study should be performed to better understand the influence of anions on the toxicity and environmental fate of ILs.

Experimental

Ionic liquids and other chemicals

1-Butyl-3-methylimidazolium tetrafluoroborate [BMIM][BF₄] (purity > 98%), 1-butyl-3-methylimidazolium hexafluorophosphate [BMIM][PF₆] (purity > 98%), 1-butyl-3-methylimidazolium bromide [BMIM][Br] (purity > 98%) and 1-butyl-3-methylimidazolium hexafluoroantimonate [BMIM][SbF₆] (purity > 98%) were purchased from C-TRI, Korea. 1-Butyl-3-methylimidazolium chloride [BMIM][Cl] (purity > 98%), 1-butyl-3-methylimidazolium octylsulfate [BMIM][C₈H₁₇SO₄] (purity > 95%) and 1-butyl-3-methylimidazolium trifluoromethanesulfonate [BMIM][CF₃SO₃] (purity > 95%) were purchased from Sigma-Aldrich. Sodium tetrafluoroborate [NaBF₄] (purity > 98%), sodium hexafluorophosphate [NaPF₆] (purity > 98%), sodium chloride [NaCl] (purity > 99.5%), sodium bromide [NaBr] (purity > 99%), sodium trifluoromethanesulfonate [NaCF₃SO₃] (purity > 98%), potassium fluoride [KF] (purity > 99%) and potassium hexafluoroantimonate [KSbF₆] (purity > 99%) were purchased from Sigma-Aldrich, and sodium octylsulfate [NaC₈H₁₇SO₄] (purity > 99%) from Lancaster. 2-Propanol (purity > 99.5%) and dimethylformamide (purity > 99.5%) were purchased from Sigma-Aldrich and methanol (purity > 99.5%) from Samchun Pure Chemical Co. (Korea).

Microalgal strain and cultivation

The green microalga, *Selenastrum capricornutum* ATCC-22662, was obtained from the National Institute Environmental Research (Korea), and used as the model algal strain in this study. The stock alga was cultivated in a 250 ml Erlenmeyer flask containing 200 ml of sterilized nitrate-enriched BBM medium, which was made from triple distilled water to avoid nitrogen limitation in the high-density culture.³⁹ The culture flask was continuously agitated on a rotary shaker at 170 rpm, with air bubbling (1 volume of air/volume of liquid/min) but without a sparger. Continuous illumination of $30 \pm 5 \mu\text{E m}^{-2} \text{s}^{-1}$ was provided by overhead warm-white fluorescent tubes (Korea General Electric, Korea), with the temperature controlled at $25 \pm 2 \text{ }^\circ\text{C}$.

Toxicity tests

The ILs toxicity tests were conducted using the methods recommended in the EPA²⁹ and the OECD guidelines.³⁰ Experiments were conducted in a 250 ml Erlenmeyer flask, containing 55 ml of sterilized culture medium, inoculated with 5 ml of 7-day cultured algal samples. Subsequently, a known concentration of the ILs was added to each flask, placed on a

shaking incubator maintained at 170 rpm and 25 °C, and with 24 h illumination from warm-white fluorescent tubes, which provided an average illumination of $30 \pm 5 \mu\text{E m}^{-2} \text{s}^{-1}$. At each determined exposure period date, the optical density of the algal biomass was estimated at 438 nm, using a spectrophotometer (UV mini-1240, Shimadzu, Kyoto, Japan). The dry cell weight corresponding to the optical density was determined through the linear relation Dry cell weight = $0.1329 \times$ optical density, and expressed in g l^{-1} . In this study, two replicates were set up for each treatment, whereas there were three replicates for controls, because the control is the basis for evaluation of toxicity, and if the control is not precise the EC50 may contain a large error.

Analytical methods

Ion chromatography was used to determine the fluoride ions generated during the hydrolysis of imidazolium-based ILs incorporating BF_4^- , PF_6^- and SbF_6^- as the counter-anions. All chromatographic analyses³⁷ were performed at room temperature using a Metrohm Model 792 Basic IC (Metrohm, Herisau, Switzerland), with a suppressor module, and equipped with a Metrosep A Supp 5 column (150×170 mm). The anions were detected using a conductivity detector. The eluent was comprised of a 3.2 mM Na_2CO_3 and 1.0 mM NaHCO_3 mixture, with H_2SO_3 used as the suppressor regenerating solution. Prior to preparing the eluent mixture and regenerating solution, the deionized water was filtered through a 0.45 μm filter.

Data treatment

The protocol used for the growth inhibition bioassay was based on the standard procedures in the OECD guidelines.³⁰ The average specific growth rate, μ , for a specific period was calculated as the logarithmic increase in biomass:

$$\mu_{i-f} = \frac{\ln C_f - \ln C_i}{t_f - t_i} \text{d}^{-1} \quad (2)$$

where μ_{i-f} is the average specific growth rate from the initial time, i , to the final time, f ; C_i and C_f are the initial and final biomass concentrations (mg l^{-1}), respectively; and t_i and t_f the initial and final times (d), respectively.

The proportion of cell growth (I) for each treatment replicate can be calculated from:

$$I = \frac{\mu_T}{\mu_C} \quad (3)$$

where μ_C and μ_T are the specific growth rates in the control and treatment (d^{-1}), respectively.

Where feasible, the concentration–response curves were fitted, using the nonlinear least-squares method, to the multinomial data employing the logistic model for the relationship of the cell viability and inhibition to the decadic logarithm of the examined concentrations, which can be written as follows:

$$I = \frac{1}{1 + (x/x_0)^b} \quad (4)$$

where x is the substance concentration to which the cells were exposed, I the proportion of cell growth, normalized with the negative controls (*i.e.*, controls consisting of the same nutrient medium conditions, procedures, and algal seeds from the same culture, except that none of the test substance (ILs) is added) to intervals from 1 ($x = 0$) to 0 (negative control); x_0 represents the EC50, and b the slope of the function on a logit-log scale. Calculations were carried out using the Sigma Plot program (Sigma-Plot 8.02).

References

- J. D. Holbrey and K. R. Seddon, *Clean Prod. Process.*, 1999, **1**, 223–236.
- H. Olivier-Bourbigou and L. Magna, *J. Mol. Catal. A: Chem.*, 2002, **182–183**, 419–437.
- K. N. Marsh, J. A. Boxall and R. Lichtenthaler, *Fluid Phase Equilib.*, 2004, **219**, 93–98.
- J. Fuler, R. T. Carlin and R. A. Osteryoung, *J. Electrochem. Soc.*, 1997, **144**, 3881–3886.
- T. Welton, *Chem. Rev.*, 1999, **99**, 2071–2083.
- R. Sheldon, *Chem. Commun.*, 2001, 2399–2407.
- J. Dupont, R. F. De Souza and P. A. Z. Suarez, *Chem. Rev.*, 2002, **102**, 3667–3691.
- D. S. H. Wong, J. P. Chen, J. M. Chang and C. H. Chou, *Fluid Phase Equilib.*, 2002, **194–197**, 1089–1095.
- B. Jastorff, K. Mölter, P. Behrend, U. Bottin-Weber, J. Filser, A. Heimersm, B. Ondruschka, J. Ranke, M. Schaefer, H. Schröder, A. Stark, P. Stepnowski, F. Stock, R. Störmann, S. Stolte, U. Welz-Biermann, S. Ziegert and J. Thöming, *Green Chem.*, 2005, **7**, 362–372.
- J. Pernak, J. Rogoża and I. Mirska, *Eur. J. Med. Chem.*, 2001, **36**, 313–320.
- J. Pernak, J. Kalewska, H. Ksycińska and J. Cybulski, *Eur. J. Med. Chem.*, 2001, **36**, 899–907.
- J. Pernak, K. Sobaszekiewicz and I. Mirska, *Green Chem.*, 2003, **5**, 52–56.
- J. Pernak and P. Chwała, *Eur. J. Med. Chem.*, 2003, **38**, 1035–1042.
- J. Pernak, I. Goc and I. Mirska, *Green Chem.*, 2004, **6**, 323–329.
- F. Stock, J. Hoffmann, J. Ranke, R. Störmann, B. Ondruschka and B. Jastorff, *Green Chem.*, 2004, **6**, 286–290.
- J. Ranke, K. Mölter, F. Stock, U. Bottin-Weber, J. Poczobutt, J. Hoffmann, B. Ondruschka, J. Filser and B. Jastorff, *Ecotoxicol. Environ. Saf.*, 2004, **58**, 396–404.
- K. M. Docherty and C. F. Kulpa, Jr., *Green Chem.*, 2005, **7**, 185–189.
- P. Stepnowski, A. C. Składanowski, A. Ludwiczak and E. Łaczyńska, *Hum. Exp. Toxicol.*, 2004, **23**, 513–517.
- R. J. Swatloski, J. D. Hobrey, S. B. Memon, G. A. Caldwell, K. A. Caldwell and R. D. Rogers, *Chem. Commun.*, 2004, 668–669.
- R. J. Bernot, E. E. Kennedy and G. A. Lamberti, *Environ. Toxicol. Chem.*, 2005, **24**(7), 1759–1765.
- R. J. Bernot, M. A. Brueseke, M. A. Evans-White and G. A. Lamberti, *Environ. Toxicol. Chem.*, 2005, **24**(1), 87–92.
- S.-M. Lee, W.-J. Chang, A.-R. Choi and Y.-M. Koo, *Korean J. Chem. Eng.*, 2005, **22**(5), 687–690.
- S. Stole, J. Arning, U. Bottin-Weber, M. Matzke, F. Stock, K. Thiele, M. Uerdingen, U. Welz-Biermann, B. Jastorff and J. Ranke, *Green Chem.*, 2006, **8**, 621–629.
- A. S. Wells and V. T. Coombe, *Org. Process Res. Dev.*, 2006, **10**, 794–798.
- C. Pretti, C. Chiappe, D. Pieraccini, M. Gregori, F. Abramo, G. Monni and L. Intorre, *Green Chem.*, 2006, **8**, 238–240.
- C. R. Blaise, in *Ecotoxicology Monitoring*, ed. M. L. Richardson, VCH, Weinheim, 1993, pp. 83–108.
- M. A. Lewis, in *Fundamentals of aquatic toxicology: Effects, environment fate, and risk assessment*, ed. G. M. Rand, Taylor and Francis, Washington, DC, USA, 2nd edn., 1995, pp. 135–170.
- A. Latała, P. Stepnowski, M. Nędzi and W. Mroziak, *Aquat. Toxicol.*, 2005, **73**(1), 91–98.
- U.S. Environmental Protection Agency, Ecological Effect Test Guidelines, OPPTs 850.5400, Algal Toxicity, Tiers I and II, 1996.

- 30 Organization for Economic Cooperation and Development, Guidelines for the testing of chemicals, Proposal for updating guideline 201, Freshwater alga and cyanobacteria, Growth Inhibition Test, 2002.
- 31 D. Zhao, Y. Liao and Z. Zhang, *Clean*, 2007, **35**, 42–48.
- 32 M. T. Garcia, N. Gathergood and P. J. Scammells, *Green Chem.*, 2005, **7**, 9–14.
- 33 P. Wasserscheid, R. van Hal and A. Boesmann, *Green Chem.*, 2002, **4**, 401–404.
- 34 J. E. Griffiths and G. E. Walrafen, *Inorg. Chem.*, 1972, **2**, 427–429.
- 35 A. E. Visser, R. P. Swatloski, W. M. Reichert, S. T. Griffin and R. D. Rogers, *Ind. Eng. Chem. Res.*, 2000, **39**, 3596–3604.
- 36 R. P. Swatloski, J. D. Hobrey and R. D. Rogers, *Green Chem.*, 2003, **5**, 361–363.
- 37 C. Villagrán, M. Deetlefs, W. R. Piter and C. Hardacre, *Anal. Chem.*, 2004, **76**, 2118–2123.
- 38 G. A. Baker and S. N. Baker, *Aust. J. Chem.*, 2005, **58**, 172–177.
- 39 Y.-S. Yun and J. M. Park, *Korean J. Chem. Eng.*, 1997, **14**, 1297–1300.

Find a SOLUTION

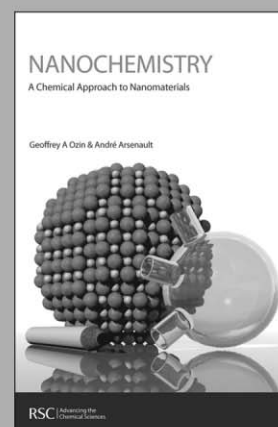
... with books from the RSC

Choose from exciting textbooks, research level books or reference books in a wide range of subject areas, including:

- Biological science
- Food and nutrition
- Materials and nanoscience
- Analytical and environmental sciences
- Organic, inorganic and physical chemistry

Look out for 3 new series coming soon ...

- RSC Nanoscience & Nanotechnology Series
- Issues in Toxicology
- RSC Biomolecular Sciences Series



28040542

RSC Publishing

www.rsc.org/books

The methylation of benzyl-type alcohols with dimethyl carbonate in the presence of Y- and X-faujasites: selective synthesis of methyl ethers

Maurizio Selva,* Enrico Militello and Massimo Fabris

Received 23rd May 2007, Accepted 18th October 2007

First published as an Advance Article on the web 9th November 2007

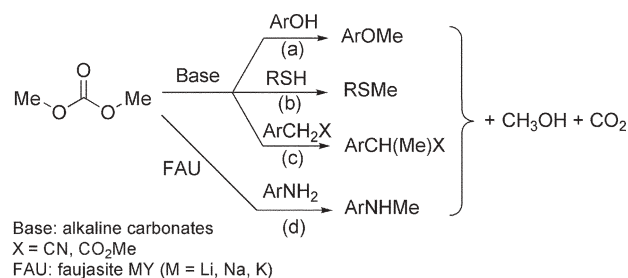
DOI: 10.1039/b707774b

At 165–200 °C, in the presence of sodium-exchanged faujasites (NaX or NaY) as catalysts, the reaction of dimethyl carbonate with benzyl-, *o*- and *p*-methoxybenzyl-, *p*-hydroxybenzyl-, diphenylmethyl-, and triphenylmethyl-alcohols (**1a**, **2a,b**, **3a**, **4a**, and **4c**, respectively), produces the corresponding methyl ethers in up to 98% yields. A peculiar chemoselectivity is observed for hydroxybenzyl alcohols (compounds **3a** and **3b**, *para*- and *ortho*-isomers) whose etherification takes place without affecting the OH aromatic groups. Acid–base interactions of alcohols and DMC over the faujasite surface offer a plausible explanation for the catalytic effect of zeolites NaY and NaX, as well as for the trend of reactivity shown by the different alcohols (primary > secondary > tertiary). However, in the case of substrates with mobile protons in the β -position (*i.e.* 1-phenylethanol and 1,1-diphenylethanol), the dehydration reaction to olefins is the major, if not the exclusive, process.

Introduction

Conventional techniques for the synthesis of benzyl methyl ethers are mainly based on the classical base-promoted Williamson reaction of benzyl-type alcohols with methyl halides, dimethyl sulfate or diazomethane.¹ Though efficient, these procedures pose a great concern from both safety and environmental standpoints: they use highly noxious methylating agents, often in the presence of toxic solvents (THF, hexane, benzene), and they consume over-stoichiometric amounts of strong bases which imply work-ups with aqueous solutions and the co-generation of by-products and polluted effluents to be disposed of. A viable alternative is the methanolysis of alcohols which has been reported over a variety of Brønsted and Lewis acidic compounds such as HCl,² H₂SO₄,³ *p*-MeC₆H₄SO₃H,⁴ CF₃SO₃H,⁵ CAN [(NH₄)₂Ce(NO₃)₆],⁶ FeX₃ (X = Cl, NO₃),⁷ RE(OTf)₃ (RE = Yb, Sc),⁸ and NaHSO₄/SiO₂.⁹ These methods, however, are limited to secondary and tertiary substrates,^{2–7} or to primary benzyl alcohols only if activated by OH and OR *para*-substituents.^{8,9}

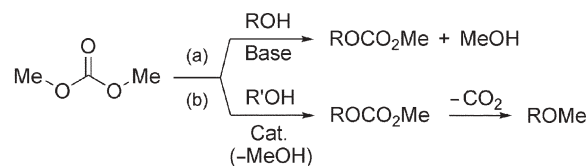
Safer and selective methylation protocols can be conceived with the non-toxic dimethyl carbonate (MeOCO₂Me, DMC).¹⁰ In the presence of weak bases or alkali metal-exchanged Y-faujasites (FAU) as catalysts,¹¹ a number of O-, S-, C- and N-nucleophiles (*e.g.* phenols, thiols, CH₂-active compounds, and primary amines) react with DMC to produce the corresponding methyl derivatives [Scheme 1, paths (a)–(d)] in very high yields (85–95%).¹² Of particular note are the cases of CH₂-active substrates and anilines whose reactions proceed with unprecedented high mono-*C*- and mono-*N*-methyl selectivity (up to 99%) towards ArCH(Me)X, and ArNHMe products [paths (c) and (d)].



Scheme 1 Methylation reactions mediated by DMC.

Under basic catalysis, however, the reaction of alcohols with DMC goes through an exclusive transesterification process (B_{Ac}2 mechanism) to yield methyl alkyl carbonates as sole products [ROCO₂Me; Scheme 2(a)].¹³ A selective synthesis of methyl ethers from DMC has been recently reported only for a few substrates, in the presence of alumina and hydrotalcite promoters:¹⁴ final products (ROME) are obtained in two steps *via* an initial transesterification reaction followed by an *in situ* decarboxylation process [Scheme 2(b)].

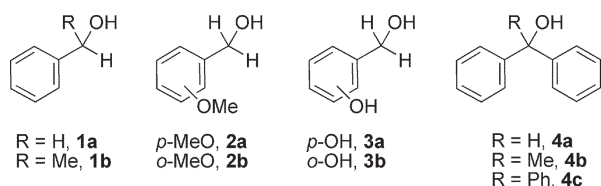
Based on our previous results on DMC-mediated methylation reactions catalyzed by zeolites,^{12,15} we decided to explore both Y- and X-faujasites as catalysts for the preparation of methyl ethers of primary, secondary and tertiary benzyl-type alcohols (Scheme 3).



Base: alkaline carbonates, CsF/ α -Al₂O₃
R' = 1-C₈H₁₇; 1-C₈H₁₇; 2-C₈H₁₇; PhCH₂
Cat.: Basic Al₂O₃, Hydrotalcite

Scheme 2 Reactions of DMC with alcohols.

Dipartimento di Scienze Ambientali dell'Università Ca' Foscari, Calle Larga S. Maria, 2137, Venezia, 30123, Italy. E-mail: selva@unive.it; Fax: +39 041 2348 584; Tel: +39 041 2348 687



Scheme 3

We wish to report herein that the combined use of DMC and Y- or X-faujasites offers an excellent tool to set up an innovative etherification protocol: at 165–200 °C, six out of nine of the tested alcohols (**1a**, **2a,b**, **3a**, **4a** and **4c**) undergo a clean *O*-methylation to produce methyl ethers in up to 98% isolated yields. Compound **3b** instead gives the corresponding ether in a 46% yield, and alcohols **1b** and **4b**, are preferably dehydrated to the corresponding olefins. To further elucidate the scope and limitations of the method, commercial NaY and NaX zeolites are also compared to a conventional basic catalyst (K₂CO₃) used for methylations promoted by DMC.

Results

Benzyl alcohol, **1a**

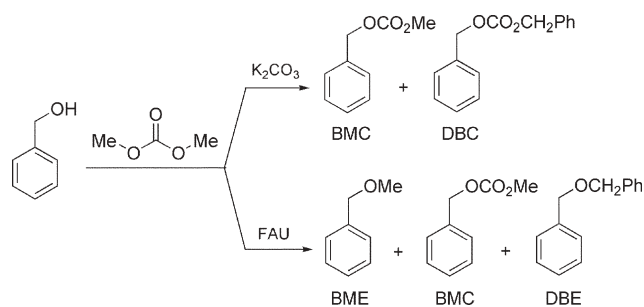
Initially, the model reaction of benzyl alcohol with DMC was investigated. A solution of compound **1a** (0.2 g, 1.9 mmol) in DMC (6×10^{-2} M, 30 mL; DMC serving both as a reagent and the solvent) was set to react at 165–200 °C in a stainless steel autoclave (90 mL), in the presence of different faujasites NaY and NaX [weight ratio zeolite : substrate (*Q*) = 3]. All reactions were carried out under a N₂ atmosphere and they were monitored by GC–MS.

At 165 °C, the same procedure was also used to perform experiments with K₂CO₃ (weight ratio K₂CO₃ : substrate of 3), in place of faujasites. Table 1 reports the results.

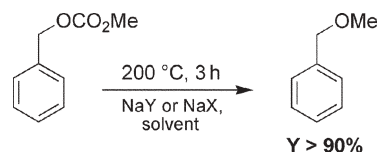
In the absence of K₂CO₃ or of faujasites, benzyl alcohol was recovered unreacted after 3 h at 180 °C (entry 1). Otherwise, different products were observed: benzyl methyl ether (BME), benzyl methyl carbonate (BMC), dibenzyl carbonate (DBC), and dibenzyl ether (DBE), respectively (Scheme 4).

The nature of the catalyst controlled the relative amounts of these products.

In particular, at 165–180 °C, in the presence of K₂CO₃, the transesterification of dimethyl carbonate was the exclusive



Scheme 4



Scheme 5

process, and BMC or a mixture of BMC and DBC was obtained (entries 2, 3).

The use of faujasites instead allowed simultaneous methylation and carboxymethylation processes (entries 4, 5). Minor amounts of dibenzyl ether were also observed, plausibly due to the dehydration of benzyl alcohol. However, when the reaction was carried out at 200 °C, BME could be isolated in up to 96% yield (entries 6–7).¹⁶ The high temperature, in fact, promoted the quantitative decarboxylation of the transesterification product (BMC). Good evidence for this behavior was gathered from separate experiments, in which solutions (0.2 M, 30 mL) of BMC (0.3 g, 1.9 mmol) in either cyclohexane or dimethoxyethane were heated up to 200 °C in the presence of both NaX and NaY solids (weight ratio for zeolite : BMC of 1.5). In all cases, after 3 h, benzyl methyl ether was the sole product (Scheme 5).

The excellent selectivity towards BME prompted us to investigate possible effects associated with the character and the amount of the two zeolites. Under the conditions of entry 6 in Table 1 (200 °C; 6×10^{-2} M solution of **1a** in DMC, 30 mL), a set of experiments was carried out using different quantities of both NaY and NaX catalysts. The *Q* ratio (weight ratio cat. : **1a**) was ranged from 0.2 to 3, and for each test the reaction was monitored until a complete conversion of benzyl alcohol was obtained.

Table 1 Reaction of benzyl alcohol **1a** with dimethyl carbonate in the presence of NaY, NaX and K₂CO₃ catalysts^a

Entry	Catalyst	<i>Q</i> ^b (wt : wt)	<i>t</i> /h	<i>T</i> /°C	Conv. (%) ^c	Products (% by GC) ^c			Y (%) ^d
						PhCH ₂ OMe	PhCH ₂ OCO ₂ Me	(PhCH ₂) ₂ O	
1	None		3	180	—	—	—	—	
2	K ₂ CO ₃	3	4	165	100	—	100	—	
3	K ₂ CO ₃	3	4	180	100 ^e	—	93	—	
4	NaY	3	7	165	35	10	23	—	
5	NaY	3	7	180	80	53	19	6	
6	NaY	3	5	200	100	93	3	4	92
7	NaX	3	3	200	100	99	—	—	96

^a All reactions were carried out using a solution of **1a** (0.2 g, 1.9 mmol) in DMC (6×10^{-2} M, 30 mL). ^b *Q* was the weight ratio of catalyst : substrate. ^c Both conversion and % amounts of BME, BMC, and DBE were determined by GC analyses. ^d Y: Isolated yield of benzyl methyl ether. ^e Also, dibenzyl carbonate (7%) was detected.

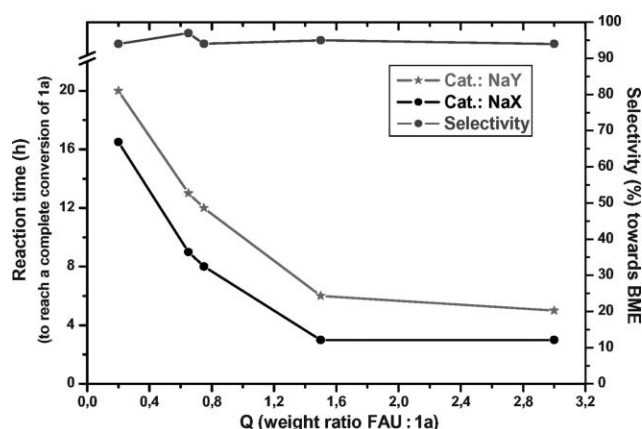


Fig. 1 Synthesis of BME over NaY and NaX catalysts.

Results are described in Fig. 1, in which the reaction time necessary to reach a quantitative substrate conversion was plotted against Q (left to right). The grey and black profiles refer to NaY and NaX zeolites, respectively. To complete the picture, the figure also reports the selectivity towards the formation of BME (right to left).

Four major aspects emerged from this analysis. (i) Both faujasites (NaY and NaX) acted as genuine catalysts: after 16–20 h (left ordinate), benzyl alcohol was totally converted even using Q as low as 0.2. (ii) When Q was increased from 0.2 to 1.5, reaction times dropped considerably: the etherification could be accomplished up to 4–5 times faster (3–5 h, $Q = 1.5$). However, the rate was not substantially improved by a further increasing of the amount of the zeolite (Q from 1.5 to 3). (iii) The change of Q (0.2–3) never appreciably affected the selectivity towards BME, which remained always very high

(93–97%: right ordinate).¹⁷ (iv) The comparison of the two zeolites showed that reactions catalyzed by the NaX faujasite took place quicker than those carried out over the NaY one. This difference was particularly pronounced at $Q \geq 1.5$: under these conditions, reaction times were nearly halved (3 h) when NaX was used.

Additional experiments were performed to scale up the reaction. At 200 °C, in the presence of NaY ($Q = 0.2$), benzyl alcohol (2.5 g, 23.1 mmol) was set to react with different amounts of DMC (10, 40, 58, and 117 mL). The corresponding range of the DMC : **1a** molar ratio (W) was from 5 to 60. Each test was carried out for 24 h. Table 2 reports the results.

The reaction selectivity was dramatically affected by the W ratio. At the lowest W (5: entry 1), the dehydration of benzyl alcohol took place to a large extent: at a conversion of 82%, dibenzyl ether was produced at 34%. However, as the DMC : **1a** molar ratio was increased up to 30, a quantitative reaction was observed and the amount of DBE decreased markedly to 10% (entries 2 and 3). Finally, at $W = 60$, the BME yield was of 94% (by GC, entry 4). This last result substantially matched that reported in Fig. 1 (at $Q = 0.2$). In other words, a selective synthesis of BME was possible only if a large-to-moderate excess of DMC was used. This reagent/solvent, however, could be quantitatively recovered by distillation, and recycled several times.¹⁸

Other benzyl-type alcohols (**1b**, **2a,b**, **3a,b**, **4a–c**)

According to the above-described procedure for **1a**, solutions of primary, secondary, and tertiary benzyl-type alcohols **1b**, **2a,b**, **3a,b**, and **4a–c** in DMC (6×10^{-2} M, 30 mL) were made to react at 165–200 °C, in the presence of both faujasites NaY and NaX. If not otherwise specified, the weight ratio of zeolite : substrate (Q) was set to 1.5. Table 3 reports the results.

Table 2 Reaction of benzyl alcohol **1a** with different amounts of dimethyl carbonate in the presence of the NaY catalyst

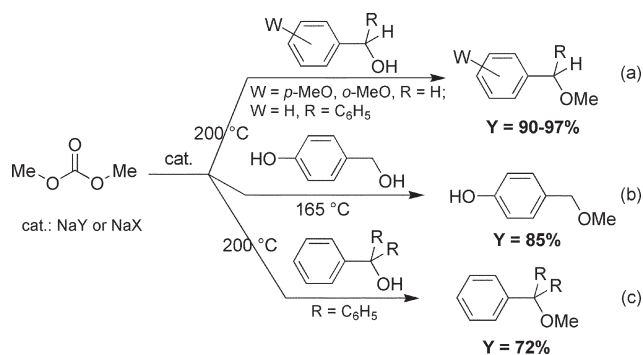
Entry	NaY (Q) ^a	DMC : 1a (W) ^b	t/h	$T/^\circ\text{C}$	Conv. (%) ^c	Products (% by GC) ^c			
						PhCH ₂ OMe	PhCH ₂ OCO ₂ Me	(PhCH ₂) ₂ O	Others ^d
1	0.2	5	24	200	82	42	1	34	5
2	0.2	20	24	200	98	76	1	19	2
3	0.2	30	24	200	100	90	—	8	2
4	0.2	60	24	200	100	94	3	3	—

^a Q was the weight ratio of catalyst : substrate. ^b W was the DMC : **1a** molar ratio. ^c Both conversion and % amounts of BME, BMC, and DBE were determined by GC analyses. ^d Total amount of other unidentified products.

Table 3 Reaction of alcohols **2**, **3**, and **4** with dimethyl carbonate in the presence of NaY and NaX catalysts^a

Entry	Substrate XC ₆ H ₄ CR(R')OH	Cat. (Q) ^b	t/h	$T/^\circ\text{C}$	Conv. (%) ^c	Products (% by GC) ^c	Y (%) ^d
1	2a : X = <i>p</i> -MeO; R = R' = H	NaY (1.5)	6	200	100	<i>p</i> -MeOC ₆ H ₄ CH ₂ OMe (94)	98
2	2a : X = <i>p</i> -MeO; R = R' = H	NaX (1.5)	4	200	100	<i>p</i> -MeOC ₆ H ₄ CH ₂ OMe (98)	—
3	2b : X = <i>o</i> -MeO; R = R' = H	NaY (1.5)	6.5	200	100	<i>o</i> -MeOC ₆ H ₄ CH ₂ OMe (98)	97
4	2b : X = <i>o</i> -MeO; R = R' = H	NaX (1.5)	4	200	100	<i>o</i> -MeOC ₆ H ₄ CH ₂ OMe (99)	—
5	3a : X = <i>p</i> -OH; R = R' = H	NaY (3)	5	165	100	<i>p</i> -(HO)C ₆ H ₄ CH ₂ OMe (100)	85
6	4a : X = R = H; R' = C ₆ H ₅	NaY (1.5)	9	200	96	(C ₆ H ₅) ₂ CHOMe (89) (C ₆ H ₅) ₂ CHOCO ₂ Me (7)	90
7	4a : X = R = H; R' = C ₆ H ₅	NaX (1.5)	5	200	100	(C ₆ H ₅) ₂ CHOMe (99)	96
8	4c : X = H; R = R' = C ₆ H ₅	NaY (1.5)	11	200	88	(C ₆ H ₅) ₃ COMe (74) (C ₆ H ₅) ₃ CH (14)	72

^a All reactions were carried out using a solution of the substrate (1.9 mmol) in DMC (6×10^{-2} M, 30 mL). ^b Q was the weight ratio of faujasite : substrate. ^c Both conversion and % amounts of different products were determined by GC analyses. ^d Y: Isolated yield of methyl ethers.



Scheme 6

At 200 °C, alcohols **2a,b** and **4a** gave the corresponding methyl ethers [Scheme 6(a)] in >95% purity (by GC–MS, entries 1–4 and 6–7). These products were isolated in 90–98% yields by simple filtration of the zeolite and removal of DMC under vacuum.

A similar result was obtained also for alcohol **3a** on the condition that a lower temperature was used (entry 5: 165 °C; 85% yield) [Scheme 6(b)].¹⁹ In this case, the high chemoselectivity was a further added value of the procedure: a clean *O*-methylation of the alcohol group took place, the aromatic OH function being fully preserved from any possible methylation or carboxymethylation process (see also Scheme 1). It should be noted that only a very few methods are available in the literature, for a straightforward high-yield synthesis of methyl *p*-hydroxybenzyl ether.^{6c,9}

In the case of triphenylcarbinol (**4c**), at 200 °C, the reaction still proceeded with a high conversion (88%, entry 8); however, it required a longer time than for previous compounds, and the etherification selectivity was not as excellent as before. Methyl triphenylmethyl ether was isolated in 72% yield [Scheme 6(c)].²⁰

The reactivity of alcohols **2–4** reflected some aspects already observed for benzyl alcohol: (i) the NaX faujasite generally allowed faster reactions with respect to NaY (compare entries 1–2, 3–4, and 6–7); (ii) etherification reactions were truly catalytic processes which could be simply scaled up to 1–2 g. For instance, in separate experiments, when compounds **2a** (1.5 g, 10.9 mmol) and **4a** (1.5 g, 8.2 mmol) were set to react at 200 °C in the presence of DMC (70 mL) and NaY (*Q* = 0.2), the corresponding methyl ethers were obtained in amounts of 97 and 91%, respectively, after 11 and 21 h. Under the same conditions, the reaction of **4c** (1.5 g, 5.8 mmol) showed a conversion of only 52% (methyl ether: 44%), after 26 h; (iii) if zeolites were replaced with K₂CO₃, the synthesis of methyl ethers of alcohols **2–4** was never possible. At 165–200 °C, the reaction of **2a** and **4a**, with DMC and K₂CO₃ (molar ratio substrate : DMC : base of 1 : 60 : 1.5, respectively) gave transesterification products exclusively (ROCO₂Me, R = *p*-hydroxybenzyl and 1,1-diphenylmethyl).

By contrast to the good result obtained for *p*-hydroxybenzyl alcohol (**3a**), both NaY and NaX catalysts offered a poor selectivity in the reaction of the *ortho*-isomer **3b**. Under the conditions of entry 5 in Table 3 (NaY, 165 °C, 5 h, *Q* = 3), the conversion of **3b** was quantitative, but its methyl ether [*o*-(HO)C₆H₄CH₂OMe] was detected in only a 47% amount (by GC–MS), other products being *o*-cresol [*o*-(HO)C₆H₄CH₃,

28%] and *o*-hydroxybenzaldehyde [*o*-(HO)C₆H₄CHO, 27%].²¹ Yet, no methylation of the aromatic OH group took place.

Faujasites did not succeed in the reaction of DMC with alcohols **1b** and **4b**. In these cases, methyl ethers were minor products or they were not obtained at all. For example, under the conditions of entry 5 in Table 3 (NaY, 165 °C, 5 h, *Q* = 3), 1-phenylethanol (**1b**) was converted into a mixture of methyl 1-phenylethyl ether (9%) and styrene (56%), whereas 1,1-diphenylethanol (**4b**) yielded 1,1-diphenylethylene as the sole product.

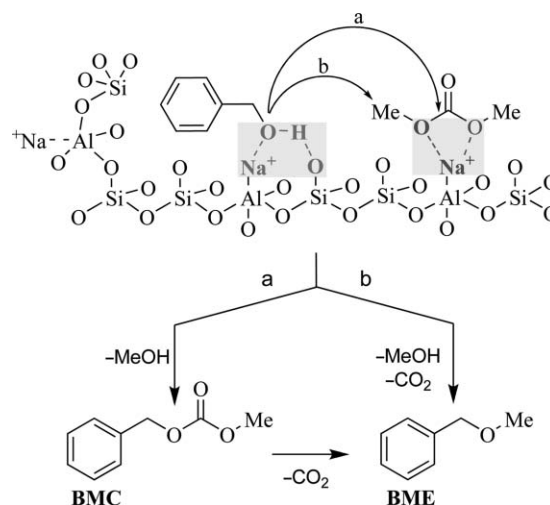
Discussion

The role of the NaX and NaY zeolites

Alkali metal-exchanged faujasites are often reported as amphoteric solids.^{11c,22} Accordingly, the interactions of these zeolites with alcohols, particularly of the benzyl type, and with DMC as well, are basically described through H-bonds and acid–base reactions occurring at the surface of the solid catalyst.^{23,24} Scheme 7 offers a plausible mechanistic pattern for the synthesis of benzyl methyl ether promoted by DMC, over both NaY and NaX catalysts.

At the catalyst surface, benzyl alcohol and DMC undergo a nucleophilic (shaded section, left) and an electrophilic (shaded section, right) activation, respectively.²⁵ The so-formed alcoholate-like species attacks methyl and carbonyl carbons of DMC to produce both BMC and BME (paths a and b), through tetrahedral and S_N2 mechanisms. Then, at a high temperature (preferably over 180 °C), the decarboxylation of BMC takes place to yield BME as the sole product (see Scheme 5). This last reaction of BMC is reported also over basic alumina or hydrotalcite solids in the presence of dimethyl carbonate.¹⁴

Data of Tables 1 and 3, and of Fig. 1, suggest that NaX and NaY faujasites exhibit a different activity: in particular, according to the acid–base scale proposed by Barthomeuf (Scheme 6),^{11c,22} one would conclude that the more basic NaX has a better performance than NaY. This is consistent with our



Scheme 7 Pictorial view of the reaction of benzyl alcohol and DMC over a faujasite.

previous findings on the reactions of indolyl carboxylic acids with DMC, promoted by zeolites.^{15b} In the present case, however, Fig. 1 also shows that the difference in reaction times observed for the two faujasites is rather constant (3–4 h), regardless of the amount of catalyst used (compare black and grey lines with *Q*). This trend might imply the occurrence of an induction period for the less active NaY faujasite. At the moment, this behavior has no clear reasons.

Traces of water (and Brønsted acidity) in the catalysts may also explain the dehydration of benzyl alcohol to form dibenzyl ether (Tables 1 and 2).²⁶ Not surprisingly, the process becomes significant when a high concentration of the alcohol is available at the zeolite surface (entries 1 and 2, Table 2). Notwithstanding, the onset of this side-reaction can be substantially prevented if a large-to-moderate excess of DMC is used.

The different reactivity of alcohols

A reactivity scale can be highlighted for the different alcohols. In particular, primary substrates react more rapidly than secondary and tertiary ones (Tables 1 and 3). This result is likely ascribed to the modes of surface interactions illustrated in Scheme 7: the higher the steric crowding around the OH group, the worse the adsorption and the contact of reagents, the poorer the catalysis is. Aromatic substituents also modify the reactivity of alcohols **2** and **3**, though a general tendency cannot be inferred. For instance, compounds **3a,b** bearing an electron-donating OH aryl substituent undergo the etherification reaction at a relatively low temperature (165 °C). Methoxybenzyl alcohols would then be expected to be more reactive than benzyl alcohol, but they are not: at 200 °C, the reaction rate for compounds **2a,b** is comparable (if not lower) to that of **1a** (Fig. 1 and Table 3). A rationale for this incongruity is perhaps on the nature and the geometry of adsorption of reagents over the catalyst: since OH aryl substituents are able to interact directly with the zeolite surface,^{11c,22,27} it is plausible that hydroxybenzyl alcohols (**3a,b**) are adsorbed more strongly than other compounds, such that the resulting catalysis is favored.

In the case of 1-phenyl- and 1,1-diphenyl-ethanol (compounds **1b** and **4b**, respectively), the co-presence of mobile methyl protons and of traces of Brønsted acidity in the catalysts allows the dehydration reaction to olefins, to be the major, if not the exclusive, process.

Conclusions

The combination of dimethyl carbonate and alkali metal-exchanged Y- and X-faujasites offers unique possibilities to accomplish selective methylations of a variety of N- and S-nucleophiles. This work discloses a further important application of the same system: in the presence of both NaY and NaX zeolites, a highly selective and straightforward etherification of benzyl-type alcohols is possible using dimethyl carbonate as a reagent and a solvent. Typically, methyl ethers of primary, secondary and tertiary substrates (**1–4**) can be isolated in 72–98% yields. In the case of hydroxybenzyl alcohols, the reaction is also very chemoselective: for instance, at 200 °C, methyl *p*-hydroxybenzyl ether is obtained

in 85% yield, the aromatic OH-substituent being fully preserved from methylation and/or methoxycarbonylation side-reactions.

Under the same reaction conditions, if zeolites are replaced with K₂CO₃ (a conventional basic catalyst for DMC-mediated reactions), alcohols undergo an exclusive transesterification process to produce the corresponding methyl alkyl carbonates (ROCO₂Me).

The possible reaction mechanism involves the initial activation of both DMC and the reactant alcohols over the zeolite surface. This occurs through the formation of H-bonds and acid–base interactions with basic oxygen atoms and weakly acidic cations, which belong to the zeolite framework. Then, a sequence of tetrahedral and S_N2-type processes followed by a decarboxylation reaction takes place to yield methyl ethers as the final products. The overall reactivity of compounds **1–4** is sensitive to the steric crowding around the alcoholic function: primary substrates are more reactive than secondary and tertiary ones. The reaction rate is also modified by aromatic substituents whose presence plausibly alters the adsorption of reagents on the catalysts.

Although the reported protocol is rather energy intensive, several *green* features can be recognized: (i) DMC is used as a non-toxic reagent and solvent; (ii) commercially available sodium-exchanged faujasites (NaY and NaX) are eco-safe materials which can be easily separated by filtration, reactivated, and recycled without any loss of activity and/or selectivity;¹⁵ (iii) except for MeOH and CO₂, no organic/inorganic by-products are observed; and (iv) thanks to the excellent *O*-methylation selectivity, high-quality methyl ethers are obtained with simple and cheap purification methods.

Experimental

Compounds **1a,b**, **2a,b**, **3a,b**, **4a–c** and DMC were ACS grade and were employed without further purification. Zeolites NaY and NaX were from Aldrich (art. # 334448 and 283592, respectively): before each reaction, these solids were dried under vacuum (65 °C; 8 mbar) overnight.

MS (EI, 70 eV) analyses were run using a HP5/MS capillary column (30 m). ¹H NMR spectra were recorded on a 300 MHz spectrometer, using CDCl₃ as solvent. Chemical shifts were reported in δ values downfield from TMS.

Reactions carried out in autoclave. General procedure

A stainless-steel autoclave (150 mL of internal volume) was charged with a solution (6×10^{-2} M; 30 mL) of the chosen substrate (**1a,b**, **2a,b**, **3a,b**, and **4a–c**; 1.9 mmol), dimethyl carbonate (0.36 mol) and NaY or NaX [the weight ratio (*Q*) of faujasite : substrate was in the range of 0.2–3; see Tables 1 and 2 and Fig. 1 for details]. At room temperature and before the reaction, air was carefully removed by a purging valve with a N₂ stream. The autoclave was then electrically heated, while the mixture was kept under magnetic stirring throughout the reaction. A thermocouple fixed onto the autoclave head checked the temperature (165–200 °C). After different time intervals (3–20 h), the autoclave was cooled to rt, purged from CO₂, and finally, opened. The reaction mixture was analysed by GC–MS.

The same procedure was also used for the following:

(i) scale up of the reaction to the gram level. In this case, compounds **1a** (1.5 g, 13.9 mmol), **2a** (1.5 g, 10.9 mmol), **4a** (1.5 g, 8.2 mmol), and **4c** (1.5 g, 5.8 mmol) were set to react at 200 °C in the presence of DMC (70 mL) and NaY ($Q = 0.2$).

(ii) carrying out experiments with K_2CO_3 as a catalyst. In this case, the reaction temperature was set to 165–180 °C, and the molar ratio of K_2CO_3 : substrate was in the range of 1.5–2.3.

The synthesis and the decarboxylation of benzyl methyl carbonate (BMC)

BMC was prepared according to a procedure previously reported by us:^{13b} a mixture of benzyl alcohol (1.0 g, 9.3 mmol), dimethyl carbonate (30 mL) and K_2CO_3 (2.6 g, 18.5 mmol) was set to react at 90 °C for 15 h. After filtration of the solid base and removal of DMC under vacuum, BMC was isolated in 98% purity (yield: 1.28 g, 83%). The structure of BMC was assigned by GC–MS and by comparison to an authentic sample. The crude product was used as such for the decarboxylation step of Scheme 5: the reaction was carried out in an autoclave, under conditions similar to those described above (see general procedure). A solution of BMC (0.2 g, 1.2 mmol) in a given solvent (cyclohexane or dimethoxyethane, 30 mL) was charged in an autoclave of 90 mL in the presence of NaY or NaX faujasite (the weight ratio of faujasite : BMC was 1.5). After purging with a N_2 stream, the reactor was heated at 200 °C for 3 h, while the mixture was kept under magnetic stirring throughout the reaction. The final product (benzyl methyl ether) was characterised by GC–MS.

The isolation and characterisation of methyl ethers

Crude methyl ethers of benzyl, *p*- and *o*-methoxybenzyl-, *p*-hydroxybenzyl-, and diphenylmethyl-alcohols were isolated in 96–98% GC-purity, by simple filtration of the zeolite and removal of DMC under vacuum (35 °C/250 mm). Methyl triphenylmethyl ether was further purified by flash column chromatography on silica gel F60 (eluant : petroleum ether/diethyl ether in 5 : 1 v/v). The products were characterized by GC–MS and 1H NMR. In the case of *o*-hydroxybenzyl methyl ether and methyl 1-phenylethyl ether, which were not isolated from the reaction mixture, the respective structures were assigned only by GC–MS.

Spectroscopic and physical properties of all ethers were in agreement with those reported in the literature.

Benzyl methyl ether

Pale-yellow liquid [lit.^{1d} bp 29–30 °C/0.1 mm] 1H NMR (300 MHz, $CDCl_3$) δ 3.40 (s, 3H), 4.47 (s, 2H), 7.29–7.39 (m, 5H). MS (EI), m/z (relative int.): 122 (M^+ , 61%), 121 ($M^+ - H$, 61), 92 (24), 91 ($M^+ - OMe$, 100), 77 (28), 65 (16).

p-Methoxybenzyl methyl ether

Yellow liquid [lit.^{1f} bp 47–50 °C/ 1.5×10^{-3} mm]. 1H NMR (300 MHz, $CDCl_3$) δ 3.36 (s, 3H), 3.81 (s, 3H), 4.39 (s, 2H), 6.88 (d, 2H, $J = 8.5$ Hz), 7.27 (d, 2H, $J = 8.7$ Hz). MS (EI), m/z

(relative int.): 152 (M^+ , 29 %), 151 ($M^+ - H$, 19), 122 (11), 121 ($M^+ - OMe$, 100), 77 (15).

o-Methoxybenzyl methyl ether

Pale-yellow liquid [lit.²⁸ bp 168–169 °C]. 1H NMR (300 MHz, $CDCl_3$) δ 3.42 (s, 3H), 3.84 (s, 3H), 4.50 (s, 2H), 6.84–7.00 (m, 2H), 7.23–7.38 (m, 2H). MS (EI), m/z (relative int.): 152 (M^+ , 55 %), 151 ($M^+ - H$, 16), 122 (16), 121 ($M^+ - OMe$, 100), 92 (12), 91 (99), 77 (24), 65 (16).

p-Hydroxybenzyl methyl ether

Mp 79–82 °C (white solid) [lit.⁴ mp 80–81 °C]. 1H NMR (300 MHz, $CDCl_3$) δ 3.37 (s, 3H), 4.36 (s, 2H), 6.72 (d, 2H, $J = 8.3$ Hz), 7.21 (d, 2H, $J = 8.6$ Hz). MS (EI), m/z (relative int.): 138 (M^+ , 35 %), 137 ($M^+ - H$, 24), 121 (15), 107 ($M^+ - OMe$, 100), 106 (28), 78 (14), 77 (27), 51 (12).

o-Hydroxybenzyl methyl ether

(Not isolated), MS (EI), m/z (relative int.): 138 (M^+ , 44 %), 107 ($M^+ - OMe$, 19), 106 (65), 78 (100), 77 (34), 51 (12).

Diphenylmethyl methyl ether

Viscous oil [lit.² bp 157–158 °C/20 mm]. 1H NMR (300 MHz, $CDCl_3$) δ 3.34 (s, 3H), 5.21 (s, 1H), 4.50 (s, 2H), 7.17–7.35 (m, 10H). MS (EI), m/z (relative int.): 198 (M^+ , 66 %), 197 ($M^+ - H$, 18), 168 (16), 167 ($M^+ - OMe$, 100), 166 (22), 165 (55), 152 (25), 121 ($M^+ - Ph$, 99), 105 (21), 91 (17), 77 (49).

Methyl triphenylmethyl ether

Mp = 81–82 °C (pale-yellow solid) [lit.^{6a} mp 83–84 °C]. 1H NMR (300 MHz, $CDCl_3$) δ 3.06 (s, 3H), 7.18–7.37 and 7.41–7.49 (m, 15H). MS (EI), m/z (relative int.): 274 (M^+ , 29 %), 243 ($M^+ - OMe$, 45), 197 ($M^+ - Ph$, 100), 166 ($M^+ - Ph - OMe$, 12), 165 (62), 105 ($PhCO^+$, 73), 77 (53).

Methyl 1-phenylethyl ether

(Not isolated), MS (EI), m/z (relative int.): 136 (M^+ , 2%), 121 ($M^+ - Me$, 100), 105 ($M^+ - OMe$, 24), 91 (12), 77 (25).

By-products

The structures of *o*-cresol, *o*-hydroxybenzaldehyde, styrene, and 1,1-diphenylethylene were assigned by GC–MS.

o-Cresol

MS (EI), m/z (relative int.): 108 (M^+ , 100 %), 107 (85), 91 ($M^+ - OH$, 10), 90 (22), 79 (36), 77 (36).

o-Hydroxybenzaldehyde

MS (EI), m/z (relative int.): 122 (M^+ , 100 %), 121 ($M^+ - H$, 91), 93 ($M^+ - CHO$, 18), 76 (19), 65 (29).

Styrene

MS (EI), m/z (relative int.): 104 (M^+ , 100 %), 103 ($M^+ - H$, 46), 78 (41), 77 (19).

1,1-Diphenylethylene

MS (EI), m/z (relative int.): 180 (M^+ , 100 %), 179 ($M^+ - H$, 73), 178 (62), 165 (92), 89 (20), 77 (12).

Acknowledgements

MIUR (Italian Ministry of University and Research) and Consorzio Interuniversitario 'La Chimica per l'Ambiente' are gratefully acknowledged for financial support. We also thank Dr A. Perosa for his helpful comments.

References and notes

- (a) G. W. Griffin and A. Manmade, *J. Org. Chem.*, 1972, **37**, 2589–2599; (b) B. A. Stoochnoff and L. Benoiton, *Tetrahedron Lett.*, 1973, 21–24; (c) H. Ogawa, Y. Ichimura, T. Chihara, S. Teratami and K. Taya, *Bull. Chem. Soc. Jpn.*, 1986, **59**, 2481–2483; (d) J. Blagg, S. G. Davies, N. J. Holman, C. A. Laughton and B. E. Mobbs, *J. Chem. Soc., Perkin Trans. 1*, 1986, 1581–1589; (e) H. Ogawa, T. Hagiwara, T. Chihara, S. Teratami and K. Taya, *Bull. Chem. Soc. Jpn.*, 1987, **60**, 627–629; (f) E. Baciocchi, M. Bietti and M. Mattioli, *J. Org. Chem.*, 1993, **58**, 7106–7110; (g) X.-K. Fu and S.-Y. Wen, *Synth. Commun.*, 1995, **25**, 2435–2442; (h) H. Surya Prakash Rao, S. P. Senthilkumar, D. Srinivasa Reddy and G. Mehta, *Indian J. Chem., Sect. B: Org. Chem. Incl. Med. Chem.*, 1999, **38**, 260–263; (i) J. J. Gajewski, W. Bocian, N. J. Harris, L. P. Olson and J. P. Gajewski, *J. Am. Chem. Soc.*, 1999, **121**, 326–324; (j) R. Shu, J. F. Harrod and A.-M. Lebuis, *Can. J. Chem.*, 2002, **80**, 489–495; (k) B. Branchi, M. Bietti, G. Ercolani, M. A. Izquierdo, M. A. Miranda and L. Stella, *J. Org. Chem.*, 2004, **69**, 8874–8885.
- G. E. Hartzell and E. S. Huyser, *J. Org. Chem.*, 1964, **29**, 3341–3344.
- H. A. Smith and R. J. Smith, *J. Am. Chem. Soc.*, 1948, **70**, 2400–2402; E. A. Mayeda, L. L. Miller and J. F. Wolf, *J. Am. Chem. Soc.*, 1972, **94**, 6812–6816.
- J. M. Saa, A. Llobera, A. Garcia-Raso, A. Costa and P. M. Deya, *J. Org. Chem.*, 1988, **53**, 4263–4273.
- G. Olah and J. Welch, *J. Am. Chem. Soc.*, 1978, **100**, 5396–5401.
- (a) N. Iranpoor and E. Mothaghineghad, *Tetrahedron*, 1994, **50**, 1859–1870; (b) J.-M. Chapuzet, S. Beauchemin, B. Daouzet and J. Lessard, *Tetrahedron*, 1996, **52**, 4175–4180; (c) B. Das, B. Venkataiah and P. Madhusudhan, *J. Chem. Res. (S)*, 2000, 266–268.
- P. Salehi, N. Iranpoor and F. K. Behbahani, *Tetrahedron*, 1998, **54**, 943–948; V. V. Namboodiri and R. S. Varma, *Tetrahedron Lett.*, 2002, **43**, 4593–4595.
- A. Kawada, K. Yasuda, H. Abe and T. Harayama, *Chem. Pharm. Bull.*, 2002, **50**, 380–383.
- R. Ramu, R. Nath, M. R. Reddy and B. Das, *Synth. Commun.*, 2004, **34**, 3135–3145.
- A.-A. G. Shaik and S. Sivaram, *Chem. Rev.*, 1996, **96**, 951–976; P. Tundo and M. Selva, *Acc. Chem. Res.*, 2002, **35**, 706–716.
- Alkali metal-exchanged Y-faujasites are a class of zeolites in which the negative charge of the aluminosilicate framework is counterbalanced by an alkali metal cation. For example, a NaY faujasite possesses the general formula $Na_{56}[(AlO_2)_{56}(SiO_2)_{136}] \cdot 250H_2O$. For morphological details and properties, see: (a) F. Schwochow and L. Puppe, *Angew. Chem., Int. Ed. Engl.*, 1975, **14**, 620; (b) G. C. Bond, *Heterogeneous Catalysis Principles and Applications*, Clarendon Press, Oxford, 2nd edn, 1987; (c) D. Barthomeuf, *J. Phys. Chem.*, 1984, **88**, 42–45.
- P. Tundo, *Continuous Flow Methods in Organic Synthesis*, Horwood Publishers, Chichester (UK), 1991; Z.-H. Fu and Y. Ono, *Catal. Lett.*, 1993, **22**, 277–281; M. Selva, C. A. Marques and P. Tundo, *J. Chem. Soc., Perkin Trans. 1*, 1994, 1323–1328; Z.-H. Fu and Y. Ono, *J. Catal.*, 1994, **145**, 166–170; M. Selva, A. Bomben and P. Tundo, *J. Chem. Soc., Perkin Trans. 1*, 1997, 1041–1045; A. Bomben, M. Selva, P. Tundo and L. Valli, *Ind. Eng. Chem. Res.*, 1999, **38**, 2075–2079; M. Selva, P. Tundo, A. Perosa and S. Memoli, *J. Org. Chem.*, 2002, **67**, 1071–1077; M. Selva, P. Tundo and A. Perosa, *J. Org. Chem.*, 2003, **68**, 7374–7378; M. Selva, P. Tundo and T. Foccardi, *J. Org. Chem.*, 2005, **70**, 2476–2485.
- (a) P. Tundo, F. Trotta and G. Moraglio, *Ind. Eng. Chem. Res.*, 1988, **27**, 1565–1571; (b) M. Selva, F. Trotta and P. Tundo, *J. Chem. Soc., Perkin Trans. 2*, 1992, 519–522; (c) B. Veldurthy, J.-M. Clacens and F. Figueras, *J. Catal.*, 2005, **229**, 237–242.
- P. Tundo, S. Memoli, D. Herault and K. Hill, *Green Chem.*, 2004, **6**, 609–612. Hydrotalcite is a mixed Mg–Al oxide of the general formula $Mg_{0.7}Al_{0.3}O_{1.15}$.
- (a) M. Selva and P. Tundo, *J. Org. Chem.*, 2006, **71**, 1464–1470; (b) M. Selva, P. Tundo, D. Brunelli and A. Perosa, *Green Chem.*, 2007, **9**, 463–468.
- The product was easily separated in >95 % purity (by GC) by filtration of the solid zeolite and removal of DMC under vacuum. To obtain pure samples of BME, air had to be carefully purged with a N_2 stream before the reaction. Otherwise, the oxidation of benzyl alcohol took place. Under the conditions of entries 6 and 7 of Table 1, in a single experiment where moisture was not excluded, benzaldehyde was detected in a 10% amount (by GC) at a conversion of 85%.
- For brevity, the selectivity reported in Fig. 1 (uppermost curve) was averaged over the values obtained in the reactions catalyzed by both NaY and NaX faujasites. At complete conversion of **1a**, these values did not differ by more than 3% from each other.
- The number of recycling episodes, however, might be limited by the formation of an azeotropic mixture DMC–MeOH (70 : 30 v/v); see: W. Wona, X. Feng and D. Lawless, *Sep. Purif. Technol.*, 2003, **31**, 129–140; M. Fuming, P. Zhi and L. Guangxing, *Org. Process Res. Dev.*, 2004, **8**, 372–375. In the reported reaction, this problem was not experienced after three recycling tests.
- At 200 °C, the reaction of *p*-hydroxybenzyl alcohol (**3a**) afforded *p*-cresol as the major product.
- Methyl triphenylmethyl ether was purified by FCC (see Experimental section).
- A similar disproportionation reaction was also observed in the heating (200–400 °C) of benzyl alcohol in the presence of spinels as well as H-ZSM5 zeolites. See: G. R. Dube and V. S. Darshane, *J. Chem. Soc., Faraday Trans.*, 1992, **88**, 1299–1304; I. L. Yatovt, E. I. Kotov and N. R. Bursian, *J. Appl. Chem. USSR*, 1986, **59**, 604–609 (Engl. Transl.).
- B. Su and D. Barthomeuf, *Stud. Surf. Sci. Catal.*, 1995, **94**, 598.
- C. Bezoukhanova and Y. A. Kalkachev, *Catal. Rev. Sci. Eng.*, 1994, **36**, 125–143; C. Bezoukhanova, Y. A. Kalkachev, V. Nenova and H. Lechert, *J. Mol. Catal.*, 1991, **68**, 295–300.
- T. Beutel, *J. Chem. Soc., Faraday Trans.*, 1998, **94**, 985; F. Bonino, A. Damin, S. Bordiga, M. Selva, P. Tundo and A. Zecchina, *Angew. Chem., Int. Ed.*, 2005, **44**, 4774–4777.
- The OH function of benzyl alcohol undergoes a double interaction over the solid surface: the OH-oxygen atom reacts with the weak Lewis acidic sodium cation of the zeolite, while H-bonding takes place between the OH-hydrogen atom and a basic oxygen available in the lattice (see ref. 21). Simultaneously, an acid–base complex is formed between oxygen atoms of DMC and another Na cation.
- G. Öztürk and B. Gümgüm, *React. Kinet. Catal. Lett.*, 2004, **82**, 395–399; S. R. Kirumakki, N. Nagaraju and S. Narayanan, *Appl. Catal., A*, 2004, **273**, 1–9.
- The interaction of X and Y zeolites with OH groups of phenols is similar to that reported in Scheme 7; see: T. Beutel, M.-J. Peltre and B. L. Su, *Colloids Surf., A*, 2001, **187–188**, 319–325.
- P. Wan and B. Chak, *J. Chem. Soc., Perkin Trans. 2*, 1986, 1751–1756.

The relationship between solvent polarity and molar volume in room-temperature ionic liquids†

Mark N. Kobra*^{*}

Received 6th August 2007, Accepted 18th October 2007

First published as an Advance Article on the web 12th November 2007

DOI: 10.1039/b711991g

Solvent polarity is a subject of great interest to chemists. A significant component of a solvent's polarity is its capacity for nonspecific electrostatic interactions, which is often parameterized using the dielectric constant ϵ or the Kamlet–Taft dipolarity/polarizability parameter π^* . Recent theoretical work has established a connection between the molar volume of an ionic liquid and its capacity for nonspecific electrostatic interactions with a neutral dipolar solute. In this work, we make use of a recently-developed theoretical method to estimate the molar volume of a series of ionic liquids, and explore the variation of experimentally-measured ϵ and π^* values with molar volume. Both variables are found to vary with molar volume, and we observe an anomaly in the behavior of π^* that offers insight on the nanoscale inhomogeneity of ionic liquids. An important outcome of this work is a simple scheme for the estimation of the relative polarities of ionic liquids; while not quantitatively accurate, the scheme permits prediction of the change in solvent polarity on ionic substitution or derivitization. The approach is sufficiently simple that for most commonly-used ionic liquids it can be implemented on a pocket calculator in a matter of minutes, making it a practical aid to researchers seeking to design task-specific ionic liquids.

I. Introduction

In recent years, there has been considerable interest in a novel class of molten salts known as room-temperature ionic liquids (ILs).^{1–5} ILs possess many physical properties that make them useful as solvents, and have been found capable of solvating a wide range of organic and inorganic compounds. However, the nature of the solvation process in ILs remains poorly understood, and the relationship between ionic structure and solvent polarity is particularly opaque.

Like all molten salts, ILs are highly structured materials. Much of the crystal structure of the solid state is retained on melting, and the best model of the liquid environment is a crystalline lattice with a high population of voids and defects.⁶ Simulations^{7,8} and experiments⁹ suggest that nanoscale structures emerge in ILs incorporating long-chain hydrocarbon substituents. In these systems, a three-dimensional network of ionic charge centers forms, with aliphatic tails forming separate nanoscale domains interspersed in the medium. Further simulation data¹⁰ indicates that solutes may partition preferentially into one or the other domain, suggesting that regions of multiple polarity exist.

The definition of solvent polarity is simple neither in theory nor in practice,¹¹ but polarity is generally taken as an indicator of the combined strength of specific solute–solvent interactions (e.g. hydrogen bonding) and nonspecific (electrostatic) solute–solvent interactions. Previous studies of polarity in ILs have

shown that specific interactions in ionic liquids can, with few exceptions,¹² be understood from the same principles at work in molecular solvents. The binary nature of ionic materials can complicate the implementation of these principles through the creation of competing ion–solute and ion–counterion interactions,^{13,14} but the nature of, for example, the hydrogen bond, appears the same in both molecular and ionic liquids.

In this work, we focus on understanding electrostatic solute–solvent interactions, and consider both the macroscopic, static dielectric constant ϵ and the Kamlet–Taft dipolarity/polarizability parameter π^* . The static dielectric constant is defined by the zero-frequency polarization response of the medium,¹⁵ and is used to estimate the electrostatic energy (or free energy) of solute–solvent interactions in dielectric continuum models such as the Polarizable Continuum Model.¹⁶ While there are many subtleties in the application of the macroscopically-measured dielectric constant to molecular solvation, it has proven highly successful in understanding solute–solvent interactions in molecular liquids. However, for many well-studied ILs, the measured dielectric constants fall in the range of 10–15.¹⁷ Characterizations of IL polarity based on molecular spectroscopy^{17–23} and solubility^{24–28} generally indicate nonspecific electrostatic interactions of ILs that are equal to those of molecular liquids possessing significantly higher macroscopically-measured dielectric constants. This may have to do with the strong wavelength-dependence of the dielectric constant of fused salts,²⁹ as the dielectric constant measured in macroscopic (long-wavelength) experiments may not be the same as that associated with the response to a microscopic (molecular) field.

One may circumvent this possible discrepancy by using a molecular measurement of electrostatic polarization, such as

Department of Chemistry, Brooklyn College and the Graduate Center of the City University of New York, 2900 Bedford Ave., Brooklyn, NY, 11210, USA. E-mail: mkobra@brooklyn.cuny.edu

† Electronic supplementary information (ESI) available: Ionic volume calculations. See DOI: 10.1039/b711991g

the Kamlet–Taft scheme.^{30–32} The Kamlet–Taft scheme is a semi-empirical description of solvent polarity based on a linear free energy relationship describing the solvatochromic response of a series of dye molecules. The dyes are chosen to possess different electrostatic and hydrogen-bonding properties, permitting derivation of parameters for the solvent representing its ability to donate and accept hydrogen bonds, and its capacity for nonspecific electrostatic interactions. This last parameter is labeled π^* , and is referred to as representing the dipolarity/polarizability of the solvent. In molecular liquids, it includes both the reorientation of static molecular dipoles and the polarization of the electron cloud of individual molecules. In addition to permitting us to evaluate electrostatic solute–solvent interactions at a molecular level, the value of π^* is known to be an important determinant of reaction outcomes.^{33–36} Understanding the relationship between π^* and molecular structure is thus critically important in designing IL solvents.

We recently³⁷ derived an expression describing the electrostatic energy of interaction between a neutral, dipolar solute and an ionic solvent. While the expression was not analytically solvable, its form indicated that, in the lowest order electrostatic description of solvation, the only ionic property relevant to solute–solvent interactions is ionic volume. This prediction was confirmed by comparison to experimental data, in which the measured value of π^* was plotted against the number density of the solvent. The result showed a clear trend in which π^* decreased with increasing molar volume. This contrasts with the situation for molecular liquids, where the correlation between the two variables is very weak.

While the dataset was sufficient to confirm the predicted trend, experimental data on liquid density were not available for all species of known π^* value. In this work, we take advantage of a model prepared by Ye and Shreeve³⁸ that allows estimation of ionic volumes based solely on chemical structure. We use this method to estimate molar volumes for 40 ILs of known π^* value, and analyze the observed trend. We find that the predictions of the theory are further born out by the data, and we also find indirect evidence of the partitioning of solute species into aliphatic regions predicted above. We also examine the relationship between the static dielectric constant and the molar volume, though the dataset is more limited. The results are of interest to researchers seeking to design task-specific ionic liquids of a given polarity.

II. Methodology

The dataset for the present study, given in Table 1, represents the result of an extensive search of the literature for IL species with known Kamlet–Taft π^* and/or ϵ value. Ion identities are given in Table 2. Molar volumes were calculated according to the procedure in ref. 38. As we discuss below, there were some cases in which volume parameters had to be estimated, or for which the estimation of the volume in this way was ambiguous. However, the errors associated with these limitations of the model are small. The goal of the present study is to establish a qualitative rather than quantitative relationship between molar volume and solvent polarity, and the values employed are sufficiently accurate for that purpose.

Where possible, ionic volumes were taken directly from Table I of ref. 38. For organic species, it was necessary to apply the authors' rules regarding additivity of functional groups to estimate the molar volume. The rules for imidazolium, pyrrolidinium and pyridinium species are straightforward and can be applied without ambiguity. For tetraalkylammonium species, however, one obtains slightly different results depending on whether one “builds up” from Ye and Shreeve's tetramethylammonium cation or from a simple ammonium ion. We make a simple rule: Alkylammonium species incorporating only one or two alkyl substituents are constructed from the ammonium ion, while those incorporating three or four substituents are constructed from the tetramethylammonium cation. The latter is consistent with Ye and Shreeve's calculation of tetraalkylammonium species, though those authors do not consider mono- and dialkylammonium species. Details of the construction of each ion are given in the ESI;† in the most extreme case, the difference in volumes computed between the two pathways leads to an uncertainty of 6% in the calculated RTIL volumes. This is sufficiently low that it will not obscure the underlying trend in the data that is of interest in the present study.

No parameters were available describing the ring of the 1-ethyl-2-methylpyrazolium (EMP) ion. We estimated the volume to be equal to that of the 1-ethyl-3-methylimidazolium (C2MIM) ion, on the grounds that both are composed of five-membered aromatic rings incorporating 2 nitrogen atoms and decorated with equivalent alkyl substituents. In their discussion of heterocyclic cationic species, Ye and Shreeve assign a single ionic volume to a nitrogen atom in an aromatic ring, regardless of whether it is bonded to neighboring carbon or nitrogen atoms. Their results, which include examination of triazolium and tetrazolium species, suggest this approximation is sufficiently accurate that we may assign the pyrazolium and imidazolium rings the same molar volume (and by extension, equivalent volumes for C2MIM and EMP).

For ions and functional groups not explicitly discussed in Ye and Shreeve, it was necessary to follow their example and obtain estimated volumes from thermochemical radii reported in Jenkins *et al.*³⁹ Volumes for SbF_6^- and SCN^- were obtained from this source and used without modification. A number of organoanions in the present study incorporate an SO_3^- substituent, the volume of which cannot be directly calculated from data in either source. We therefore took the value of the volume for $\text{S}_2\text{O}_6^{2-}$ from Jenkins *et al.* and divided it in half, assigning a value of 76 Å for the SO_3^- substituent. This is similar to the value one would obtain from, for example, subtracting the molar volume of a fluoride ion (or fluorine atom) from the volume of FSO_3^- , also reported by Jenkins *et al.*³⁹ The potential error associated with this estimate is in any case small relative to the volumes of the ILs in question.

The values of π^* are taken from the experimental literature, with references included in Table 1. Experimental values of the static dielectric constant, estimated from microwave spectroscopy, are also included. Where we were aware of multiple, significantly different values reported for the same liquid, all are reported and their average used in graphical analysis.

Table 1 Molar volumes and π^* values for some ionic liquids

Cation	Anion	Cation volume/ \AA^3	Anion volume/ \AA^3	Total volume/ \AA^3	π^*	ϵ
Group A						
C1MIM	DCA	154	86	240	1.11 ⁵¹	
C2MIM	DCA	182	86	268	1.07 ⁵¹	
C2MIM	BF ₄ ⁻	182	73	255		12.9 ¹⁷
C2MIM	C2OSO ₃	182	147	329		27.9 ¹⁷
C2MIM	C4OSO ₃	182	203	385		17.5 ¹⁷
C2MIM	Tf	182	129	311		15.1 ¹⁷
C2MIM	Tf ₂ N	182	230	412		12.3 ¹⁷
						12.2 ⁴⁵
						Avg: 12.2
C3MIM	Tf ₂ N	210	230	440		11.8 ¹⁷
C4MIM	BF ₄ ⁻	238	73	311	1.05 ¹³	11.7 ¹⁷
C4MIM	Cl ⁻	238	47	285	1.17 ⁵	
C4MIM	DCA	238	86	324	1.05 ⁵¹	
C4MIM	PF ₆ ⁻	238	107	345	1.03 ¹³	11.4 ¹⁷
					0.92 ¹⁸	
					0.91 ⁵	
					Avg: 0.95	
C4MIM	SbF ₆ ⁻	238	121	359	1.04 ¹³	
C4MIM	Tf	238	129	367	1.01 ¹³	13.2 ¹⁷
C4MIM	Tf ₂ N	238	230	468	0.98 ⁵²	11.6 ¹⁷
						11.5 ⁴⁵
						Avg: 11.6
C5MIM	Tf ₂ N	266	230	496		11.4 ¹⁷
C6MIM	DCA	294	86	380	1.05 ⁵¹	
C6MIM	Tf	294	129	423	0.98 ⁵³	
C6MIM	Tf ₂ N	294	230	524	0.98 ⁵³	
C6MIM	PF ₆ ⁻	294	345	639		8.9 ⁴²
C8MIM	Cl ⁻	350	47	397	1.09 ⁵	
C8MIM	PF ₆ ⁻	350	107	457	0.88 ⁵	
C8MIM	Tf ₂ N	350	230	580	0.97 ⁵³	
C4MMIM	BF ₄ ⁻	266	73	339	1.08 ¹³	
C4MMIM	Tf ₂ N	266	230	496	1.01 ⁵³	11.6 ¹⁷
						11.4 ⁴⁵
						Avg: 11.5
C6MMIM	Tf ₂ N	322	230	552	0.99 ⁵³	
EMP	DCA	182	86	268	1.10 ⁵¹	
MPyrim4	Tf ₂ N	258	230	488	0.96 ⁵³	
MPyrim6	Tf ₂ N	314	230	544	0.98 ⁵³	
MPyrim8	Tf ₂ N	370	230	600	0.96 ⁵³	
MDMAPyrim6	Tf ₂ N	383	230	613	0.98 ⁵³	
N2HHH	NO ₃ ⁻	71	64	135	1.12 ¹³	26.2 ¹⁷
					1.24 ⁴¹	
					Avg: 1.18	
N33HH	SCN ⁻	183	71	254	1.16 ⁵	
N3HHH	NO ₃ ⁻	99	64	163	1.17 ⁴¹	
N4HHH	SCN ⁻	127	71	198	1.23 ⁴¹	
N(B2)HHH	SCN ⁻	127	71	198	1.28 ⁴¹	
N4111	Tf ₂ N	220	230	450		12.5 ⁴³
N444H	NO ₃ ⁻	360	64	424	0.97 ⁴¹	
N5222	Tf ₂ N	332	230	562		10.0 ¹⁷
Pyrim4	Tf ₂ N	230	230	455		11.3 ⁴³
						11.5 ¹⁷
						Avg: 11.4
Pyrr12	DCA	197	86	283	1.03 ⁵¹	
Pyrr14	Tf	253	129	382	1.02 ⁵²	
Pyrr14	Tf ₂ N	253	230	483	0.95 ⁵²	11.9 ¹⁷
						11.7 ⁴³
						Avg: 11.8
Pyrr15	Tf ₂ N	281	230	511		11.1 ¹⁷
Group B						
N3333	CHES	360	272	632	1.08 ⁴¹	
N3333	MOPSO	360	279	639	1.05 ⁴¹	
N4444	BES	472	280	752	1.07 ⁴¹	
N4444	CHES	472	272	744	1.01 ⁴¹	
N4444	MOPSO	472	279	751	1.07 ⁴¹	
N5555	BES	584	280	864	0.99 ⁴¹	
N5555	CHES	584	272	856	1.00 ⁴¹	
N5555	MOPSO	584	279	863	1.02 ⁴¹	

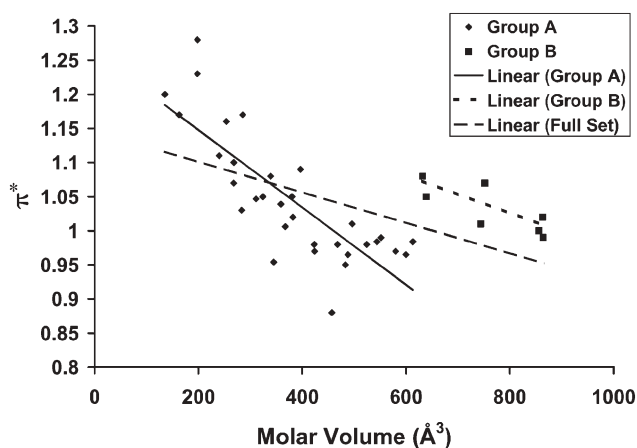
Table 2 Definitions of acronyms used in the present study

Cations	
C_nMIM	1-Alkyl-3-methylimidazolium <i>n</i> denotes alkyl chain length (methyl, butyl, hexyl, octyl)
C_nMMIM	1-Alkyl-2,3-dimethylimidazolium <i>n</i> denotes alkyl chain length (butyl, hexyl, octyl)
EMP	1-Ethyl-2-methylpyrazolium
Pyrr1 <i>n</i>	1-Alkyl-1-methylpyrrolidinium <i>n</i> denotes alkyl chain length (ethyl, butyl)
Pyrim <i>n</i>	1-Alkylpyridinium <i>n</i> denotes alkyl chain length (butyl)
MPyrim <i>n</i>	1-Alkyl-3-methylpyridinium <i>n</i> denotes alkyl chain length (butyl, hexyl, octyl)
MDMAPyrim6 <i>Nijkl</i>	1-Hexyl-3-methyl-4-dimethylaminopyridinium Indicates an alkylammonium species <i>ijkl</i> denote a hydrogen (H) or carbon chain length (1–5) (B2) denotes a <i>sec</i> -butyl group
Anions	
$ClOSO_3$	<i>n</i> -Alkylsulfate; <i>i</i> denotes alkyl chain length (ethyl, butyl)
DCA	Dicyanamide
Tf	Trifluoromethylsulfonate
Tf_2N	Bis(trifluoromethylsulfonyl)imide
CHES	2-(Cyclohexylamino)ethane sulfonate
BES	2-[Bis(2-hydroxyethyl)amino] ethanesulfonate
MOPSO	2-Hydroxy-4-morpholinopropane sulfonate
All other anions are denoted by their chemical formula.	

III. Results and discussion

A. The Kamlet–Taft dipolarity/polarizability

A plot of π^* vs. molar volume is shown in Fig. 1. The theoretical results that motivated this work³⁷ predict no specific functional form for the relationship between π^* and molar volume, only a general inverse relationship. The overall trend in the total dataset, indicated by the dashed line, confirms this expectation (see Table 3 for the details of the regression), and analysis of the linear correlation coefficient⁴⁰ for the sample confirms a correlation between π^* and molar volume to 99.9% certainty. The π^* parameter accounts for both the electronic and nuclear components of the solvent polarization, so one might question whether the correlation is really with the density of charge centers in the liquid or some other phenomenon that correlates with the polarizability of the

**Fig. 1** Graphical analysis of π^* . See text for discussion.**Table 3** Regression analyses. See text for discussion

Set	Slope/ $\times 10^{-4} \text{ \AA}^{-3}$	Intercept	R^2
π^* Regression parameters (Fig. 1)			
Group A	−5.67	1.26	0.65
Group B	−2.80	1.25	0.55
Full Set	−2.24	1.15	0.28
ϵ Regression parameters (Fig. 2)			
Full Set	−0.0272	24.78	0.42
Outliers	−0.0121	17.38	0.42
Dropped			

electron clouds of individual ions. However, our previous study³⁷ explored the relationship between molar volume and π^* for molecular liquids, and found only a very weak correlation. The observed pattern in Fig. 1 must therefore arise from the number density of charge centers, as predicted by theory.

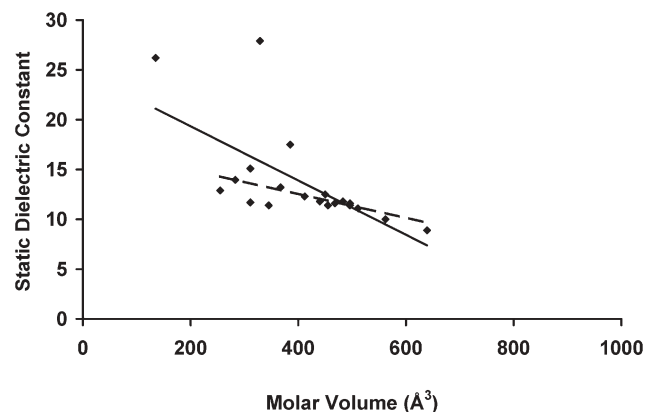
The sharp discontinuity in π^* at 620 \AA^3 , and the relatively small scatter in the data on either side of the step suggests it is productive to look for a detailed explanation of this phenomenon. For purposes of analysis, we divide the sample into two groups: Group A corresponds to liquids with a molar volume of less than 620 \AA^3 , and Group B corresponds to liquids with higher molar volumes. Examination of Table 1 reveals three facts:

(1) The data for all liquids in Group B is reported in a single reference.

(2) Group B contains *all* ILs incorporating symmetric tetraalkylammonium cations (*i.e.* tetraalkylammonium ions based on four equivalent substituents), and *only* cations of this type.

(3) Group B contains *all* ILs incorporating anions of molar volume greater than 250 \AA^3 , and contains *only* anions of this type.

In light of (1), one might question whether the deviation is an artifact of experimental methodology. The study, ref. 41, represents an early (indeed, pioneering) study in the field, when concerns about aqueous and other impurities were not fully developed. However, the authors' experimental protocol does not appear flawed, and of the 13 ILs reported in the same study, five fall in Group A and are well within the observed trend. Further, the scatter of points within Group B is considerably narrower than the size of the step in the value of π^* at 620 \AA^3 . It is conceivable that the behavior of Group B

**Fig. 2** Graphical analysis of ϵ . See text for discussion.

arises from some artifact that is unique to the ILs of highest molar volume and leads to a consistent shift in the value of π^* without an increase in its variance, but there is no evidence to suggest that this is the case.

It is therefore likely that the increase in π^* is a physical effect associated with the ionic structures of the Group B ions. We hypothesize that the increase in π^* is associated with the alteration or elimination of the nanoscale structure associated with Group A ILs. As discussed in the Introduction, the formation of nanoscale regions of aliphatic character reduces the effective polarity by creating a relatively low polarity domain into which molecular solutes may partition. Reduction of the volume of this domain, or its elimination, would therefore increase the observed (ensemble-averaged) polarity.

The high volume and symmetry of the Group B cations is the most likely culprit in such a scenario. The formation of nanoscale regions of well-defined ionic character requires the close coordination of ions, and the bulky, highly-symmetric character of the tetraalkylammonium cations may frustrate such close association. The presence of four equivalent neutral substituents prevents the formation of a well-defined aliphatic domain, and ionic volume and symmetry also hinder the close association of cation and anion charge centers that could facilitate the creation of an ionic domain. Group A includes more conventional IL structures, which include highly asymmetric cations and relatively small anions. Tf_2N , the largest Group A anion, is something of an exception to this trend, but it is highly flexible and possesses a symmetric and diffuse distribution of charge; it should thus be capable of strongly coordinating to cations. In contrast, the Group B anions are not only bulky, but (as shown in Fig. 3) they are asymmetric, with charge largely centered at the sulfonate moiety. Thus, both cations and anions in Group B contain structures that hinder the close association of ionic centers, and cation symmetry hinders the formation of a well-defined aliphatic domain.

These arguments suggest that the relationship between ionic structure and polarity is quite complex. Derivatization of a molecular solvent by a nonpolar substituent almost inevitably leads to a reduction in solvent polarity. By contrast, such derivitization of an ionic liquid can lead to an *increase* in solvent polarity if it disrupts the formation of aliphatic nanostructures in the liquid. This is a useful insight for the design of task-specific ILs.

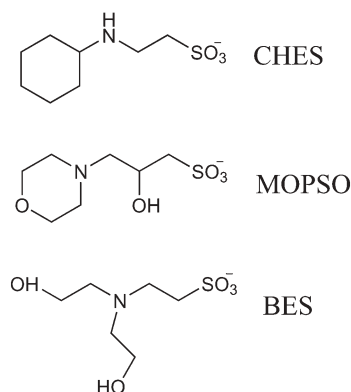


Fig. 3 Structures of anions in Group B. See text for details, and Table 2 for full nomenclature.

Note that while the partitioning of the solute into nanoscale domains appears to reduce the effective polarity of the solvent, the values of π^* for ionic liquids are still substantially larger than those observed in molecular liquids. This implies that electrostatic interactions with the ionic domain are still of great importance in the determination of polarity. While the proper account of the structural inhomogeneity of ILs requires extension of previous theory,³⁷ it does not invalidate the basic principles identified in that work as governing solute–solvent electrostatic interactions.

B. The static, macroscopic dielectric constant

Table 1 also presents experimental data on the dielectric constants of ILs, taken from the literature. The conductive nature of ILs makes measurement of the dielectric constant challenging, and the reported values are based on microwave dielectric relaxation spectroscopy, with the static values estimated by extrapolation from the relaxation data.^{17,42–45} Such extrapolation is difficult, but where multiple datasets are available, results from different studies are very consistent (see Table 1).

The available dataset of experimental values for ϵ (20 datapoints) is smaller than that for π^* , and includes neither Group B ionic liquids nor any of obviously similar chemical structure. We therefore consider the entire dataset for ϵ as similar in character to Group A. The most obvious question is whether ϵ varies with molar volume, and the answer is that it does. Statistical analysis of the linear correlation coefficient⁴⁰ indicates a correlation between the two variables with 99.8% certainty, and a simple linear regression of the data also indicates some variation (see Table 3). This regression analysis is applied both to the full dataset, and to a truncated dataset in which two outlying datapoints of $\epsilon > 25$ ($[\text{N2HHH}][\text{NO}_3^-]$ and $[\text{C2MIM}][\text{C2OSO}_3]$) are arbitrarily dropped to eliminate their disproportionate influence on the trend.

Our previously-developed theory³⁷ does not consider the macroscopic dielectric response, and so offers no insight on the nature of this relationship. Hydrodynamic theories based on the product of molecular (ionic) volume and viscosity are sometimes used to interpret the dynamics observed in dielectric relaxation experiments,⁴⁵ but such dynamic theories are not applicable to the static dielectric constant.

Two recent papers^{46,47} spell out the formulation relating the dielectric response of the IL to translational and rotational ionic motion. This formalism employs the dipole moment associated with the ionic center of mass, and rotational motion represents a component of the polarization response in a manner analogous to the rotation of dipoles in molecular liquids. Many ILs in the present study are structurally analogous families synthesized by the derivitization of parent ions with successively longer alkyl substituents; such derivitization would tend to increase both the dipole moment (by moving the center of mass away from charge centers) and the molar volume. One might therefore expect an increase in molar volume to correlate with an increase in dielectric constant, yet this is the reverse of the observed trend. It is possible that ionic dynamics are more weakly correlated in systems possessing a larger molar volume, so that the collective motion responsible

for the macroscopic dielectric response is weaker, decreasing the static dielectric constant.

It may be that ILs should be viewed as possessing characteristics similar to those of glasses rather than liquids. Simulation results⁴⁸ are indicative of supercooled or glassy dynamics in ILs, and broadband dielectric studies⁴⁹ observe secondary relaxation processes that are similar to those observed in molecular glasses. Schrödle *et al.*⁴⁴ have noted a secondary relaxation process in their microwave dielectric relaxation studies that is at least superficially similar to that observed in molecular glasses; similar secondary relaxations are observed in other experimental studies,⁴³ though the authors do not draw explicit analogy to glassy systems. Disordered ionic solids owe much of their dielectric response to the behavior of defects in their crystalline structure, which are known to display slow, complex relaxation dynamics.⁵⁰ If similar “defects” (nonuniformities in the liquid charge distribution) are responsible for the macroscopic dielectric response in ILs, the probability for the formation of these defects could reasonably be expected to vary inversely with the molar volume, if only because of the larger number of possible defects per unit volume. It may also be true that the creation of such defects polarizes the medium on some length scale in a manner analogous to polarization by a molecular solute. In this case, the free energy associated with the formation of the defect would be reduced by the lower IL molar volume by the same mechanism at work in the response to a molecular dipole.³⁷ However, this is speculative. We do not claim to have a clear interpretation of the relationship between the static, macroscopic dielectric constant and the molar volume of the IL, and simply lay the issue before the community for further discussion.

It would be desirable to study the relationship between π^* and ϵ directly, since their joint variation with molar volume implies some level of correlation. However, as indicated in Table 1, we are aware of only seven liquids for which both parameters are available. While the reader can easily construct the analysis from the data provided, we find that the sample is simply too limited to support any useful conclusions. We therefore forego discussion in the interest of brevity.

IV. Conclusions

We have used the method of Ye and Shreeve³⁸ to estimate molar volumes for a series of ionic liquids, and have confirmed our previously-derived theory that the value of the π^* dipolarity/polarizability factor should vary inversely with the molar volume of an IL. In so doing, we have also uncovered evidence that the IL nanostructures identified in simulation affect the solvation properties of an IL. We have also identified a relationship between the static, macroscopic dielectric constant and the molar volume of an ionic liquid, which suggests there may be a relationship between the macroscopic dielectric response and the microscopic (molecular) electrostatic behavior of the IL, though this relationship appears quite different than that observed in molecular liquids.

The results concerning π^* are of interest to researchers seeking to design task-specific ILs. For example, the work demonstrates that if a high dipolarity/polarizability is desired

for a certain task, the liquid should either (1) incorporate very small ions, or (2) incorporate ionic structures that frustrate the formation of nanoscale domains. Such frustration is observed in the present study for ILs incorporating large, asymmetric anions in combination with symmetric tetraalkylammonium cations, though it is not yet clear whether either or both features are necessary for this phenomenon. Further studies comparing π^* and molar volume may provide additional insight and reveal alternative strategies.

A major advantage of the present theory is its ease of implementation. For common cations and anions, Ye and Shreeve's³⁸ method for estimating molar volumes can be implemented on a pocket calculator in a matter of minutes. And while the relationship between π^* and molar volume is not sufficiently robust to permit quantitative predication of π^* , the relative change of polarity associated with chemical derivitization or ionic substitution can be estimated. Solvent polarity can be an important determinant of reaction outcomes, and the technique presented here is thus a simple and powerful aid to chemists seeking to design task specific ILs.

Acknowledgements

Grateful acknowledgement is made to the donors of the American Chemical Society Petroleum Research Fund for support of this research.

References

- J. L. Anderson, D. W. Armstrong and G. Tzo, *Anal. Chem.*, 2006, **78**, 2893–2902.
- J. B. Harper and M. N. Kobrak, *Mini-Rev. Org. Chem.*, 2006, **3**, 253–269.
- T. Welton, *Coord. Chem. Rev.*, 2004, **248**, 2459–2477.
- J. Dupont, R. F. de Souza and P. A. Z. Suarez, *Chem. Rev.*, 2002, **102**, 3667–3692.
- P. Wasserscheid and T. Welton, *Ionic Liquids in Synthesis*, Wiley-VCH, Mörlenbach, Germany, 2002.
- M. Blander, Some Fundamental Concepts in the Chemistry of Molten Salts, in *Molten Salts: Characterization and Analysis*, ed. G. Mamantov, Marcel-Dekker, New York, 1969.
- Y. Wang and G. A. Voth, *J. Phys. Chem. B*, 2006, **110**, 18601–18608.
- J. N. Canongia-Lopes and A. A. H. Pádua, *J. Phys. Chem. B*, 2006, **110**, 3330–3335.
- A. Triolo, O. Russina, H.-J. Bleif and E. D. Cola, *J. Phys. Chem. B*, 2007, **111**, 4641–4644.
- J. N. Canongia-Lopes, M. F. C. Gomes and A. A. H. Pádua, *J. Phys. Chem. B*, 2006, **110**, 16816–16818.
- C. Reichardt, *Chem. Rev.*, 1994, **94**, 2319–2358.
- C. Hanke, A. Johansson, J. Harper and R. Lynden-Bell, *Chem. Phys. Lett.*, 2003, **374**, 85–90.
- L. Crowhurst, P. Mawdsley, J. Perez-Arlandis, P. Salter and T. Welton, *Phys. Chem. Chem. Phys.*, 2003, **5**, 2790–2794.
- V. I. Znamenskiy and M. N. Kobrak, *J. Phys. Chem. B*, 2004, **108**, 1072–1079.
- J. D. Jackson, *Classical Electrodynamics*, 2nd edn., John Wiley & Sons, New York, 1975.
- C. J. Cramer and D. G. Truhlar, *Chem. Rev.*, 1999, **99**, 2161–2200.
- H. Weingärtner, *Z. Phys. Chem.*, 2007, **220**, 1395–1405.
- S. N. Baker, G. A. Baker and F. V. Bright, *Green Chem.*, 2002, **4**, 165–169.
- S. V. Dzyuba and R. A. Bartsch, *Tet. Lett.*, 2002, **43**, 4657–4659.
- K. A. Fletcher and S. Pandey, *Appl. Spectrosc.*, 2002, **56**, 266–271.
- M. J. Muldoon, C. M. Gordon and I. R. Dunkin, *Perkin Trans.*, 2001, **2**, 433–435.
- S. N. V. K. Aki, J. F. Brennecke and A. Samanta, *Chem. Commun.*, 2001, 413–414.

- 23 A. J. Carmichael and K. R. Seddon, *J. Phys. Org. Chem.*, 2000, **13**, 591–595.
- 24 M. H. Abraham, A. M. Zissimos, J. G. Huddleston, H. D. Willauer, R. D. Rogers and W. E. Acree, *J. Ind. Eng. Chem. Res.*, 2003, **42**, 413–418.
- 25 J. G. Huddleston, H. D. Willauer, R. P. Swatloski, A. E. Visser and R. D. Rogers, *Chem. Commun.*, 1998, 1765–1766.
- 26 J. L. Anderson and D. W. Armstrong, *Anal. Chem.*, 2003, **75**, 4851–4858.
- 27 J. L. Anderson, J. Ding, T. Welton and D. W. Armstrong, *J. Am. Chem. Soc.*, 2002, **124**, 14247–14254.
- 28 D. W. Armstrong, L. He and Y.-S. Liu, *Anal. Chem.*, 1999, **71**, 3873–3876.
- 29 M. Rovere and M. P. Tosi, *Rep. Prog. Phys.*, 1986, **49**, 1001–1081.
- 30 T. Yokoyama, R. W. Taft and M. J. Kamlet, *J. Am. Chem. Soc.*, 1976, **98**, 3233–3237.
- 31 R. W. Taft and M. J. Kamlet, *J. Am. Chem. Soc.*, 1976, **98**, 2886–2894.
- 32 M. J. Kamlet and R. W. Taft, *J. Am. Chem. Soc.*, 1976, **98**, 377–383.
- 33 M. H. Abraham, P. L. Grellier, J.-L. M. Abboud, R. M. Doherty and R. W. Taft, *Can. J. Chem.*, 1988, **66**, 2673–2686.
- 34 K. Dernbecher and G. Gauglitz, *J. Chem. Phys.*, 1992, **97**, 3245–3251.
- 35 M. Jonsson, A. Houmam, G. Jocys and D. D. M. Wayner, *J. Chem. Soc., Perkin Trans. 2*, 1999, 425–429.
- 36 P. M. Mancini, G. Fortunato, C. Adam, L. R. Vottero and A. J. Terenzani, *J. Phys. Org. Chem.*, 2002, **15**, 258–269.
- 37 M. N. Kobraj, *J. Phys. Chem. B*, 2007, **111**, 4755–4762.
- 38 C. Ye and J. M. Shreeve, *J. Phys. Chem. A*, 2007, **111**, 1456–1461.
- 39 H. D. B. Jenkins, H. K. Roobottom, J. Passmore and L. Glasser, *Inorg. Chem.*, 1999, **38**, 3609–3620.
- 40 R. J. Larsen and M. L. Marx, *An introduction to mathematical statistics and its applications*, 2nd edn, Prentice-Hall, Englewood Cliffs, 1986.
- 41 S. K. Poole, P. H. Shetty and C. F. Poole, *Anal. Chim. Acta*, 1989, **218**, 241–264.
- 42 C. Wakai, A. Oleinikova, M. Ott and H. Weingärtner, *J. Phys. Chem. B*, 2005, **109**, 17028–17030.
- 43 H. Weingärtner, P. Sasisanker, C. Daguene, P. J. Dyson, I. Krossing, J. M. Slattery and T. Schubert, *J. Phys. Chem. B*, 2007, **111**, 4775–4780.
- 44 S. Schrödle, G. Annat, D. R. MacFarlane, M. Forsyth, R. Bucher and G. Heftler, *Chem. Commun.*, 2006, 1748–1750.
- 45 C. Daguene, P. J. Dyson, I. Krossing, A. Oleinikova, J. Slattery, C. Wakai and H. Weingärtner, *J. Phys. Chem. B*, 2006, **110**, 12682–12688.
- 46 C. Schröder, T. Rudas and O. Steinhauser, *J. Chem. Phys.*, 2006, **125**, 244506.
- 47 C. Schröder, C. Wakai, H. Weingärtner and O. Steinhauser, *J. Chem. Phys.*, 2007, **126**, 084511.
- 48 C. J. Margulis, H. A. Stern and B. J. Berne, *J. Phys. Chem. B*, 2002, **106**, 12017–12021.
- 49 A. Rivera and E. A. Rössler, *Phys. Rev. B*, 2006, **73**(212201), 1–4.
- 50 W. Dieterich and P. Maass, *W. Dieterich and P. Maass*, 2002, **284**, 439–467.
- 51 Y. Yoshida, O. Baba and G. Saito, *J. Phys. Chem. B*, 2007, **111**, 4742–4749.
- 52 L. Crowhurst, R. Falcone, L. Lancaster, V. Llopis-Mestre and T. Welton, *J. Org. Chem.*, 2006, **71**, 8847–8853.
- 53 B. R. Mellein, S. N. V. K. Aki, R. L. Ladewski and J. F. Brennecke, *J. Phys. Chem. B*, 2007, **111**, 131–138.

Desulfurisation of oils using ionic liquids: selection of cationic and anionic components to enhance extraction efficiency†

John D. Holbrey,^{*a} Ignacio López-Martin,^a Gadi Rothenberg,^b Kenneth R. Seddon,^a Guadalupe Silvero^c and Xi Zheng^a

Received 11th July 2007, Accepted 24th October 2007

First published as an Advance Article on the web 14th November 2007

DOI: 10.1039/b710651c

Extraction of dibenzothiophene from dodecane using ionic liquids as the extracting phase has been investigated for a range of ionic liquids with varying cation classes (imidazolium, pyridinium, and pyrrolidinium) and a range of anion types using liquid–liquid partition studies and QSPR (quantitative structure–activity relationship) analysis. The partition ratio of dibenzothiophene to the ionic liquids showed a clear variation with cation class (dimethylpyridinium > methylpyridinium > pyridinium \approx imidazolium \approx pyrrolidinium), with much less significant variation with anion type. Polyaromatic quinolinium-based ionic liquids showed even greater extraction potential, but were compromised by higher melting points. For example, 1-butyl-6-methylquinolinium bis{(trifluoromethyl)sulfonyl}amide (mp 47 °C) extracted 90% of the available dibenzothiophene from dodecane at 60 °C.

Introduction

The current state of the art for removing sulfur-containing compounds in refineries is catalytic hydrogenation.¹ However, there is an increased interest in alternative processes to hydrodesulfurisation driven by regulatory requirements to reduce the content of sulfur in fuels and the current limitations of hydrodesulfurisation technologies to fully remove refractory aromatic sulfur compounds, particularly alkylated benzothiophenes and dibenzothiophenes.² Approaches³ based on adsorption⁴ or complexation,⁵ oxidative extraction,⁶ biodesulfurisation,⁷ and ultrasonic treatments⁸ have been explored.

Liquid–liquid extractive desulfurisation (EDS) systems using ionic liquids as the extracting phase have been reported.^{9–12} Many ionic liquids are immiscible, or only partially miscible, with hydrocarbons,¹³ and these studies have attempted to use the unique solvent characteristics of ionic liquids^{13,14} to provide high extraction ratios and greater selectivity compared to molecular solvents.¹⁵ The principal focus of these studies is the extraction of refractory sulfur-containing polyaromatics, such as dibenzothiophene (DBT, Fig. 1) and 4,6-dimethyldibenzothiophene from dodecane as a model oil system.

The ionic liquids studied have been chosen principally for their ready availability at relatively low cost and environmental impact. Following the initial report by Bösmann *et al.*,⁹

Jess and co-workers have promoted 1,3-dialkylimidazolium alkylsulfates,¹⁰ whereas Li and co-workers¹² favour 1,3-dialkylimidazolium alkylphosphates as candidates for extractive desulfurisation technologies.

While simple hydrocarbons are poorly soluble in many ionic liquids,¹³ aromatic compounds, such as benzene and toluene, can be highly soluble,¹⁶ with interactions between the ionic liquid ions and aromatic solutes leading to liquid clathrate and solid-state inclusion complexes.^{17,18} However, despite these favourable interactions,¹⁹ ionic liquids have not proven to be exceptional solvents for liquid–liquid separation of aromatics from aliphatic hydrocarbons.^{20,21}

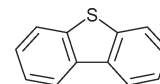


Fig. 1 Chemical structure of dibenzothiophene (DBT).

For sulfur-containing aromatics, such as DBT, 1-butyl-3-methylimidazolium octylsulfate ([C₄mim][C₈H₁₇SO₄]) was reported¹⁰ to have the highest partition ratio (K_D) for DBT from dodecane ($K_D = 1.9$) of all the ionic liquids, with the exception of chloroaluminate ionic liquids, which are hydrolytically unstable and reactive to many substrates. An alternative reaction/extraction approach has also been described combining hydrogen peroxide/ethanoic acid oxidation of the aromatic sulfur compounds to sulfones and sulfoxides, which are then extracted with much higher partition ratios to the ionic liquid phase.²²

Interestingly, most of the published data relates to ionic liquids with imidazolium cations.^{9–12} 1-Alkylpyridinium salts, for example, are described in the patent literature only as organic salt additives in liquid–liquid separations.²³ With the variety of ionic liquids available, especially considering those with different types of cations, we reasoned that a more general study to examine the influence of different cationic and

^aThe QUILL Research Centre, School of Chemistry and Chemical Engineering, The Queen's University of Belfast, Belfast BT9 5AG, Northern Ireland, UK. E-mail: quill@qub.ac.uk; Tel: +44 28 90975420

^bYan't Hoff Institute for Molecular Sciences, Universiteit van Amsterdam, Nieuwe Achtergracht 166, 1018 WV Amsterdam, The Netherlands

^cDepartamento de Química Orgánica, Universidad de Extremadura, Avenida de la Universidad, 10071 Cáceres, Spain

† Electronic supplementary information (ESI) available: QSPR analysis of solvent group contributions to extraction. See DOI: 10.1039/b710651c

anionic species on the partitioning might lead to better ionic liquid extracting systems.

Here, we describe an investigation of the role of different cationic and anionic components of an ionic liquid extracting phase on the efficiency of partitioning of DBT from dodecane as a model for extractive desulfurisation of oils.

Results and discussion

Extraction of a model system consisting of dodecane containing DBT as a source of polyaromatic sulfur with a sulfur content of 500 ppm (2880 ppm, 0.0156 mole l^{-1} of DBT) was studied with a range of ionic liquids, chosen in order to assess the role of the different cation classes (imidazolium, pyridinium, methylpyridinium, pyrrolidinium, see Fig. 2), and anion types, respectively, both with common counterions. This enabled the study of the respective roles of cation, anion or cation–anion pairs on the extraction profile.

Extraction experiments were performed on a 4 cm³ scale using equal volumes (2 cm³ each) of ionic liquid as the extracting phase and dodecane containing DBT at 0.0156 molar concentration (corresponding to 500 ppm of sulfur) in the initial organic phase. The volume of the ionic liquid phase was not observed to change during the contact and mixing with dodecane, indicating low co-solubility of the phases. The hydrocarbon phase was analysed before and after extraction for DBT by GC-MS.

Initially, we compared selected systems from the literature to establish that the experimental protocol used in this work could replicate previously reported results at 25 and 60 °C from Jess and co-workers.^{9,10} Comparing the data in Table 1 indicates a reasonable compatibility between the results for 1-butyl-3-methylimidazolium octylsulfate ([C₄mim][C₈H₁₇SO₄]), and 1-ethyl-3-methylimidazolium ethylsulfate ([C₂mim][C₂H₅SO₄]) at 25 °C and 1-butyl-3-methylimidazolium hexafluorophosphate ([C₄mim][PF₆]), 1-butyl-3-methylimidazolium tetrafluoroborate ([C₄mim][BF₄]), and [C₄mim][C₈H₁₇SO₄], at 60 °C. We obtained a reasonable correlation with the

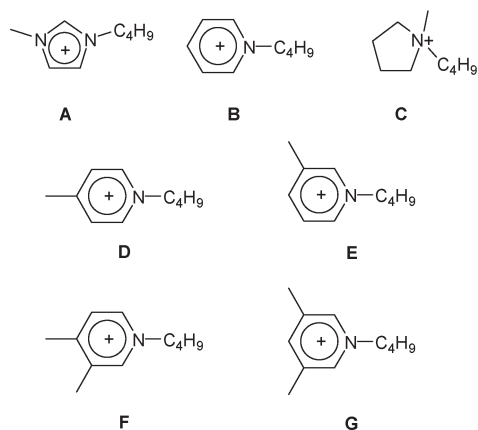


Fig. 2 Chemical structure of seven of the ionic liquid cations studied here: (A) 1-butyl-3-methylimidazolium ([C₄mim]⁺); (B) 1-butylpyridinium ([C₄py]⁺); (C) 1-butyl-1-methylpyrrolidinium ([C₄mpyr]⁺); (D) 1-butyl-4-methylpyridinium ([C₄⁴mpy]⁺); (E) 1-butyl-3-methylpyridinium ([C₄³mpy]⁺); (F) 1-butyl-3,4-dimethylpyridinium ([C₄^{2,4}dmpy]⁺); (G) 1-butyl-3,5-dimethylpyridinium ([C₄^{2,5}dmpy]⁺).

Table 1 Comparison of DBT partition ratios (K_D), with literature data from references 9 and 10 in parentheses^a

Ionic liquid	K_D	
	25 °C	60 °C
[C ₄ mim][PF ₆], 4	—	0.8 (0.7/0.9)
[C ₄ mim][BF ₄], 1	—	0.9 (1.0)
[C ₄ mim][C ₈ H ₁₇ SO ₄], 2	1.7 (1.9)	1.6 (2.1)
[C ₂ mim][C ₂ H ₅ SO ₄]	0.9 (0.8)	—

^a General conditions: 25 or 60 °C, volume ratio model oil : ionic liquid = 1 : 1, mixing time 1 h, equilibration time 15 min, initial sulfur content 500 ppm as DBT.

literature results[‡] confirming the consistency of the experimental methodology, although we notably obtained a consistently lower K_D in the [C₄mim][C₈H₁₇SO₄] system.

Having established that this protocol was consistent with the previous literature, subsequent screening experiments were performed at 40 °C. This enabled better experimental stability of temperature and gave improved mixing characteristics for some of the more viscous ionic liquids.

The ionic liquids used contained [C₄mim]⁺ (**1–7**), [C₄py]⁺ (**8,9**), [C₄⁴mpy]⁺ (**10–13**), [C₄³mpy]⁺ (**14–17**), [C₄^{2,4}dmpy]⁺ (**18**), [C₄^{2,5}dmpy]⁺ (**19**), and [C₄mpyr]⁺ (**20**) cations (see Fig. 2); the extraction results for removing DBT (at 500 ppm sulfur content) from dodecane for each ionic liquid with the anions hexafluorophosphate [PF₆][−], octylsulfate [OcSO₄][−], trifluoromethanesulfonate [OTf][−], tetrafluoroborate [BF₄][−], bis((trifluoromethyl)sulfonyl)amide [NTf₂][−], thiocyanate [SCN][−], and ethanoate [CH₃CO₂][−] are shown in Table 2 as percentage extracted and as the partition ratio K_D .

Anion dependence with common [C₄mim]⁺ cation

The influence of the ionic liquid anion on the partitioning was explored for [C₄mim]⁺ ionic liquids with the series of anions; [PF₆][−] (**1**), [C₈H₁₇SO₄][−] (**2**), [OTf][−] (**3**), [BF₄][−] (**4**), [NTf₂][−] (**5**), [SCN][−] (**6**), and [CH₃CO₂][−] (**7**). EDS data for the first four ionic liquids here have previously been reported (as described above); the last three ionic liquids have not been previously studied in the context of desulfurisation.

Comparison of the data for these ionic liquids shows that the choice of anion has little direct effect on the extraction ability in most cases (shown as percentage DBT extracted in Fig. 3). Only a relatively small variation in partition ratio with anion type was observed, with K_D in the range 0.9–1.9, which corresponds to DBT extraction between 47 and 66%. The ordering of the partition ratio with anion type is [BF₄][−] < [NTf₂][−] < [OTf][−] < [PF₆][−] < [C₈H₁₇SO₄][−] < [CH₃CO₂][−] < [SCN][−]. The four ionic liquids [C₄mim][PF₆], [C₄mim][C₈H₁₇SO₄], [C₄mim][OTf], and [C₄mim][BF₄] have similar partition ratios (K_D = 1–1.2), which are also comparable with

[‡] The variation in partition ratio (K_D) quoted over the range 1–3 correspond to only small changes in actual percentages of DBT extracted, for example, the differences between K_D = 1.6 and K_D = 1.9, for DBT extraction with the ionic liquid [C₄mim][C₈H₁₇SO₄] here, and in the literature, represent percentage extracted of 62 and 66%, overall—only 4% variation, which is probably within the experimental errors between different methods. Similarly, this experimental variation is exemplified by the differences between results published in references 9 and 10 by the same researchers.

Table 2 Ionic liquids screened and extraction of dibenzothiophene (concentration equivalent to 500 ppm of sulfur) from dodecane at 40 °C using equal volumes of ionic liquid and dodecane, expressed as percent extracted and as partition ratio (K_D)^a

	Ionic liquid	Percent extracted (%)	K_D	Standard error (%)
1	[C ₄ mim][BF ₄]	47	0.9	0.6
2	[C ₄ mim][C ₈ H ₁₇ SO ₄]	63	1.7	0.9
3	[C ₄ mim][CF ₃ SO ₃]	50	1.0	0.6
4	[C ₄ mim][PF ₆]	53	1.2	0.5
5	[C ₄ mim][NTf ₂]	50	1.0	2.8
6	[C ₄ mim][SCN]	66	1.9	1.4
7	[C ₄ mim][CH ₃ CO ₂]	61	1.6	0.1
8	[C ₄ py][NTf ₂]	55	1.2	3.4
9	[C ₄ py][BF ₄]	43	0.8	1.1
10	[C ₄ ⁴ mpy][NTf ₂]	76	3.3	1.0
11	[C ₄ ⁴ mpy][BF ₄]	70	2.3	0.4
12	[C ₄ ⁴ mpy][SCN]	79	3.8	0.87
13	[C ₄ ⁴ mpy][CF ₃ SO ₃]	72	2.6	0.58
14	[C ₄ ³ mpy][NTf ₂]	77	3.4	0.5
15	[C ₄ ³ mpy][BF ₄]	70	2.3	0.4
16	[C ₄ ³ mpy][SCN]	83	4.9	0.5
17	[C ₄ ³ mpy][CF ₃ SO ₃]	69	2.3	1.6
18	[C ₄ ^{2,4} dmpy][NTf ₂]	83	4.9	0.28
19	[C ₄ ^{2,5} dmpy][NTf ₂]	81	4.0	0.53
20	[C ₄ mpyrr][NTf ₂]	47	0.9	1.9

^a General conditions: 40 °C, volume ratio model oil : ionic liquid = 1 : 1, mixing time 1 h, equilibration time 15 min, initial sulfur content 500 ppm as DBT

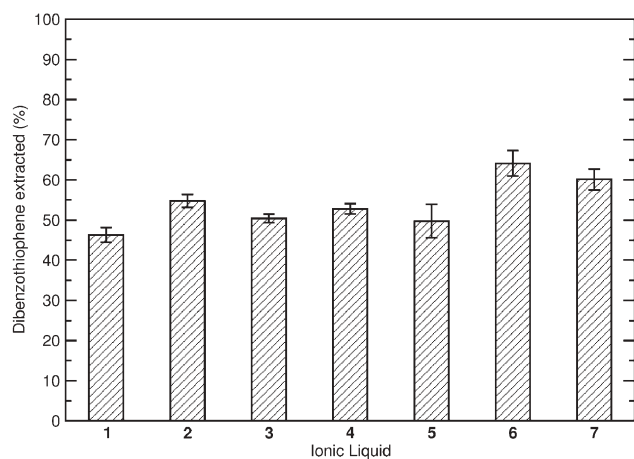


Fig. 3 Percentage DBT extracted by [C₄mim]X (1–7) from dodecane at 40 °C (1 : 1 volumes, 500 ppm sulfur in dodecane phase as DBT).

the data from Jess and co-workers^{9,10} for [C₄mim]X ionic liquids measured at 60 °C.

Interestingly, the ionic liquids with the ethanoate and thiocyanate anions ([C₄mim][CH₃CO₂] and [C₄mim][SCN]) gave the highest partition ratios of all the [C₄mim]⁺ salts studied here. Jess and co-workers^{9,10} have suggested that anion size was an important factor in achieving better extraction, supported by the high value of K_D for [C₄mim][C₈H₁₇SO₄]. However, our data suggest that high relative ionicity, rather than the size, of the anion may be more significant in promoting extraction.

Cation dependence with common anion

Having established that changing the anion of the ionic liquid has only a small variation on K_D for dibenzothiophene, despite

the significant variation in the usual physical properties of ionic liquids driven by the anion type,¹⁵ the influence of the cation type was investigated. The key common classes of cations used to prepare ionic liquids were studied as bis{(trifluoromethyl)sulfonyl}amide salts. Data for [C₄mim][NTf₂] (5), [C₄py][NTf₂] (8), [C₄⁴mpy][NTf₂] (10), [C₄³mpy][NTf₂] (14), [C₄^{2,4}dmpy][NTf₂] (18), [C₄^{2,5}dmpy][NTf₂] (19), and [C₄mpyrr][NTf₂] (20) gave a much wider distribution in K_D , ranging from 0.9 to 4.9 (47–83% extraction of DBT), than that observed from the change in anion type, and are shown graphically in Fig. 4.

The ability of the ionic liquids to extract DBT follows the order, pyrrolidinium ≈ imidazolium ≈ pyridinium < methylpyridinium < dimethylpyridinium, with the two 1-butyl-dimethylpyridinium isomers ([C₄^{2,4}dmpy][NTf₂] and [C₄^{2,5}dmpy][NTf₂]) giving the highest partition ratios for DBT observed for any of the systems. Both of these ionic liquids extracted between 81–83% of the DBT from dodecane, followed by the 1-butyl-methylpyridinium systems ([C₄⁴mpy][NTf₂] and [C₄³mpy][NTf₂]), which were able to extract 76–77% of the available DBT in a single contact. The three remaining bis{(trifluoromethyl)sulfonyl}amide ionic liquids ([C₄mim][NTf₂], [C₄py][NTf₂], and [C₄mpyrr][NTf₂]), showed poorer extraction ability, removing between 47–55% of DBT.

A comparable trend was also observed for the smaller set of corresponding tetrafluoroborate ionic liquids; [C₄mim][BF₄] and [C₄py][BF₄] gave similar, poor, extraction of DBT (K_D = 0.9 and 0.8, respectively), whereas [C₄⁴mpy][BF₄], and [C₄³mpy][BF₄] exhibited good extraction of DBT (K_D = 2.3 in each case), almost comparable to the high partition ratios measured in the corresponding bis{(trifluoromethyl)sulfonyl}amide containing ionic liquids, extracting 69–70% of the DBT from the dodecane phase.

Four additional ionic liquids with 1-butyl-4-methylpyridinium and 1-butyl-3-methylpyridinium cations; [C₄⁴mpy][SCN], [C₄⁴mpy][CF₃SO₃], [C₄³mpy][SCN], and [C₄³mpy][CF₃SO₃] also were examined. All showed good extraction characteristics, comparable to those of the corresponding bis{(trifluoromethyl)sulfonyl}amide analogues. [C₄⁴mpy][CF₃SO₃]

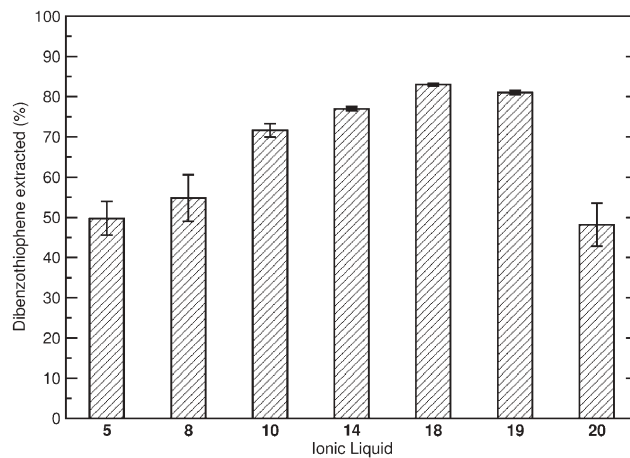


Fig. 4 Percentage DBT extracted by [A][NTf₂] (5, 8, 10, 14, 18–20) from dodecane at 40 °C (1 : 1 volumes, 500 ppm sulfur in dodecane phase as DBT).

and $[C_4^3\text{mpy}][CF_3SO_3]$ with trifluoromethanesulfonate anions extracted around 70% of the DBT with a single contact, comparable with the corresponding bis{(trifluoromethyl)sulfonyl}amide and tetrafluoroborate ionic liquids. Even higher partition ratios were measured with the thiocyanate-containing ionic liquids $[C_4^4\text{mpy}][SCN]$ and $[C_4^3\text{mpy}][SCN]$ ($K_D = 3.8$ and 4.9 respectively, corresponding to 79 and 83% extraction). For each group of cations examined, the ionic liquids with thiocyanate anions consistently showed the greatest ability to extraction DBT from dodecane. These results support the observations of cation dominance in the partitioning efficiency, and significantly less importance of the anion, although the effect of the anion is incontrovertible.

Influence of cation isomerisation

There are few data to differentiate between the extraction ability of the two sets of isomeric ionic liquids with 1-butyl-methylpyridinium cations ($[C_4^4\text{mpy}]^+$ and $[C_4^3\text{mpy}]^+$), or between the two results for 1-butyl-dimethylpyridinium isomers ($[C_4^{2,4}\text{dmpy}][NTf_2]$ and $[C_4^{2,5}\text{dmpy}][NTf_2]$). Only small variations in K_D with the positions of the methyl groups on the ring with comparable partition ratios are observed for each pair of ionic liquids.

QSPR analysis of solvent group contributions to extraction

Explaining the differences in the extraction of DBT by the different ionic liquids is challenging. Factors such as the size/shape/aromaticity and/or charge distribution appears to be the important criteria. Both $[C_4\text{mim}]^+$ and $[C_4\text{py}]^+$ cations contain ten non-hydrogen atoms, compared to eleven for $[C_4^3\text{mpy}]^+$ and $[C_4^4\text{mpy}]^+$ and twelve for the $[C_4^{2,4}\text{dmpy}]^+$ and $[C_4^{2,5}\text{dmpy}]^+$ cations, which may lead to the small relative increase in affinity for aromatic components. However, the methyl group is not usually considered to have a significant inductive effect on aromatic rings. Similarly, the presence, or absence, of aromaticity may not be the only feature of importance; $[C_4\text{mpyrr}]^+$ also contains ten non-hydrogen atoms, but in contrast is neither flat nor an aromatic cation.

Quantitative structure–property relationship (QSPR) approaches have been used with some success in predicting the physical properties of ionic liquids.^{24–30} A QSPR analysis of the partitioning data was used to identify whether a correlation could be obtained, and which, if any, of the resulting descriptors could be related to the extracting ability of the ionic liquids. The study focused on the influence of the cation using data from twelve ionic liquids with the common bis{(trifluoromethyl)sulfonyl}amide anion (4, 8, 10, 14, 18–20 from Table 2 and five additional ionic liquids§).

§ Additional ionic liquids incorporated in the QSPR data analysis, with experimentally determined DBT distribution ratio and percentage extracted: (a) 1-(methoxyethyl)-3-methylimidazolium bis{(trifluoromethyl)sulfonyl}amide ($[CH_3OC_2H_4\text{mim}][NTf_2]$), $K_D = 0.6$, 28%; (b) *N*-methyl-*N*-butyl-*N,N*-di(2-hydroxyethyl)ammonium bis{(trifluoromethyl)sulfonyl}amide ($[NMeBu(CH_2CH_2OH)_2][NTf_2]$) $K_D = 0.26$, 21%; (c) 1-(2-hydroxyethyl)-1-methylmorpholinium bis{(trifluoromethyl)sulfonyl}amide ($[HOCH_2CH_2\text{mmor}][NTf_2]$) $K_D = 0.7$, 41%; (d) 1-butyl-4-cyanopyridinium bis{(trifluoromethyl)sulfonyl}amide ($[C_4^4\text{CNpy}][NTf_2]$) $K_D = 1.6$, 61%; (e) 1-hexyl-4-cyanopyridinium bis{(trifluoromethyl)sulfonyl}amide ($[C_6^4\text{CNpy}][NTf_2]$) $K_D = 2.0$, 66%.

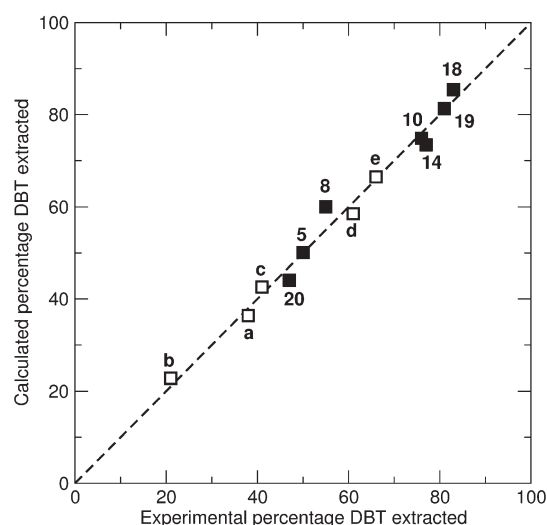


Fig. 5 Comparison of experimental and calculated percentage DBT extraction from the regression analysis ($r^2 = 0.9835$, $c_{vr}^2 = 0.9452$) for the ionic liquids 4, 8, 10, 14, 18–20 and five additional ionic liquids; (a) $[CH_3OC_2H_4\text{mim}][NTf_2]$; (b) $[NMeBu(CH_2CH_2OH)_2][NTf_2]$; (c) $[HOEtmmor][NTf_2]$; (d) $[C_4^4\text{CNpy}][NTf_2]$; (e) $[C_6^4\text{CNpy}][NTf_2]$.

An initial series of one-, two- and four-parameter correlations were screened using the heuristic method³¹ implemented in CODESSA,³² a complete description of the QSPR treatment and analysis is available as supplementary material.† The descriptors identified from the one-, two- and four-parameter correlations indicated that the size, shape and aromaticity of the cation were important contributors. However, with such a small number of observations (12), chance correlations are likely if the number of screened variables is large.³³ Notably, a number of descriptors from the four parameter correlation ($WPSA_1$, $WPSA_2$ and $FPSA_3$) were related and describe weighted positive charge size and distribution (suggesting that the cation size has a significant correlation with extraction ability). Topliss and Edwards suggest that all duplicate descriptors with intercorrelation $r^2 > 0.8$ should be discarded for the final modelling,³³ which also dramatically reduces the likelihood of chance correlations, since the number of descriptors screened is reduced.

The four-descriptor correlation was rescreened using a more stringent rejection criterion for duplicate descriptors (2-parameter intercorrelation $r^2 \geq 0.80$); this reduced the descriptor pool to 31. The best regression correlation, shown in Fig. 5 ($r^2 = 0.9835$, $c_{vr}^2 = 0.9452$) was:

$$\%_{\text{Extract}} = 2.9504e01(\epsilon_{\text{HOMO}-1}) - 1.3835e04(P_{\sigma-\sigma}) - 7.9048e02(P'^C_{AB}) - 1.2512e02(S_{YZ}) + 1.5082e04$$

$\epsilon_{\text{HOMO}-1}$: HOMO-1 energy (2nd ionisation potential)

$P_{\sigma-\sigma}$: maximum $\sigma-\sigma$ bond order

P'^C_{AB} : minimum (>0.1) bond order for a C atom

S_{YZ} : YZ shadow/YZ rectangle

With this correlation, the best interpretation of the descriptors is that the extraction is governed by a combination of solute–solvent interactions with the aromatic system ($\epsilon_{\text{HOMO}-1}$, $P_{\sigma-\sigma}$, P'^C_{AB}) and is also controlled by the topology of the cation, with larger/flatter cations (ZY shadow/XY

rectangle) performing best. However, these criteria can also be interpreted in a number of alternative ways: for example, in order to obtain a larger/flatter cation, additional carbon atoms can be added (pyridinium, methylpyridinium, dimethylpyridinium, *etc.*), which increases the number of carbon atoms and the reduction in sigma–sigma bond order all as intercorrelated descriptors.

Given the small number of observations, caution must be exerted when interpreting these results. Yet, where overall conclusions can be drawn, they point towards transfer interaction ability, aromaticity and the shape of the molecule as being influential with this extraction process and suggest that ionic liquids containing cations with greater aromatic character, for example containing polyaromatic cations, would give enhanced extraction. Ionic liquids containing a polyaromatic quinolinium and isoquinolinium cations are known, but tend to have relatively high melting points, a common feature of the larger ring structure.^{34,35} Two examples, 1-butyliisoquinolinium bis{(trifluoromethyl)sulfonyl}amide (mp 56 °C), and 1-butyl-6-methylquinolinium bis{(trifluoromethyl)sulfonyl}amide (mp 47 °C) were prepared and tested for extraction of DBT at 60 °C. Both ionic liquids performed exceptionally well, giving 80% extraction ($K_D = 4$) with 1-butyliisoquinolinium bis{(trifluoromethyl)sulfonyl}amide and 90% extraction ($K_D = 9$) for 1-butyl-6-methylquinolinium bis{(trifluoromethyl)sulfonyl}amide, consistent with the QSPR predictions.

Practical considerations for implementation and scale-up

These results show how the partition ratio (K_D) for dibenzothiophene between dodecane and ionic liquids is strongly influenced, and can be controlled, by the selection of the cation and to a much lesser extent anion of the ionic liquid. Using these data to develop practical liquid–liquid extraction processes using real refinery feeds requires a number of additional considerations.

Real feeds (such as kerosene or diesel) contain a mixture of components, including paraffinic, aromatic, alkylaromatic and a range of polyaromatic hydrocarbons. The co-miscibility of the ionic liquids and feeds, selectivity and specificity of the extracting phase for polyaromatic sulfur compounds over hydrocarbons and polyaromatic hydrocarbons become important, and in this case should show high capacity with rejection of hydrocarbons. Initial tests have shown that the partition ratio for 4,6-dimethyldibenzothiophene (DMDBT) follows a similar trend to those for DBT, although with lower K_D (0.77 for DMDBT compared to 1.6 for DBT with $[C_4^4CNpy][NTf_2]$, (d), consistent with the data previously described by Eßer and co-workers¹⁰ for $[C_4mim][C_8H_{17}SO_4]$ ($K_D = 1.9$ for DBT and 0.8 for DMDBT). These results are part of continuing work to examine the effects of specific target ionic liquids in real feeds, considering selectivity, extraction and recovery of the extractants from the ionic liquids.

Secondly, the question of removal (and recovery) of extracted materials from the ionic liquid phase needs to be considered. In a conventional liquid–liquid extraction process, secondary stripping stages would be used to recover extracted material. In practical terms, the need for efficient re-extraction often negates the advantages of high K_D values from the initial extraction. An alternative to extraction is distillation, however,

this is not an appealing approach to recover high boiling polyaromatic sulfur compounds, such as DBT (bp 332–333 °C), even when the relatively high thermal stability of many ionic liquids is taken into consideration.

However, since liquid–liquid EDS is not currently considered competitive with conventional hydrodesulfurisation technologies,³ advancing this approach to desulfurisation may also require non-conventional re-extraction techniques. Nie and co-workers¹² have shown that polyaromatic sulfur compounds can be reprecipitated from water-soluble ionic liquids on addition of water, as one approach to recovery and reuse of ionic liquid phases. Electrochemical approaches to hydrodesulfurisation recovering the hydrocarbon-portion of the molecules may also be appropriate, especially if significantly higher concentration factors and loadings can be obtained using ionic liquids (or other) novel extracting phases.

Summary

Liquid–liquid extraction of dibenzothiophene from dodecane has been investigated for a range of ionic liquids with varying cation classes (imidazolium, pyridinium, pyrrolidinium, and quinolinium) and with a range of anion types. Partition ratios for dibenzothiophene to the ionic liquids ranged from 0.8 to 9, and showed clear variation with cation class. The polyaromatic quinolinium-based ionic liquids demonstrated the best extractive ability. However, these and other polyaromatic cations, such as 1,3-dialkylbenzimidazolium, are technically limited by their higher melting points and only tend to form low-melting point ionic liquids with highly flexible perfluorinated anions, such as bis{(trifluoromethyl)sulfonyl}amide. This highlights the importance of only using theoretical predictions in tandem with empirical data on rheological and thermophysical properties in order to obtain realistic target materials.

Amongst the monocyclic systems, the ionic liquids can be ranked by cation; methylpyridinium \geq pyridinium \approx imidazolium \approx pyrrolidinium, with much less significant variation with anion type. The ionic liquids with $[C_4^{2,4}dmpy]^+$ and $[C_4^{2,5}dmpy]^+$ cations showed the best extraction performance with 81–83% of the DBT removed in a single contact. Ionic liquids containing 1-butyl-*n*-methylpyridinium cations ($n = 3$ or 4) gave good DBT extraction (70–83%), irrespective of the anion present.

Surprisingly, the ionic liquids with ethanoate and thiocyanate anions gave the best extraction performance with each cation, indicating that more benign (and much cheaper) anions could be used as alternatives to the perfluorinated bis{(trifluoromethyl)sulfonyl}amide and tetrafluoroborates, especially when coupled to cations, such as 1-butyl-3-methylpyridinium (83% extraction).

Experimental

Reagents

Dodecane and dibenzothiophene were purchased from Aldrich and used as received. Solutions of dibenzothiophene in dodecane (2880 ppm, 0.0156 mole l^{-1} of DBT, corresponding to 500 ppm of sulfur) were prepared by dissolving dibenzothiophene (288 mg, 0.00156 mole) in dodecane (100 cm^3).

Ionic liquids

The ionic liquids **2**, **3**, **6**, **7**, and **11** were purchased from Fluka, **9** was purchased from Acros. All were used as received. The ionic liquids **1**, **4**, **5**, **8**, **10**, and **12–20** were synthesised by alkylation of the respective 1-methylimidazole, pyridine, 4-methylpyridine, 3-methylpyridine, 3,4-dimethylpyridine, 3,5-dimethylpyridine or 1-methylpyrrolidine heterocyclic bases with 1-bromobutane, followed by anion metathesis. 1-Ethyl-3-methylimidazolium ethylsulfate was prepared using the previously published synthetic route.³⁶ The ionic liquids were characterised by proton NMR spectroscopy, ion-chromatography and Karl Fisher titration.

Partitioning experiments

Extraction experiments were performed under standardised conditions: equal volumes (2 cm³) of dodecane (containing 500 ppm sulfur as dibenzothiophene) and ionic liquid were mixed for 1 h at 950 rpm in 25 × 75 mm vials with 10 mm triangular magnetic stirring bars, using an Anachem stem-block for 1 h at 25, 40, or 60 °C, followed by equilibration at temperature for 15 min without stirring. A sample (1 cm³) of the upper dodecane phase was taken by pipette, taking care not to disturb the phase boundary, and was analysed by GC-MS (PerkinElmer Clarus 500 with an ESGE SolGel column) for dibenzothiophene using direct injection of the samples, and comparing the integral with the phase before extraction. The percentage of DBT extracted and partition ratio of DBT to the ionic liquid were calculated by difference from the integral of the dibenzothiophene signal using the equation:

$$K_D = [\text{DBT}]_{\text{ionic liquid}}/[\text{DBT}]_{\text{dodecane}}$$

which reduces, when the phase volumes are equal, to

$$K_D = [I_{\text{initial}} - I_{\text{dodecane}}]/[I_{\text{dodecane}}]$$

where I is the peak integral analysed by GC-MS.

Measurements were performed in triplicate, and replicate experiments using different batches of ionic liquid, where available, were also performed. Mass balance was confirmed by analysis of both phases (dodecane and ionic liquid) using HPLC (Agilent 1200 series with RP18 column in acetonitrile/water) in a number of cases.

Acknowledgements

We thank BP (JDH, XZ, IL-M), QUILL and its Industrial Advisory Board, EPSRC through the Portfolio Partnership Scheme Grant EP/D029538/1 (KRS), and the *Ministerio de Educación y Ciencia* of Spain (grant CTQ2005-07676 to GS) for funding and support.

References

1 J. G. Speight, in 'Kirk-Othmer Encyclopaedia of Chemical Technology', ed. A. Seidel, Vol. 18, John Wiley & Sons, Inc., Hoboken, New Jersey, 2007, pp. 1–49.

- 2 G. C. A. Schuit and B. C. Gates, *AIChE J.*, 1973, **19**, 417; X. L. Ma, K. Y. Sakanishi and I. Mochida, *Ind. Eng. Chem. Res.*, 1994, **33**, 218.
- 3 E. Ito and J. A. R. van Veen, *Catal. Today*, 2006, **116**, 446.
- 4 G. P. Khare, *World Pat.*, WO0132805, 2001.
- 5 M. Macaud, M. Sévignon, A. Favre-Réguillon, M. Lemaire, E. Schulz and M. Vrinat, *Ind. Eng. Chem. Res.*, 2004, **43**, 7843; M. Sévignon, M. Macaud, A. Favre-Réguillon, J. Schulz, M. Rocault, R. Faure, M. Vrinat and M. Lemaire, *Green Chem.*, 2005, **7**, 413.
- 6 J. T. Sampanthar, H. Xiao, J. Dou, T. Y. Nah, X. Rong and W. P. Kwan, *Appl. Catal., B*, 2005, **63**, 85.
- 7 F. Li, P. Xu, J. Feng, L. Meng, Y. Zheng, L. Luo and C. Ma, *Appl. Environ. Microbiol.*, 2005, **71**, 276; S. A. Denome, C. Oldfield, L. J. Nash and K. D. Young, *J. Bacteriol.*, 1994, **176**, 6707.
- 8 R. W. Gunnerman, *US Pat.* 6,827,844, 7 Dec 2004.
- 9 A. Bösmann, A. Datsevich, A. Jess, A. Lauter, C. Schmitz and P. Wasserscheid, *Chem. Commun.*, 2001, 2494.
- 10 J. Eßer, P. Wasserscheid and A. Jess, *Green Chem.*, 2004, **6**, 316.
- 11 S. Zhang, Q. Zhang and Z. C. Zhang, *Ind. Eng. Chem. Res.*, 2004, **43**, 614.
- 12 Y. Nie, C. Li, A. Sun, H. Meng and Z. Wang, *Energy Fuels*, 2006, **20**, 2083.
- 13 P. Wasserscheid and W. Keim, *Angew. Chem.*, 2000, **112**, 3926.
- 14 T. Welton, *Chem. Rev.*, 1999, **99**, 2071; J. D. Holbrey and K. R. Seddon, *Clean Prod. Proc.*, 1999, **1**, 223.
- 15 J. L. Anderson, J. Ding, T. Welton and D. W. Armstrong, *J. Am. Chem. Soc.*, 2002, **124**, 14247.
- 16 L. A. Blanchard and J. Brennecke, *J. Ind. Eng. Chem. Res.*, 2001, **40**, 287.
- 17 J. D. Holbrey, W. M. Reichert, M. Nieuwenhuyzen, O. Sheppard, C. Hardacre and R. D. Rogers, *Chem. Commun.*, 2003, 476.
- 18 A. R. Choudhury, N. Winterton, A. Steiner and K. A. Johnson, *CrystEngComm*, 2006, **8**, 742.
- 19 S. Tsuzuki, M. Mikami and S. Yamada, *J. Am. Chem. Soc.*, 2007, **129**, 8656.
- 20 G. W. Meindersma, A. J. G. Podt and A. B. de Haan, *Fuel Proc. Technol.*, 2005, **87**, 59.
- 21 A. Arce, M. J. Earle, H. Rodríguez and K. R. Seddon, *Green Chem.*, 2007, **9**, 70.
- 22 W.-H. Lo, H.-Y. Yang and G.-T. Wei, *Green Chem.*, 2003, **5**, 639.
- 23 Y. Horii, H. Onuki, S. Doi, T. Mori, T. Takeo, H. Sato, T. Ookuro and T. Sugawara, *US Pat.*, 5,494,572, February 27, 1996.
- 24 A. R. Katritzky, A. Lomaka, R. Petrukhin, R. Jain, M. Karelson, A. E. Visser and R. D. Rogers, *J. Chem. Inf. Comput. Sci.*, 2002, **42**, 71.
- 25 A. R. Katritzky, R. Jain, A. Lomaka, R. Petrukhin, M. Karelson, A. E. Visser and R. D. Rogers, *J. Chem. Inf. Comput. Sci.*, 2002, **42**, 225.
- 26 D. M. Eike, J. F. Brennecke and E. J. Maginn, *Green Chem.*, 2003, **5**, 323.
- 27 S. Trohalaki, R. Pachter, G. W. Drake and T. Hawkins, *Energy Fuels*, 2005, **19**, 279.
- 28 S. Trohalaki and R. Pachter, *QSAR Comb. Sci.*, 2005, **24**, 485.
- 29 N. Sun, X. He, K. Dong, X. Zhang, X. Lu, H. He and S. Zhang, *Fluid Phase Equilib.*, 2006, **246**, 137.
- 30 I. López-Martin, E. Burello, P. N. Davey, K. R. Seddon and G. Rothenberg, *ChemPhysChem*, 2007, **8**, 690.
- 31 A. R. Katritzky, V. S. Lobanov and M. Karelson, *Chem. Soc. Rev.*, 1995, 279.
- 32 A. R. Katritzky, V. S. Lobanov and M. Karelson, CODESSA: Reference Manual; Version 2, University of Florida, 1994.
- 33 J. G. Topliss and R. P. Edwards, *J. Med. Chem.*, 1979, **22**, 1238.
- 34 A. E. Visser, J. D. Holbrey and R. D. Rogers, *Chem. Commun.*, 2001, 2484.
- 35 D. F. Wassell, PhD thesis, The Queen's University of Belfast., Sept 2003; D. F. Wassell and K. R. Seddon, Abstracts of Papers, 223rd ACS National Meeting, Orlando, FL, United States, April 7–11, 2002, 2002, IEC-147.
- 36 J. D. Holbrey, W. M. Reichert, R. P. Swatloski, G. A. Broker, W. R. Pitner, K. R. Seddon and R. D. Rogers, *Green Chem.*, 2002, **4**, 407.

The bulk oxypropylation of chitin and chitosan and the characterization of the ensuing polyols

Susana Fernandes, Carmen Sofia Rocha Freire,* Carlos Pascoal Neto and Alessandro Gandini

Received 30th July 2007, Accepted 23rd October 2007

First published as an Advance Article on the web 14th November 2007

DOI: 10.1039/b711648a

Chitin and chitosan were converted into viscous polyols through a simple oxypropylation reaction, with the aim of valorising the less noble fractions or by-products of these valuable renewable resources. This process bears “green” connotations, given that it requires no solvent, leaves no by-products and no specific operations (separation, purification, *etc.*) are needed to isolate the entire reaction product. Chitin or chitosan samples were preactivated with KOH and then reacted with an excess of propylene oxide (PO) in an autoclave. In all instances, the reaction product was a viscous liquid made up of oxypropylated chitin or chitosan and PO homopolymer. The two fractions were separated and thoroughly characterized by FTIR and NMR spectroscopy, DSC, TGA and viscosity.

Introduction

The exploitation of renewable resources for both energy and materials has been attracting considerable attention recently, mainly in response to the economical and environmental problems associated with the use of fossil counterparts. In particular, the vast quantities of by-products arising from agricultural, marine and forestry activities represent a very promising first generation of natural resources, available for specific chemical modifications aimed at generating novel materials. Two aspects are relevant here, *viz.*, the fact of (i) selecting only the less noble parts of these commodities for the modifications, leaving the more valuable ones for well-established uses (food, timber, papermaking, pharmaceuticals, *etc.*) and (ii) valorising all the components of a given resource through the biorefinery working hypothesis, instead of selecting only that or those which appear to be more valuable. Indeed, a growing number of studies show that the so-called by-products can in fact be the precursors to materials with remarkable properties and high added value.

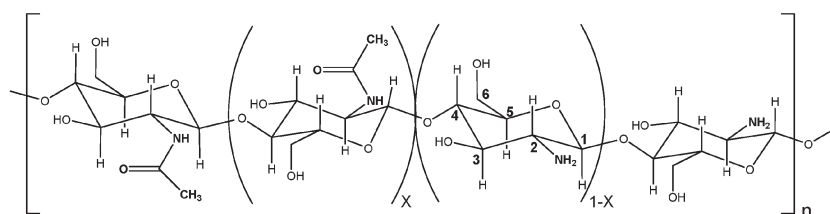
Among the numerous approaches investigated within this context,^{1–4} only the bulk oxypropylation of natural polymeric substrates is discussed here. Lignin, sugar beet pulp and cork powder are secondary products of major industrial activities, mainly used today as sources of energy by combustion. In previous studies, they have been efficiently

converted by a single-step oxypropylation reaction into liquid viscous polyols,^{5–11} which are interesting macromonomers for the synthesis of polyurethanes and polyesters.^{6,12,13} These systems are particularly straightforward in terms of their implementation, since they only involve the mixing of the activated solid substrate with propylene oxide (PO) in an autoclave and the subsequent heating of the ensuing suspension until the total consumption of the added PO. The recovery of the final polyol mixture is extremely simple, because it does not require the removal of any solvent or other component, nor any separation or purification procedure. The green connotations of the entire operation are therefore quite relevant. However, it is important to emphasize that PO is a hazardous chemical in terms of toxicity and flammability. In our systems, both in the past and in the present context, the fact that PO was always totally used up in the oxypropylation represents an element of safety, but, of course, particular care must be taken during these reactions to avoid any loss of control, which might lead to PO contamination.

Chitin is the second most abundant natural polymer and its partly deacetylated derivative, chitosan, represents one of the most actively investigated materials because of its unique properties and applications.¹⁴

To the best of our knowledge, this specific approach had never been applied to chitin, and only once very succinctly to chitosan.⁹ The studies related to the preparation of hydroxypropyl chitin and chitosan bearing very short grafts^{15–22} and destined to biomedical applications, all involved the use of a solvent and therefore required a laborious workup, isolation, and purification of the final product. This state of affairs

CICECO and Department of Chemistry, University of Aveiro, Campus de Santiago, 3810-193 Aveiro, Portugal. E-mail: cfreire@ua.pt; Fax: +351 234 370 084; Tel: +351 234 401 507



Structures of chitin ($x \gg 1-x$) or chitosan ($1-x \gg x$)

prompted us to extend to chitin and chitosan the successful approach already applied to other natural polymers,^{5–13} with the aim of valorising the less noble fractions and by-products arising from the industrial process consisting of the extraction of chitin and its conversion into chitosan.

This paper describes a preliminary study of the bulk oxypropylation of chitin and chitosan and the characterization of the ensuing polyols.

Experimental

Materials

The chitin ($M_w \sim 6 \times 10^5$) and chitosan ($M_w = 5.4 \times 10^5$) samples used in this work were generously provided by Mahtani Chitosan Pvt. Ltd. (India). The deacetylation degree (DDA) of the chitosan was 92%. Propylene oxide (PO) 99% was supplied by Sigma–Aldrich and employed as received.

Oxypropylation

The oxypropylation reactions were carried out in a 300 cm³ stainless steel autoclave equipped with stirring, a heating resistance and temperature and pressure sensors. The chitin and chitosan samples (10 g) were preactivated in the reaction vessel with an ethanol–KOH solution for 1 h at room temperature under a nitrogen atmosphere. The dried activated-substrate was then mixed with PO (40 and 20 mL, respectively for chitin and chitosan) and allowed to react, with constant mechanical stirring at 1000 rpm, at 140 °C (set 1) and 120 °C (set 2). The higher amount of PO in the experiments with chitin was employed to guarantee a thorough impregnation of the substrate, which was particularly fluffy. The onset of the oxypropylation reaction was revealed by a rapid increase in temperature (max. 220 °C) and pressure (max. 15 bar) and its completion by the return of the pressure to its atmospheric value. The reaction time varied between 1 and 2 h. In all these experiments, no unreacted PO was detected after opening the autoclave.

The viscous products were diluted with dichloromethane and filtered through a highly porous cotton fabric. The solid residues (SR) were washed several times with dichloromethane, dried and weighed in order to determine the percentage of unreacted, or poorly reacted, substrate. The solvent and other volatile components of the filtrates were removed in a rotary evaporator leaving a viscous polyol, which was then extracted with n-hexane in order to separate the oxypropylated chitin or chitosan (hexane insoluble material, PL) from the PO homopolymer fraction (HP). The separation procedures were only applied in order to characterize all the products of the reaction. In practice, however, the polyol mixtures can be used, as such, without any separation or purification.

Some of the solid products were submitted to a second oxypropylation in the same conditions in order to verify whether they were intractable structures or simply residual polysaccharides which had not been sufficiently modified during the first treatment. The fact that in all instances, liquid polyols were obtained, proved that the latter reason had been the cause of these incomplete oxypropylations.

Characterization

The FTIR spectra were taken with a Mattson 7000 spectrophotometer equipped with a single horizontal Golden Gate ATR cell. The thermogravimetric tests were carried out with a Shimadzu TGA 50 analyser equipped with a platinum cell. Samples were heated at a constant rate of 10 °C min⁻¹ from room temperature to 800 °C, under a nitrogen flow of 20 mL min⁻¹. The thermal decomposition temperature was taken as the onset of a significant ($\geq 0.5\%$) weight loss from the heated sample, after the initial moisture loss. The elemental analyses were conducted with a Leco CNHS Elemental Analyser. The DSC thermograms were traced with a Setaram analyzer scanning at 10 °C min⁻¹ in a stream of helium. Scanning at 2 °C min⁻¹ gave essentially the same results. The ¹H–NMR (in CDCl₃ for the HP e PL fractions and in CD₃CO₂D (1%)/D₂O for chitosan) spectra were recorded with a Bruker Avance (Wissembourg, France) spectrometer working at 300.13 MHz. Chemical shifts are expressed in δ (ppm) values relative to tetramethylsilane (TMS) as the internal reference. The viscosities of the chitin- and chitosan-based polyols (PL) were measured with a controlled-stress AR 1000 TA rheometer, fitted with a cone-plate geometry (40 mm diameter and 4° angle).

Results and discussion

The purpose of this investigation was to establish the feasibility of converting chitin and chitosan into viscous polyols *via* a simple oxypropylation reaction, without any attempt to optimize the processes through a systematic study of the role of each parameter. The mechanism of these bulk oxypropylations calls upon the activation of some of the substrate OH groups by a Brønsted or Lewis base to produce the corresponding oxanions, from which PO oligomers are grafted by its ring-opening anionic polymerization. Because transfer reactions inevitably occur in this process, the formation of some PO homopolymer (PPO) always accompanies the actual oxypropylation.

With the conditions described above, the extent of oxypropylation of both chitin and chitosan was relatively high, but not complete, as measured by the relatively modest amounts of unreacted or poorly oxypropylated solid residues (5–15% and ~25%, respectively for chitin and chitosan). The lower reactivity of chitosan was interpreted on the basis of its higher cohesive energy²³ arising from the very strong intermolecular hydrogen bonds involving both its OH and NH₂ groups, because the reoxypropylation of the corresponding solid residue gave the same result (~25% of unreacted material), suggesting that the added amount of PO had not been the limiting factor in the first treatment. It is important to emphasize here that there is no doubt in our minds that the systematic study of both these systems will provide the appropriate conditions insuring total conversion of the substrates into liquid products.

As mentioned above, the oxypropylation of OH-containing substrates, such as polysaccharides, inevitably gives two products, namely the oxypropylated macromolecules and some PPO.^{5–8,11} Their relative proportion, which depends on the reaction conditions, obviously influences the physical properties, as well as the reactivity of these polyol mixtures. It has been shown that these two polymers can be efficiently separated by extracting the reaction mixture with n-hexane,⁸ since the HP

fraction is selectively removed by this solvent. In the present study, the proportion of HP formed was systematically around ~40%, in close agreement with that obtained with other natural substrates oxypropylated under similar reaction conditions.^{5,6,8}

FTIR analysis

Fig. 1 shows typical FTIR spectra of chitosan and the two liquid polyol fractions (HP and PL) resulting from its oxypropylation. As expected, the spectrum of HP displayed the same bands as those of a commercial sample of PPO, *viz.* around 3380 cm^{-1} , assigned to the OH stretching modes; in the range 2870–2970 cm^{-1} for the C–H stretching modes of the aliphatic CH_3 , CH_2 and CH groups; and around 1080 cm^{-1} for the C–O–C moieties.²⁴ The spectrum of the chitosan PL also showed the latter features, plus an additional peak around 1590 cm^{-1} , assigned to the N–H deformation mode of primary amines,²⁴ arising from the chitosan monomer units. These results corroborated the occurrence of the oxypropylation reaction through the grafting of PPO chains onto the polysaccharide backbone and the efficiency of the use of *n*-hexane as a discriminating solvent.

The two polyol fractions obtained in the oxypropylation of chitin also presented different FTIR spectra, but with the carbonyl amide band at 1680–1630 cm^{-1} , resulting from the chitin monomer units, as the main distinguishing feature.

The solid residues isolated in both chitin and chitosan modification reactions showed evidence of a modest oxypropylation, since their infrared spectra differed from those of the

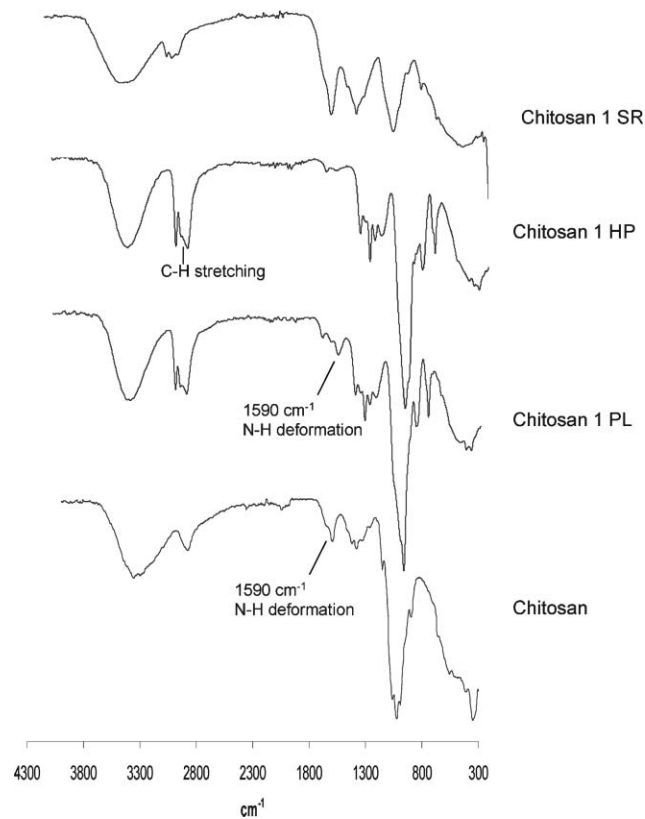


Fig. 1 Typical FTIR spectra of chitosan, the two liquid polyol fractions (HP and PL) and the solid residue (SR) resulting from its oxypropylation at 140 °C.

respective initial substrates, mostly because of the presence of the characteristic PO-unit CH_3 peak around 2960 cm^{-1} .

^1H -NMR analysis

Fig. 2 shows typical ^1H -NMR spectra of native chitosan and of the two chitosan-related products, following the extraction with *n*-hexane. The ^1H spectrum of chitosan, obtained in an acidic solution at 50 °C, is in close agreement with the literature.^{25,26} On the other hand, the soluble material gave a spectrum very similar to that of commercial PPO, except for a slightly higher integration in the 3–5 ppm region, characteristic of CH–O and CH_2 –O protons, compared with that of the methyl groups around 1 ppm, suggesting that small amounts of the oxypropylated chitosan had also been extracted, since for PPO alone those integrations are identical. The spectrum of the *n*-hexane-insoluble polyol showed, as expected, a higher contribution of the ether-type peaks, reflecting the presence of the chitosan backbones. In the case of the corresponding products relative to the oxypropylation of chitin, the extracted

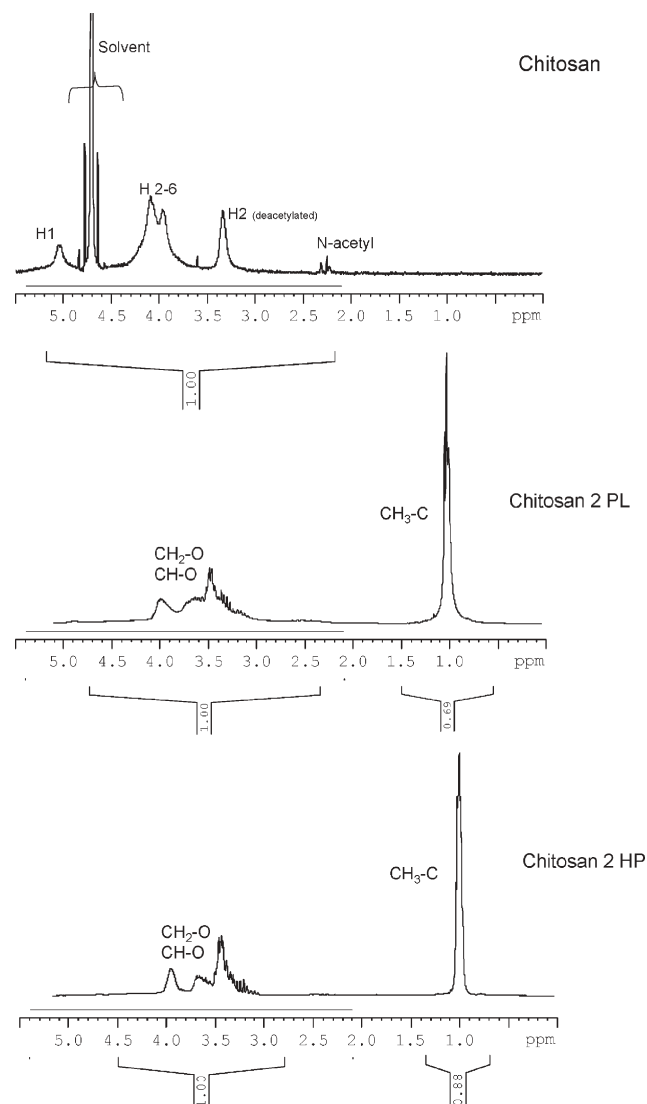


Fig. 2 ^1H -NMR spectra of chitosan and of the two fractions (HP and PL) obtained after its oxypropylation at 120 °C.

material gave a spectrum virtually identical to that of PPO, whereas that of the residue showed a less pronounced relative integration of the ether protons, compared with the chitosan-based counterpart. These results corroborated the previous indication related to the lower reactivity of chitosan in these oxypropylation conditions.

Elemental analysis

Table 1 gives a selection of results related to the elemental analysis of the different fractions isolated following the oxypropylation of both substrates. The low, but non-zero nitrogen content of the HP fractions confirmed the conclusions drawn from the $^1\text{H-NMR}$ spectra concerning the fact that n-hexane actually extracted the PPO and a very small amount of oxypropylated substrate, more so in the case of chitosan. The nitrogen content of the oxypropylated chitin and chitosan fractions was however much higher than that of their corresponding homopolymeric fractions, as expected for these truly grafted samples.

In addition, the nitrogen contents of the solid residues were lower than those of the initial substrates, but higher than those of the corresponding n-hexane insoluble products, confirming that the residues were composed mainly of weakly oxypropylated chitin or chitosan, as already suggested on the basis of the FTIR analysis and of the reoxypropylation experiments. Interestingly, these second experiments gave, not only a similar percentage of solid residue, but also elemental analyses which replicated those related to the corresponding first run, as shown in Table 1.

Thermogravimetric analysis

The two fractions resulting from the oxypropylation of these natural substrates showed in all cases markedly different TGA profiles (Fig. 3). Thus, the HP fractions displayed a typical single weight loss and a maximum decomposition temperature at 240–290 °C, characteristic of POP. On the other hand, the oxypropylated counterparts gave profiles which were a combination of those of the corresponding natural polymer and of PPO, with two main losses at 250–270 and 350–370 °C, indicating that the grafted architecture of these materials did

Table 1 Elemental composition of the fractions isolated following the oxypropylation of chitin and chitosan at 140 °C and 120 °C. ROx refers to the reoxypropylation experiments

Sample	C	N	H
Chitin	41.87	6.03	6.41
Chitosan	37.22	7.16	6.86
Chitin1 HP	57.79	0.42	9.90
Chitin2 HP	57.42	0.47	10.22
Chitin1 PL	56.25	1.82	8.79
Chitin2 PL	55.24	1.84	8.25
SR chitin	52.54	2.57	8.10
ROx chitin HP	57.72	0.47	9.70
ROx chitin PL	53.19	1.59	8.46
Chitosan1 HP	53.09	1.21	10.16
Chitosan2 HP	54.85	0.65	9.86
Chitosan1 PL	54.29	2.23	8.45
Chitosan2 PL	53.75	2.67	8.20
SR chitosan	42.36	4.54	6.55
ROx chitosan HP	56.16	0.41	9.79
ROx chitosan PL	47.52	2.04	7.67

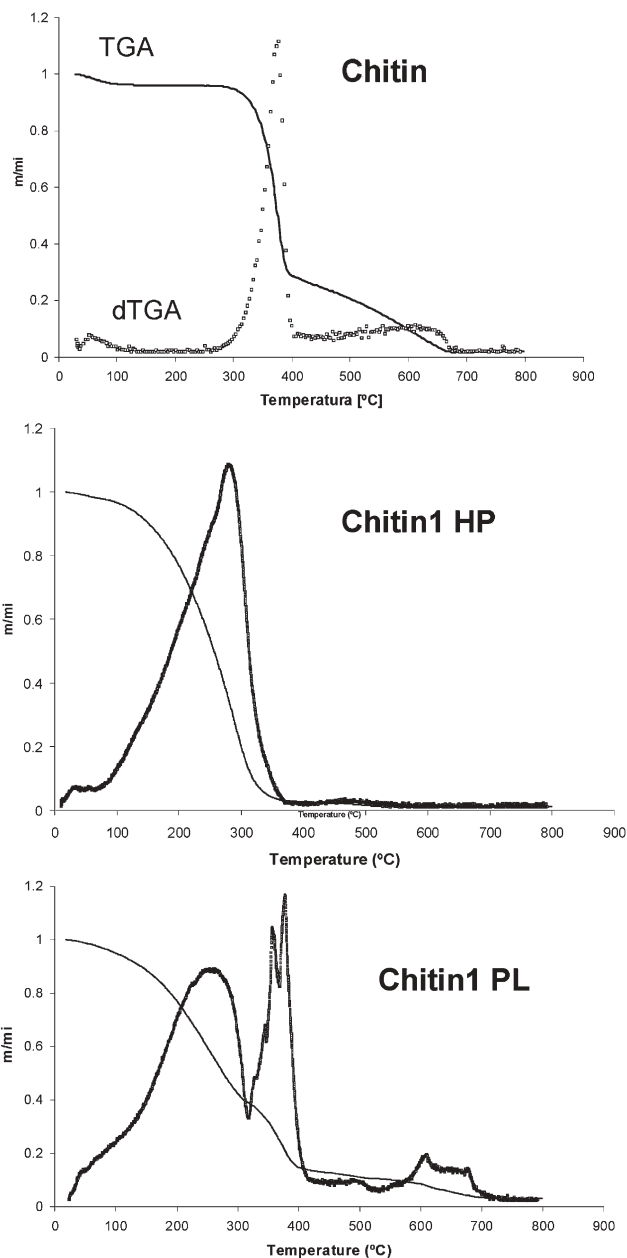


Fig. 3 TGA thermograms of the two fractions (HP and PL) obtained from the oxypropylation of chitin at 140 °C.

not alter their thermal degradation in relation to their separate components.

Differential scanning calorimetry

The T_g of the HP products were consistently around -75 °C, *i.e.* the typical value for low molecular-weight PPO (Fig. 4). The n-hexane-insoluble products gave T_g values of about -55 °C for both oxypropylated polysaccharides (Fig. 4). This increase in T_g reflects the stiffening role of the natural polymer backbone, but the modest increment suggests that the PPO grafts played a predominant plasticizing role in these structures. These results are in good agreement with those previously published for similar products obtained in the oxypropylation of other natural substrates.^{6,7}

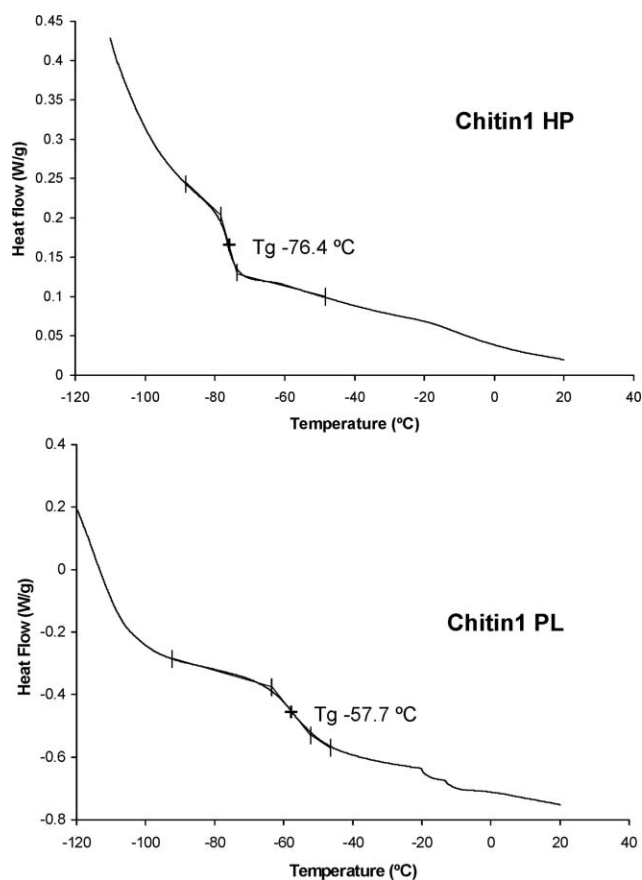


Fig. 4 DSC thermograms of the two fractions (HP and PL) obtained from the oxypropylation of chitin at 140 °C.

Viscosity

The viscosities of chitosan's PLs (50 000 Pa s) were some 5 times higher than those of chitin's homologues. This further confirmed the lower reactivity of the former polysaccharide. Of course, all the polyol mixtures before extraction were some 100 times less viscous, given the low viscosity of the accompanying PPO oligomers.

Hence, these mixtures, as recovered after the oxypropylation reaction, without any separation or purification, are the actual polyols which constitute the interesting macromonomers to be exploited in polycondensations based on the use of their OH groups. The oxypropylated polymer has a high OH functionality, indeed the same as that of the substrate, since the grafting reaction only brings the OH group out of its initial core structure. The PPO has an OH functionality of two and will therefore act as a chain extender during the polycondensation reactions in which the grafted polymer is responsible for branching and ultimately cross-linking.

Conclusions

This short study provides irrefutable qualitative evidence about the possibility of transforming chitin and chitosan into viscous polyol mixtures, by an extremely simple process which only involves the activated substrate and propylene oxide. It is extremely important to underline that the various separation

procedures described above were only applied in order to characterise the different products of these reactions. In practice, the polyol mixtures can be simply removed as such from the reaction vessel, without the need of any other operation, since they constitute viable macromonomers for the synthesis of polyurethanes, polyethers or polyesters. In other words, these systems are a good example of green chemistry, in that they do not require any solvent, leave no residue and call upon the exploitation of renewable resources.

Acknowledgements

The authors thank Mahtani Chitosan Pvt. Ltd. (India) for their generous gifts of chitosan and chitin. Susana Fernandes thanks the Fundação para a Ciência e a Tecnologia (Portugal) for a Scientific Research grant (SFRH/B1/33050/2007).

References

- 1 D. S. Argyropoulos, *ACS Symp. Ser.*, 2007, vol. 954.
- 2 *Renewable Bioresources*, ed. C. V. Stevens, R. Verhé, John Wiley, New York, 2004.
- 3 A. J. Ragauskas, C. K. Williams, B. H. Davison, G. Britovsek, J. Cairney, C. A. Eckert, W. J. Frederick, J. P. Hallett, D. J. Leak, C. L. Liotta, J. R. Mielenz, R. Murphy, R. Templer and T. Tschaplinski, *Science*, 2006, **311**(5760), 484–489.
- 4 L. Yu, K. Dean and L. Li, *Prog. Polym. Sci.*, 2006, **31**(6), 576–602.
- 5 M. Evtiouguina, A. M. Barros, J. J. Cruz-Pinto, C. P. Neto, M. N. Belgacem, C. Pavier and A. Gandini, *Bioresour. Technol.*, 2000, **73**(2), 187–189.
- 6 M. Evtiouguina, A. Barros-Timmons, J. J. Cruz-Pinto, C. P. Neto, M. N. Belgacem and A. Gandini, *Biomacromolecules*, 2002, **3**(1), 57–62.
- 7 C. Pavier and A. Gandini, *Ind. Crops Prod.*, 2000, **12**(1), 1–8.
- 8 C. Pavier and A. Gandini, *Carbohydr. Polym.*, 2000, **42**(1), 13–17.
- 9 P. Velazquez-Morales, J. F. Le Nest and A. Gandini, *Electrochim. Acta*, 1998, **43**(10–11), 1275–1279.
- 10 A. Gandini, M. N. Belgacem, Z. X. Guo and S. Montanari, in *Chemical Modification, Properties, and Usage of Lignin*, ed. T. Q. Hu, Kluwer Academy/Plenum Publishers, 2002, pp. 57–80.
- 11 H. Nadji, C. Bruzzese, M. N. Belgacem, A. Benaboura and A. Gandini, *Macromol. Mater. Eng.*, 2005, **290**(10), 1009–1016.
- 12 M. Evtiouguina, A. Gandini, C. P. Neto and M. N. Belgacem, *Polym. Int.*, 2001, **50**(10), 1150–1155.
- 13 C. Pavier and A. Gandini, *Eur. Polym. J.*, 2000, **36**(8), 1653–1658.
- 14 M. Rinaudo, *Prog. Polym. Sci.*, 2006, **31**(7), 603–632.
- 15 D. Asahina, T. Matsubara, Y. Miyashita and Y. Nishio, *Sen-I Gakkaishi*, 2000, **56**(9), 435–442.
- 16 S. J. Kim, S. S. Kim and Y. M. Lee, *Macromol. Chem. Phys.*, 1994, **195**(5), 1687–1693.
- 17 S. S. Kim, S. J. Kim, Y. D. Moon and Y. M. Lee, *Polymer*, 1994, **35**(15), 3212–3216.
- 18 Y. Liu, G. Chen and K. A. Hu, *J. Mater. Sci. Lett.*, 2003, **22**(19), 1303–1305.
- 19 I. K. Park and Y. H. Park, *J. Appl. Polym. Sci.*, 2001, **80**(13), 2624–2632.
- 20 Y. F. Peng, B. Q. Han, W. S. Liu and X. J. Xu, *Carbohydr. Res.*, 2005, **340**(11), 1846–1851.
- 21 Y. Wan, K. A. M. Creber, B. Peppley and T. V. Bui, *J. Polym. Sci., Part B: Polym. Phys.*, 2004, **42**(8), 1379–1397.
- 22 W. M. Xie, P. X. Xu, W. Wang and Q. Liu, *Carbohydr. Polym.*, 2002, **50**(1), 35–40.
- 23 M. N. Belgacem, A. Blayo and A. Gandini, *J. Colloid Interface Sci.*, 1996, **182**(2), 431–436.
- 24 L. J. Bellamy, in *The Infrared Spectra of Complex Molecules*, Chapman and Hall, London, 3rd edn, 1975, p. 433.
- 25 A. Hirai, H. Odani and A. Nakajima, *Polym. Bull.*, 1991, **26**, 87–94.
- 26 K. M. Varum, M. W. Anthonsen, H. Grasdalen and O. Smitsrod, *Carbohydr. Res.*, 1991, **211**, 17–23.

The continuous synthesis of ϵ -caprolactam from 6-aminocapronitrile in high-temperature water

Chong Yan,^a Joan Fraga-Dubreuil,^a Eduardo Garcia-Verdugo,^a Paul A. Hamley,^a Martyn Poliakov,*^a Ian Pearson^b and A. Stuart Coote^b

Received 2nd July 2007, Accepted 22nd October 2007

First published as an Advance Article on the web 15th November 2007

DOI: 10.1039/b710041h

Caprolactam (CPL) is a widely used chemical intermediate for the production of Nylon-6. However, existing synthetic routes in industry have severe drawbacks. The development on the synthesis of CPL from 6-aminocapronitrile (ACN), using near- and supercritical water as the solvent, reactant and catalyst, is described in this paper. The two-step reaction (hydrolysis and cyclization) to produce CPL is combined in a single process, by using a continuous-flow system. Effects of pressure, temperature, residence time and the concentration of ACN were studied. The high-temperature high-pressure environment possesses unique properties which result in very efficient catalysis. The overall CPL yield reaches 90% within a short residence time (<2 min).

Background

The production of ϵ -caprolactam (CPL), the primary use of which is in the production of Nylon-6, is a most industrially important process. About 90% of the CPL is manufactured in processes which are based on (or partially based on) the cyclohexanone route.¹ However, two main drawbacks make the process costly and environmentally harmful. Firstly, cyclohexanone is made by the aerobic oxidation of cyclohexane, where the conversion must be kept at only 3–6% to maintain a high selectivity.¹ Secondly, although the total yield of CPL from cyclohexanone can approach 98%, the major product generated by the process is actually ammonium sulfate, with CPL as a mere “by-product” in weight terms. Ammonium sulfate is sold as a fertilizer, but it has a limited market as it is only useful in sulfur-deficient soils, and the H₂SO₄ formed on decomposition acidifies the soil.

Most process improvements are focussed on avoiding the production of (NH₄)₂SO₄. Many of these efforts have been introduced.^{2,3} Some of these developments have been introduced industrially. There are three ammonium sulfate free methods which might be commercialized in the near future:⁴ (1) ammoxidation, (2) vapour phase Beckmann rearrangement and (3) butadiene-based processes. The catalysts involved are often the key factor in these three processes. Both the ammoxidation and the vapour phase Beckmann processes are based on the existing reaction route from benzene or toluene, and a 60 000 tonnes year⁻¹ plant was commissioned in 2003 in Japan⁵ to commercialise the technology which combines a proprietary vapour-phase Beckmann rearrangement^{6,7} with Italian company EniChem's direct ammoxidation method.⁸ The only by-product is H₂O and no ammonium sulfate is co-produced. However, the butadiene-based processes not only avoid co-production of ammonium sulfate, but also decrease

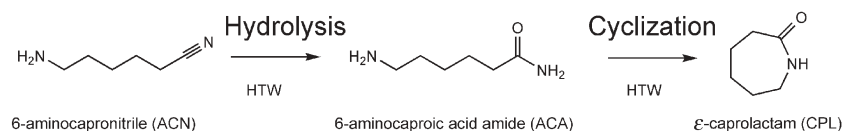
the monetary cost by utilising butadiene as a raw material, which is less expensive than benzene or toluene. Also, problems associated with cyclohexane oxidation^{9,10} can be avoided by using butadiene feedstock. Such processes involve the formation of ACN *via* adiponitrile.

Our work describes the preparation of CPL and NH₃ from ACN in a continuous-flow reactor, using high-temperature water (HTW) as an alternative, environmentally benign solvent (Scheme 1). The patent literature has several reports of this reaction being carried out catalytically in organic solvents.^{11,12} The reaction of ACN to form CPL in the absence of catalysts and organic solvent is quite rare. In one patent from BASF,¹³ a solution of 10% by weight of ACN in H₂O was heated to 300 °C in a tube reactor (volume 300 mL) with an average residence time of 1 h. All of the ACN was converted but some components with high boiling point were produced during this process and needed to be recycled; thus a yield of 93% CPL could be achieved. Also, Vogel *et al.* described results from this reaction in supercritical water in their reviews;^{14,15} an ACN conversion of *ca.* 70% and a selectivity of CPL of *ca.* 66% (*i.e.*, a CPL yield of less than 50%) was obtained at 350 °C and 250 bar with a residence time of 240 s. Compared to these studies, our method for CPL production from ACN, using near- and supercritical water as the solvent, reactant and catalyst, provides advantages of efficiency, productivity and green technology.

From an industrial aspect, the use of supercritical water can be advantageous. H₂O is abundant, inexpensive, non-flammable and non-toxic, but the use of ambient water is limited by its high polarity and the consequent poor solubility of organic molecules. However, water becomes a tunable solvent for organics under high-temperature and high-pressure conditions. Two important properties—adjustable static dielectric constant (ϵ) and ionic product (K_w)—make supercritical water a unique reaction medium. As the temperature is increased, the dielectric constant of water becomes successively comparable to those of conventional organic solvents at ambient conditions (*e.g.*, methanol, ethanol, acetone, and

^aThe School of Chemistry, The University of Nottingham, Nottingham, UK NG7 2RD. E-mail: martyn.poliakov@nottingham.ac.uk

^bINVESTA Performance Technologies, Wilton, Cleveland, UK TS10 4XX



Scheme 1 Hydrolysis of ACN followed by cyclization of ACA to CPL in HTW.

hexane).¹⁶ Thus, small organic compounds and most gases are highly soluble in near- and supercritical water. At a constant pressure of 250 bar, the ionic product of water first increases with temperature until it reaches a maximum (10^{-11}) at 250 °C, and then decreases to 10^{-19} at 400 °C and 10^{-22} at 500 °C. This not only allows acid- and base-catalysed reactions to be performed in HTW without additional catalyst, but also allows the medium to be varied between ionic and radical environments. Our group has reported the hydrolysis of esters¹⁷ and nitriles,¹⁸ the reduction of nitroarenes and subsequent cyclization to quinolines,¹⁹ the partial oxidation of *p*-xylene (to terephthalic acid) and other xylenes,^{20–22} the use of water as a reactant in hydrogen exchange reactions,²³ and synthesis of benzimidazoles.²⁴ In these reactions, water plays an important role as a solvent, reactant, catalyst, or a combination of these.

Experimental

Caution: these reactions involve high pressures and should only be carried out in an apparatus with the appropriate pressure rating at the reaction temperature. A thorough safety assessment should be made. All experiments were conducted using a tubular continuous-flow reactor, Fig. 1. Generally, an aqueous solution of feedstock is pumped through the pre-heater to the reactor. After reaction, the mixture is cooled, filtered and released via the back pressure regulator (BPR) which maintains the system pressure. The pre-heater and the reactor are similar in construction, consisting of 1/16 inch stainless steel tubing coiled around an aluminium block. A cartridge heater and a band heater are used to supply heat. The temperature of the fluid is measured by thermocouples secured in a Swagelok T-piece with the tip of the thermocouple in the flow. The reason for using the combination of pre-heater and reactor instead of a single reactor with longer tubing is that the heating is more uniform and a temperature monitoring point can be inserted between the pre-heater and the reactor. Before each run, the apparatus was hydrostatically pressure tested when cold, and was then heated with a flow of pure water (1.5 mL min^{-1}) at a given pressure. Once the operating temperature had been reached, the feedstock was switched

from pure water to the ACN aqueous solution. Thirty minutes were allowed for the apparatus to equilibrate, and samples were collected every 15 min for a period of 3 min. Typically, an experiment was performed over approximately 2 h.

ACN was supplied by INVISTA Performance Technologies. All the other chemicals were used as received (Aldrich) and H₂O was HPLC grade triply distilled. Residence time was calculated from the total reactor volume (*i.e.*, the volume of the pre-heater plus that of the reactor) divided by the volumetric flow rate at operating temperature and pressure. The volumetric flow rate of the reaction mixture was calculated using the physical properties of H₂O at the high-temperature high-pressure reaction conditions, as published by the US National Institute of Science and Technology (NIST). Samples were analysed by gas chromatography (GC), using a temperature programmable PERKIN ELMER AutoSystem instrument equipped with a 30 m × 0.32 mm × 1.0 mm non-polar capillary column, a flame ionization detector, and He as the carrier gas. The temperature gradient was 20 °C min⁻¹ from 100 °C to 300 °C. The retention times were 4.6 min (ACN), 5.6 min (CPL) and 6.7 min (ACA). The calculation of yields and selectivity was based on the molar amount of each compound.

Since the thermo-physical properties of the reaction mixture are unknown, pure H₂O is taken as the model fluid. Density and viscosity data are from NIST; Static dielectric constant and ionic product data were calculated by using the empirical equations from Franck *et al.*^{25,26}

Results and discussion

Stability of CPL in HTW

To check the feasibility of the synthetic route from ACN to CPL (see Scheme 1), the stability of CPL was initially examined. A solution of CPL in H₂O (2.4 mol l^{-1}) was pumped through the system at the flow rates, pressures and temperatures shown in Table 1. Greater decomposition of CPL was observed at lower flow rates. However, the stability cannot be attributed only to the effect of residence time as suggested by entries 2 and 5 because the real properties of this mixture and its flow type in the tubular reactor are uncertain.

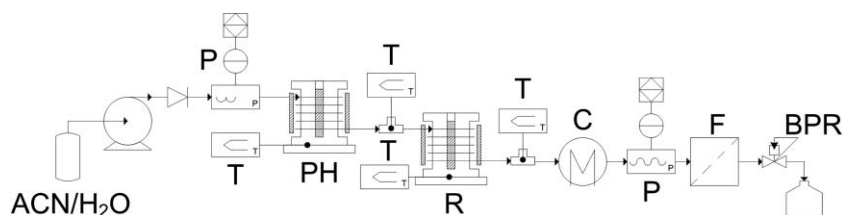


Fig. 1 Scheme of the supercritical water continuous-flow reactor for the reaction of ACN to CPL (P: pressure monitor; T: thermocouple; PH: pre-heater; R: reactor; C: cooler; F: filter; BPR: back pressure regulator).

Table 1 Stability of CPL in HTW. CPL was stable in HTW with recoveries higher than 85% under different conditions

Entry ^a	T/°C	p/bar	Flow rate/ mL min ⁻¹	Recovery of CPL (%) ^b	Residence time/s ^c
1	25	200	1.5	100	—
2	400	200	1.5	85	9
3	400	350	1.5	84	44
4	400	200	5	96	3
5	400	350	5	97	13

^a The starting material was an aqueous solution of CPL (2.4 mol l⁻¹).
^b The recovery of CPL was calculated by GC, reproducible to ±2%.
^c For calculation of residence time, see Experimental.

Even at the longest residence time (44 s), the recovery of CPL was still over 80%. Therefore CPL is sufficiently stable for the reaction to be carried out in HTW.

Effect of temperature

Temperature is one of the important parameters in HTW, because it affects the yield not only by changing the solvent properties of H₂O, but also by modifying the rate of the reaction. Vogel *et al.*¹⁴ reported that the conversion of ACN at high temperature and 250 bar displayed *pseudo*-first-order kinetics with a low temperature dependency.

We have studied the effect of temperature (250–450 °C) on the synthesis of CPL from ACN in HTW at 200 bar (a pressure in the near-critical region where the concentrations of H⁺ and OH⁻ can change greatly with temperature), with a flow rate of 1.5 mL min⁻¹. The concentration of feedstock was 30% (v/v). At the highest temperature (450 °C), oil-like and even solid by-products (insoluble in methanol) were formed, and were not characterised by GC. For all the other runs, CPL was formed selectively as the sole, stable final product from the intermediate ACA. From Fig. 2, it can be seen that the conversion

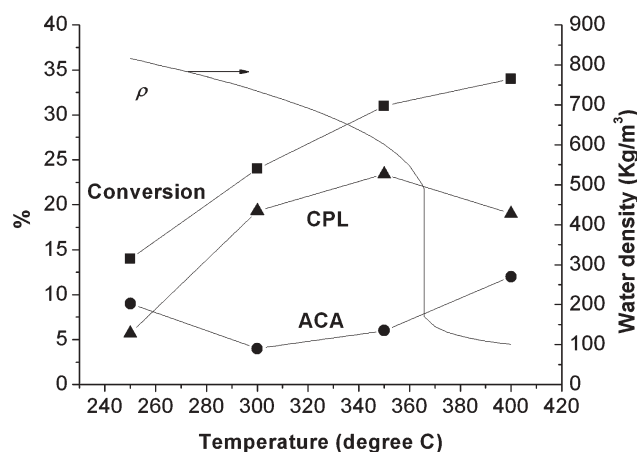


Fig. 2 The effect of temperature on the reaction of 30% (v/v) ACN in HTW with a flow rate of 1.5 mL min⁻¹ and a pressure of 200 bar. When the temperature increased, the conversion of ACN increased up to 34%; the yield of CPL first increased to the maximum of 23% and then decreased; and the yield of ACA first decreased to the minimum of 4% and then increased. The density of H₂O decreased with temperature from 816 kg m⁻³ to 101 kg m⁻³, causing a decrease of calculated residence time from 75 s to 6 s (■: conversion of ACN; ●: yield of ACA; ▲: yield of CPL).

of ACN rose from 14% to 34% with increasing temperature. The selectivities to ACA and CPL vary with temperature; the yield of ACA first decreased to its minimum (less than 5%) and then started to increase (>10%), while the yield of CPL first increased to its maximum (up to 24%) and then started to decrease.

Vogel *et al.* also noticed that the selectivity to CPL decreased considerably above 380 °C. However, this could also be the effect of fluid density. In a continuous-flow system, a compressible fluid will expand when the system temperature is increased at constant pressure; this results in a decrease in density and consequently in the residence time of the substrate. In these runs, the calculated residence time decreased from 75 s at 250 °C to 6 s at 400 °C. Thus, the effect of temperature on the reaction can be rationalised as follows: high temperatures improve the conversion of ACN and ACA, but the conversion of the intermediate ACA to CPL is limited by the reduction in residence time. However, it is also possible that the rate coefficients of the two reaction steps respond differently to changes in temperature. Furthermore, the hydrolysis of nitriles is known to follow a proton-catalysed mechanism, involving several proton transfers.²⁷ At higher temperature, therefore, the factors of faster molecular motion, lower solvent viscosity (from 1.1 × 10⁻⁴ Pa s at 250 °C to 2.6 × 10⁻⁵ Pa s at 400 °C) and breakdown of H-bond network²⁸ enhance the efficiency of the reaction even though the ionic product is lower.

Effect of pressure

Since the conversion of ACN was found to be favoured at 400 °C, a series of experiments was carried out to study the effect of pressure at this temperature at a constant flow rate of 1.5 mL min⁻¹. The same concentration of ACN aqueous solution, 30% (v/v), was used at pressures between 150 and 400 bar. For all runs, CPL was formed selectively as the stable final product from the intermediate ACA. It can be seen from Fig. 3 that the conversion of ACN and the yield of CPL were

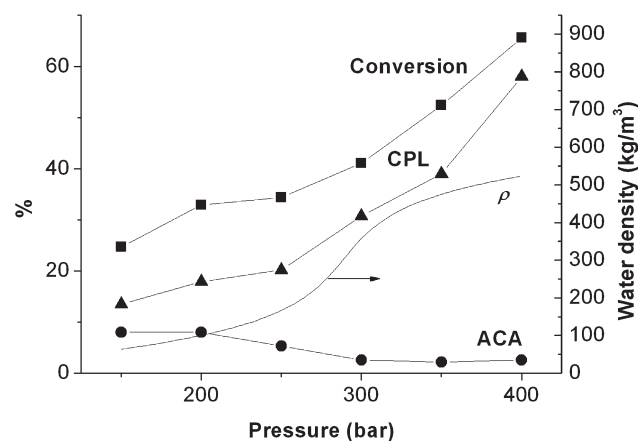


Fig. 3 Observed effect of pressure on the reaction of 30% (v/v) ACN in HTW with a flow rate of 1.5 mL min⁻¹ and a temperature of 400 °C. The conversion of ACN (up to 66%) and yield of CPL (up to 58%) increased with pressure. The yield of ACA decreased to less than 5% at higher pressures. The corresponding increase in the density of H₂O is from 64 kg m⁻³ to 523 kg m⁻³, as indicated on the right hand axis.

favoured at higher pressure (increasing to 66% and 58% respectively), while the yield of ACA was reduced at higher pressure (lowered to less than 3%).

One of the advantages of HTW compared to traditional solvents, is that pressure can be used to adjust the solvent power of the fluid, and also to alter the concentration of H^+ and OH^- in a reaction environment. In the present reaction, pressure can tune the solvent properties of HTW to favour formation of CPL; the ionic product of pure H_2O increases with pressure at 400 °C, up to $10^{-12.5}$ at 400 bar (compared to 10^{-14} for H_2O at ambient temperatures). Also, according to isothermal molecular dynamics simulations by Laria *et al.*,²⁹ the overall proton transport increases with pressure. The catalytic properties of H_2O are therefore enhanced at elevated pressure. At the same time, higher pressure favours the addition of H_2O to the nitrile group of ACN, since the activation volume ΔV^\ddagger is negative.

Furthermore, when this compressible fluid (HTW) is under plug flow conditions in a continuous-flow system, increasing pressure at constant temperature (isothermally) will increase the density of the fluid, and hence increase the residence time of the substrate. For the study of pressure at 400 °C with a constant flow rate of 1.5 mL min^{-1} , the calculated residence time increased from 6 s at 150 bar, to 48 s at 400 bar. Since the reaction in HTW is very selective, longer residence time will lead to a higher yield of the final product and less ACA will remain.

Reproducibility of the synthesis

Although there are no deactivation issues because H_2O is the only catalyst, the reproducibility of this process is important from an industrial point of view. Therefore, reaction was carried out for 12 h by pumping a 30% (v/v) aqueous solution of ACN continuously into the unit at 1.5 mL min^{-1} and at 400 °C and 400 bar, giving a calculated residence time of 48 s, with a sample being collected every hour (for a period of 3 min) and analysed by GC. The results shown in Fig. 4 suggest that CPL was formed reproducibly over this extended period with yields of CPL between 53–57%, and with ACN conversions remaining constant *ca.* 65%.

Effect of feedstock concentration

In this system, both the starting material (ACN) and the product (CPL) have a high solubility in H_2O at 20 °C; CPL is 82% (w/w),¹ and ACN is 50% (v/v). From an economic point of view, there is an obvious interest in producing CPL in HTW at the highest feedstock concentration. The reaction was therefore investigated with feedstock concentrations between 5% and 40% (v/v) at 400 °C and 400 bar using a total flow rate of 1.5 mL min^{-1} (see Fig. 5). In all the runs, CPL was formed selectively as the stable final product *via* the intermediate 6-aminocaproic acid amide (ACA), which was obtained in less than 5% yield. Although no exotherm was observed, a higher concentration of starting material led to higher conversion (up to 73%) and higher yield of the product (up to 61%) with the same calculated residence time of 48 s. The feedstock from 5% to 40% changed the yield from 47% to 61%. This suggests the high productivity is a function of the solubility of the starting

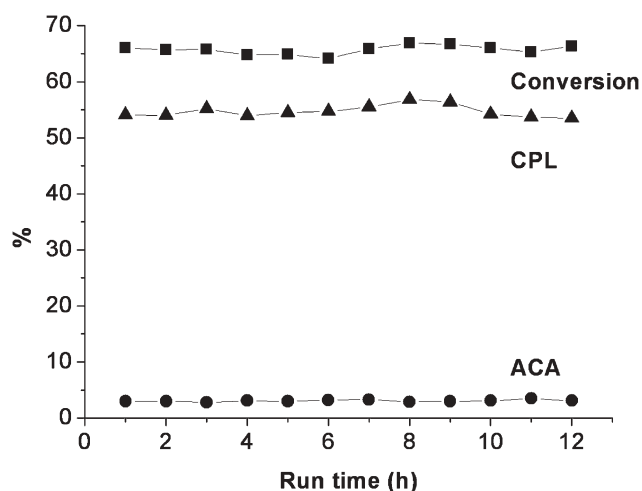


Fig. 4 Study of the reproducibility on the reaction of 30% (v/v) ACN in HTW with a flow rate of 1.5 mL min^{-1} under a temperature of 400 °C and a pressure of 400 bar. CPL yields between 53–57% were achieved (with an average of 54.7% and standard deviation of 1.1%), while ACN conversions remained constant *ca.* 65% ($65.7 \pm 0.8\%$). The yield of ACA was kept below 5%.

material in H_2O . For practical reasons, a 30% concentration was favoured because particles of ACN could possibly precipitate and cause a blockage, at higher concentration of feedstock.

Vogel *et al.* reported that the conversion of 5% (w/w) ACN in HTW could be described by *pseudo*-first order kinetics.¹⁴ However, we found that the conversion of ACN increased with increasing feedstock concentration, so that this reaction is unlikely to be first order but could possibly be second order. Alternatively, increasing feedstock concentration might change the properties of the reaction mixture and hence change the reaction rate.

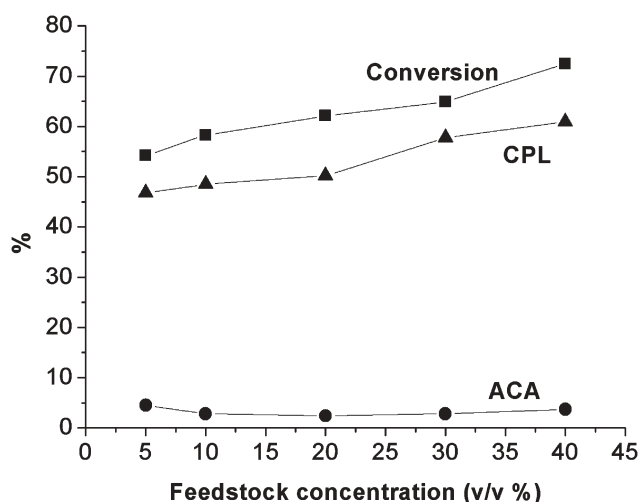


Fig. 5 Effect of feedstock concentration on the reaction of ACN in HTW at 400 °C and 400 bar, with a flow rate of 1.5 mL min^{-1} (calculated residence time = 48 s). The conversion of ACN and yield of CPL increase with increasing feedstock concentration (-■-: conversion of ACN; -●-: yield of ACA; -▲-: yield of CPL).

Table 2 Effect of residence time on the reaction of ACN in HTW with a flow rate of 1.5 mL min⁻¹ under a temperature of 400 °C and a pressure of 400 bar. A high CPL yield of 90% was achieved after two sequential runs, with a total calculated residence time of 96 s

Entry	Feedstock concentration (v/v%)	Conversion of ACN (%) ^a	Yield of ACA (%) ^a	Yield of CPL (%) ^a	Calculated residence time ^b /s
1 ^c	5	70	4	45	240
2	5	53	5	47	48
3	5	68	—	67	2 × 48
4	5	85	—	80	3 × 48
5	30	65	2	58	48
6	30	94	1	90	2 × 48

^a The conversion and yields were calculated by GC, reproducible to ±2%. ^b For calculation of residence time, see Experimental. ^c The results of Vogel *et al.*¹⁴

Effect of the residence time

Our final objective was establishing whether the conversion of ACN could be improved at higher residence time. A simple way of increasing the residence time is to collect the solution emerging from the reactor and to pump it through the reactor a second or even a third time under the same conditions of temperature and pressure. Our experiments were carried out as before at 400 °C and 400 bar at a flow rate of 1.5 mL min⁻¹ and a calculated residence time of 48 s. To compare with the results of Vogel *et al.*,¹⁴ two concentrations of ACN, 5% (v/v) and 30% (v/v), were used, see Table 2.

It can be seen from Table 2 that 3 runs were needed for the 5% (v/v) feedstock to achieve an ACN conversion of 85% and a CPL yield of 80%, while only 2 runs were necessary for the 30% (v/v) feedstock to obtain an ACN conversion of 94% and a CPL yield of 90%. According to the best result of Vogel *et al.*,¹⁴ an ACN conversion of *ca.* 70% and a selectivity of CPL of *ca.* 66% gave an actual CPL yield of <50% at 350 °C and 250 bar with a residence time of 240 s. Thus, it is evident that our process, using a higher temperature, pressure and concentration of ACN, is an improvement on the previously published method. However, it should be noted that our process of repeated runs not only increases the residence time, but also, during the depressurization between the runs, releases the NH₃ generated from hydrolysis, which appears to inhibit further reaction. The same idea of using two or more reactors in series with provision for mid-process pressure let-down and “refluxing” at atmospheric pressure or less to remove intermediate NH₃ was suggested more than 60 years ago in a patent,³⁰ where the reaction was conducted at temperatures below 300 °C. However, we found that this “refluxing” method worked better with 30% (v/v) feedstock than that with 5% (v/v), suggesting that it could be a combined effect of releasing NH₃ and phase behaviour of the reaction mixture.

Conclusion

The results presented here demonstrate that CPL can be formed selectively and continuously from ACN in HTW. A yield of 90% CPL and a conversion of 94% ACN have been achieved within a calculated residence time of 96 s at 400 °C and 400 bar. Also increasing the concentration of ACN

(up to 40% v/v aqueous solution) improves the efficiency of the reaction.

A study of the effect of temperature, pressure and residence time performed here shows that HTW is an easily adjustable environment which allows simple optimisation of the reaction.

Compared to previous studies of this reaction, our process in HTW is the first to achieve a high conversion and high yield without using either an additional catalyst or an organic solvent. Also the reaction time has been shortened from hours to seconds, compared to those patented processes discussed in this paper. In addition, the higher temperatures used permit more efficient recovery of reaction exotherm. This highly efficient and eco-friendly system has promise for industrial applications.

Acknowledgements

We thank S. D. Housley, W. B. Thomas, G. R. Aird and M. L. Thomas for their advice. The authors would also like to thank M. Guylar, R. Wilson and P. A. Fields for their help and INVISTA Performance Technologies and the University of Nottingham for financial support.

References

- 1 F. Ullmann, *Ullmann's encyclopaedia of industrial chemistry [electronic resource]*, John Wiley & Sons, Inc., New York, 2002.
- 2 K. Weissermel and H.-J. Arpe, *Industrial Organic Chemistry*, VCH, New York, 1997.
- 3 G. Dahlhoff, J. P. M. Niederer and W. F. Hoelderich, *Catal. Rev. Sci. Eng.*, 2001, **43**(4), 381–441.
- 4 H. Ichihashi and H. Sato, *Appl. Catal., A*, 2001, **221**(1–2), 359–366.
- 5 C. O'Driscoll, *Eur. Chem. News*, 2004, **81**(2111), 16.
- 6 H. Sato, K. Hirose, N. Ishii and Y. Umada, Sumitomo Chemical Co., Ltd., Japan, JP 62123167, 1987.
- 7 H. Sato, K. Hirose, M. Kitamura, Y. Umada, N. Ishii and H. Tojima, Sumitomo Chemical Co., Ltd., Japan, EP 242960, 1987.
- 8 P. Roffia, M. Padovan, E. Moretti and G. De Alberti, Montedipe S.p.A., Italy, EP 208311, 1987.
- 9 U. Schuchardt, W. A. Carvalho and E. V. Spinace, *Synlett*, **1993**(10), 713–718.
- 10 U. Schuchardt, D. Cardoso, R. Sercheli, R. Pereira, R. S. da Cruz, M. C. Guerreiro, D. Mandelli, E. V. Spinace and E. L. Pires, *Appl. Catal., A*, 2001, **211**(1), 1–17.
- 11 L. Gilbert, N. Laurain, P. Leconte and C. Nedez, Rhone-Poulenc Fiber & Resin Intermediates, Fr.; Rhodia Polyamide Intermediates, EP 748797, 1996.
- 12 F. Ohlbach, A. Ansmann, P. Bassler, R.-H. Fischer, H. Luyken, S. Maixner and J.-P. Melder, BASF Aktiengesellschaft, Germany, WO 2001083441, 2001.
- 13 G. Achhammer and E. Fuchs, BASF A.-G., Germany, US 5495016, 1996.
- 14 A. Kramer, S. Mittelstadt and H. Vogel, *Chem. Eng. Technol.*, 1999, **22**(6), 494–500.
- 15 D. Broll, C. Kaul, A. Kramer, P. Krammer, T. Richter, M. Jung, H. Vogel and P. Zehner, *Angew. Chem., Int. Ed.*, 1999, **38**(20), 2999–3014.
- 16 *CRC Handbook of Chemistry and Physics: a ready-reference book of chemical and physical data*, ed. D. R. Lide, CRC Press, Boca Raton, FL, 2002.
- 17 P. A. Aleman, C. Boix and M. Poliakoff, *Green Chem.*, 1999, **1**(2), 65–68.
- 18 E. Venardou, E. Garcia-Verdugo, S. J. Barlow, Y. E. Gorbaty and M. Poliakoff, *Vib. Spectrosc.*, 2004, **35**(1–2), 103–109.
- 19 C. Boix, J. M. de la Fuente and M. Poliakoff, *New J. Chem.*, 1999, **23**(6), 641–643.
- 20 P. A. Hamley, T. Ilkenhans, J. M. Webster, E. Garcia-Verdugo, E. Venardou, M. J. Clarke, R. Auerbach, W. B. Thomas, K. Whiston and M. Poliakoff, *Green Chem.*, 2002, **4**(3), 235–238.

- 21 E. Garcia-Verdugo, E. Venardou, W. B. Thomas, K. Whiston, W. Partenheimer, P. A. Hamley and M. Poliakoff, *Adv. Synth. Catal.*, 2004, **346**(2–3), 307–316.
- 22 E. Garcia-Verdugo, J. Fraga-Dubreuil, P. A. Hamley, W. B. Thomas, K. Whiston and M. Poliakoff, *Green Chem.*, 2005, **7**(5), 294–300.
- 23 C. Boix and M. Poliakoff, *Tetrahedron Lett.*, 1999, **40**(23), 4433–4436.
- 24 L. M. Dudd, E. Venardou, E. Garcia-Verdugo, P. Licence, A. J. Blake, C. Wilson and M. Poliakoff, *Green Chem.*, 2003, **5**(2), 187–192.
- 25 M. Uematsu and E. U. Franck, *J. Phys. Chem. Ref. Data*, 1981, **9**(4), 1291–1306.
- 26 W. L. Marshall and E. U. Franck, *J. Phys. Chem. Ref. Data*, 1981, **10**(2), 295–304.
- 27 J. Clayden, N. Greeves, S. Warren and P. Wothers, *Organic Chemistry*, Oxford University Press, Oxford, 2001.
- 28 M. Boero, T. Ikeshoji, C. C. Liew, K. Terakura and M. Parrinello, *J. Am. Chem. Soc.*, 2004, **126**(20), 6280–6286.
- 29 D. Laria, J. Marti and E. Guardia, *J. Am. Chem. Soc.*, 2004, **126**(7), 2125–2134.
- 30 E. L. Martin, E. I. du Pont de Nemours & Co., US 2301964, 1942.

		<p>Comments received from just a few of the thousands of satisfied RSC authors and referees who have used ReSource - the online portal helping you through every step of the publication process.</p> <p>authors benefit from a user-friendly electronic submission process, manuscript tracking facilities, online proof collection, free pdf reprints, and can review all aspects of their publishing history</p> <p>referees can download articles, submit reports, monitor the outcome of reviewed manuscripts, and check and update their personal profile</p> <p>NEW!! We have added a number of enhancements to ReSource, to improve your publishing experience even further.</p> <p>New features include:</p> <ul style="list-style-type: none"> ● the facility for authors to save manuscript submissions at key stages in the process (handy for those juggling a hectic research schedule) ● checklists and support notes (with useful hints, tips and reminders) ● and a fresh new look (so that you can more easily see what you have done and need to do next) <p>Go online today and find out more.</p>
	<p>'I wish the others were as easy to use.'</p>	
<p>'ReSource is the best online submission system of any publisher.'</p>		

Registered Charity No. 207890

RSC Publishing

www.rsc.org/resource

Toxicity of imidazolium ionic liquids to freshwater algae

Konrad J. Kulacki* and Gary A. Lamberti

Received 21st June 2007, Accepted 31st October 2007

First published as an Advance Article on the web 20th November 2007

DOI: 10.1039/b709289j

Room-temperature ionic liquids (ILs) are a class of novel green chemicals being designed to replace traditional volatile organic solvents in industrial processes. The potential effects of ILs on aquatic ecosystems have been poorly studied, despite the possibility of unintentional discharge into rivers and lakes, and their intentional disposal in wastewater treatment plants. We studied the effects of three imidazolium ionic liquids, 1-butyl-, 1-hexyl- and 1-octyl-3-methylimidazolium bromide, on the growth rates of two freshwater algae, *Scenedesmus quadricauda* and *Chlamydomonas reinhardtii*, in 96 h standard toxicity bioassays. Increases in alkyl chain length increased the toxicity of these ionic liquids to both *S. quadricauda* (EC₅₀ values of 0.005–13.23 mg L⁻¹) and *C. reinhardtii* (EC₅₀ values of 4.07–2138 mg L⁻¹). Bioassays were performed in both nutrient-amended media and low-nutrient groundwater to evaluate if test conditions altered IL toxicity. EC₅₀ values for *S. quadricauda* were similar between nutrient media and groundwater for all ILs tested, while the presence of nutrient media appeared to partially mitigate the toxicity of ILs to *C. reinhardtii* (groundwater EC₅₀ < media EC₅₀). Overall, *S. quadricauda* was much more sensitive than *C. reinhardtii* to all ILs tested, perhaps reflecting differences in cell wall structure. EC₅₀ values suggest that ILs are more, or just as, toxic to algae than many of the solvents they are intended to replace. Results of this study show that ionic liquids can elicit a range of algal responses, suggesting that a diversity of target organisms be tested in order to predict the effects of ILs in natural environments.

Introduction

New chemicals are constantly being designed to meet the needs of industry and society, both to improve existing processes and to facilitate new ones. Increasingly, these chemicals are being designed specifically to reduce toxicity, enhance biodegradability, and prevent waste at its source, all of which are fundamental principles of green chemistry.¹ While these ‘green’ chemicals are often intended to be more efficient and/or safer, this is not always the case.² Thorough chemical and toxicological research is needed to ensure that the chemicals that are, or may some day be, in widespread use are indeed safe for humans and the environment. Such proactive research is currently underway with a novel class of industrial solvents: room-temperature ionic liquids.³

Room-temperature ionic liquids (ILs) are non-volatile organic solvents being designed to replace traditional volatile organic solvents (VOS),⁴ such as benzene and toluene.^{5–7} Ionic liquids typically consist of a bulky cation, often an imidazolium or pyridinium ring; side chains that vary in length, number, and position; and a variable anion (Fig. 1). They are often referred to as ‘designer’ chemicals, since the cation and anion can be easily manipulated to change the solvent’s properties and thus tailor it to a specific industrial process.⁸ Ionic liquids could be used, for example, as lubricants, battery electrolytes, catalysts, and in the manufacture of

nanomaterials.^{3,9} However, recent studies have shown that the toxicity of many ionic liquids can be similar to those of the industrial solvents they may replace.^{10–13} While ILs pose little threat of airborne toxicity, a growing body of evidence suggests that they can be toxic to aquatic organisms, including bacteria, plants, invertebrates, and fish.^{3,12,14–16} However, varying the anion and length of the side chains of ionic liquids can modify their toxicity to organisms^{17,18} and thus provide one way to design ionic liquids in which function is balanced by low toxicity should ILs ever be released into the environment.

If ILs were released, either intentionally after industrial waste processing or accidentally during a spill, they would

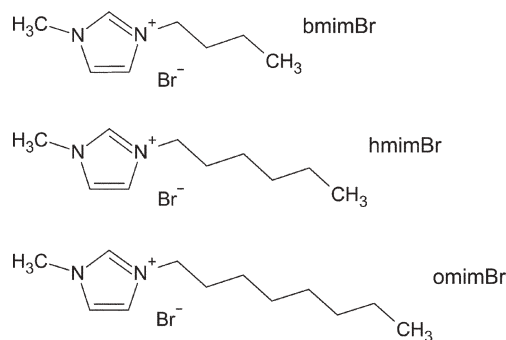


Fig. 1 Structures of the imidazolium ionic liquids used in this study: 1-butyl-3-methylimidazolium bromide (bmimBr), 1-hexyl-3-methylimidazolium bromide (hmimBr), 1-octyl-3-methylimidazolium bromide (omimBr).

Department of Biological Sciences, University of Notre Dame, Notre Dame, IN 46556, USA. E-mail: kkulacki@nd.edu

likely enter aquatic ecosystems ranging from groundwater to surface water. Because many ILs are water soluble,^{19,20} they are likely to move readily through the environment and contact the biota. Primary producers, such as freshwater algae, are essential to aquatic food webs, serving roles in nutrient cycling and conversion of carbon dioxide into biomass,²¹ and could be vulnerable to chemical stressors due to their ubiquity, small size, large population numbers, and short life cycles.²² To date, few studies have examined the effects of ILs on algal primary producers.^{12,16,23} Latała *et al.*²³ studied two marine algae, and found that the two species differed dramatically in their ability to recover from IL exposure, and that IL toxicity declined with increasing salinity. Wells and Coombe¹² studied one freshwater alga, *Pseudokirchneriella subcapitata*, in 48 h bioassays and found that longer alkyl chains on the ILs increased toxicity, a trend not evident in the work of Latała *et al.*²³ Matzke *et al.*¹⁶ studied *Scenedesmus vacuolatus* in rapid (24 h) screening assays, and found it to be sensitive to several different ILs. To better assess the potential effects of ILs on aquatic primary producers, studies of different species at the same trophic level are needed to begin to generalize responses to higher taxonomic groups.

The objective of our study was to determine the effects of imidazolium-based ionic liquids on two contrasting freshwater algae, *Scenedesmus quadricauda* and *Chlamydomonas reinhardtii*, using standard toxicity bioassays. *Scenedesmus* and *Chlamydomonas* are two common genera of freshwater algae, are easily cultured in the laboratory, and have been used as model organisms in toxicology studies.^{24–26} *Scenedesmus* (Order: Chlorococcales) are non-motile green algae, often forming colonies of four, eight, or sixteen ellipsoidal cells joined laterally.²⁷ By contrast, *Chlamydomonas* (Order: Volvocales) are mobile, possessing two flagella of equal length, and occur as individual, spherical cells.²⁸ Our hypothesis was that the two algae would respond similarly to ILs if toxicity can be generalized over broad taxonomic groups. However, morphological and physiological differences between species could result in differential responses. Furthermore, we hypothesized that the nutrient environment of the algae could influence toxicity. We predicted that the presence of replete nutrients, as provided by typical algal media, would mitigate IL toxicity to some extent.

Results

Scenedesmus quadricauda

The ionic liquid most toxic to *S. quadricauda* was omimBr, followed by hmimBr, and then bmimBr (Table 1); however, even bmimBr exhibited high toxicity to this alga (96 h EC₅₀ = 13.2 mg L⁻¹). Growth inhibition increased with increasing IL concentration in all cases (Fig. 2A,B). Growth rates declined rapidly with increasing IL concentration until zero or negative growth was exhibited. Algae exposed to omimBr, even in algal media, not only stopped growing, but also died during the experiment, as reflected in negative 96 h growth rates (Fig. 2B). *S. quadricauda* growth rates were more variable in groundwater than in the algal media. However, the addition of media did not significantly affect the toxicity of these ILs to *S. quadricauda*.

Chlamydomonas reinhardtii

The ionic liquid most toxic to *C. reinhardtii* was omimBr, followed by hmimBr, and then bmimBr (96 h EC₅₀ = 2140 mg L⁻¹; Table 1). Growth inhibition increased with increasing IL concentration (Fig. 3A,B). EC₅₀ values for the ILs tested were 10³–10⁵ higher for *C. reinhardtii* than for *S. quadricauda*. Algae exposed to 400 mg L⁻¹ bmimBr in groundwater exhibited slight hormesis (*i.e.* increased growth at low concentrations of otherwise toxic substances), although growth rates were not significantly different from controls. The presence of algal media increased the EC₅₀ of omimBr to *C. reinhardtii* by an order of magnitude, and had similar effects for bmimBr and hmimBr (Table 1). At 64 mg L⁻¹ in groundwater, omimBr halted the growth of *C. reinhardtii* and killed cells (Fig. 3A).

Discussion

Traditionally, phytotoxicity data have not played an important role in the regulation of hazardous chemicals, based on the perception that plants and algae were less sensitive to most chemicals than were invertebrates and fish.²⁹ Only recently has this assumption been re-examined, as many algal species have been found to be just as sensitive, if not more, as animals to a wide array of chemicals, including surfactants.²² We reviewed

Table 1 EC₅₀ values for 1-alkyl-3-methylimidazolium ionic liquids for *S. quadricauda* and *C. reinhardtii*

Algae	Media	Ionic liquid	EC ₅₀ /mg L ⁻¹	95% confidence interval
<i>S. quadricauda</i>	Groundwater	bmimBr	4.76	(n.c.) ^a
	Groundwater	hmimBr	0.078	(0.045–0.191)
	Groundwater	omimBr	0.005	(0.0003–0.057)
	Enriched	bmimBr	13.2	(4.48–29.9)
	Enriched	hmimBr	0.052	(0.006–0.126)
	Enriched	omimBr	0.005	(n.c.) ^a
<i>C. reinhardtii</i>	Groundwater	bmimBr	1070	(1020–1110)
	Groundwater	hmimBr	260	(232–284)
	Groundwater	omimBr	4.07	(2.43–6.44)
	Enriched	bmimBr	2140	(1180–2640)
	Enriched	hmimBr	851	(401–14 600)
	Enriched	omimBr	50.7	(36.6–65.3)

^a n.c. = not computable.

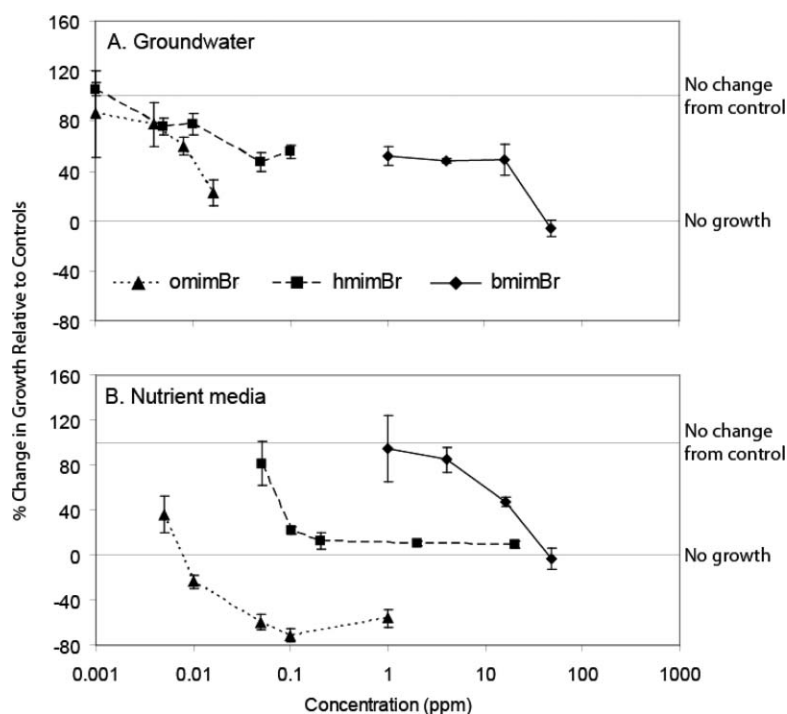


Fig. 2 Effects of bmimBr, hmimBr, and omimBr on the growth of *S. quadricauda* in groundwater (A) and nutrient media (B). All results were normalized to controls for each test. 100% response indicates no difference between treatment and control; 0% response indicates zero growth. Bars represent ± 1 SE for each treatment mean.

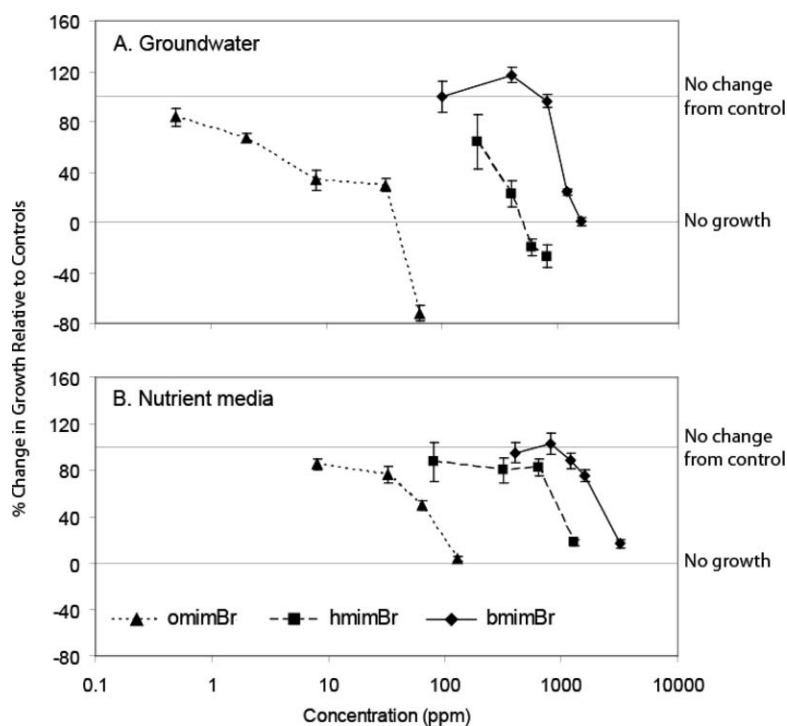


Fig. 3 Effects of bmimBr, hmimBr, and omimBr on the growth of *C. reinhardtii* in groundwater (A) and nutrient media (B). All results were normalized to controls for each test. 100% response indicates no difference between treatment and control; 0% response indicates zero growth. Bars represent ± 1 SE for each treatment mean.

the published literature for data on the toxicity of ILs to any freshwater or marine alga (Table 2), and also compared those values to the toxicity of common industrial solvents

(Table 3). Ionic liquids have been shown to be as toxic, or more so, as their volatile counterparts to freshwater algae (Table 3).

Table 2 Comparison of toxicities of various imidazolium ionic liquids to algae

Ionic liquid	Algae	Duration/h	EC ₅₀ /mg L ⁻¹	Ref.
emimBF ₄ ^a	<i>Oocystis submarina</i>	72	0.99 < EC ₅₀ < 9.9	23
emimBF ₄ ^a	<i>Cyclotella meneghiniana</i>	96	9.9 < EC ₅₀ < 99	23
emim(2-OPhO) ₂ B ^b	<i>Scenedesmus vacuolatus</i>	24	9.15	16
bmimBF ₄	<i>O. submarina</i>	72	>113	23
bmimBF ₄	<i>C. meneghiniana</i>	96	>113	23
bmimPF ₆	<i>Pseudokirchneriella subcapitata</i>	48	45	12
bmimCl	<i>P. subcapitata</i>	48	38.5	12
bmimBr	<i>S. quadricauda</i>	96	13.23 (media); 4.76 (water)	p.w. ^c
bmimBr	<i>Chlamydomonas reinhardtii</i>	96	2138 (media); 1066 (water)	p.w. ^c
bmim(CF ₃) ₂ N	<i>S. vacuolatus</i>	24	244.4	16
bmimX ^{-d}	<i>S. vacuolatus</i>	24	20.9–29.4	16
hmimBF ₄	<i>O. submarina</i>	72	12.7 < EC ₅₀ < 127	23
hmimBF ₄	<i>C. meneghiniana</i>	96	12.7 < EC ₅₀ < 127	23
hmimBr	<i>S. quadricauda</i>	96	0.052 (media); 0.078 (water)	p.w. ^c
hmimBr	<i>C. reinhardtii</i>	96	850.51 (media); 259.95 (water)	p.w. ^c
omimBr	<i>S. quadricauda</i>	96	0.005 (media); 0.006 (water)	p.w. ^c
omimBr	<i>C. reinhardtii</i>	96	50.69 (media); 4.07 (water)	p.w. ^c
omimBF ₄	<i>S. vacuolatus</i>	24	0.001	16
C ₁₂ mimC ^e	<i>P. subcapitata</i>	48	0.0011	12
C ₁₄ mimCl ^e	<i>P. subcapitata</i>	48	0.0041	12
C ₁₆ mimCl ^e	<i>P. subcapitata</i>	48	0.0129	12

^a 1-Ethyl-3-methylimidazolium tetrafluoroborate. ^b 1-Ethyl-3-methylimidazolium bis(1,2-benzenediolato)borate. ^c p.w. = present work. ^d Four anions were used: chloride, tetrafluoroborate, octylsulfate, and bis(trifluoromethylsulfonyl)imide. ^e The ILs used in this study had alkyl chains of 12, 14, and 16 carbons.

Table 3 Toxicity of common industrial solvents to *Scenedesmus* (top) and *Chlamydomonas* (bottom) species, compared to ionic liquids

Chemical	Species	Endpoint reported	Duration/h	Concentration/mg L ⁻¹	Ref.
Acetone	<i>S. quadricauda</i>	Growth LOEC ^a	n/r ^c	7500	49
	<i>S. pannonicus</i>	Growth NOEC ^b	48	4740	50
Benzene	<i>S. quadricauda</i>	Growth LOEC ^a	n/r ^c	>1400	49
	<i>S. abundans</i>	Growth EC ₅₀	96	>1360	51
Toluene	<i>S. quadricauda</i>	Growth LOEC ^a	n/r ^c	>400	49
	<i>S. subspicatus</i>	Growth EC ₅₀	48	125	52
Phenol	<i>S. quadricauda</i>	Growth LOEC ^a	n/r ^c	7.5	49
Ionic liquids	<i>S. vacuolatus</i>	Growth EC ₅₀	24	0.001–244	16
	<i>S. quadricauda</i>	Growth EC ₅₀	96	0.005–13.23	p.w. ^d
Chloroform	<i>C. angulosa</i>	Photosynthesis EC ₅₀	3	382.1	53
Toluene	<i>C. reinhardtii</i>	Fluorescence EC10	2	13	54
	<i>C. angulosa</i>	Photosynthesis EC ₅₀	3	0.13	53
Hexane	<i>C. angulosa</i>	Photosynthesis EC ₅₀	3	8.1	53
Benzene	<i>C. angulosa</i>	Photosynthesis EC ₅₀	3	0.46	53
Ionic liquids	<i>C. reinhardtii</i>	Growth EC ₅₀	96	4.07–2138	p.w. ^d

^a LOEC: Lowest Observed Effect Concentration. ^b NOEC: No Observed Effect Concentration. ^c n/r = not reported. ^d p.w. = present work.

In our study, we focused on two algal genera that have been used in several previous toxicological studies. For *S. quadricauda* and *C. reinhardtii*, we observed several orders of magnitude difference between their EC₅₀ values for the same IL. In previous studies, the relative sensitivities of these two genera have ranged from *Chlamydomonas* being the more sensitive of the two,³⁰ to no differences,³¹ to *Scenedesmus* being more sensitive (present study). Compared with previous studies^{12,16,23} of the same imidazolium ILs, but with different anions, *Scenedesmus* is the most sensitive algal genus tested, with *S. quadricauda* responding similarly to *S. vacuolatus*. By contrast, *Chlamydomonas* appears to be less sensitive to ILs than any other algal genus studied (Table 2). While the differences among these studies are noteworthy, it should be kept in mind that the anion of the ionic liquid can have a limited effect on its toxicity,^{16,18} at least compared to the cation, and that the duration of these tests differed among

studies. The differences seen here between algal taxa and in comparison to previous studies may be explained by addressing the mechanism of IL toxicity.

While the specific mechanism of IL toxicity remains unclear, the structures of many ILs are similar to those of surfactants,³² for which the mode of toxic action is likely narcosis via membrane disruption.³³ Ionic liquids can disrupt synthetic membranes,³⁴ but the concentrations used in that study were several orders of magnitude higher than those shown to have toxic effects in the present study, suggesting a more subtle mechanism of IL toxicity to freshwater algae. One clue to this mechanism may be the very different cell wall structures of the two species we studied. The cell wall of *S. quadricauda* is composed primarily of cellulose,²⁷ while that of *C. reinhardtii* is composed primarily of glycoprotein.^{25,35} Latała *et al.*²³ also proposed that the differences they saw in algal sensitivity were due to cell wall structure differences, with their diatom

(silica-based cell wall) being more sensitive than their green alga (cellulose cell wall). The cell wall of algae is known to play a critical role in the transport of materials in and out of the cell, including toxins.³⁶ Thus, differences in the cell wall structure could affect the abilities of cells to resist or repair membrane disruption. Taken together, our results and those of Latała *et al.*²³ suggest that glycoprotein cell walls may be more resistant to IL disruption than cellulose cell walls, which in turn may be more resistant than silica-based walls. However, more studies are needed to fully investigate these cell wall structural differences with ionic liquids in particular. If differences in cell walls are shown to affect susceptibility to ionic liquids, we should be able to scale the effects of ILs across organisms more accurately and improve our ability to predict their effects in natural environments.

Nutrient media is commonly used to maintain laboratory cultures of algae, including during experimentation.³⁷ We found that the presence of nutrient media had a mitigating effect on the toxicity of these ionic liquids to *C. reinhardtii*, but not to *S. quadricauda*, in comparison to low-nutrient groundwater. Similarly, the presence of nutrient media has been shown to have little effect on the toxicity of another surfactant, FFD-6, to *Scenedesmus obliquus*.³⁸ Since the conductivities of the Bold's Basal media and the groundwater used in our tests were similar (666 and 742 μS , respectively), the observed differences in response to ILs between test media types were unlikely to be due to an ionic strength effect, as was seen by Latała *et al.*²³ when altering test media salinity. The fact that we did not see a difference in IL effects on *S. quadricauda* between the modified COMBO media and the groundwater, though the conductivities were different (373 and 742 μS , respectively), supports this point. Established protocols²² for testing the (eco)toxicity of chemicals to freshwater algae do not consider the issue of nutrient conditions, and from the literature it is common practice to use whichever media is appropriate for a given taxon, with no consideration of the potential interactions between the media and toxicity. More broadly, aquatic ecologists are well aware of the influence that nutrient concentrations have on the community composition of pelagic algal communities.²¹ The differences we observed could reflect the higher nutrient concentrations in Bold's Basal media used with *C. reinhardtii* relative to the modified COMBO media used with *S. quadricauda*.^{37,39} This difference in nutrient levels might enable a taxon to cope better with the higher stress levels associated with a particular ionic liquid. In general, organisms that are stressed by other factors, such as starvation or disease, are more sensitive to toxins.³³ Clearly, information about the abiotic conditions under which an organism will likely be exposed to a toxic substance is needed to properly predict the potential responses. Furthermore, we suggest some standardization across ecotoxicology protocols, such as those of the USEPA, to include nutrient media for algal toxicity tests. However, many examples currently in the literature and in databases lack consistency, often for practical reasons. Such inconsistencies severely limit our ability to make informed generalizations from single-species bioassays about the impacts of hazardous chemicals on organisms, including ionic liquids.

Single-species bioassays are considered a rapid, cost-effective way to determine the toxicity of chemicals to target

organisms.⁴⁰ These tests are often based on several assumptions, including that the test organism: (1) is the most sensitive of all the possible choices; (2) will be the most sensitive to a wider array of chemicals represented by the test chemical; and (3) will exhibit responses representative of those observed for other organisms in similar environments. In other words, results should be scalable across similar organisms, conditions, and chemicals.⁴¹ While these assumptions may not always hold true, we have addressed some deficiencies of single-species bioassays by studying two different organisms and contrasting environment conditions. In the published literature, *Scenedesmus* is the most sensitive algal genera to IL toxicity to date. With additional testing, other algal taxa may be shown to be equally or more sensitive to the ILs tested here. Indeed, such marked differences between two genera of freshwater algae suggests that more taxa should be considered, especially given that more than 770 genera of freshwater algae are known to exist in North America alone.⁴² Laboratory tests, such as the present study, provide a straightforward comparison of LC₅₀ values across compounds (be it individual ILs or more broadly) and organisms. Such tests are a critical step to determining the potential effects of chemicals in the environment, and provide important background information for future multi-species testing, especially given the complexity of response to just two variables (species, nutrient media) apparent from this study.

The wide range of toxicity values seen here and in other studies^{12,16,23} illustrates the difficulty of extrapolating the results of laboratory bioassays across taxa. Furthermore, the abiotic conditions used in these tests do not span the range of conditions found in natural environments. We feel that this presents a challenge and opportunity for the field of ecotoxicology. Standard protocols typically require a defined test media, a strict light–dark regime, and a constant temperature,⁴³ conditions rarely found in nature. To meet the challenge of making realistic predictions about the potential effects of chemicals in the environment, tests should be performed across a range of conditions in order to (1) determine how abiotic factors affect the toxicity of a chemical, and (2) enhance applicability to field conditions. While this study showed that nutrient environment can affect the toxicity of ILs to algae, further studies are needed to determine if changes in other abiotic factors, such as light and temperature, can modify toxicity. This could be especially relevant to ionic liquids, due to their countless possible structures and subsequent possible interactions with abiotic factors.

Ionic liquids can be produced in a myriad of different chemical forms, estimated to include up to 10¹⁸ possible compounds.⁴⁴ One way in which ILs can be modified is by changing the length of the alkyl chain, such as from butyl to hexyl to octyl. We observed an increase in toxicity with an increase in the length of the alkyl chain, a result consistent with that of several other studies.^{15,17} Accordingly, in order to minimize the potential for environmental harm, the development of ionic liquids should focus on compounds with shorter alkyl chains (*e.g.* butyl, propyl, ethyl). We have also shown that even at low concentrations ($<0.005 \text{ mg L}^{-1}$), ILs can have strong negative effects on freshwater algae. The broader ecological consequences of IL toxicity to algae are substantial,

given that algae represent the base of the food web of most aquatic ecosystems. The design of ionic liquids to minimize the risk to algae and other primary producers will help to protect aquatic ecosystems from unintended harm.

Conclusions

Room-temperature ionic liquids are considered to be an improvement over conventional industrial solvents due to their flexibility in design and non-volatility.⁴ However, these compounds have been shown to be as toxic, or more so, as their volatile counterparts to aquatic organisms, including freshwater algae. We observed considerable variation in toxicity between chemicals and organisms. To ensure the safety of natural ecosystems, additional testing should be performed on other IL structures and algal taxa using standard toxicity tests, as well as with more ecologically complex systems. Ideally, such systems would mimic the natural systems that chemicals might enter, in terms of species diversity and abiotic conditions. The 'perfect solvent' that has all the desirable chemical properties with none of the toxicity is unlikely to exist. However, ecologists and toxicologists can guide the development of environmentally safe ionic liquids by providing direct feedback to chemical engineers about the ecotoxicology of the compounds they generate.

Experimental

Test chemicals

The three ILs used in this study were different forms of 1-alkyl-3-methylimidazolium bromide, where the alkyl chain was either four (butyl; bmimBr), six (hexyl; hmimBr), or eight (octyl; omimBr) carbons long (Fig. 1). The K_{ow} values for these and other similar ILs range from 0.0033 to 11.1,²⁰ suggesting that they are unlikely to bioaccumulate. The ILs used in these bioassays were synthesized in the Department of Chemical and Biomolecular Engineering, University of Notre Dame, Notre Dame, IN, USA using established synthesis procedures.^{45,46} These specific ILs were chosen because imidazolium ionic liquids are already commercially available, and are beginning to be used in industrial processes (Sigma Aldrich, St. Louis, MO, USA).

Test organisms

S. quadricauda was obtained from the University of Texas Culture Collection (UTCC #76), and *C. reinhardtii* from the University of Toronto Culture Collection (UTCC #243). Both algae were batch-cultured in nutrient media at a constant temperature of 24 °C on a 12 h : 12 h light–dark cycle. Culture flasks were decanted and refilled with fresh nutrient media weekly to maintain exponential population growth. *S. quadricauda* was cultured and tested in modified COMBO media.³⁹ Media was modified to include higher concentrations of nitrogen and phosphorus (7 mg L⁻¹ P, as KH₂PO₄⁻; 0.7 mg L⁻¹ N, as NaNO₃) to promote algal growth. *C. reinhardtii* was cultured and tested in Bold's Basal Media (BBM).³⁷ Different media were used because the two algae have different nutrient requirements.³⁷

Groundwater used in tests was low in all major nutrients (<1 mg L⁻¹ DOC, <15 µg L⁻¹ N, <10 µg L⁻¹ P), and was not chlorinated or fluorinated. The specific conductivities of the COMBO, BBM, and groundwater were 373, 666, and 742 µS, respectively.

Test methods

All bioassays were performed according to standard protocols.⁴⁷ Tests were performed in 500 mL Erlenmeyer flasks containing the appropriate alga, test media, and a range of concentrations of bmimBr, hmimBr, or omimBr. Each algae/media/IL combination was tested separately. Range-finding tests were performed initially to establish concentrations for definitive testing. All test concentrations were replicated four or five times. Experimental flasks were completely randomized and placed on a rotary shaker table (140 rpm) under a full spectrum light source (20 µM photons m⁻² s⁻¹) set for a 12 h photoperiod. All experiments were performed at a constant temperature of 24 °C. Samples for chlorophyll *a* (chl *a*) analysis were taken daily for five days (96 h) and analyzed on a fluorometer (TD-700, Turner Designs) using a methanol extraction method.⁴³ Algal growth rates [Δ chl *a* (µg L⁻¹ d⁻¹)] were determined for each flask from changes in chl *a* over 96 h and then averaged across replicates. Growth rates for each IL concentration were then compared to the controls for that experiment to determine percent response relative to controls.

Statistical analyses

EC₅₀ values and associated 95% confidence intervals for the algal growth rate for each algae/media/IL combination were determined by fitting the dose–response curves to a logistic model using the maximum likelihood method.⁴⁸ In some cases, 95% confidence intervals could not be calculated because of high variability in algal response. All analyses were performed using SAS[®] (Version 9.1) statistical software (SAS, Cary, NC, USA).

Acknowledgements

We would like to thank Nicole Gifford and Michael Brueseke for laboratory assistance. Discussions with Randall Bernot led to the development of this study, and Dominic Chaloner provided useful comments on previous versions of the manuscript. This study was supported by grants from the US Department of Education's GAANN Program (Graduate Assistance in Areas of National Need) and the US National Oceanic and Atmospheric Administration (NOAA Awards No. NA04OAR4600076 and NA05OAR4601153).

References

- 1 P. T. Anastas and J. C. Warner, *Green Chemistry: Theory and Practice*, Oxford University Press, New York, 1998.
- 2 W. Hartley, A. Engle, Jr. and D. Harrington, *Water Sci. Technol.*, 1999, **39**, 305–310.
- 3 B. Jastorff, K. Mölter, P. Behrend, U. Bottin-Weber, J. Filser, A. Heimers, B. Ondruschka, J. Ranke, M. Schaefer, H. Schröder, A. Stark, P. Stepnowski, F. Stock, R. Störmann, S. Stolte, U. Welz-Biermann, S. Ziegert and J. Thöming, *Green Chem.*, 2005, **7**, 362–372.

- 4 J. F. Brennecke and E. J. Maginn, *AIChE J.*, 2001, **47**, 2384–2389.
- 5 Y. Chauvin and H. Olivier-Bourbigou, *Chemtech*, 1995, **25**, 26–30.
- 6 R. D. Rogers and K. R. Seddon, *Ionic Liquids: Industrial Applications for Green Chemistry*, Oxford University Press, San Diego, CA, 2002.
- 7 R. D. Rogers and K. R. Seddon, *Ionic Liquids IIIA: Fundamentals, Progress, Challenges, and Opportunities: Properties and Structure*, Oxford University Press, San Diego, CA, 2005.
- 8 K. N. Marsh, A. Deev, A. C. T. Wu, E. Tran and A. Klamt, *Korean J. Chem. Eng.*, 2002, **19**, 357–362.
- 9 P. L. Short, *Chem. Eng. News*, 2006, **84**, 15–21.
- 10 J. Ranke, S. Stolte, J. Störmann, J. Arning and B. Jastorff, *Chem. Rev.*, 2007, **107**, 2183–2206.
- 11 R. J. Bernot, M. A. Brueske, M. A. Evans-White and G. A. Lamberti, *Environ. Toxicol. Chem.*, 2005, **24**, 87–92.
- 12 A. S. Wells and V. T. Coombe, *Org. Process Res. Dev.*, 2006, **10**, 794–798.
- 13 K. M. Docherty and C. F. Kulpa, Jr., *Green Chem.*, 2005, **7**, 185–189.
- 14 C. Pretti, C. Chiappe, D. Pieraccini, M. Gregori, F. Abramo, G. Monni and L. Intorre, *Green Chem.*, 2006, **8**, 238–240.
- 15 R. J. Bernot, E. E. Kennedy and G. A. Lamberti, *Environ. Toxicol. Chem.*, 2005, **24**, 1759–1765.
- 16 M. Matzke, S. Stolte, K. Thiele, T. Juffernholz, J. Arning, J. Ranke, U. Welz-Biermann and B. Jastorff, *Green Chem.*, 2007, **9**, 1198–1207.
- 17 D. J. Couling, R. J. Bernot, K. M. Docherty, J. K. Dixon and E. J. Maginn, *Green Chem.*, 2006, **8**, 82–90.
- 18 S. Stolte, J. Arning, U. Bottin-Weber, M. Matzke, F. Stock, K. Thiele, M. Uerdingen, U. Welz-Biermann, B. Jastorff and J. Ranke, *Green Chem.*, 2006, **8**, 621–629.
- 19 J. L. Anthony, E. J. Maginn and J. F. Brennecke, *J. Phys. Chem.*, 2001, **105**, 10942–10949.
- 20 L. Ropel, L. S. Belvèze, S. N. V. K. Aki, M. A. Stadtherr and J. F. Brennecke, *Green Chem.*, 2005, **7**, 83–90.
- 21 R. G. Wetzel, *Limnology*, Academic Press, San Diego, CA, 2001.
- 22 M. A. Lewis, in *Fundamentals of Aquatic Toxicology*, ed. G. M. Rand, Taylor & Francis, London, 2003, pp. 135–169.
- 23 A. Latała, P. Stepnowski, M. Nędzi and W. Mrozik, *Aquat. Toxicol.*, 2005, **73**, 91–98.
- 24 A. E. Girling, D. Pascoe, C. R. Janssen, A. Peither, A. Wenzel, H. Schäfer, B. Neumeier, G. C. Mitchell, E. J. Taylor, S. J. Maund, J. P. Lay, I. Jüttner, N. O. Crossland, R. R. Stephenson and G. Personne, *Ecotoxicol. Environ. Safety*, 2000, **45**, 148–176.
- 25 E. H. Harris, *The Chlamydomonas Sourcebook*, Academic Press, San Diego, CA, 1989.
- 26 T. Zbigniew and P. Wojciech, *Ecotoxicol. Environ. Safety*, 2006, **65**, 323.
- 27 L. E. Shubert, in *Freshwater Algae of North America*, ed. J. D. Wehr and R. G. Sheath, Academic Press, Amsterdam, 2003, ch. 7.
- 28 H. Nozaki, in *Freshwater Algae of North America*, ed. J. D. Wehr and R. G. Sheath, Academic Press, Amsterdam, 2003, ch. 6.
- 29 E. E. Kenaga and R. J. Moolenaar, *Environ. Sci. Technol.*, 1979, **13**, 1479–1480.
- 30 J. F. Fairchild, D. S. Ruessler and A. R. Carlson, *Environ. Toxicol. Chem.*, 1998, **17**, 1830–1834.
- 31 R. Rojíčková-Padrťová and B. Maršálek, *Chemosphere*, 1999, **38**, 3329–3338.
- 32 P. J. Scammells, J. L. Scott and R. D. Singer, *Aust. J. Chem.*, 2005, **58**, 155–169.
- 33 G. M. Rand, P. G. Wells and L. S. McCarty, in *Fundamentals of Aquatic Toxicology*, ed. G. M. Rand, Taylor & Francis, London, 2003, pp. 3–67.
- 34 K. O. Evans, *Colloids Surf. A*, 2006, **274**, 11–17.
- 35 J. Voigt, *Planta*, 1988, **173**, 373–384.
- 36 F. Kasai and S. Hatakeyama, *Chemosphere*, 1993, **27**, 899–904.
- 37 R. A. Andersen, *Algal Culturing Techniques*, Academic Press, New York, 2005.
- 38 M. Lurling, *Chemosphere*, 2006, **62**, 1351–1358.
- 39 S. S. Kilham, D. A. Kreeger, S. G. Lynn, C. E. Goulden and L. Herrera, *Hydrobiologia*, 1998, **377**, 147–159.
- 40 G. M. Rand and S. R. Petrocelli, *Fundamentals of Aquatic Toxicology*, Hemisphere, New York, 1985.
- 41 J. Cairns, Jr., *BioScience*, 1986, **36**, 670–672.
- 42 *Freshwater Algae of North America*, ed. J. D. Wehr and R. G. Sheath, Academic Press, Amsterdam, 2003.
- 43 American Public Health Association, *Standard Methods for the Examination of Water and Wastewater*, Port City Press, Baltimore, 1999.
- 44 A. E. Visser, R. P. Swatloski, W. M. Reichert, R. Mayton, S. Sheff, A. Wierzbicki, J. H. Davis and R. D. Rogers, *Environ. Sci. Technol.*, 2002, **36**, 2523–2529.
- 45 L. Cammarata, S. G. Kazarian, P. A. Salter and T. Welton, *Phys. Chem. Chem. Phys.*, 2001, **3**, 5192–5200.
- 46 P. Bonhote, A. P. Dias, N. Papageorgiou, K. Kalyanasundaram and M. Gratzel, *Inorg. Chem.*, 1996, **35**, 1168–1178.
- 47 *Annual Book of ASTM Standards*, E1218–1290, American Society for Testing and Materials, Philadelphia, PA, 1990.
- 48 M. C. Newman, *Quantitative Methods in Aquatic Ecotoxicology*, Lewis, Boca Raton, FL, 1995.
- 49 G. Bringmann and R. Kuhn, *Vom Wasser*, 1978, **50**, 45–60.
- 50 W. Sloof, J. H. Canton and J. L. M. Hermens, *Aquat. Toxicol.*, 1983, **4**, 113–128.
- 51 H. Geyer, I. Scheunert and F. Korte, *Chemosphere*, 1985, **14**, 1355–1369.
- 52 R. Kuhn and M. Pattard, *Water Res.*, 1990, **24**, 31–38.
- 53 T. C. Hutchinson, J. A. Hellebust, D. Tam, D. Mackay, R. A. Mascarenhas and W. Y. Shiu, *Environ. Sci. Res.*, 1980, **16**, 577–586.
- 54 W. Brack and H. Frank, *Ecotoxicol. Environ. Safety*, 1998, **40**, 34–41.

Downloaded by Lomonosov Moscow State University on 13 October 2010
Published on 20 November 2007 on http://pubs.rsc.org | doi:10.1039/B709289J

Green synthesis of carbamates from CO₂, amines and alcohols

Angelica Ion,^a Charlie Van Doorslaer,^a Vasile Parvulescu,^b Pierre Jacobs^a and Dirk De Vos^{*a}

Received 23rd July 2007, Accepted 1st November 2007

First published as an Advance Article on the web 20th November 2007

DOI: 10.1039/b711197e

Various carbamates can be prepared in a halogen-free way starting from cheap and readily available reagents such as amines, alcohols and carbon dioxide. Basic catalysts were able to convert both linear and branched aliphatic amines to the corresponding carbamates with good yields, in mild reaction conditions (2.5 MPa CO₂) and even in the absence of dehydrating agents.

Introduction

The continuous increase of carbon dioxide concentrations in the atmosphere is of worldwide concern due to the impact on global warming. Thus, utilization and transformation of CO₂ into useful chemicals is an area of major interest. Among the few major industrial processes using CO₂, urea synthesis is the most important one, with a production of about 100 million tonnes per year.¹ Other organic compounds such as salicylic acid and its derivatives, and cyclic carbonates are produced in smaller amounts.^{1,2} One of the most promising fields for CO₂ utilization is the synthesis of carbamates, since the carbon atom in CO₂ does not need to be reduced in this reaction. Carbamates are important raw materials for the manufacture of a variety of polymers used in foams, coatings, adhesives, plastics and fibres.³ Current commercial processes for production of carbamates are alcoholysis of isocyanates or aminolysis of chloroformates.⁴ The preparation of isocyanates and chloroformates requires use of the highly toxic and corrosive phosgene (COCl₂). Alternative routes imply the utilization of poisonous carbon monoxide,⁵ or rather expensive dialkyl carbonates.⁶

Use of CO₂ in carbamate synthesis is particularly attractive since CO₂ is a non-toxic, non-corrosive, inflammable, abundant and cheap C₁ source. Despite its stability, it easily combines with amines at ambient temperature and atmospheric pressure to form the corresponding carbamic acids.⁷ However, when alcohols are used as the alkyl source, the subsequent dehydrative condensation to the carbamate proceeds much less easily, partly because the reaction is equilibrium limited. As one solution, alkyl halides have been used as the electrophilic alkyl source. Even if several catalysts exist for this reaction,⁸ the co-production of HCl remains a drawback. Thus, the use of alcohols would be a major advance, since alcohols are cheap and would allow to make the process completely halogen-free.

Few reports exist on direct synthesis of carbamates from CO₂, amines and alcohols.⁹ The known catalytic systems

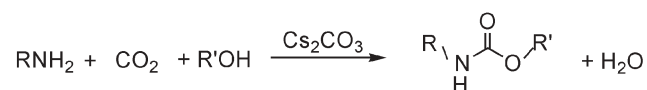
contain a homogeneous metal catalyst (Sn, Ni) and reactions are preferentially performed at very high CO₂ pressures (e.g. 30 MPa of CO₂). An excess of a dehydrating ketal is mostly used to overcome the equilibrium limitations. Even then, the only reactions reported concern sterically congested amines, such as *tert*-butylamine or cyclohexylamine. In another approach, it has been reported that 1,2-aminoalcohols react with CO₂ at 150–180 °C to form the cyclic carbamate products, either in the presence of Sn¹⁰ or Sb¹¹ or even in absence of a catalyst.¹² However, the cyclic nature of the oxazolidinone product has a decisive influence on the reaction, and the same reaction conditions fail when it is attempted to make non-cyclic carbamates.

Clearly, there is a lack of knowledge regarding the one-step production of carbamates from preferred reagents, *viz.* amines, alcohols and carbon dioxide. In the present paper we report that basic catalysts are suitable to convert a broad variety of amines and alcohols into the corresponding carbamates using carbon dioxide as a carbonyl source (Scheme 1).

Results and discussion

Catalysts for the synthesis of carbamates

In previous work, Cs⁺ compounds were shown to be very active in the catalytic activation of carbon dioxide and amines to give symmetric and asymmetric urea derivatives selectively.¹³ Therefore, we decided to investigate the activity of these catalysts for the synthesis of carbamates starting from amines, alcohols and CO₂. A series of basic catalysts were tested for two model reactions, *viz.* *n*-octylamine/*n*-PrOH and *n*-butylamine/MeOH (Table 1). In the absence of a catalyst, almost no reaction occurred and carbamate yields were negligible (entries 1 and 7). For the couple *n*-octylamine/*n*-PrOH, the selectivity to carbamate increases in going from K⁺ to Cs⁺ in the series of alkali carbonates, reaching 67% for Cs₂CO₃ after 24 h (entries 2–4). The identity of the carbamates was confirmed by GC-MS (see Experimental section). The main side-products were the corresponding symmetric urea derivatives. Note that the reactions proceed to appreciable



Scheme 1

^aCatholic University of Leuven, Centre for Surface Science and Catalysis, Kasteelpark Arenberg 23, 3001, Leuven, Belgium.

E-mail: dirk.devos@biw.kuleuven.be; Fax: 32 1632 1998;

Tel: 32 1632 1639

^bUniversity of Bucharest, Department of Catalysis, B-dul R. Elisabeta 4-12, 030016, Bucharest, Romania.

E-mail: v_parvulescu@chem.unibuc.ro; Fax: 40 2131 59249;

Tel: 40 2141 00241

Table 1 Catalytic activities of various bases for the synthesis of carbamates using CO₂^a

Entry	Catalyst	Amine	Alcohol	X ^b (%)	S _c ^c (%)	S _u ^d (%)	Y _c ^e (%)
1	—	<i>n</i> -OctNH ₂	<i>n</i> -PrOH	2	—	100	—
2	K ₂ CO ₃	<i>n</i> -OctNH ₂	<i>n</i> -PrOH	48	52	48	25
3	Rb ₂ CO ₃	<i>n</i> -OctNH ₂	<i>n</i> -PrOH	37	66	34	25
4	Cs ₂ CO ₃	<i>n</i> -OctNH ₂	<i>n</i> -PrOH	51	67	33	34
5	CsF	<i>n</i> -OctNH ₂	<i>n</i> -PrOH	57	63	37	36
6	CH ₃ COOCs	<i>n</i> -OctNH ₂	<i>n</i> -PrOH	60	46	34	28
7	—	<i>n</i> -BuNH ₂	MeOH	5	22	78	1
8	K ₂ CO ₃	<i>n</i> -BuNH ₂	MeOH	55	22	78	12
9	Rb ₂ CO ₃	<i>n</i> -BuNH ₂	MeOH	45	28	72	13
10	Cs ₂ CO ₃	<i>n</i> -BuNH ₂	MeOH	48	26	74	13
11	MgO	<i>n</i> -BuNH ₂	MeOH	4	23	77	1
12	DMAP ^f	<i>n</i> -BuNH ₂	MeOH	27	30	70	8
13	TBD ^g	<i>n</i> -BuNH ₂	MeOH	24	14	86	3
14	KF/Al ₂ O ₃	<i>n</i> -BuNH ₂	MeOH	41	24	76	10

^a Conditions: 50 mmol alcohol (molar ratio amine : alcohol = 1 : 10), 0.1 g catalyst, 200 °C, 24 h, 2.5 MPa CO₂. ^b X = amine conversion. ^c S_c = carbamate selectivity. ^d S_u = urea selectivity. ^e Y_c = carbamate yield. ^f DMAP = 4-dimethylaminopyridine. ^g TBD = 1,5,7-triazabicyclo[4.4.0]dec-5-ene.

conversion even in the absence of dehydrating agents. The conversions are also far higher than usually achieved in the synthesis of organic carbonates from alcohols and CO₂.¹⁴

Concerning the amine conversion, Cs₂CO₃ proved again to be the most active of the alkali carbonates. The counter-anions of Cs⁺ have strong effects as well. With F⁻ or CH₃COO⁻ salts, the amine conversion increases but the carbamate selectivity decreases, especially for Cs acetate (entries 5–6). Even if the couple *n*-butylamine/MeOH is considerable less reactive than *n*-octylamine/*n*-PrOH, a more than 10-fold increase of the amine conversion was observed when alkali carbonates were used as catalysts (entries 7–10). The presence of such catalysts also slightly enhances the selectivity to carbamate. Traces of alkylated amines were observed, but only when MeOH was used as the alcohol.

Other strongly basic compounds such as MgO, 4-dimethylaminopyridine (DMAP) or 1,5,7-triazabicyclo[4.4.0]dec-5-ene (TBD) generated carbamates in poor yields (entries 11–13). Employment of a heterogeneous basic catalyst such as KF/Al₂O₃ did not improve the yield of carbamate either.

Table 2 Optimization of the reaction conditions^a

Entry	T/°C	Catalyst/g	Alcohol	Amine : alcohol (molar ratio)	X ^b (%)	S _c ^c (%)	S _u ^d (%)	Y _c ^e (%)
1	170	0.1	<i>n</i> -PrOH	1 : 10	15	14	86	2
2	200	0.1	<i>n</i> -PrOH	1 : 10	51	67	33	34
3	220	0.1	<i>n</i> -PrOH	1 : 10	37	62	38	23
4	200	0.05	<i>n</i> -PrOH	1 : 10	42	28	72	12
5	200	0.15	<i>n</i> -PrOH	1 : 10	44	64	36	28
6	200	0.25	<i>n</i> -PrOH	1 : 10	48	62	38	30
7	200	0.1	<i>n</i> -PrOH	1 : 8	44	34	66	15
8	200	0.1	<i>n</i> -PrOH	1 : 15	56	79	21	44
9 ^f	200	0.1	MeOH	1 : 15	35	58	41	20
10	200	0.1	EtOH	1 : 15	51	58	42	30
11	200	0.1	<i>n</i> -BuOH	1 : 15	51	60	40	30
12	200	0.1	<i>n</i> -HexOH	1 : 15	55	72	28	42
13	200	0.1	2-PrOH	1 : 15	44	43	57	19
14	200	0.1	2-BuOH	1 : 15	55	49	51	27

^a Conditions: 50 mmol alcohol, Cs₂CO₃, 24 h, 2.5 MPa CO₂. ^b X = amine conversion. ^c S_c = carbamate selectivity. ^d S_u = urea selectivity. ^e Y_c = carbamate yield. ^f Alkylated compounds were formed as side products (~1%).

Summarizing, alkali-metal compounds seem to be the best choice for this reaction.

Reaction conditions

In order to select the optimum reaction conditions, experiments focused on the reaction temperature, time, amount of catalyst, amine to alcohol ratio and type of alcohol. Influences of the reaction temperature were investigated using the *n*-octylamine/*n*-PrOH system and Cs₂CO₃ as a catalyst. As shown in Table 2 for reactions of 24 h, a temperature of 200 °C seems the optimum to reach the highest carbamate yields (entries 1–3). Lower temperatures were unfavorable, likely because the reaction is simply too slow. At a higher temperature of 220 °C there was again a decrease of the conversion. This probably indicates that the reaction is exothermic, as was previously found for the formation of urea compounds from amines and CO₂.¹³ Hence, the equilibrium shifts to the left with increasing temperature, and the conversion decreases.

Next, the effect of the amount of the catalyst on the reaction was examined. 0.1 g of Cs₂CO₃ was found to be necessary to achieve good yields of carbamates (entry 2). This most likely corresponds to a solubility maximum of cesium carbonate in the alcoholic reaction mixture, as confirmed by further tests with a higher amount of catalyst (entries 5, 6). In the presence of a smaller amount of catalyst (*e.g.* 0.05 g) the selectivity to carbamate was quite poor (entry 4). Variation of the amine : alcohol ratio showed that a larger alcohol excess promoted the reaction (entries 2, 7, 8). Both conversion and selectivity for carbamate increased with increasing the excess of alcohol, reaching their highest values for a ratio of amine to alcohol of 1 : 15.

In order to study the influence of the alcohol type, *n*-octylamine was subjected to reactions with *n*-alcohols of varying chain length. The reactivity of the alcohols was lowest for MeOH, and increased with the alkyl chain length (entries 8–12). Clearly, as the acidity of the alcohol decreases,¹⁵ the reaction rate increases. A simple explanation is that basicity of the Cs₂CO₃ catalyst is least affected by long chain aliphatic alcohols, while it is weakened by a large excess of the more acidic methanol. In the case of reactions in methanol, this even results in formation of by-products by alkylation of

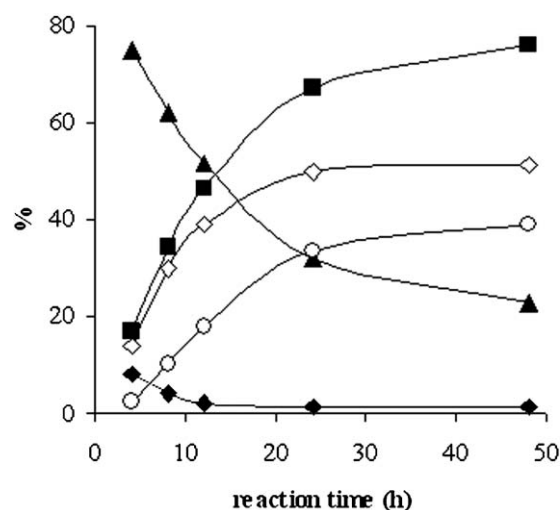


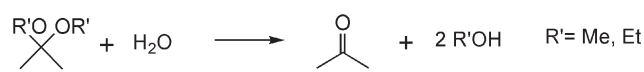
Fig. 1 Change of product distribution in time: (◇) amine conversion, (■) selectivity for carbamate, (▲) selectivity for urea derivative, (◆) isocyanate selectivity, (○) yield of carbamate. *Conditions:* 50 mmol *n*-PrOH, *n*-OctNH₂ : *n*-PrOH = 1 : 10, 0.1 g Cs₂CO₃, 200 °C, 2.5 MPa CO₂.

the amine, which is normally an acid-catalyzed reaction. The fact that a high yield is reached for *n*-hexanol is also in line with a nucleophilic substitution mechanism, and with the increased nucleophilicity of alcohols with larger alkyl substituents. Secondary alcohols are in this reaction less reactive than their primary homologs, which is ascribed to increased steric hindrance of the nucleophile's attack (entries 13, 14). Again a similar order of reactivity is observed, with 2-BuOH giving higher yields than isopropanol.

In order to follow the evolution of the product distribution in time, reactions were performed at 4, 8, 12, 24 and 48 h (Fig. 1). While in the first stage of the reaction mainly dialkylurea is formed, the selectivity shifts towards the formation of carbamate for longer reaction times. The isocyanate is initially detected in small concentration as well, but its concentration becomes negligible after 24 h. While the carbamate selectivity increases continuously, the conversion reaches a maximum value at 24 h. A further increase of the reaction time to 48 h produced no change in conversion, while the selectivity and yield of carbamate marginally increased.

Reaction scope

With the best conditions in hand, other carbamates were successfully synthesized in considerable yields as shown in



Scheme 2

Table 3. Experiments performed at different amine : alcohol ratios reconfirmed the necessity of a high alcohol excess in the reaction mixture to achieve good yields of carbamates (entries 2–4). Compared with the *n*-amines, internal amines such as 2-heptylamine reacted more selectively, most probably due to the steric hindrance. However, they were considerably less reactive than the linear amines (entries 5–7).

Reactions in the presence of a dehydrating agent

As the carbamate formation produces water,⁹ it can be attempted to shift the equilibrium of the reaction to the right by withdrawing water from the medium. Besides, an excess of water could also cause catalyst deactivation. Acetals such as dimethoxypropane (DMP) or diethoxypropane (DEP), molecular sieves and urea were used as dehydrating agents to selectively remove water from the reaction system. Acetals react with water to produce a ketone and two alcohols (Scheme 2).

The influence of the dehydrating agents on the catalytic performance is shown in Table 4. The acetals bring about a significant increase of the amine conversion and of the carbamate yield (compare Table 4, entries 2, 3 with Table 4, entry 1 and Table 2, entry 10). A clear disadvantage, however, is that imines are formed from the side reaction between acetone and the amines. Moreover, in the presence of the basic catalysts, a series of other side-products is formed from acetone, such as mesityl oxide, isophorone and 4-methoxy-4-methyl-2-pentanone.

Since zeolites have a well known water absorption capacity, and since potassium salts catalyze the reaction, commercially available K-zeolites such as molecular sieves 3A and L were tested as dehydrating agents. In each case, the reactions were compared to those catalysed by alkali carbonates in absence of a zeolite. Unfortunately, both conversion and selectivity of carbamate decreased upon zeolite addition (Table 4), probably because part of the Cs⁺ or Rb⁺ ions were exchanged on the molecular sieves. On the other hand, one may expect that the uptake of water by these sieves is limited at the reaction temperature of 200 °C. Much better results were obtained in the presence of urea, with a 69% yield of propyl *N*-octyl-carbamate (Table 4, entry 8). However, further tests performed in nitrogen instead of carbon dioxide atmosphere revealed that

Table 3 Synthesis of other carbamates^a

Entry	Amine	Alcohol	Amine : alcohol (molar ratio)	X ^b (%)	S _c ^c (%)	S _u ^d (%)	Y _c ^e (%)
1	<i>n</i> -BuNH ₂	<i>n</i> -PrOH	1 : 15	40	50	50	20
2	<i>n</i> -HexNH ₂	<i>n</i> -PrOH	1 : 8	38	37	63	14
3	<i>n</i> -HexNH ₂	<i>n</i> -PrOH	1 : 10	45	43	57	19
4	<i>n</i> -HexNH ₂	<i>n</i> -PrOH	1 : 15	51	61	39	31
5	2-HeptNH ₂	<i>n</i> -PrOH	1 : 10	26	70	30	18
6	2-HeptNH ₂	<i>n</i> -PrOH	1 : 15	31	73	27	23
7	2-OctNH ₂	<i>n</i> -PrOH	1 : 15	30	76	24	23

^a *Conditions:* 50 mmol alcohol, 0.1 g Cs₂CO₃, 24 h, 200 °C, 2.5 MPa CO₂. ^b X = amine conversion. ^c S_c = carbamate selectivity. ^d S_u = urea selectivity. ^e Y_c = carbamate yield.

Table 4 Influence of dehydrating agents on carbamate formation^a

Entry	Amine	Alcohol	Amine : alcohol (molar ratio)	Catalyst/g	Dehydrating agent/g	X ^b (%)	S _c ^c (%)	S _u ^d (%)	Y _c ^e (%)
1	<i>n</i> -OctNH ₂	MeOH	1 : 10	Cs ₂ CO ₃ (0.1)	—	56	30	70	17
2	<i>n</i> -OctNH ₂	MeOH	1 : 10	Cs ₂ CO ₃ (0.1)	DMP	68	37	14	25
3	<i>n</i> -OctNH ₂	EtOH	1 : 15	Cs ₂ CO ₃ (0.1)	DEP	82	56	5	46
4	<i>n</i> -OctNH ₂	<i>n</i> -PrOH	1 : 15	Cs ₂ CO ₃ (0.25)	3A (0.2) ^f	57	60	40	34
5	<i>n</i> -OctNH ₂	<i>n</i> -PrOH	1 : 15	Rb ₂ CO ₃ (0.25)	—	64	67	33	43
6	<i>n</i> -OctNH ₂	<i>n</i> -PrOH	1 : 15	Rb ₂ CO ₃ (0.25)	3A (0.2) ^f	47	57	43	27
7	<i>n</i> -OctNH ₂	<i>n</i> -PrOH	1 : 15	Rb ₂ CO ₃ (0.25)	L (0.2) ^g	63	64	36	40
8	<i>n</i> -OctNH ₂	<i>n</i> -PrOH	1 : 15	Cs ₂ CO ₃ (0.1)	Urea ^h	82	84	16	69

^a Conditions: 50 mmol alcohol, molar ratio amine : DMP/DEP = 1 : 2, 24 h, 200 °C, 2.5 MPa CO₂. ^b X = amine conversion. ^c S_c = carbamate selectivity. ^d S_u = urea selectivity. ^e Y_c = carbamate yield. ^f Zeolite 3A in the K-form. ^g Zeolite L in the K-form. ^h 3.3 mmol urea.

Table 5 Synthesis of carbamates from sterically hindered amines (*t*-BuNH₂)^a

Entry	Catalyst/g	Alcohol	<i>t</i> -BuNH ₂ : alcohol (molar ratio)	Dehydrating agent	t/h	X ^b (%)	S _c ^c (%)	Y _c ^d (%)
1	0.1	MeOH	1 : 10	—	24	4	>99	4
2	—	MeOH	1 : 10	DMP	24	—	—	—
3	0.1	MeOH	1 : 10	DMP	24	36	>99	36
4	0.25	MeOH	1 : 10	DMP	24	47	>99	47
5	0.25	EtOH	1 : 10	DEP	24	52	>99	52
6	0.25	EtOH	1 : 10	DEP	48	62	>99	62
7	0.25	EtOH	1 : 11.5	DEP	48	71	>99	71
8	0.25	EtOH	1 : 15	DEP	48	68	>99	68
9	0.25	EtOH	1 : 11.5	DEP + 3A ^e	48	64	>99	64
10	0.25	EtOH	1 : 11.5	Urea	24	37	90	33
11 ^f	0.25	EtOH	1 : 11.5	Urea	24	33	90	30
12 ^g	0.25	<i>t</i> -BuOH	1 : 10	—	24	28	54	15

^a Conditions: 50 mmol alcohol, 10 mmol DMP/DEP or 5 mmol urea, Cs₂CO₃ as catalyst, 200 °C, 2.5 MPa CO₂. ^b X = amine conversion. ^c S_c = carbamate selectivity. ^d Y_c = carbamate yield. ^e 0.2 g zeolite 3A (K-form). ^f N₂ instead of CO₂. ^g Selectivity of urea derivative = 28%, yield of urea = 8%.

rather than CO₂, urea is employed as the carbonyl source in this case.

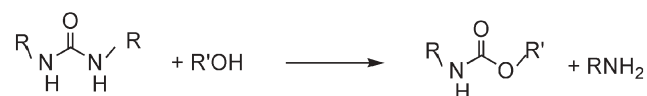
The use of dehydrating agents appeared particularly effective when sterically hindered amines were used as starting compounds for the carbamate synthesis. As an example, *tert*-butylamine was investigated (Table 5). No reaction took place in the absence of a catalyst (entry 2). Using cesium carbonate as a catalyst, and in the absence of a dehydrating agent, the amine conversion was very poor, even if the carbamate was almost exclusively obtained (entry 1). With Cs₂CO₃ and the DMP dehydrating agent combined, a dramatic increase in conversion was observed, with preservation of the >99% carbamate selectivity (entry 3). A higher amount of catalyst produced higher yields of carbamate (entry 4). This was expected since the total reaction volume has increased due to the presence of acetals; hence a higher amount of catalyst can be solubilized in the reaction mixture. In the presence of methanol, traces (<1%) of alkylated compounds and urea were occasionally observed. Side products derived from acetone such as mesityl oxide were also present. In agreement with the results obtained for the linear amines, the EtOH/DEP couple proved to be slightly more effective than the MeOH/DMP system (entry 5).

While in reactions without dehydrating agent a ceiling conversion is attained after 24 h due to the presence of water (see Fig. 1), this is not the case when DMP or DEP are added, as water is efficiently eliminated from the reaction mixture. By allowing the reaction to proceed for 48 h and by adjusting the

amine : alcohol ratio, a 71% yield in carbamate was attained with Cs₂CO₃ in 48 h using only 2.5 MPa of carbon dioxide (entries 6–8). A combination of acetals with molecular sieves did not further improve the carbamate yield (entry 9). *t*-BuNH₂ reacts selectively and in acceptable yield when urea is used instead of an acetal, but it was again proven that urea itself, rather than CO₂, is the source of the inserted carbonyl group (entries 10 and 11).

Mechanism of carbamate formation over Cs catalysts

As can be observed from Fig. 1, mainly dialkylurea is formed in the first stage of the reaction of *n*-alkylamines. Indeed, the urea formation is much faster in comparison with the reaction of an alcohol, amine and carbon dioxide towards a carbamate.¹³ The strong initial increase in conversion is mainly due to urea formation. The decrease of urea selectivity with time and the increase of carbamate selectivity suggest that the carbamates may be produced *via* urea alcoholysis, with the amine as a coproduct (Scheme 3). The sharp dependence of carbamate selectivity on the concentration of the base catalyst suggests that the alcoholysis step is speeded up by the base (Table 2, entries 4 vs. 5). In order to gather more information

**Scheme 3**

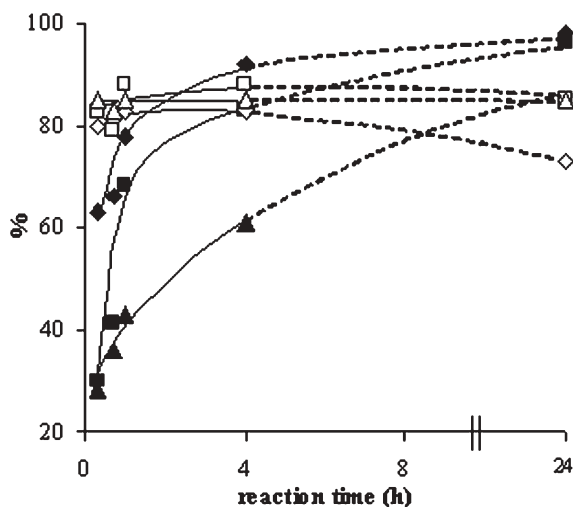
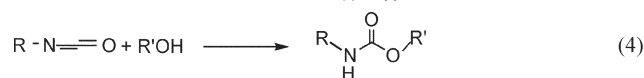
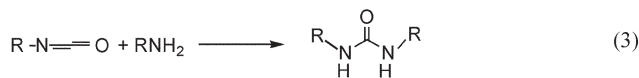
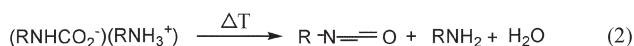


Fig. 2 *N,N'*-Dibutylurea (DBU) alcoholysis with *n*-PrOH: (◆) conversion and (◇) carbamate selectivity when 0.125 mmol DBU were used, (■) conversion and (□) carbamate selectivity when 0.25 mmol DBU were used, (▲) conversion and (△) carbamate selectivity when 0.375 mmol DBU were used. Other conditions: 50 mmol *n*-PrOH, 0.1 g Cs₂CO₃, 200 °C, 2.5 MPa CO₂.

concerning this reaction pathway, the alcoholysis of *N,N'*-dibutylurea (DBU) with *n*-PrOH was conducted under the same experimental conditions as the initial reaction. Tests were performed at various reaction times and at DBU concentrations corresponding to 5, 10 and 15% conversion of amine in the initial reaction. The data presented in Fig. 2 suggest that indeed *N,N'*-dialkylureas are gradually transformed into the corresponding carbamates. The main by-product detected was *n*-propyl butyrate. Although this compound was formed in significant amounts in the *N,N'*-dibutylurea alcoholysis, only traces of this product were observed in the reaction of *n*-BuNH₂, *n*-PrOH and carbon dioxide.

A second possibility for carbamate formation is that in the high-temperature reaction conditions, the unstable carbamic acid undergoes a thermal dehydration to form the corresponding isocyanate (Scheme 4, eqn (2)), which can further condense with an alcohol or an amine (Scheme 4, eqn (3) and (4)) to form the carbamate or urea derivative respectively. Evidence for this mechanism is supplied by the presence of small amounts of isocyanates in the reaction mixtures, particularly at short reaction times (see Fig. 1). An isocyanate pathway could also explain the lack of reactivity of secondary amines. Isocyanates may well intervene at several places in the reaction



Scheme 4

network, since they have also been proposed as intermediates in urea alcoholysis.¹⁶

While evidence for both routes is available for *n*-alkylamines, the mechanism is less clear for *t*-BuNH₂. The urea alcoholysis pathway is improbable for a sterically hindered amine such as *t*-BuNH₂. It has indeed been demonstrated that the base-catalyzed urea formation from *t*-BuNH₂ is poorly effective;¹³ in the present experiments (Table 5), the *N,N'*-di-*tert*-butylurea is only detected in trace amounts, except in the reaction of *t*-BuNH₂ with *t*-BuOH, where it was formed in 8% yield (Table 5, entry 12).

Remarkably, isocyanate concentrations were below the detection limit in the reactions of *t*-BuNH₂ with various alcohols. For these reactions, indirect evidence for an isocyanate route comes from the strong promotion of the carbamate formation by the addition of an acetal (Table 5, entries 1 vs. 3); indeed, the formation of the isocyanate is a dehydration. The reaction of *t*-BuNH₂ with *t*-BuOH was the only reaction of *t*-BuNH₂ that gave an appreciable carbamate yield even in the absence of a dehydrating agent (Table 5, entry 12 vs. entry 1); this may well be ascribed to the high reactivity of *t*-BuOH.

In conclusion, there are two, most probably parallel routes that lead to carbamates using this catalytic system, either *via* ureas or *via* isocyanates. Their relative importance likely depends on the amine structure.

Conclusions

In summary, this is the first systematic study proving that basic catalysts can promote the transformation of a large variety of amines and alcohols into carbamates in appreciable yields. The most active among the catalysts tested were Cs₂CO₃ and Rb₂CO₃. The proposed catalytic system was able to convert both linear and branched aliphatic amines to their corresponding carbamates in mild reaction conditions (*i.e.* 2.5 MPa CO₂), even in the absence of dehydrating agents. Only when a sterically hindered amine such as *tert*-butylamine was involved, a dehydrating agent was necessary. Mechanistic investigations revealed two main pathways for carbamate formation, *viz.* a direct pathway with isocyanates as reaction intermediates, and an indirect one *via* urea alcoholysis.

Experimental

All reactions were conducted under pressurized CO₂ in small stainless steel autoclaves (10 ml inner volume). In a typical experiment, the amine (5 mmol), alcohol (50 mmol) and the catalyst (0.1 g) were charged in the reactor, which was then saturated with CO₂ under a pressure of 2.5 MPa at room temperature. The mixture was magnetically stirred and heated to 170–220 °C in a temperature-controlled electrical heater for 4–48 h. After heating, the reactor was cooled to room temperature (0 °C in the case of the more volatile amines) and carefully depressurized. The liquid reaction mixture was diluted in MeOH and analyzed with a Shimadzu 2014 gas chromatograph (flame ionization detector) with CP-Sil5 CB capillary column (50 m × 0.25 μm). The reaction products were identified by GC-MS using an Agilent 5973 Network

Mass Selective Detector coupled to an Agilent 6890N GC with HP5MS capillary column (30 m × 0.25 mm). The reaction products could easily be separated from the catalyst by extraction with ethyl acetate from an aqueous solution of the reaction mixture. For product isolation, the reaction mixture was poured into distilled water (8 ml) and then extracted thrice with 6 ml ethyl acetate. The GC analysis of both organic and water phases after extraction confirmed the complete uptake of the carbamate by the organic layer. For urea alcoholysis, *N,N'*-dibutylurea (0.125–0.375 mmol), *n*-PrOH (50 mmol) and Cs₂CO₃ (0.1 g) were charged in the reactor after which the same procedure as for the initial reaction was applied. Spectroscopic data for the synthesized carbamates are given below.

Methyl *N*-butylcarbamate

GC-MS, *m/z*: 57 (10%), 88 (100), 102 (3), 116 (3), 131 (8).

Methyl *N*-octylcarbamate

GC-MS, *m/z*: 59 (10%), 76 (19), 88 (100), 116 (4), 130 (4), 144 (3), 172 (3), 187 (4).

Ethyl *N*-octylcarbamate

GC-MS, *m/z*: 57 (14%), 71 (6), 85 (8), 99 (24), 116 (2), 130 (3), 144 (2), 172 (8), 201 (2).

Propyl *N*-octylcarbamate

GC-MS, *m/z*: 57 (16%), 71 (9), 85 (5), 99 (12), 113 (2), 116 (100), 130 (5), 144 (3), 158 (5), 172 (18), 186 (1), 215 (5).

Isopropyl *N*-octylcarbamate

GC-MS, *m/z*: 57 (46%), 74 (45), 116 (100), 130 (7), 144 (3), 172 (26), 200 (1), 215 (3).

Butyl *N*-octylcarbamate

GC-MS, *m/z*: 57 (100%), 74 (28), 118 (17), 130 (83), 174 (30), 186 (4), 229 (6).

2-Butyl *N*-octylcarbamate

GC-MS, *m/z*: 57 (100%), 130 (21), 156 (14), 174 (30), 200 (1), 214 (1), 229 (2).

Hexyl *N*-octylcarbamate

GC-MS, *m/z*: 57 (46%), 74 (30), 85 (26), 116 (6), 130 (6), 158 (40), 174 (100), 186 (3), 200 (3), 214 (2), 257 (2).

Propyl *N*-hexylcarbamate

GC-MS, *m/z*: 57 (6%), 85 (11), 99 (4), 116 (100), 144 (13), 158 (4), 172 (1), 187 (7).

Propyl *N*-(2 heptyl)carbamate

GC-MS, *m/z*: 57 (18%), 70 (14), 88 (9), 99 (7), 113 (8), 130 (100), 186 (3).

Methyl *N*-*tert*-butylcarbamate

GC-MS, *m/z*: 57 (37%), 72 (24), 84 (21), 116 (100), 131 (1).

Hexyl isocyanate

GC-MS, *m/z*: 56 (100%), 69 (12), 85 (32), 99 (100), 112 (20).

Ethyl *N*-*tert*-butylcarbamate

GC-MS, *m/z*: 58 (100%), 86 (11), 130 (64), 145 (1).

Butyl isocyanate

GC-MS, *m/z*: 56 (100%), 70 (16), 98 (26).

Octyl isocyanate

GC-MS, *m/z*: 56 (55%), 70 (30), 85 (31), 99 (100), 113 (31), 126 (14), 140 (3), 154 (3).

Acknowledgements

Angelica Ion is grateful to the K.U. Leuven Research Fund for a doctoral fellowship. The authors appreciate funding of this work in the frame of a Bilateral Agreement Flanders/Romania and of IAP, GOA and CECAT projects.

References

- 1 I. Omae, *Catal. Today*, 2006, **115**, 33.
- 2 M. Shi and Y. Shen, *Curr. Org. Chem.*, 2003, **7**, 737.
- 3 R. Srivastava, M. D. Manju, D. Srinivas and P. Ratnasamy, *Catal. Lett.*, 2004, **97**, 41.
- 4 *Ullmann's Encyclopedia of Industrial Chemistry*, 6th edn, electronic version, 2000.
- 5 (a) F. Shi, J. Peng and Y. Deng, *J. Catal.*, 2003, **219**, 372; (b) B. Chen and S. S. C. Chuang, *J. Mol. Catal. A: Chem.*, 2003, **195**, 37; (c) B. Chen and S. S. C. Chuang, *Green Chem.*, 2003, **5**, 484.
- 6 (a) Z. H. Fu and Y. Ono, *J. Mol. Catal.*, 1994, **91**, 399; (b) S. Carloni, D. De Vos, P. A. Jacobs, R. Maggi, G. Sartori and R. Sartorio, *J. Catal.*, 2002, **205**, 199; (c) N. Katada, H. Fujinaga, Y. Nakamura, K. Okumura, K. Nishigaki and M. Niwa, *Catal. Lett.*, 2002, **80**, 47.
- 7 E. M. Hampe and D. M. Rudkevich, *Tetrahedron*, 2003, **59**, 9619.
- 8 (a) R. N. Salvatore, F. Chu, A. S. Nagle, E. A. Kapxhiu, R. M. Cross and K. W. Jung, *Tetrahedron*, 2002, **58**, 3329; (b) W. D. McGhee, Y. Pan and D. P. Riley, *J. Chem. Soc., Chem. Commun.*, 1994, 699; (c) M. Yoshida, N. Hara and S. Okuyama, *Chem. Commun.*, 2000, 151; (d) R. Srivastava, D. Srinivas and P. Ratnasamy, *J. Catal.*, 2005, **233**, 1.
- 9 (a) M. Abla, J. C. Choi and T. Sakakura, *Chem. Commun.*, 2001, 2238; (b) M. Abla, J. C. Choi and T. Sakakura, *Green Chem.*, 2004, **6**, 524.
- 10 K.-I. Tominaga and Y. Sasaki, *Synlett*, 2002, **2**, 307.
- 11 R. Nomura, M. Yamamoto and H. Matsuda, *Ind. Eng. Chem. Res.*, 1987, **26**, 1056.
- 12 B. M. Bhanage, S. Fujita, Y. Ikushima and M. Arai, *Green Chem.*, 2003, **5**, 340.
- 13 A. Ion, V. Parvulescu, P. Jacobs and D. De Vos, *Green Chem.*, 2007, **9**, 158.
- 14 (a) T. Sakakura, J. Choi, Y. Saito and T. Sako, *Polyhedron*, 1999, **19**, 573; (b) C. Jiang, Y. Guo, C. Wang, C. Hu, Y. Wu and E. Wang, *Appl. Catal., A*, 2003, **256**, 203; (c) M. Aresta, A. Dibenedetto, C. Pastore, I. Papai and G. Schubert, *Top. Catal.*, 2006, **40**, 71.
- 15 (a) W. M. Olmstead, Z. Margolin and F. G. Bordwell, *J. Org. Chem.*, 1980, **45**, 3295; (b) W. L. Mock and J. Z. Zhang, *Tetrahedron Lett.*, 1990, **31**, 5687.
- 16 Q. Li, N. Zhao, W. Wei and Y. Sun, *J. Mol. Catal.*, 2007, **270**, 44.

Ionic liquid effects on the activity of monooxygenase P450 BM-3

Kang Lan Tee,^a Danilo Roccatano,^a Stefan Stolte,^b Jürgen Arning,^b Bernd Jastorff^b and Ulrich Schwaneberg^{*c}

Received 24th September 2007, Accepted 1st November 2007

First published as an Advance Article on the web 20th November 2007

DOI: 10.1039/b714674d

P450 monooxygenases oxidize a broad range of substrates including fatty acids, alcohols, aliphatic and aromatic hydrocarbons which are often poorly soluble in water and have K_m values in the millimolar range. Cosolvent and host–guest chemistry have thus been supplemented to increase catalytic efficiencies. Ionic liquids are alternative solvents and cosolvents in biocatalysis and have received an escalating interest due to unique properties such as tunable hydrophobicity and hydrophilicity. Effects of ten ionic liquids on cytochrome P450 BM-3 activity were investigated by evaluating the influence of hydrophobicity and ion pairs on P450 BM-3. Investigated ionic liquids comprised a range of four anions, four 1-alkyl-3-methylimidazolium derivatives differing in hydrophobic chain length, two altered head groups (pyridinium and pyrrolidinium) and an additional functional group in the side chain (nitrile). Results indicate that varying the chain length of the 1-alkyl-3-methylimidazolium has apparent effects on the resistance of P450 BM-3 (based on EC_{50}), with increasing inhibition in the order of EMIM Cl (232 ± 8) > BMIM Cl (148 ± 5) > HMIM Cl (32 ± 2) > OMIM Cl (9 ± 1).

Introduction

Ionic liquids have received increasing attention in recent years as alternative solvents in biocatalysis.^{1–4} These studies were performed on isolated/immobilized enzymes or whole cell systems, in biphasic or homogenous ionic liquid–water mixtures and pure ionic liquids.^{2,5–7} Stability, activity and enantioselectivity were altered through the use of ionic liquids for enzyme classes such as hydrolases (lipase,^{5,8} esterase⁶ and protease⁹) and oxidoreductases (formate dehydrogenase,¹⁰ horseradish peroxidase¹¹ and cytochrome *c*¹²). Research on biocatalysis in ionic liquids is driven by solubility properties, low vapor pressure, and high thermal stability of ionic liquids which lead to lower inhalatory exposure and non-flammability. The latter are important considerations in large-scale industrial processes.

Cytochrome P450s are oxidoreductases and form a ubiquitous enzyme family which plays key roles in biochemical pathways, xenobiotic metabolism and detoxification. Cytochrome P450s can hydroxylate or epoxidize substrates by inserting a single oxygen molecule from oxygen into an organic compound.^{13–15} These oxygenation reactions are often difficult to achieve through organic syntheses, especially when regio- or stereoselective oxygenation at ambient temperature, using oxygen as oxidant is required. P450 monooxygenases are attractive industrial biocatalysts due to their selectivity and wide spectrum of substrates accepted (alkanes, alkenes,

alcohols, fatty acids, amides, polyaromatic hydrocarbons and heterocyclics).^{16–19} However hydrophobic substrates of P450s often have K_m values in the millimolar range thus requiring the use of organic solvents or cosolvents for efficient biotransformations. P450 enzymes often cannot tolerate required amounts of organic solvents or cosolvents.^{20,21}

P450 BM-3 is one of the most well-studied and industrially important P450 enzymes (structure,^{22–24} catalytic efficiency^{18,25} and substrate specificity^{16,26}) due to its robustness and design as a single component system (reductase and heme domain being fused on a single polypeptide²⁷). Ionic liquids represent an alternative to solvents and cosolvents for industrial important P450 BM-3 substrates such as fatty acids, alcohols, aliphatic and aromatic hydrocarbons which are known to be totally or partially miscible with ionic liquids.^{28–30} The influence of ionic liquids has barely been studied for cytochrome P450s, and only one report for a multi-component system (CYP3A4) has been published.³¹ There have been no reports on the study of ionic liquid effects on enzymatic activity for single component P450 monooxygenases.

In this study, effects of ionic liquids and their hydrophobic side chains on P450 BM-3 activity are quantified. First hypotheses on inhibitory influences are further generated by measuring the OMIM Cl resistance of P450 BM-3 mutant F87A, in which the F87A substitution decreases tolerance of P450 BM-3 towards organic solvents.²¹

Results

The pNCA (*p*-nitrophenoxycarboxylic acid) assay³² was used to determine the activity of P450 BM-3 under the influence of ionic liquids using *p*-nitrophenoxydodecanoic acid (12-pNCA) as substrate. The pH remained stable under assay conditions. Concentration range of ten ionic liquids as well as calculated

^aJacobs University, School of Engineering and Science, Campus Ring 8, 28759, Bremen, Germany

^bUFT - Center for Environmental Research and Environmental Technology, Leobenerstr., 28359, Bremen, Germany

^cAssociate Professor of Biochemical Engineering, Jacobs University Bremen, Campus Ring 1, 28759, Bremen, Germany.

E-mail: u.schwaneberg@jacobs-university.de; Fax: +49 (421) 200 3640; Tel: +49 (421) 200 3543

Table 1 Compounds, abbreviations, concentrations of ionic liquids used for P450 BM-3 activity measurements and calculated EC_{50} values of ionic liquids employed in inhibitory studies of P450 BM-3. All parameters were determined from triplicate measurements

Compound	Abbreviation	Concentration range/mM	EC_{50}^a /mM
1-Ethyl-3-methylimidazolium chloride	EMIM Cl	0–420	232 ± 8
1-Ethyl-3-methylimidazolium trifluoromethanesulfonate	EMIM CF_3SO_3	0–180	94 ± 6
1-Ethyl-3-methylimidazolium trifluoroacetate	EMIM CF_3COO	0–180	72 ± 3
1-Ethyl-3-methylimidazolium tetrafluoroborate	EMIM BF_4	0–100	42 ± 3
1-Butylpyridinium chloride	Bpy Cl	0–264	195 ± 9
1-Cyanomethyl-3-methylimidazolium chloride	1M11CN Cl	0–360	182 ± 8
1-Butyl-1-methylpyrrolidinium chloride	BMPyr Cl	0–300	175 ± 8
1-Butyl-3-methylimidazolium chloride	BMIM Cl	0–240	148 ± 5
1-Hexyl-3-methylimidazolium chloride	HMIM Cl	0–72	32 ± 2
1-Octyl-3-methylimidazolium chloride	OMIM Cl	0–15	9 ± 1
Sodium chloride	NaCl	0–600	202 ± 9
Sodium trifluoromethanesulfonate	$NaCF_3SO_3$	0–300	166 ± 8
Sodium trifluoroacetate	$NaCF_3COO$	0–360	162 ± 7
Sodium tetrafluoroborate	$NaBF_4$	0–360	119 ± 8

^a EC_{50} values determined based on triplicate measurements (confidence intervals $\alpha = 0.025$)

EC_{50} values are listed in Table 1. The statistical calculations for EC_{50} were performed using software library drfit for the R language and environment.³³ The tolerance of P450 BM-3 towards the investigated ionic liquids varies between EC_{50} values of 9 and 232 mM. Among the ten ionic liquids, P450 BM-3 has the highest tolerance towards EMIM Cl ($EC_{50} = 232 \pm 8$ mM) and the least tolerance towards OMIM Cl ($EC_{50} = 9 \pm 1$ mM).

Effect of the anions and EMIM cation on P450 BM-3 activity

The EC_{50} values of EMIM with different anions (Cl^- , $CF_3SO_3^-$, CF_3COO^- and BF_4^-) show that P450 BM-3 has the lowest tolerance towards EMIM BF_4 . The residual activities for each anion are normalized to the activity when no ionic liquid is added and are shown in Fig. 1. It can be observed from Fig. 1 that EMIM Cl has a visibly lower inhibitory effect compared to the other EMIM anions.

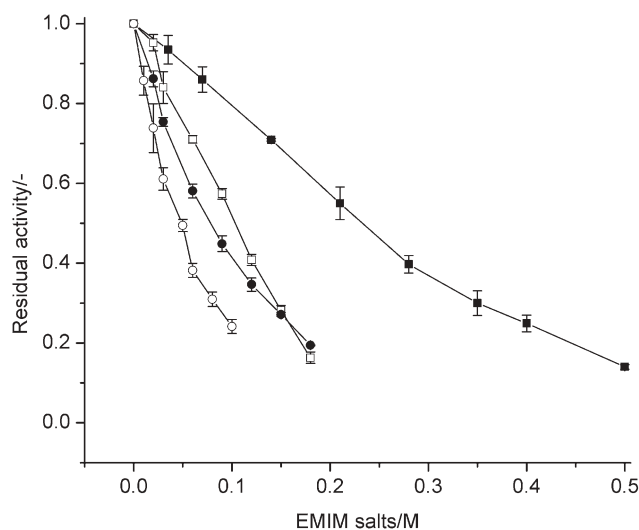


Fig. 1 Residual activities of P450 BM-3 in presence of EMIM and anions (Cl^- , $CF_3SO_3^-$, CF_3COO^- , BF_4^-). Residual activity is given as ratio of initial catalytic turnover number in the presence of ionic liquids to that in the absence of ionic liquids. —■—: EMIM Cl; —□—: EMIM CF_3SO_3 ; —●—: EMIM CF_3COO ; —○—: EMIM BF_4 .

Inhibition is also reflected by the absolute decrease of EC_{50} from EMIM Cl to EMIM CF_3SO_3 , which is at least 2.7-fold higher than any difference between the three other investigated EMIM salts (EMIM CF_3SO_3 , EMIM CF_3COO and EMIM BF_4). In fact Fig. 1 shows that the order of inhibition for EMIM CF_3SO_3 and EMIM CF_3COO changes around 150 mM suggesting very similar inhibitions by these two ionic liquids.

The Na^+ salts of the above four anions (Cl^- , $CF_3SO_3^-$, CF_3COO^- and BF_4^-) show lower inhibitory influences than the corresponding EMIM salts except NaCl (EC_{50} value 0.9-fold of the EMIM Cl). These results suggest that reduced activity of P450 BM-3 can mainly be attributed to an anion effect. Differences in the extend of inhibition indicate that inhibitory differences between the Na^+ and EMIM salts are not solely due to an anion effect, but rather depend on EMIM and Na^+ counter ion effects on corresponding anions.

As the chloride anion has the lowest inhibition among the tested anion, it was used as the counter ion for all subsequent tests on ionic liquids with different cations.

Effect of the alkyl-chain length of EMIM cations on P450 BM-3 activity

Effects of alkyl chain length for the imidazolium cation were investigated by using 1-alkyl-3-methylimidazolium chlorides in which the alkyl-chain at one N-atom was stepwise elongated from ethyl- (C_2) to octyl- (C_8). Fig. 2 shows a decreasing tolerance of P450 BM-3 with stepwise increased alkyl chain length. From the EC_{50} values in Table 1, the tolerance of P450 BM-3 towards OMIM Cl is almost 20-fold lower than EMIM Cl. Fig. 2 and EC_{50} values in Table 1 show a clear increase in inhibition in accordance to alkyl-chain elongations from C_2 to C_8 .

Effect of cation aromaticity, size and free electron pair in alkyl-chain of imidazolium cation

Three other cationic structures were investigated: Bpy Cl, BMPyr Cl and 1M11CN Cl. The resulted EC_{50} are in between EMIM Cl and BMIM Cl. Bpy Cl has a pyridinium head group which is larger compared to the imidazolium head group

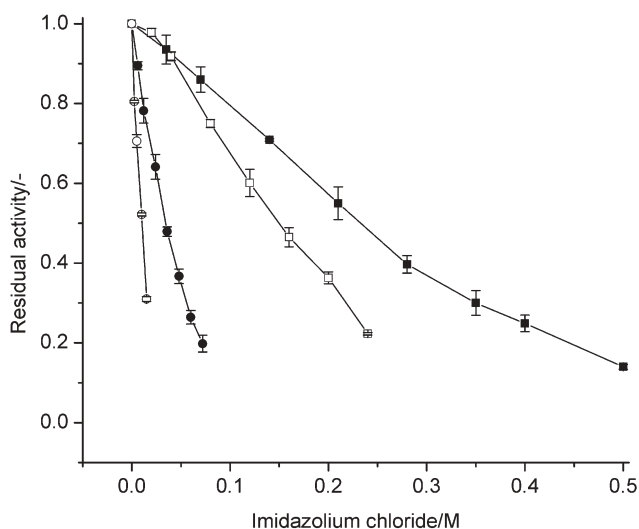


Fig. 2 Effect of hydrophobic side chain of 1-alkyl-3-methylimidazolium on residual activities of P450 BM-3. Residual activity is given as ratio of initial catalytic turnover number in the presence of ionic liquids to that in the absence of ionic liquids. —■—: EMIM Cl; —□—: BMIM Cl; —●—: HMIM Cl; —○—: OMIM Cl.

(six- compared to five-membered ring). However this does not seem to have large effects on the inhibition ($EC_{50} \sim 1.3$ -fold of BMIM Cl) and EC_{50} remains lower than EMIM Cl. BMPyr Cl has a side chain on its cation which is the same as BMIM, but unlike the imidazolium (BMIM) head group, the pyrrolidinium (BMPyrH) head group does not have an aromatic ring system. Aromaticity however has only a minor effect on the inhibition. The BMPyr Cl EC_{50} value is ~ 1.2 -fold higher than that of BMIM Cl (Table 1). The side chain carrying the nitrile functional group on IM11CN Cl has a chain length that is in between EMIM and BMIM. Differing from the alkyl imidazolium side chains, a polar nitrile functional group was introduced. Possible electrostatic interactions have however no notable influence on P450 BM-3 inhibition (EC_{50} for IM11CN Cl lies between EMIM Cl and BMIM Cl).

k_{cat} and K_m values for P450 BM-3 in ionic liquid–water mixture

As seen in Table 1 and Fig. 2, the effect of the length of side chain has an apparent influence on the inhibition of P450 BM-3. For further insight, the kinetic parameters of the

P450 BM-3 hydroxylation of 12-pNCA were determined in the presence of the imidazolium chlorides (Table 2). For each of the 1-alkyl-3-methylimidazolium chlorides (BMIM Cl, HMIM Cl and OMIM Cl), the amount of ionic liquid equivalent to the EC_{50} concentration was employed. In all three ionic liquids a lower k_{cat} and a higher K_m was obtained which led to a 4.0–4.6-fold lower catalytic efficiency (k_{cat}/K_m) when compared to the P450 BM-3 activity in no ionic liquid. In detail, the k_{cat} was reduced to 0.50–0.62-fold while the K_m increased 2.0–2.6-fold. Kinetic constants (k_{cat} , K_m , K_i) were calculated by assuming mixed inhibition kinetics of P450 BM-3 (Table 2). Table 2 shows that K_i decreases 18-fold as the side chain length increases from BMIM to OMIM. Changes in K_i suggest that the increasing inhibition as side chain length increases can be attributed to a stronger association of the ionic liquid to P450 BM-3. Increasing from BMIM Cl to HMIM Cl shows largest decrease in K_i (5.6-fold) and EC_{50} values (4.6-fold) when comparing 1-alkyl-3-methylimidazolium from C₄ to C₈.

Role of amino acid position 87 in P450 BM-3 ionic liquid tolerance

The amino acid residue phenylalanine 87 is important for the organic solvent resistance of P450 BM-3. Mutating this residue to alanine resulted in a significant drop in resistance of P450 BM-3 towards DMSO, THF, ethanol and acetonitrile.²¹ The catalytic efficiency of P450 BM-3 F87A mutant in the presence of OMIM Cl decreased 35-fold compared to when no ionic liquid was added, which is significantly larger than the 4.3-fold decrease observed in wildtype P450 BM-3 (see Table 2). The change in K_m is of the same order of magnitude between the wildtype and F87A mutant while the major contributor of this drastic difference in catalytic efficiency is the 12.5-fold decrease in k_{cat} in F87A compared to the 1.6-fold decrease seen in the wildtype. A lower K_i is also observed suggesting better association of OMIM Cl in F87A mutant compared to the wildtype.

NADPH consumption and P450 spectra using ionic liquids as substrate

The NADPH consumption assay was used to investigate the possibility of the ionic liquids being substrates of P450 BM-3, particularly the long chain 1-alkyl-3-methylimidazolium.

Table 2 Effect of 1-alkyl-3-methylimidazolium chlorides on the kinetic parameters (k_{cat} , K_m , K_i) of P450 BM-3 wildtype and mutant F87A. All parameters were determined from triplicate measurements

Inhibitor	Inhibitor added/mM	k_{cat}/min^{-1}	$K_m/\mu\text{M}$	K_{cat}/K_m	k_{cat} ratio ^a	K_m ratio ^a	K_i^b/mM
Wild type							
No inhibitor	0	136.6 ± 2.6	2.8 ± 0.3	48.8	—	—	—
BMIM Cl	148	68.2 ± 0.7	5.6 ± 0.3	12.2	0.50	2.0	49.2
HMIM Cl	32	77.8 ± 1.0	7.4 ± 0.4	10.5	0.57	2.6	8.8
OMIM Cl	9	84.2 ± 2.2	7.4 ± 0.7	11.4	0.62	2.6	2.7
Mutant F87A							
No inhibitor	0	404.8 ± 5.7	7.2 ± 0.4	56.2	—	—	—
OMIM Cl	9	31.4 ± 1.8	20.2 ± 2.8	1.6	0.08	2.8	0.3

^a k_{cat} and K_m ratio is the ratio of kinetic parameters in the presence of ionic liquids to that in the absence of ionic liquids. ^b K_i = dissociation constant of inhibitor to enzyme.

Except for IM11CN Cl, no NADPH consumption higher than the negative control was observed. For IM11CN Cl, a NADPH consumption of <12% of employed NADPH was detected after 20 min in absence of any other substrate. All employed ionic liquids except IM11CN Cl are therefore not or very poor substrates of P450 BM-3. NADPH consumption assay also shows that OMIM Cl is not a substrate of the F87A variant. Spectral measurements of P450 BM-3 in the presence of 1-alkyl-3-methylimidazoliums (BMIM Cl, HMIM Cl, OMIM Cl) did not result in any spectral changes (absorbance decrease around 420 nm and increase around 390 nm). These spectral changes are characteristic of substrate binding in P450 BM-3 which leads to perturbation of the sixth water ligand from the heme iron center. The iron changes thereby from a low spin to a high spin configuration that subsequently leads to an increase in the heme iron reduction potential, a pre-requisite for the electron transfer from the redox partner. All experimental results suggest a lack of inhibitor coordination to the heme iron as reported for the cosolvent DMSO.²²

Discussion

Principles of structure–function relationships of enzymes and biological systems in ionic liquids have been discovered and quantified.^{34–36} There has been so far only one study on the effects of ionic liquids on cytochrome P450 activities³¹ and this report does not evaluate the potential use of ionic liquids for industrial biotransformations. In this manuscript, we have performed a systematic study to quantify ionic liquid effects on P450 BM-3 activity. In detail we studied the influence of four anions and EMIM cation, the effect of alkyl-chain length of 1-alkyl-3-methylimidazolium cations, cation aromaticity and size as well as an additional free electron pair in the alkyl-chain of imidazolium cation on P450 BM-3 activity. These influences of the P450 BM-3 activity were quantified by determining the EC₅₀ values, k_{cat} , K_{m} and K_{i} using the pNCA activity assay.³² Based on these results the EMIM Cl (EC₅₀ = 232 ± 8 mM) is a preferred candidate for biotransformations in ionic liquids.

EC₅₀ values are at least an order of magnitude higher for P450 BM-3 wildtype when compared to studies on acetylcholinesterase.³⁴ When compared to hydrolases P450 BM-3 resistance to ionic liquids is however low. Hydrolases even function in pure ionic liquid solutions.^{5,6,37} The Cl[−] anion has a significantly lower inhibitory effect than CF₃SO₃[−], CF₃COO[−] and BF₄[−] in both cations (EMIM, Na⁺; see Table 1 and Fig. 1). For the cations (EMIM, Na⁺), no general anion trends could be observed. The EMIM and Na⁺ cations however have similar inhibitory effects when Cl[−] ion is used as counter anion (Table 1 and Fig. 1). One possible explanation of the different anion effects is the Hofmeister series which suggests that kosmotropic anions stabilize enzymes while chaotropic anions destabilize biocatalysts. According to the Hofmeister series, chaotropicity increases in the order of CF₃COO[−] > Cl[−] > BF₄[−].^{38,39} The observed inhibition does show that the most chaotropic anion BF₄[−] is most inhibitory for P450 BM-3, while CF₃COO[−] and Cl[−] behave differently from the Hofmeister series. Such exceptions are also reported for bovine carbonic anhydrase, succinate dehydrogenase and NADH oxidase.³⁸

The most significant activity effect due to changes in the cation was seen when the alkyl chain length of the 1-alkyl-3-methylimidazolium cation was increased, which has also been previously observed in acetylcholinesterase.³⁴ Additionally, a decreased enantioselectivity of a protease from *Bacillus licheniformis* had been reported with increasing cation side-chain length (EMIM CF₃COO > BMIM CF₃COO > HMIM CF₃COO).⁴⁰ It had been suggested that increased destabilization with increased alkyl chain length follows the Hofmeister series where longer side-chain length increases hydrophobicity and kosmotropicity of cations.³⁹ The Hofmeister series remains the best possible postulation for enzyme destabilization by cations but it is difficult to generalize for all the enzyme systems that have been studied so far (lipase, esterase, dehydrogenase and P450s).³⁸ For example the kinetic resolution of 1-phenylethanol by *Candida antarctica* lipase A and *Candida antarctica* lipase B improves when the 1-alkyl-3-methylimidazolium cation chain length increases from BMIM BF₄ to HMIM BF₄ and OMIM BF₄.⁴¹

Increasing the alkyl side chain from ethyl- to octyl- leads to more than 25-fold decrease in the EC₅₀ value for P450 BM-3 wildtype. Table 2 summarizes the kinetic parameters (k_{cat} , K_{m} , K_{i}) of BMIM Cl, HMIM Cl and OMIM Cl. Analysis of the P450 BM-3 structure shows a substrate binding pocket close to heme that is lined by hydrophobic residues (F42, Y51, L181, M185, L188, A328, A330 and M354).⁴² The increased inhibition can be attributed to the extended hydrophobicity of longer side chains which cause stronger associations with the hydrophobic patches in the P450 BM-3 substrate channel. Consequently the K_{m} increases as substrate access is adversely affected due to competition from the 1-alkyl-3-methylimidazolium cation. Changing the cation to pyrrolidinium or addition of a nitrile functional group (Table 1 and 2) does not impact significantly on the EC₅₀ values (Table 1 and 2).

As the full crystal structure of P450 BM-3 has not been resolved, one can only base hypotheses on the crystallized heme domain of P450 BM-3. One possible explanation of the lower K_{m} and k_{cat} of P450 BM-3 is the binding of 1-alkyl-3-methylimidazolium cation at the entrance of the substrate access channel. To obtain further insight, short molecular dynamics (MD) simulation of BMIM, HMIM and OMIM at the entrance of the substrate channel and inside the channel were performed. For the MD at the substrate channel entrance, the final conformations show the head group pointing towards Glu13, likely due to electrostatic interaction; the hydrophobic tail points into the substrate channel (see Fig. 3). Glu13 lies within the hydrophobic patch (P11, L14, L17, P18, P45 and A191) which is believed to be a site important for initial binding of lipophilic substrates.⁴² The presence of the 1-alkyl-3-methylimidazolium cation may interfere with this initial binding thereby affecting substrate binding and leading to higher K_{m} values (Table 2). Despite the substrate channel being hydrophobic and having a positively charged R47 which coordinates the carboxylate terminal of the fatty acid substrates, it is known that positively charged substrates can enter and be converted by P450 BM-3.⁴³ MD of the positively charged 1-alkyl-3-methylimidazoliums inside the substrate channel were performed and the positively charged head group moves away from Arg47 and orients towards

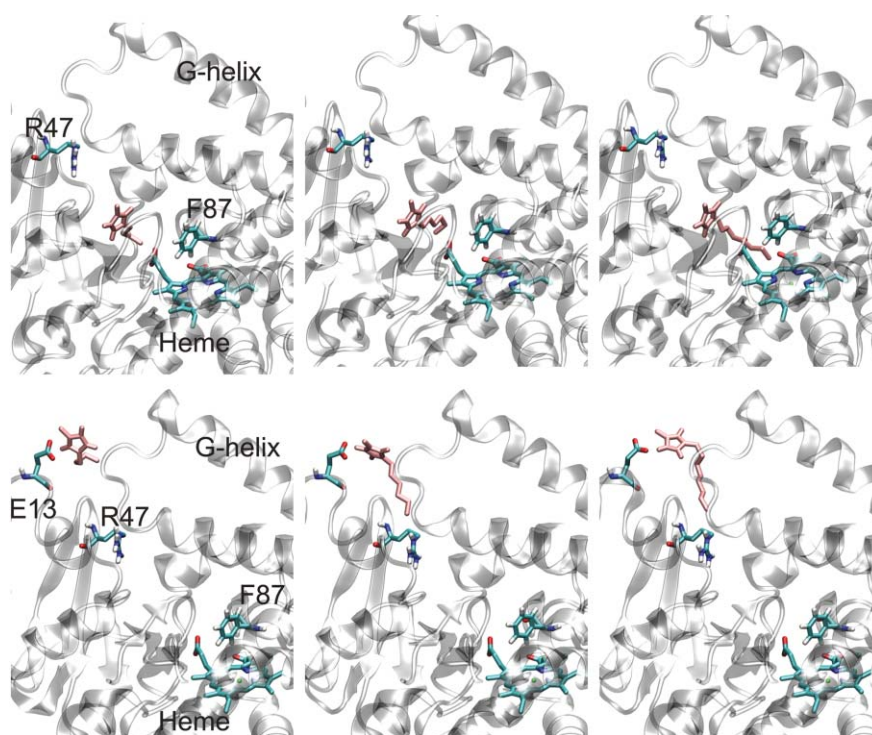


Fig. 3 Final conformations from molecular dynamics docking simulations. Top row (substrate channel entrance; from left to right): BMIM, HMIM, OMIM; Bottom row (inside substrate binding channel; from left to right): BMIM, HMIM, OMIM. Figures on the left are labeled by highlighting important P450 BM-3 positions/regions. The 1-alkyl-3-methylimidazolium is colored in pink.

Glu435 with the hydrophobic tail pointing towards the heme (see Fig. 3). OMIM, which has the longest hydrophobic tail of the investigated ionic liquids, is located ~ 5 Å from the Fe iron, 9 Å from Y51 and 13 Å from R47 according to the MD simulations. The 1-alkyl-3-methylimidazoliums in the substrate channel in such a configuration can interfere with the orientation of the substrate with respect to the heme, thereby affecting the terminal hydroxylation of 12-pNCA and lead to the lower k_{cat} values.

The mutation F87A is known to influence P450 BM-3's tolerance towards organic solvents.²¹ The OMIM Cl resistance of P450 BM-3 F87A was thus determined. The change in phenylalanine 87 to alanine led to a lower resistance of P450 BM-3 to OMIM Cl as reflected in the 35-fold decrease in $k_{\text{cat}}/K_{\text{m}}$ compared to the 4-fold decrease observed in P450 BM-3 wildtype (Table 2). The change in $k_{\text{cat}}/K_{\text{m}}$ is contributed largely by the 12.5-fold lower k_{cat} value (Table 2). The presence of phenylalanine 87 at the end of channel can possibly interact further with the *p*-nitrophenyl group of the 12-pNCA substrate through π - π interaction and contribute to a catalytic "active" orientation of 12-pNCA, especially if the OMIM inside the substrate channel affects substrate orientation. Changing F87 to alanine removes this interaction and leads to a much lower k_{cat} value. More extensive studies are currently being performed to elucidate the actual mode of inhibition by the 1-alkyl-3-methylimidazoliums.

Conclusion

EMIM Cl is identified as a preferred ionic liquid as cosolvent for biotransformations catalyzed by P450 BM-3. Increasing

alkyl side chain from ethyl- to octyl- in the imidazolium cation significantly increases (26-fold) the inhibitory effect of ionic liquids which can likely be attributed to increase hydrophobicity of the alkyl chain. Potential binding sites lie at the hydrophobic mouth of the substrate access channel (OMIM head group pointing towards Glu13) and inside the substrate channel (OMIM head group pointing towards Glu435). P450 BM-3 shows, based on the EC_{50} values, a lower resistance to ionic liquids compared to previously studied organic solvents such as DMSO (50% residual activity at ~ 3 M), acetonitrile (50% residual activity at ~ 1 M) and ethanol (50% residual activity at ~ 1 M).²¹ However for EMIM Cl, IM11CN Cl, Bpy Cl and BMPyr Cl, higher resistances were observed compared to THF (50% residual activity at ~ 0.1 M). Changing of the cation to pyridinium and pyrrolidinium or addition of the nitrile functional group did not generate obvious changes in EC_{50} .

Directed P450 BM-3 evolution studies employing EMIM Cl are currently being performed for discovering principles on how P450 BM-3 and monooxygenases in general can be reengineered to operate efficiently in EMIM Cl.

Experimental

Materials

All chemicals used were of analytical reagent grade or higher quality and purchased from Sigma-Aldrich Chemie (Taufkirchen, Germany), Applichem (Darmstadt, Germany) and Carl Roth (Karlsruhe, Germany). NADPH tetrasodium salt was purchased from Codexis (Redwood city, CA, United States), *p*-nitrophenoxydodecanoic acid (12-pNCA)

was synthesized as previously described³² and the ionic liquids used were from Merck KGaA (Darmstadt, Germany).

P450 BM-3 expression and purification

P450 BM-3 wildtype and mutants were expressed in 1-L Erlenmeyer flask containing 250 mL of terrific broth (100 mg L⁻¹ ampicillin, 250 μ L of trace elements as previously described²¹). The cells were harvested by centrifugation (4 °C, 3220 g, 15 min) and the cell pellet was resuspended in K_xH_{3-x}PO₄ (25 mM, pH 7.5) and lysed by high-pressure homogenization (EmulsiFlex-C3, Avestin Inc, Ottawa, Canada; two cycles of homogenizing pressure 1500–1800 bar). Cell lysate was centrifuged (20000 g, 45 min) and the supernatant was further cleared through a 0.45 μ m filter (17765 K, Sartorius, Hannover, Germany). The filtrate was loaded on a DEAE650s anion exchanger column (Tosoh Bioscience, Stuttgart, Germany) and purified as previously described.⁴⁴ P450 BM-3 concentrations were measured by CO-difference spectra as reported by Omura and Sato using $\epsilon = 91 \text{ mM}^{-1} \text{ cm}^{-1}$.⁴⁵

Determination of pH in ionic liquid–water mixture

The pH of the reaction mixture used for activity tests was determined using a laboratory pH meter (Knick, Berlin, Germany). A reaction mixture (2.5 mL) consist of 1.5 mL buffer (0.3 M Tris pH 8.2), 0.3 mL ionic liquid (0.5 M EMIM Cl; 0.18 M EMIM CF₃SO₃ and EMIM CF₃COO; 0.096 M EMIM BF₄; 0.3 M BMPyr Cl; 0.36 M 1M11CNCl; 0.24 M BMIM Cl; 0.072 M HMIM Cl; 0.015 M OMIM Cl), 75 μ M 12-pNCA and 0.5% v/v DMSO. The pH was equilibrated (10 min) or until a stable reading was obtained.

Determination of NADPH consumption and P450 spectra using ionic liquids as substrate

For NADPH consumption assay, 600 μ L tris buffer (0.3 M, pH 8.2), 0.0975 nmol P450 BM-3 WT and 10 μ L of ionic liquids (0.175 M EMIM Cl; 0.075 M EMIM CF₃SO₃ and EMIM CF₃COO; 0.04 M EMIM BF₄; 0.15 M 1M11CN Cl; 0.125 M BMPyr Cl; 0.1 M BMIM Cl; 0.03 M HMIM Cl; 0.0125 M OMIM Cl) were used. The reaction mixture was topped up by supplementing doubly-distilled H₂O (900 μ L), incubated (5 min) and initiated by adding NADPH (0.25 mM; final reaction volume 1 mL). NADPH consumption was followed spectrophotometrically (340 nm, 10 min; Specord200, Analytik Jena AG, Jena, Germany) in disposable cuvettes. A positive control was performed by adding 12-pNCA (75 μ M) and no ionic liquids to the reaction mixture; a negative control was performed in the absence of 12-pNCA substrates. For spectra measurements, 0.2 nmol of P450 BM-3 were added to phosphate buffer (25 mM, pH 7.5) with ionic liquids (148 mM BMIM Cl; 32 mM HMIM Cl; 9 mM OMIM Cl) and incubated for 5 min. Subsequently spectra measurements between 350 and 700 nm were recorded using a Specord200 (Analytik Jena AG).

Determination of P450 BM-3 activity in ionic liquid–water mixture

Residual activities of P450 BM-3 WT in the presence of ionic liquids were measured in 96-well microtiter plates

(Grenier Bio-One GmbH, Frickenhausen, Germany) and ionic liquids were always prepared freshly in doubly-distilled H₂O. The 200 μ L reaction mixture finally consists of 0.18 M Tris buffer (pH 8.2), gradient concentrations of ionic liquids, 75 μ M 12-pNCA, 0.5% DMSO and 0.0195 nmol P450 BM-3 WT. Employed concentrations of ionic liquids and the Na⁺ salts used for these activity measurements are listed in Table 1. Reaction mixtures were always incubated for 5 min before 12-pNCA conversion was initiated by adding NADPH (25 μ L, 2.5 mM). Conversion of the 12-pNCA was monitored using the Tecan Sunrise microtiter plate reader (Tecan, Zurich, Switzerland) at 405 nm for a duration of 6–10 min with an average of 3 s interval between each reading cycle. All P450 BM-3 residual activities in ionic liquid–water mixture were determined with at least triplicate measurements.

Determination of k_{cat} and K_{m} values for P450 BM-3 in ionic liquid–water mixture

The kinetic constants were determined using the 12-pNCA assay. The assay was performed in disposable cuvettes as previously described³² except that the tris buffer composition was changed (0.18 M, pH 8.2, final concentration of DMSO is 0.5%). Amount of P450 BM-3 per reaction was always 0.1 nmol. The activity was monitored at 410 nm using Specord 200 (Analytik Jena AG). 12-pNCA concentrations were varied from 2.5–125 μ M. All measurements were made in triplicates and the k_{cat} and K_{m} values were determined using GraphPad Prism software (GraphPad Software, San Diego, CA, USA) with fitting to a one-site binding hyperbola equation using non-linear regression.

Imidazolium cation docking in the substrate binding site of P450 BM-3

For MD simulations the atomic coordinates of P450 BM-3 wildtype were obtained using the crystal structure file (pdb code 1bu7).²⁴ All crystallographic water and other ligand molecules were removed except the water molecule coordinating the iron in the active site of the enzyme. Polar and aromatic hydrogen atoms were added to the crystal structure. Atomic partial charges for the protein were assigned from the GROMOS96 43b1 force field.⁴⁶ The initial structure of the three ionic liquids were optimized at HF level using 6-31G** basis set using Gaussian03 program (www.gaussian.com). The force field parameters for the ionic liquid were taken from published data.⁴⁷ Initial docked conformations were manually generated using PBD Viewer. The initial docked conformation of 1-alkyl-3-methylimidazolium at the substrate channel entrance was placed between P45 and A191,^{48,49} while initial docked conformation inside the channel was selected according to the palmitoleic acid substrate (pdb code 1fag)²³ close to R47 and Y51. Optimization of the docked structures was performed using standard energy minimization followed by a molecular dynamics simulation of at least 30 ps using position restraints on the protein backbone. All the simulation were performed using the program GROMACS (version 3.1) (www.gromacs.org). Final conformations were used to analyse the cation position.

Notes and references

- 1 S. Park and R. J. Kazlauskas, *Curr. Opin. Biotechnol.*, 2003, **14**, 432–437.
- 2 R. A. Sheldon, R. M. Lau, M. J. Sorgedraeger, F. van Rantwijk and K. R. Seddon, *Green Chem.*, 2002, **4**, 147–151.
- 3 F. van Rantwijk, R. M. Lau and R. A. Sheldon, *Trends Biotechnol.*, 2003, **21**, 131–138.
- 4 Z. Yang and W. B. Pan, *Enzyme Microb. Technol.*, 2005, **37**, 19–28.
- 5 J. L. Kaar, A. M. Jesionowski, J. A. Berberich, R. Moulton and A. J. Russell, *J. Am. Chem. Soc.*, 2003, **125**, 4125–4131.
- 6 M. Persson and U. T. Bornscheuer, *J. Mol. Catal. B: Enzym.*, 2003, **22**, 21–27.
- 7 H. Pfruender, R. Jones and D. Weuster-Botz, *J. Biotechnol.*, 2006, **124**, 182–190.
- 8 S. J. Nara, J. R. Harjani and M. M. Salunkhe, *Tetrahedron Lett.*, 2002, **43**, 2979–2982.
- 9 H. Zhao, L. Jackson, Z. Y. Song and A. Olubajo, *Tetrahedron: Asymmetry*, 2006, **17**, 2491–2498.
- 10 N. Kaftzik, P. Wasserscheid and U. Kragl, *Org. Process Res. Dev.*, 2002, **6**, 553–557.
- 11 S. Sgalla, G. Fabrizi, S. Cacchi, A. Macone, A. Bonamore and A. Boffi, *J. Mol. Catal. B: Enzym.*, 2007, **44**, 144–148.
- 12 J. A. Laszlo and D. L. Compton, *J. Mol. Catal. B: Enzym.*, 2002, **18**, 109–120.
- 13 A. Chefson and K. Auclair, *Mol. Biosyst.*, 2006, **2**, 462–469.
- 14 A. J. Fulco, *Ann. Rev. Pharm. Toxicol.*, 1991, **31**, 177–203.
- 15 D. F. V. Lewis and A. Wiseman, *Enzyme Microb. Technol.*, 2005, **36**, 377–384.
- 16 D. Appel, S. Lutz-Wahl, P. Fischer, U. Schwaneberg and R. D. Schmid, *J. Biotechnol.*, 2001, **88**, 167–171.
- 17 A. B. Carmichael and L. L. Wong, *Eur. J. Biochem.*, 2001, **268**, 3117–3125.
- 18 A. Glieder, E. T. Farinas and F. H. Arnold, *Nat. Biotechnol.*, 2002, **20**, 1135–1139.
- 19 S. Graham-Lorence, G. Truan, J. A. Peterson, J. R. Falck, S. Z. Wei, C. Helvig and J. H. Capdevila, *J. Biol. Chem.*, 1997, **272**, 1127–1135.
- 20 S. Kumar, L. Sun, B. K. Muralidhara, J. R. Halpert and J. R. Halpert, *Protein Eng. Des. Sel.*, 2006, **19**, 547–554.
- 21 T. S. Wong, F. H. Arnold and U. Schwaneberg, *Biotechnol. Bioeng.*, 2004, **85**, 351–358.
- 22 J. Kuper, T. S. Wong, D. Roccatano, M. Wilmanns and U. Schwaneberg, *J. Am. Chem. Soc.*, 2007, **129**, 5786–5787.
- 23 H. Y. Li and T. L. Poulos, *Nat. Struct. Biol.*, 1997, **4**, 140–146.
- 24 I. F. Sevrioukova, H. Y. Li, H. Zhang, J. A. Peterson and T. L. Poulos, *Proc. Natl. Acad. Sci. U. S. A.*, 1999, **96**, 1863–1868.
- 25 K. L. Tee and U. Schwaneberg, *Angew. Chem., Int. Ed.*, 2006, **45**, 5380–5383.
- 26 T. S. Wong, N. Wu, D. Roccatano, M. Zacharias and U. Schwaneberg, *J. Biomol. Screen.*, 2005, **10**, 246–252.
- 27 L. O. Narhi and A. J. Fulco, *J. Biol. Chem.*, 1987, **262**, 6683–6690.
- 28 U. Domanska and A. Marciniak, *J. Chem. Thermodyn.*, 2005, **37**, 577–585.
- 29 U. Domanska and A. Marciniak, *Fluid Phase Equilib.*, 2006, **260**, 9–18.
- 30 S. Park, F. Viklund, K. Hult and R. J. Kazlauskas, *Green Chem.*, 2003, **5**, 715–719.
- 31 A. Chefson and K. Auclair, *ChemBioChem*, 2007, **8**, 1189–1197.
- 32 U. Schwaneberg, C. Schmidt-Dannert, J. Schmitt and R. D. Schmid, *Anal. Biochem.*, 1999, **269**, 359–366.
- 33 J. Ranke, *Drfit: Dose-response data evaluation*, 2005 (computer program).
- 34 F. Stock, J. Hoffmann, J. Ranke, R. Stormann, B. Ondruschka and B. Jastorff, *Green Chem.*, 2004, **6**, 286–290.
- 35 S. Stolte, J. Arning, U. Bottin-Weber, M. Matzke, F. Stock, K. Thiele, M. Uerdingen, U. Welz-Biermann, B. Jastorff and J. Ranke, *Green Chem.*, 2006, **8**, 621–629.
- 36 S. Stolte, J. Arning, U. Bottin-Weber, A. Müller, W. R. Pitner, U. Welz-Biermann, B. Jastorff and J. Ranke, *Green Chem.*, 2007, **9**, 760–767.
- 37 R. M. Lau, F. van Rantwijk, K. R. Seddon and R. A. Sheldon, *Org. Lett.*, 2000, **2**, 4189–4191.
- 38 H. Zhao, *J. Mol. Catal. B: Enzym.*, 2005, **37**, 16–25.
- 39 H. Zhao, O. Olubajo, Z. Y. Song, A. L. Sims, T. E. Person, R. A. Lawal and L. A. Holley, *Bioorg. Chem.*, 2006, **34**, 15–25.
- 40 H. Zhao, S. M. Campbell, L. Jackson, Z. Y. Song and O. Olubajo, *Tetrahedron: Asymmetry*, 2006, **17**, 377–383.
- 41 S. H. Schofer, N. Kaftzik, P. Wasserscheid and U. Kragl, *Chem. Commun.*, 2001, 425–426.
- 42 K. G. Ravichandran, S. S. Boddupalli, C. A. Hasemann, J. A. Peterson and J. Deisenhofer, *Science*, 1993, **261**, 731–736.
- 43 C. F. Oliver, S. Modi, W. U. Primrose, L. Y. Lian and G. C. K. Roberts, *Biochem. J.*, 1997, **327**, 537–544.
- 44 U. Schwaneberg, A. Sprauer, C. Schmidt-Dannert and R. D. Schmid, *J. Chromatogr., A*, 1999, **848**, 149–159.
- 45 T. Omura and R. Sato, *J. Biol. Chem.*, 1964, **239**, 2370–2378.
- 46 W. F. van Gunsteren, S. R. Billeter, A. A. Eising, P. H. Hünenberger, P. Krüger, A. E. Mark, W. R. P. Scott and I. G. Tironi, in *Biomolecular Simulation: The GROMOS96 Manual and User Guide*, vdf Hochschulverlag, ETH Zürich, Switzerland, 1996.
- 47 N. M. Micaelo, A. M. Baptista and C. M. Soares, *J. Phys. Chem. B*, 2006, **110**, 14444–14451.
- 48 M. D. Paulsen and R. L. Ornstein, *Proteins: Struct., Funct., Genet.*, 1995, **21**, 237–243.
- 49 D. Roccatano, T. S. Wong, U. Schwaneberg and M. Zacharias, *Biopolymers*, 2006, **83**, 467–476.

Synthesis, evaluation and application of novel bifunctional *N,N*-di-isopropylbenzylamineboronic acid catalysts for direct amide formation between carboxylic acids and amines†‡

Kenny Arnold,^a Andrei S. Batsanov,^a Bryan Davies^b and Andrew Whiting^{*a}

Received 6th August 2007, Accepted 13th November 2007

First published as an Advance Article on the web 22nd November 2007

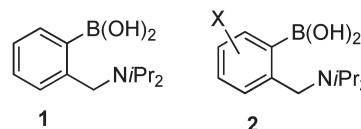
DOI: 10.1039/b712008g

Three new derivatives of *N,N*-di-isopropylbenzylamine-2-boronic acid have been prepared by directed metallation-borylation methods, to derive the 3-fluoro, 3-methoxy and 5-trifluoromethyl systems. The addition of an electron withdrawing group does increase the reactivity of such systems to act as improved direct amide formation catalysts under the most ambient conditions employed to date. In contrast, an electron donating group does result in considerable lowering of catalyst reactivity. DoE studies have been used to identify the ideal reaction conditions under which these types of catalysts should be used, typified by the parent system *N,N*-di-isopropylbenzylamine-2-boronic acid. This shows best performance at a 5 mol% loading and under higher dilution conditions, which most likely reflect the drying capacity of the solvent.

Introduction

A generally applicable, efficient direct amide formation from amines and carboxylic acids, *via* the corresponding ammonium salt, that proceeds under relatively ambient conditions remains elusive. Since the first report of ammonium carboxylate pyrolyses,¹ there have been various developments in the intervening years, including relatively small reductions in temperature,² the use of various acid catalysts³ and microwave assistance.⁴ However, none of these approaches have provided a solution to facile direct amide formation, and the more usual stoichiometric activation methods remain by far the most utilised approach.⁵ Initial reports of the application of organoboron compounds to assist amide formation,⁶ has resulted in the development of several useful boronic acid catalysts,⁷ however, the report that boric acid alone is an efficient catalyst under azeotropic conditions⁸ shows the need to be wary about the mode of action of electron deficient arylboronic acids and there is still a need to develop systems with higher reactivity, and at lower temperatures. To this end, we demonstrated the use of bifunctional amino-boronic acid derivatives⁹ for direct amide formation, and examined the previously essentially unaddressed issue of the competing degree of direct thermal amide formation. Our major aim was to develop catalytic systems which exhibit: (1) general reactivity for all types of amine and carboxylic acid substrates; (2) lower reaction temperatures to relatively ambient conditions, *i.e.* lower than

refluxing toluene where possible, and certainly below refluxing xylene or mesitylene for example; and (3) zero propensity to proto-deboration, and hence acting a source of boric acid. This resulted in the demonstration that *ortho-N,N*-di-isopropylbenzylaminoboronic acid system **1** has a bifunctional catalytic effect for direct amide formation reactions involving benzoic acid, and it could be used using refluxing fluorobenzene temperatures.¹⁰ Under these conditions, proto-deboration does not compete and a comparison of the rates of amide formation between various boron-based catalysts under two different sets of reaction conditions clearly showed the enhanced activity of catalyst **1** for the more difficult substrates under the milder set of reaction conditions. In this paper, we report our further studies aimed at better understanding the factors that control catalyst activity, including the synthesis of further examples of these bifunctional aminoarylboronic acids and an examination of their comparative reactivity in the direct amide condensation *versus* existing systems. We also report associated optimisation of reaction conditions for different substrate combinations using statistical design of experiments (DoE) methods to gain a further insight into the key reaction parameters that affect reactivity.



Results and discussion

We decided to access novel derivatives of system **1**, *i.e.* systems of type **2**, in which the hindered *N,N*-di-isopropylaminobenzyl function was retained, since in previous work, clear benefit over the less hindered *N,N*-dimethyl system was demonstrated.¹⁰ In addition, the new systems **2** were chosen with the specific aim of testing the effect of changing the Lewis acidity of the boronic acid function by suitable choice of the

^aDepartment of Chemistry, Durham University, South Road, Durham, UK, DH1 3LE E-mail: andy.whiting@durham.ac.uk

^bGlaxoSmithKline Research & Development Ltd., Gunnels Wood Road, Stevenage, Hertfordshire, UK, SG1 2NY

† Electronic supplementary information (ESI) available: General experimental methods, X-ray crystallographic data for compounds **6a** and **10**, and ¹H, ¹³C, ¹¹B and ¹⁹F NMR spectra (as appropriate) for compounds **4a**, **5a**, **6a**, **4b**, **5b**, **6b**, **4c**, **8**, **9**, **10** and 1-morpholin-4-yl-4-phenylbutan-1-one. See DOI: 10.1039/b712008g

‡ CCDC reference numbers 632237 and 632238. For crystallographic data in CIF or other electronic format see DOI: 10.1039/b712008g

functional group X, *i.e.* comparing electron withdrawing and electron donating substituents.

Catalyst synthesis

The synthesis of new catalysts based on system **2**, started with the fluoro- and methoxybenzylboronic acid, **6a** and **b**, respectively (Scheme 1). Hence, *N,N*-di-isopropyl-3-fluoro-benzylamine-2-boronic acid **6a** was prepared starting with 3-fluorobenzoyl chloride **3a**, resulting in the formation of amide **4a**, upon reaction with di-isopropylamine, which was then subjected to directed metallation. Following several attempts to achieve directed *ortho*-metallation of **4a**, attempts to directly isolate the corresponding boronic acid proved unsuccessful, and it was decided to access the pinacol ester **5a** in order to simplify isolation and purification. Hence, reaction of amide **4a** with *sec*-butyllithium followed by trimethylborate, followed by hydrolysis and esterification with pinacol derived the boronate ester **5a** (Scheme 1).

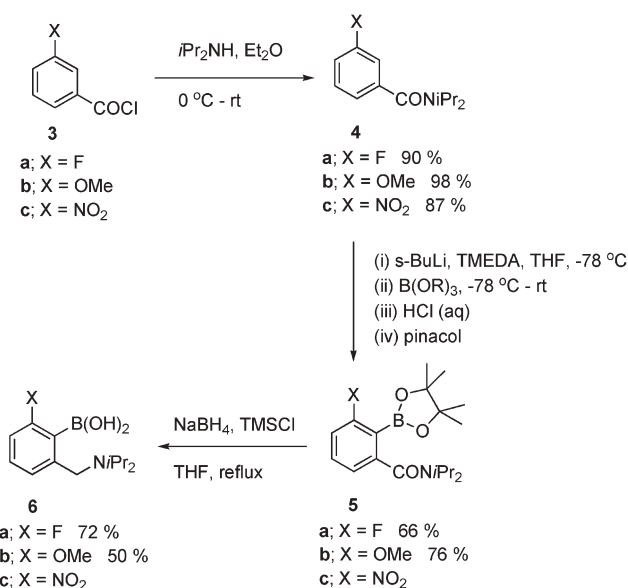
The reduction method chosen to convert the pinacol ester **5a** was selected in order to achieve both amide reduction and deprotection of the boronate ester in one step.^{9b} Although the reduction proceeded well using sodium borohydride-trimethylsilyl chloride, isolation of the amino-boronic acid **6a** proved troublesome, due to its high water solubility. However, use of an acidification-neutralisation sequence during the work up allowed direct extraction of the amino-boronic acid **6a**, which could then be efficiently precipitated to give pure product in 72 % yield.

The same strategy was employed in order to synthesise *N,N*-di-isopropyl-3-methoxybenzylamine-2-boronic acid **6b**. As before, the amidation of acid chloride **3b** was facile, efficiently providing di-isopropylamide **4b** (Scheme 1). However, the directed metallation of **4b** proved problematic at first, and resulted in low conversion to the pinacol ester **5b**, *i.e.* *sec*-butyllithium-TMEDA, $-78\text{ }^{\circ}\text{C}$. This was solved by allowing much longer reaction times for the intermediate aryllithium to

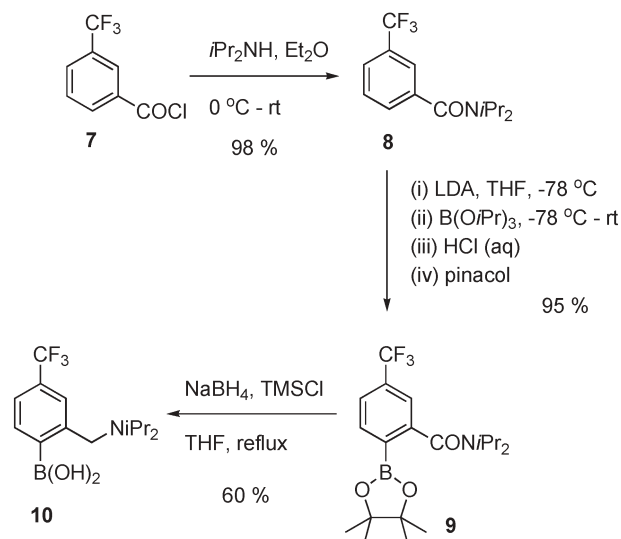
react with the borate electrophiles (*ca.* 12 h), resulting in the isolation of pinacol ester **5b** in good yield. It is worth noting that metallation-borylation of amide **4b** fails to proceed at all with *n*-butyllithium, whereas the alkylolithium source has no significant effect upon the metallation of **4a**. In addition, attempted metallation of methoxy-substituted system **4b** with lithium di-isopropylamide, followed by triisopropyl borate resulted in the formation of ester **5b**, but in only 11 % yield.

Having obtained boronate ester **5b**, reduction was attempted as for **5a**, resulting in only low yields amino-boronic acid **6b** (10 %). It appears that the methoxy system **6b** has increased water solubility compared to **6a**, and therefore, suitable changes to the work up procedure (THF evaporation and minimisation of aqueous solution and solvent volumes) resulted in a reasonably efficient isolation of **6b**, which after subsequent recrystallisation gave a 50 % yield (Scheme 1).

In order to compare catalysts of type **2**, systems with different electronic properties were required. Several attempts were made to access the system **6c**, *via* formation of the corresponding amide **4c** (Scheme 1). However, all attempts to achieve deprotonation of **4c** to access boronate **5c** led to the formation of intractable complex products, which is not in contradiction with other unsuccessful attempts to achieve lithiation of nitroaryl systems.¹¹ As an alternative to the nitro-substituted system, the final catalyst prepared was the trifluoromethyl-substituted system, *i.e.* **10**, which proved reasonably straightforward to access, as outlined in Scheme 2. Thus, amidation of acid chloride **7** provided amide **8** in 98 % yield. Directed *ortho*-metallation under the same conditions as used for systems **5** (*n*- or *s*-BuLi-TMEDA) led to a mixture of *ortho*- and *para*-CF₃ boronates, with low total conversion (*ca.* 10 %). A number of attempts at improvement (increasing reaction temperature, metallation time, *etc.*) failed to improve matters and alternative metallating agents were examined. A mixture of potassium *tert*-butoxide and BuLi¹² gave no reaction, however, use of lithium di-isopropylamide afforded the *para*-CF₃-substituted boronate **9** selectively and in high



Scheme 1 Synthesis of fluoro- and methoxy-substituted amino-boronic acids **6**.



Scheme 2 Synthesis of trifluoromethyl-substituted amine-boronic acid.

yield (95 %). Subsequent initial attempts at reduction of the amide **9** using borane-dimethyl sulfide in THF at reflux failed to give an observable reaction, however, using the TMSCl-borohydride conditions resulted in formation of boronic acid **10** after work up, albeit *via* a slow reaction, which resulted in only 40 % conversion in 40 h. The solution to this problem was to simply decrease the reaction concentration used for the reduction conditions, which resulted in complete conversion in 24 h (Scheme 2), and after modification of the work up conditions used for amino-boronic acids **6**, the trifluoromethyl-boronic acid **10** was obtained in 60 % yield after recrystallisation.

Comparison of crystal structures

Crystals of both **6a** and **10**, which were suitable for single crystal X-ray analysis, were readily prepared, however, the methoxy derivative **6b** evaded attempts to derive good quality crystals. However, fluoro and trifluoro derivatives **6a** and **10**, respectively, are essentially isostructural with one another and also with the analogue **1**.^{9b} Molecular conformations are also similar (Fig. 1). The C(1)BO(1)O(2) moiety is planar and inclined to the benzene ring plane by 25.8° (**6a**) or 21.8° (**10**). The larger twist in **6a** obviously is caused by steric repulsion between the F and O(2) atoms. One hydroxyl group, O(1)H, forms an intramolecular hydrogen bond with the amino N atom, which is slightly pyramidalised, with the mean C–N–C angle of 113°. Molecules are linked into centrosymmetric

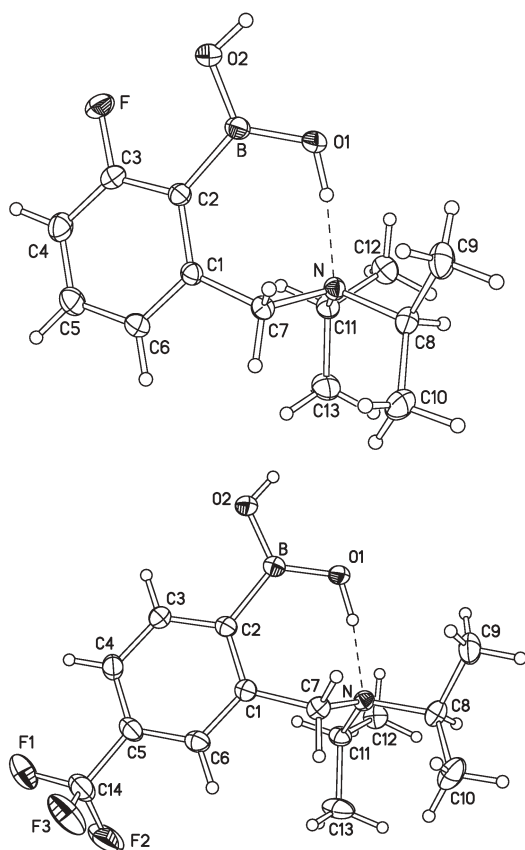


Fig. 1 X-ray molecular structures of **6a** (top) and **10**. Thermal ellipsoids are drawn at 50 % probability level.

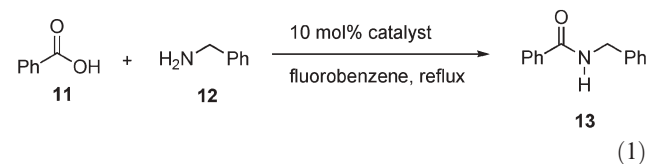
Table 1 Selected bond distances (Å)

	1	6a	10
C(2)–B	1.588(2)	1.5965(14)	1.5876(17)
B–O(1)	1.356(2)	1.3547(13)	1.3575(15)
B(1)–O(2)	1.366(2)	1.3581(13)	1.3609(16)
O(1)···N	2.637(1)	2.607(1)	2.623(1)
C(1)–C(2)	1.412(2)	1.4204(12)	1.4169(16)
C(1)–C(7)	1.522(2)	1.5171(13)	1.5187(16)
C(7)–N	1.480(1)	1.4837(12)	1.4795(15)

dimers by pairs of hydrogen bonds O(2)–H···O(1)[1–x, 1–y, 1–z]. There are only marginal differences in bond distances between **1**, **6a** and **10** (Table 1). It is interesting to note that the trifluoromethyl system **10** exhibits a shorter C–B bond length compared with the fluoro system **6a**, however, it is little different to the non-substituted system **1** (see Table 1). This probably suggests that there is not a major difference in Lewis acidity between systems **1** and **10**, though **6a** might be slightly less Lewis acidic. Unfortunately, we cannot compare these solid state structures with the methoxy derivative **6b**, and ¹¹B NMR also does not seem to suggest significant differences in the properties of the boronic acid function, which show resonances at δ 28.8,^{9b} 28.4, 29.3 and 28.5 for **1**, **6a**, **6b** and **10**, respectively.

Catalyst optimisation using design of experiments (DoE)

To gain an insight into the key reaction parameters that influence the direct amide condensation, a DoE study was carried out on the formation of amide **13** catalysed by **1** (eqn (1)).¹³ Four factors were examined (Table 2) and to simplify subsequent analysis of the results, separate designs were carried out for fluorobenzene and toluene. Temperature could not be included as a factor in these individual studies, as it has been shown previously that azeotropic reflux is desired to enable the reaction to proceed. A 2-level fractional factorial design of 8 experiments was selected¹⁴ and 4 centre points were included to provide a measure of variation and indicate curvature.



The results of the study of the reaction in fluorobenzene are summarised in Fig. 2 in the form of a half-normal probability plot in which the factors having the greatest influence appear towards the right-hand side of the graph. It can be seen that catalyst loading, time, and the two-factor interaction of catalyst loading and time are the most important factors, whilst acid stoichiometry and concentration have

Table 2 Factors and ranges chosen for the factorial design

Factor	Low	Centre	High
1 (mol%)	1	5.5	10
Acid (equiv)	0.8	1.1	1.4
Conc/M	0.1	0.3	0.5
Time/h	4	12	20

Design-Expert® Software
Yield

▲ Error from replicates

Shapiro-Wilk test

W-value = 0.729

p-value = 0.024

A: cat loading

B: acid stoichiom

C: conc

D: time

■ Positive Effects

■ Negative Effects

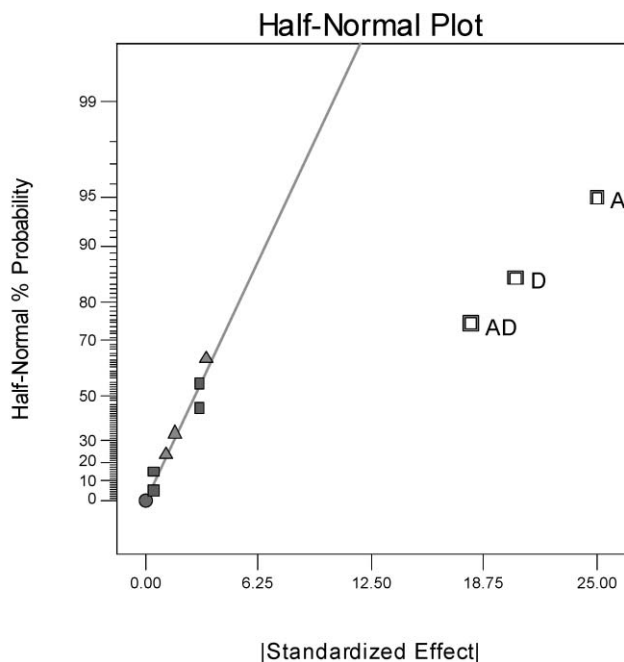


Fig. 2 Half normal plot visualizing the most important factors determining yield in the direct amide condensation in fluorobenzene.

no significant effect.¹⁵ The centre points in the interaction graph (Fig. 3) show no significant deviation from the linear relationship plotted, *i.e.* there is no significant curvature, and the linear relationship plotted is a good representative model. Thus, the DoE suggests, in order to increase yield of amide **13**, catalyst loading and time should be increased. Although increasing reaction time is a possibility, increasing the loading of **1** beyond 10 mol% would be undesirable.

The same design run in toluene shows catalyst loading is again the most important effect, followed by time, and acid

stoichiometry still has no significant effect (Fig. 4).¹⁵ However, concentration and catalyst loading are now involved in an interaction, with the model suggesting that in order to increase yields of amide **13**, both low concentration and higher catalyst loading are required (Fig. 5). The interaction graph shows significant curvature indicating that the design space is over an optimum. Since catalyst loading is the most important effect, this appears to indicate that similar yields of amide **13** could be obtained if the loading of **1** is decreased below 10 mol%. In fact, the centre points indicate that a catalyst loading of

Design-Expert® Software

Yield

● Design Points

■ D- 4.000

▲ D+ 20.000

X1 = A: cat loading

X2 = D: time

Actual Factors

B: acid stoichiom = 1.10

C: conc = 0.30

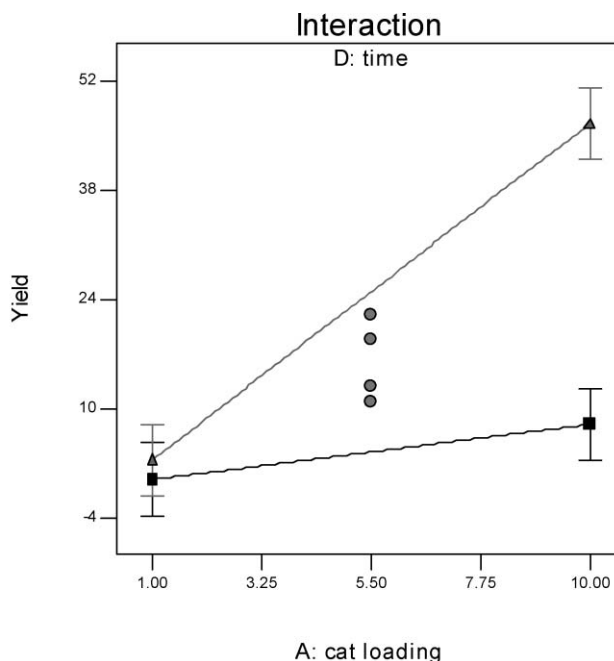


Fig. 3 Interaction graph for the direct amide condensation in fluorobenzene.

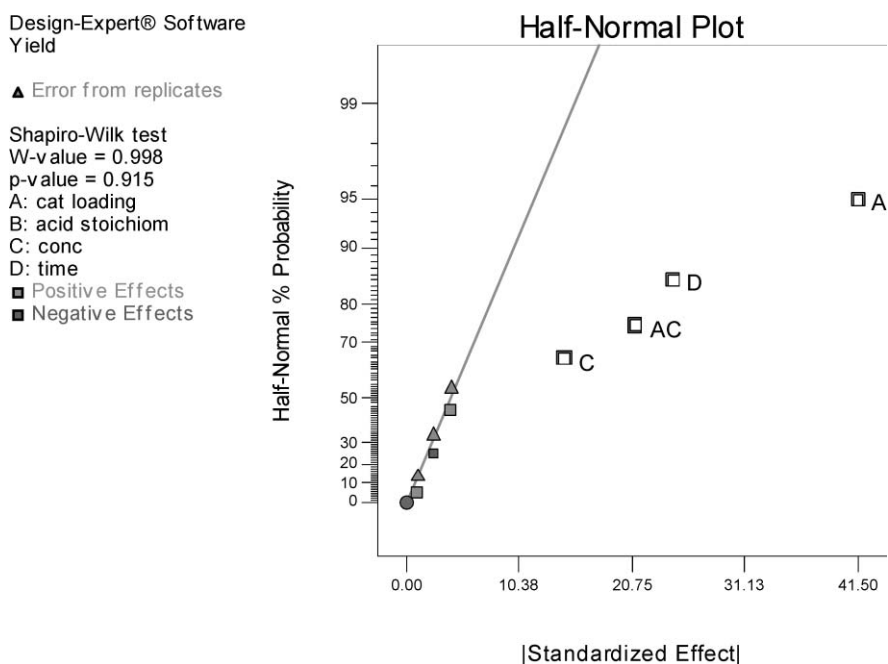


Fig. 4 Most important factors determining yield in the direct amide condensation in toluene.

5.5 mol% gives a similar effect, whilst the concentration effect suggests that reaction rate is limited by azeotropic removal of water, and therefore, low concentration is beneficial (*vide infra*). In order to model the curvature, a central composite design (CCD) could be employed to augment the existing design. Although the DoE study was carried out on the formation of amide **13**, the information obtained can clearly be used as a basis to start to improve the isolated yields of more problematic substrates (*vide infra*) and hence, these results have been taken into account in the catalyst evaluation.

Catalyst evaluation

We have previously shown¹⁰ that the boronic acid **1**, and related systems, promote amidation reactions, which are highly substrate dependent and that the use of more difficult substrates under lower temperature conditions (refluxing fluorobenzene) exposes differences in catalyst activity. With this in mind, the new catalysts were evaluated and compared using the reaction between benzoic acid and benzylamine (eqn (1)), and it had already been shown that the direct

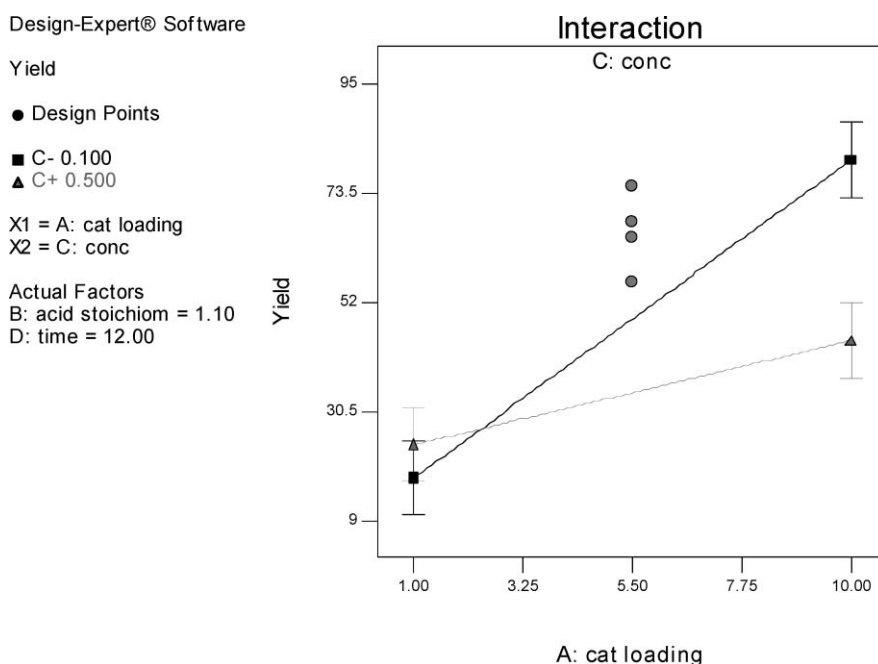


Fig. 5 Interaction graph for the direct amide condensation in toluene.

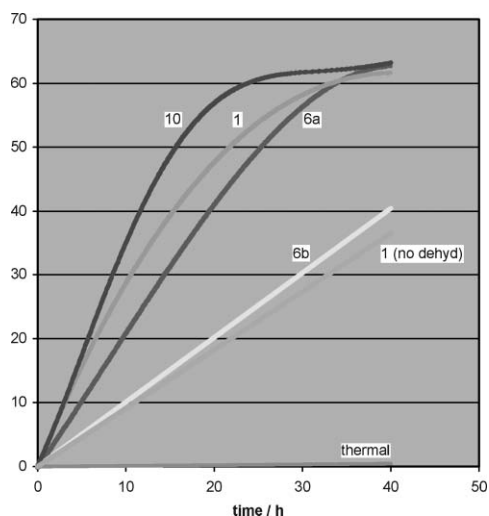


Fig. 6 Yield versus time data for catalysed and thermal direct amide condensation between benzoic acid and benzylamine in refluxing fluorobenzene.

(uncatalysed) thermal formation of amide **13** under these conditions is non-existent.¹⁰ The results of this comparison are shown in Fig. 6.

The addition of a *para*-trifluoromethyl group (catalyst **10**) is beneficial to rate of formation of *N*-benzylbenzamide **13**, compared to the unsubstituted system **1**, whereas the addition of the *ortho*-fluorine function, *i.e.* catalyst **6a**, decreases reaction rate to a small extent (Fig. 6). While the differences between catalysts **1**, **6a** and **10** are not substantial, increasing the electron density of the phenyl ring by incorporating a methoxy group, *i.e.* catalyst **6b**, leads to a significant decrease in reaction rate. This results in only 28 % conversion to amide **11** in 28 h using **6b** compared to *ca.* 63 % conversion for catalysts **1**, **10** and **6a**, which have all reached their equilibrium conversions at around this time period. The efficiency of water removal determines the equilibrium position, therefore affecting both final conversion and reaction rate, as demonstrated by the reaction catalysed by **1** without dehydration, along with the results obtained from the DoE study (*vide supra*).

Application of catalyst **1** for direct amide formation

Although the trifluoromethylbenzylboronic acid **10** is the superior catalyst according (*vide supra*), the difference between **1** and **10** is not substantial (see Fig. 6). Hence, coupled with the commercial availability of catalyst **1** and the results of the DoE optimised reaction conditions in hand (*vide supra*), we needed to evaluate the scope and limitations of the direct amide condensation catalysed by **1**. A variety of carboxylic acids and amines were examined refluxing fluorobenzene where possible, or if necessary in toluene if conversion to amide was slow, and over reaction times of up to 48 h. The results of the reactions generalised by eqn (2), are shown in Table 3.

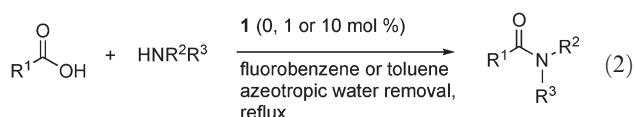


Table 3 Isolated yields for the direct amide condensation catalysed by **1**

Entry	Solvent	1 (mol %)	Time/h	Product	Yield (%)
1	PhF	0	24		16
		10			68
2	PhF	0	24		2
		10			70
3	Toluene	0	22		0 ^a
		1			46 ^a
4	PhF	0	24		4
		10			67
5	PhF	0	22		10 ^b
		10			53
6	PhF	0	24		1
		10			50
7	PhF	0	48		0
					10
		5	24		71
					10
8	PhF	0	24		0
					10
		0	24		0
					5
10	30		21		
			10	21	
9	PhF	0	48		0 ^b
		10			52 ^b
10	PhF	0	24		0
					10
		0	30		7
					5
10	59				

^a Under argon. ^b Determined by HPLC.

The results shown in Table 3 show that the majority of reactions did not proceed to 100 % completion after 48 h, though good to high isolated yields could be achieved in most cases. Fluorobenzene is certainly a suitable and practical azeotropic solvent for many of the more reactive amide formation reactions, *i.e.* entries 1, 2, 4, 5, 6, 7 and 9 (Table 3) using 10 mol% of catalyst **1**. Importantly, at this temperature (85 °C) there is a clear advantage to using the catalyst compared to the corresponding thermal conditions. For less

reactive substrates, however, for example entries 8 and 10, the use of toluene and 5 or 10 mol% catalyst loading was necessary in order to provide an improvement in the isolated yields of each of the amides (see Table 3). Although increasing the reaction temperature (*i.e.* refluxing toluene) increases reaction rates, the associated thermal reactions also become more significant in certain cases, making it harder to fully evaluate catalyst-derived performance alone. For example, reaction of 4-phenylbutyric acid and benzylamine (entry 1, Table 3) shows a significant thermal contribution, as previously reported.¹⁰ Interestingly, aniline reacts relatively well in toluene in the presence of only 1 mol% of catalyst **1**, however, the reaction must be carried out under an inert atmosphere to prevent amine oxidation (entry 3, Table 3). The case of benzoic acid and 4-phenylbutylamine (entry 7, Table 3) demonstrates the non-linear relationship between catalyst loading and yield, as observed in the DoE, with no significant difference between a 5 and 10 mol% loading of catalyst **1**. Only in the case of morpholine benzoylamide (entry 8, Table 3), could the isolated yield not be increased to a reasonable level by changing either catalyst loading or solvent boiling point. This highlights the need for further improvements in these types of direct amide formation reactions in the future, however, the majority of carboxylic acid–amine combinations are readily susceptible to this type of straightforward, clean amide formation.

Summary and conclusions

The direct reaction of amine with carboxylic acid remains the most attractive approach to preparing amide bonds in terms of avoiding reactive and toxic activated carboxylic acid derivatives, or use of *in situ* activating agents.⁵ These types of reactions are arguably best carried out without catalysis where possible, however, reaction conditions remain harsh in order to accomplish these types of direct thermal amide formation.^{1,2} The next most green alternative is arylboronic or boric acid catalysed direct amide formation, which offers generally more attractive reaction conditions of lower temperature reactions (refluxing fluorobenzene, toluene or xylene) and low catalyst loadings (1–10 mol%). In terms of green chemistry, the ability to recover and re-use the azeotropic solvents employed is important, and hence, the only by-product for this direct amide formation is water. Carboxylic acids and amines can be combined in a 1 : 1 stoichiometry, and with suitable reaction engineering, yields can be high, though dependent upon solvent boiling point, substrate combination and efficiency of the water removal (*vide supra*). Compared with, for example, an acid chloride-mediated reaction, this type of catalysed direct amide formation reaction is much more atom efficient. For example, for the reaction shown in entry 7, Table 3 in toluene, the effective mass yield (EMY)¹⁶ is 1525%, assuming that both solvent and molecular sieves are recovered and re-used efficiently, and a 5 mol% catalyst loading. This compares with preparing the same amide using, for example, thionyl chloride to prepare the acid chloride, followed by direct reaction with the amine stoichiometrically and using no additional base, giving an EMY of 87%. Clearly, the use of acylation transfer agents and bases will significantly reduce the EMY for the acid chloride-based route, hence overall, this

analysis provides a graphic example of the potential of such direct amide formation processes over conventional acylation methods.

The synthesis of novel substituted analogues of the bifunctional catalyst **1** has allowed us to begin to further probe the subtleties of the direct amide formation involving arylboronic acid-mediated catalysis. The addition of electron withdrawing functions to the aryl ring of **1**, for example trifluoromethyl derivative **10**, certainly results in increased catalytic activity for amide formation, which reinforces the view that such catalysts act by forming mixed anhydride-type analogues,¹⁰ and the electron withdrawing group increases the leaving group ability during the amide formation step. In terms of practical applications, either catalyst **1** or **10** is suitable for direct amide formation under the most ambient conditions employed to date, though commercial availability makes the use of **1** more attractive currently. Less hindered amine systems¹⁰ or more electron rich aryl systems, such as **6b**, are considerably less efficient. DoE studies on the use of catalyst **1** show that catalyst loadings above 5 mol% are not required, and most interestingly, that the water-removing capacity of the solvent is an important aspect to consider during routine use of these types of catalysts. In order to optimise reactions in the most time efficient manner, higher dilutions are preferred. Clearly, alternative drying agents, perhaps employed *in situ*, could have a major impact upon both the rate, and hence the general applicability of these processes. Further studies along these and related directions are underway and will be reported in due course.

Experimental

N,N-Di-isopropyl-3-fluorobenzamide **4a**

To a stirred solution of 3-fluorobenzoyl chloride (2.68 g, 16.9 mmol) in dry Et₂O (40 mL) under Ar at 0 °C, was added dry di-isopropylamine (6.0 mL, 42 mmol) dropwise. The reaction was allowed to warm to rt, stirred for 18 h and then quenched with 5% (w/v) HCl (25 mL). The organic layer was separated and washed again with 5% (w/v) HCl (2 × 25 mL), then brine (25 mL), 5% (w/v) NaOH (2 × 25 mL), brine (25 mL), dried over MgSO₄, and concentrated under vacuum to afford amide **4a** as a white solid; yield: 3.40 g (90%); mp 74–76 °C; ¹H NMR (500 MHz, CDCl₃): δ = 1.17 (br s, 6H, (CH₃)₂CH), 1.54 (br s, 6H, (CH₃)₂CH), 3.55 (br s, 1H, (CH₃)₂CH), 3.81 (br s, 1H, (CH₃)₂CH), 7.01–7.11 (m, 3H, ArH), 7.37 (td, *J*_{HH} = 8.0 Hz and *J*_{FH} = 5.5 Hz, 1H, ArH); ¹³C NMR (100.6 MHz, CDCl₃): δ = 20.9 (br s, (CH₃)₂CH), 46.2 (br s, (CH₃)₂CH), 51.1 (br s, (CH₃)₂CH), 113.2 (d, ²*J*_{FC} = 22 Hz, ArC), 115.9 (d, ²*J*_{FC} = 21 Hz, ArC), 121.5 (d, ⁴*J*_{FC} = 3 Hz, ArC), 130.5 (d, ³*J*_{FC} = 8 Hz, ArC), 141.1 (d, ³*J*_{FC} = 7 Hz, ArC–CONⁱPr₂), 162.9 (d, ¹*J*_{FC} = 247 Hz, ArC–F), 169.7 (d, ⁴*J*_{FC} = 2 Hz, CONⁱPr₂); ¹⁹F NMR (376.3 MHz; CDCl₃): δ = 5a–112.5 (m); IR (film): *v*_{max} (inter alia) = 3072, 2971, 1629 (s), 1583, 1437, 1344 (s), 1140 cm⁻¹; λ_{max}(MeCN)/nm 200 (ε/dm³ mol⁻¹ cm⁻¹ 12400), 267 (1400); MS (ES): *m/z* (%) = 246.1260 (100) [M + Na]⁺. [C₁₉H₁₃NOFNa]⁺ requires 246.1265; elemental analysis (%): calcd. for C₁₃H₁₈NOF: C 69.93, H 8.13, N 6.27; found: C 69.73, H 8.07, N 6.10.

N,N-Di-isopropyl-3-fluoro-2-(4,4,5,5-tetramethyl-[1,3,2]dioxaborolan-2-yl)-benzamide **5a**

To a stirred solution of **4a** (5.0 g, 22.4 mmol) and TMEDA (4.0 mL, 26.9 mmol) in dry THF (50 mL) under Ar at $-78\text{ }^{\circ}\text{C}$, was added *n*-BuLi (16.8 mL, 1.6 M, 26.9 mmol) dropwise over 10 min. Mixture left to stir for 1 h and then trimethyl borate (3.0 mL, 26.9 mmol) was added rapidly. Mixture allowed to reach rt (2 h) and then quenched with 20% (w/v) HCl (10 mL), followed by addition of pinacol (3.2 g, 26.9 mmol). Mixture extracted into ether (3×20 mL) and the organic extracts washed with sat. aq. NaHCO_3 (3×20 mL) and brine (2×20 mL). Extracts were dried over MgSO_4 and concentrated under vacuum. Column chromatography on silica gel (hexane : EtOAc, 2 : 1) afforded pinacol boronate **5a** as a white crystalline solid; yield: 5.16 g (66%); mp $104\text{--}106\text{ }^{\circ}\text{C}$; ^1H NMR (500 MHz, CDCl_3): δ = 1.19 (br s, 6H, $(\text{CH}_3)_2\text{CH}$), 1.33 (s, 12H, $4 \times \text{Me}$), 1.54 (br s, 6H, $(\text{CH}_3)_2\text{CH}$), 3.54 (br s, 1H, $(\text{CH}_3)_2\text{CH}$), 3.98 (br s, 1H, $(\text{CH}_3)_2\text{CH}$), 6.98–7.04 (m, 2H, ArH), 7.32 (td, $J_{\text{HH}} = 8.0$ Hz and $J_{\text{FH}} = 5.5$ Hz, 1H, ArH); ^{13}C NMR (125.7 MHz, CDCl_3): δ = 20.6 (br s, $(\text{CH}_3)_2\text{CH}$), 25.0 (pinacol CH_3), 46.6 (br s, $(\text{CH}_3)_2\text{CH}$), 51.2 (br s, $(\text{CH}_3)_2\text{CH}$), 83.6 (pinacol C–O), 116.0 (d, $^2J_{\text{FC}} = 25$ Hz, ArC), 120.8 (d, $^4J_{\text{FC}} = 4$ Hz, ArC), 131.5 (d, $^3J_{\text{FC}} = 9$ Hz, ArC), 144.9 (d, $^3J_{\text{FC}} = 9$ Hz, ArC–CON i Pr $_2$), 166.3 (d, $^1J_{\text{FC}} = 249$ Hz, ArC–F), 170.3 (d, $^4J_{\text{FC}} = 3$ Hz, CON i Pr $_2$); ^{11}B NMR (128.4 MHz, CDCl_3): δ = 26.9; ^{19}F NMR (376.3 MHz, CDCl_3): δ = -103.2 (s); IR (film): ν_{max} (inter alia) = 2973, 2930, 2361, 1617 (s), 1439, 1335 (vs), 1144 (s) cm^{-1} ; λ_{max} (MeCN)/nm 197 ($\epsilon/\text{dm}^3 \text{mol}^{-1} \text{cm}^{-1}$ 28100), 242 (3320), 271 (1220); MS (ES): m/z (%) = 721.4 (60), 699.5 (25), 372.2 (100, $[\text{M} + \text{Na}]^+$), 350.2295 (48, $[\text{M} + \text{H}]^+$). $[\text{C}_{19}\text{H}_{30}\text{BFNO}_3]^+$ requires 350.2297; elemental analysis (%): calcd. for $\text{C}_{19}\text{H}_{29}\text{BFNO}_3$: C 65.34, H 8.37, N 4.01; found: C 65.41, H 8.46, N 3.99.

N,N-Di-isopropyl-3-fluorobenzylamine-2-boronic acid **6a**

To a stirred solution of **5a** (5.16 g, 14.8 mmol) and NaBH_4 (5.6 g, 148 mmol) in dry THF (70 mL) under Ar was added TMSCl (37.6 mL, 296 mmol) and the mixture stirred at reflux for 20 h. Reaction quenched by slow addition of 5% (w/v) HCl then 20% (w/v) HCl taking the aqueous layer to pH 1, and extracted into Et_2O (1×50 mL, 3×100 mL). Sat. aq. NaHCO_3 was added taking the aqueous layer to pH 7 and the mixture was extracted into Et_2O (3×100 mL). Organic extracts were combined and washed with brine (2×100 mL), dried over MgSO_4 and concentrated under vacuum. Slow crystallisation from MeCN provided crystals suitable for single crystal X-ray analysis. \ddagger Recrystallisation from DCM-hexane afforded boronic acid **6a** as a white solid; yield: 2.71 g (72%); mp $110\text{--}111\text{ }^{\circ}\text{C}$; ^1H NMR (500 MHz, CDCl_3): δ = 1.10 (d, $J = 7.0$ Hz, 12H, $(\text{CH}_3)_2\text{CH}$), 3.08 (septet, $J = 7.0$ Hz, 2H, $(\text{CH}_3)_2\text{CH}$), 3.82 (s, 2H, ArCH $_2$), 6.97–7.03 (m, 1H ArH), 7.07 (d, $J = 7.5$ Hz, 1H, ArH), 7.30 (td, $J_{\text{HH}} = 7.5$ Hz and $J_{\text{FH}} = 6.5$ Hz, 1H, ArH), 9.27 (br s, 2H, B(OH) $_2$); ^{13}C NMR (125.7 MHz, CDCl_3): δ = 19.9 ($(\text{CH}_3)_2\text{CH}$), 47.7 ($(\text{CH}_3)_2\text{CH}$), 52.0 (d, $^4J_{\text{FC}} = 2$ Hz, ArCH $_2$), 115.4 (d, $^2J_{\text{FC}} = 28$ Hz, ArC), 127.7 (d, $^4J_{\text{FC}} = 2$ Hz, ArC), 131.7 (d, $^3J_{\text{FC}} = 11$ Hz, ArC), 144.7 (d, $^3J_{\text{FC}} = 8$ Hz, ArCCH $_2$ N i Pr $_2$), 168.0 (d, $^3J_{\text{FC}} = 244$ Hz, ArC–F); ^{11}B NMR (128.4 MHz, CDCl_3): δ = 28.4;

^{19}F NMR (376.3 MHz, CDCl_3): δ = -104.5 (m); IR (film): ν_{max} (inter alia) = 3307, 2971, 2539, 1604, 1565, 1450 (s), 1385 (vs), 1144 (s) cm^{-1} ; λ_{max} (MeCN)/nm 194 ($\epsilon/\text{dm}^3 \text{mol}^{-1} \text{cm}^{-1}$ 10000), 216 (6970), 272 (1280); MS (ES): m/z (%) = 254.1722 (100, $[\text{M} + \text{H}]^+$). $[\text{C}_{13}\text{H}_{22}\text{BFNO}_2]^+$ requires 246.1265; elemental analysis (%): calcd. for $\text{C}_{13}\text{H}_{29}\text{BFNO}_2$: C 61.69, H 8.36, N 5.53; found: C 61.53, H 8.41, N 5.30.

N,N-Di-isopropyl-3-methoxybenzamide **4b**

To a stirred solution of *m*-anisoyl chloride (0.82 mL, 6 mmol) in dry Et_2O (25 mL) under Ar at $0\text{ }^{\circ}\text{C}$, was added dry diisopropylamine (2.1 mL, 15 mmol) dropwise. The reaction was allowed to warm to rt, stirred for 3 h and then quenched with 5% (w/v) HCl (25 mL). The organic layer was separated and washed again with 5% (w/v) HCl (2×25 mL), brine (25 mL), 5% (w/v) NaOH (2×25 mL), brine (25 mL), dried over MgSO_4 , and concentrated under vacuum to afford amide **4b** as a white solid; yield: 1.38 g (98%); mp $92\text{--}93\text{ }^{\circ}\text{C}$; ^1H NMR (500 MHz, CDCl_3): δ = 1.16 (br s, 6H $(\text{CH}_3)_2\text{CH}$), 1.54 (br s, 6H, $(\text{CH}_3)_2\text{CH}$), 3.53 (br s, 1H, $(\text{CH}_3)_2\text{CH}$), 3.83 (s, 3H, OCH $_3$), 3.86 (br s, 1H, $(\text{CH}_3)_2\text{CH}$), 6.86 (s, 1H, ArH), 6.89 (d, $J = 8.0$ Hz, 1H, ArH), 6.91 (d, $J = 8.0$ Hz, 1H, ArH), 7.61 (t, $J = 8.0$ Hz, 1H, ArH); ^{13}C NMR (125.7 MHz, CDCl_3): δ = 20.8 ($(\text{CH}_3)_2\text{CH}$), 46.0 (br s $(\text{CH}_3)_2\text{CH}$), 51.0 (br s, $(\text{CH}_3)_2\text{CH}$), 55.4 (OCH $_3$), 111.1 (ArC), 114.7 (ArC), 117.8 (ArC), 129.7 (ArC), 140.3 (ArC–OMe), 159.7 (ArC–CON i Pr $_2$), 170.9 (CON i Pr $_2$); IR (film): ν_{max} (inter alia) = 3090, 2974, 1621 (vs), 1578, 1340 (vs), 1293, 1032 cm^{-1} ; λ_{max} (MeCN)/nm 200 ($\epsilon/\text{dm}^3 \text{mol}^{-1} \text{cm}^{-1}$ 21300) and 280 (2290); MS (ES): m/z (%) = 236.1646 (100, $[\text{M} + \text{H}]^+$). $[\text{C}_{14}\text{H}_{21}\text{NO}_2]^+$ requires 236.1645; elemental analysis (%): calcd. for $\text{C}_{14}\text{H}_{21}\text{NO}_2$: C 71.46, H 8.99, N 5.95; found: C 71.45, H 9.07, N 5.81.

N,N-Di-isopropyl-3-methoxy-2-(4,4,5,5-tetramethyl-[1,3,2]dioxaborolan-2-yl)-benzamide **5b**

To a stirred solution of **4b** (1.75 g, 7.44 mmol) and TMEDA (1.56 mL, 10.4 mmol) in dry THF (25 mL) under Ar at $-78\text{ }^{\circ}\text{C}$, was added *s*-BuLi (7.44 mL, 1.4 M, 10.4 mmol) dropwise over 10 min. Mixture left to stir for 90 min and then triisopropyl borate (1.89 mL, 8.18 mmol) was added rapidly. Mixture allowed to reach rt overnight (19 h) and then quenched with 20% (w/v) HCl (6 mL), followed by addition of pinacol (0.97 g, 8.18 mmol). Mixture allowed to stir for 10 min before being extracted into ether (3×20 mL) and the organic extracts washed with sat. aq. NaHCO_3 (3×10 mL), and brine (20 mL). Extracts were dried over MgSO_4 and concentrated under vacuum. Column chromatography on silica gel (hexane : EtOAc, 1 : 1) afforded pinacol boronate **5b** as a white solid; yield: 2.05 g (76%); mp $90\text{--}91\text{ }^{\circ}\text{C}$; ^1H NMR (500 MHz, CDCl_3): δ = 1.19 (br s, 6H, $(\text{CH}_3)_2\text{CH}$), 1.35 (s, 12H, $4 \times \text{Me}$), 1.54 (br s, 6H, $(\text{CH}_3)_2\text{CH}$), 3.50 (br s, 1H, $(\text{CH}_3)_2\text{CH}$), 3.81 (s, 3H, OMe), 4.00 (br s, 1H, $(\text{CH}_3)_2\text{CH}$), 6.82 (d, $J = 8.0$ Hz, 2H, ArH), 7.28 (1H, t, $J = 8.0$ Hz, ArH); ^{13}C NMR (125.7 MHz, CDCl_3): δ = 20.7 (br s, $(\text{CH}_3)_2\text{CH}$), 25.0 (pinacol CH_3), 46.3 (br s, $(\text{CH}_3)_2\text{CH}$), 51.0 (br s, $(\text{CH}_3)_2\text{CH}$), 55.8 (OMe), 83.5 (pinacol C–O), 110.7 (ArC), 117.3 (ArC), 130.3 (ArC), 144.0 (ArC–CON i Pr $_2$), 163.4 (ArC–OMe), 171.4 (CON i Pr $_2$); ^{11}B NMR (128.4 MHz, CDCl_3): δ = 29.0; IR (film): ν_{max} (inter

alia) = 2973, 1615 (s), 1431, 1335 (vs), 1146 cm^{-1} ; MS (ES): m/z (%) = 362.2497 (100, $[\text{M} + \text{H}]^+$). $[\text{C}_{20}\text{H}_{33}\text{BNO}_4]^+$ requires 362.2497; elemental analysis (%): calcd. for $\text{C}_{20}\text{H}_{32}\text{BNO}_4$: C 66.49, H 8.93, N 3.88; found: C 66.22, H 8.98, N 3.82.

N,N-Di-isopropyl-3-methoxybenzylamine-2-boronic acid **6b**

To a stirred solution of **5b** (0.99 g, 2.74 mmol) and NaBH_4 (1.04 g, 27.4 mmol) in dry THF (50 mL) under Ar was added TMSCl (6.95 mL, 54.8 mmol) and the mixture stirred at reflux for 21 h. Reaction quenched by slow addition of 5% (w/v) HCl (7 mL) and THF removed *in vacuo*. A further portion of 5% (w/v) HCl (15 mL) was added (aqueous layer to pH 1) and extracted into Et_2O (1 \times 25 mL, 2 \times 15 mL). Et_2O extracts washed with 5% (w/v) HCl (5 mL) and combined aqueous phase washed with Et_2O (2 \times 10 mL). Aqueous neutralised with NaOH (s) then 20% (w/v) NaOH until no further precipitation of white solid was observed (pH 9). The mixture was extracted into DCM (3 \times 15 mL), organic extracts were combined, washed with brine (15 mL), dried over MgSO_4 and concentrated under vacuum. Recrystallisation from hexane afforded boronic acid **6b** as a white solid; yield: 0.36 g (50%); mp 164–165 $^\circ\text{C}$; ^1H NMR (400 MHz, CDCl_3): δ = 1.11 (d, J = 6.8 Hz, 12H, $(\text{CH}_3)_2\text{CH}$), 3.10 (septet, J = 6.8 Hz, 2H, $(\text{CH}_3)_2\text{CH}$), 3.80 (s, 2H, ArCH_2), 3.89 (s, 3H, OMe), 6.90 (d, J = 8.0 Hz, 1H, ArH), 6.93 (d, J = 7.6 Hz, 1H, ArH), 7.31 (dd, $J_{\text{HH}} = 8.4$ Hz and $J_{\text{FH}} = 7.6$ Hz, 1H, ArH), 9.75 (br s, 2H, $\text{B}(\text{OH})_2$); ^{13}C NMR (100.6 MHz, CDCl_3): δ = 19.9 ($(\text{CH}_3)_2\text{CH}$), 47.5 ($(\text{CH}_3)_2\text{CH}$), 52.4 (ArCH_2), 56.0 (OMe), 110.5 (ArC), 125.6 (ArC), 131.2 (ArC), 144.8 (ArC), 164.8 (ArC-OMe); ^{11}B NMR (128.4 MHz, CDCl_3): δ = 29.3; IR (KBr): ν_{max} (inter alia) = 3414, 2965, 1597 (s), 1466 (s), 1249 (s), 1084 cm^{-1} ; MS (ES): m/z (%) = 266.1923 (100, $[\text{M} + \text{H}]^+$). $[\text{C}_{14}\text{H}_{25}\text{BNO}_3]^+$ requires 266.1922; elemental analysis (%): calcd. for $\text{C}_{14}\text{H}_{24}\text{BNO}_3$: C 63.42, H 9.12, N 5.28; found: C 63.82, H 9.04, N 5.16.

N,N-Di-isopropyl-3-nitrobenzamide **4c**

To a stirred solution of 3-nitrobenzoyl chloride (1.41 g, 6.71 mmol) in dry Et_2O (25 mL) under Ar at 0 $^\circ\text{C}$, was added dry di-isopropylamine (2.7 mL, 19 mmol). The reaction was allowed to warm to rt, stirred for 18 h and then quenched with 5% (w/v) HCl (25 mL). The organic layer was separated and washed again with 5% (w/v) HCl (2 \times 25 mL), then brine (25 mL), 5% (w/v) NaOH (2 \times 25 mL), brine (25 mL), dried over MgSO_4 , and concentrated under vacuum to afford amide **4c** (1.66 g, 87%) as a white solid; yield: 1.66 g (87%); mp 78–79 $^\circ\text{C}$; ^1H NMR (500 MHz, CDCl_3): δ = 1.21 (br s, 6H, $(\text{CH}_3)_2\text{CH}$), 1.56 (br s, 6H, $(\text{CH}_3)_2\text{CH}$), 3.52 (br s, 1H, $(\text{CH}_3)_2\text{CH}$), 3.55 (br s, 1H, $(\text{CH}_3)_2\text{CH}$), 7.60 (t, J = 8.1 Hz, 1H, ArH), 7.67 (d, J = 8.1 Hz, 1H, ArH), 8.20 (s, 1H, ArH), 8.25 (d, J = 8.1 Hz, 1H, ArH); ^{13}C NMR (125.7 MHz, CDCl_3): δ = 20.9 (br s, $(\text{CH}_3)_2\text{CH}$), 46.5 (br s, $(\text{CH}_3)_2\text{CH}$), 51.5 (br s, $(\text{CH}_3)_2\text{CH}$), 121.2 (ArC), 123.8 (ArC), 130.0 (ArC), 132.0 (ArC), 140.5 ($\text{ArC-CON}^i\text{Pr}_2$), 148.3 (ArC-NO_2), 168.4 (CON^iPr_2); IR (film): ν_{max} = 2930, 1625 (s), 1527, 1438, 1334, 1153; λ_{max} (MeCN)/nm 194 ($\epsilon/\text{dm}^3 \text{ mol}^{-1} \text{ cm}^{-1}$ 24000), 252 (6960); MS (ES): m/z (%) = 273.1203 (100, $[\text{M} + \text{Na}]^+$). $[\text{C}_{13}\text{H}_{18}\text{N}_2\text{O}_3\text{Na}]^+$ requires 273.1210; elemental analysis (%):

calcd. for $\text{C}_{13}\text{H}_{18}\text{N}_2\text{O}_3$: C 62.38, H 7.25, N 11.19; found: C 62.34, H 7.27, N 11.18.

N,N-Di-isopropyl-3-trifluoromethylbenzamide **8**

To a stirred solution of 3-(trifluoromethyl)benzoyl chloride (1.78 mL, 12 mmol) in dry Et_2O (30 mL) under Ar at 0 $^\circ\text{C}$, was added dry di-isopropylamine (4.24 mL, 30 mmol) dropwise. The reaction was allowed to warm to rt, stirred for 2 h and then quenched with 5% (w/v) HCl (25 mL). The organic layer was separated and washed again with 5% (w/v) HCl (25 mL), then brine (25 mL), 5% (w/v) NaOH (2 \times 25 mL), brine (25 mL), dried over MgSO_4 , and concentrated under vacuum to afford amide **8** as a white solid; yield: 3.23 g (98%); mp 58–59 $^\circ\text{C}$; ^1H NMR (500 MHz, CDCl_3): δ = 1.17 (br s, 6H, $(\text{CH}_3)_2\text{CH}$), 1.53 (br s, 6H, $(\text{CH}_3)_2\text{CH}$), 3.57 (br s, 1H, $(\text{CH}_3)_2\text{CH}$), 3.72 (br s, 1H, $(\text{CH}_3)_2\text{CH}$), 7.47–7.54 (m, 2H, ArH), 7.57 (s, 1H, ArH), 7.63 (d, J = 8.5 Hz, 1H, ArH); ^{13}C NMR (100.6 MHz, CDCl_3): δ = 20.8 ($(\text{CH}_3)_2\text{CH}$), 46.3 (br s, $(\text{CH}_3)_2\text{CH}$), 51.3 (br s, $(\text{CH}_3)_2\text{CH}$), 122.8 (q, $^3J_{\text{FC}} = 4$ Hz, ArC), 123.9 (q, $^1J_{\text{FC}} = 273$ Hz, CF_3), 125.6 (q, $^3J_{\text{FC}} = 4$ Hz, ArC), 129.1 (ArC), 129.2 (ArC), 131.1 (q, $^2J_{\text{FC}} = 33$ Hz, ArC-CF_3), 139.6 ($\text{ArC-CON}^i\text{Pr}_2$), 169.5 (CON^iPr_2); ^{19}F NMR (376.3 MHz, CDCl_3): δ = -63.2 (s); IR (film): ν_{max} = 2970, 1621 (s), 1373, 1311 (s), 1162, 1123 cm^{-1} ; λ_{max} (MeCN)/nm 200 ($\epsilon/\text{dm}^3 \text{ mol}^{-1} \text{ cm}^{-1}$ 22300), 252 (7150); MS (ES): m/z (%) = 274.1413 (100, $[\text{M} + \text{H}]^+$). $[\text{C}_{14}\text{H}_{19}\text{F}_3\text{NO}]^+$ requires 274.1413; elemental analysis (%): calcd. for $\text{C}_{14}\text{H}_{18}\text{F}_3\text{NO}$: C 61.53, H 6.64, N 5.13; found: C 61.24, H 6.59, N 4.96.

N,N-Di-isopropyl-2-(4,4,5,5-tetramethyl-1,3,2-dioxaborolan-2-yl)-5-trifluoromethyl-benzamide **9**

To a stirred solution of **6** (1.01 g, 3.70 mmol) in dry THF (20 mL) under Ar at -78 $^\circ\text{C}$, was added LDA (2.47 mL, 1.8 M, 4.44 mmol) dropwise over 15 min. Mixture left to stir for 70 min and then triisopropyl borate (0.94 mL, 4.07 mmol) was added rapidly. Mixture allowed to reach rt overnight (17 h) and then quenched with 20% (w/v) HCl (6 mL), followed by addition of pinacol (0.48 g, 4.07 mmol). Mixture allowed to stir for 15 min before being extracted into ether (2 \times 20 mL, 1 \times 10 mL) and the organic extracts washed with sat. aq. NaHCO_3 (3 \times 10 mL), and brine (20 mL). Extracts were dried over MgSO_4 and concentrated under vacuum. Column chromatography on silica gel (hexane : EtOAc , 4 : 1) afforded pinacol boronate **9** as a white solid; yield 1.40 g (95%); mp 130–131 $^\circ\text{C}$; ^1H NMR (500 MHz, CDCl_3): δ = 1.13 (d, J = 6.5 Hz, 6H, $(\text{CH}_3)_2\text{CH}$), 1.32 (s, 12H, 4 \times Me), 1.58 (d, J = 6.5 Hz, 6H, $(\text{CH}_3)_2\text{CH}$), 3.53 (m, 1H, $(\text{CH}_3)_2\text{CH}$), 3.63 (m, 1H, $(\text{CH}_3)_2\text{CH}$), 7.39 (s, 1H, ArH), 7.56 (d, J = 8.5 Hz, 1H, ArH), 7.91 (d, J = 7.5 Hz, 1H, ArH); ^{13}C NMR (125.7 MHz, CDCl_3): δ = 20.3 ($(\text{CH}_3)_2\text{CH}$), 20.5 ($(\text{CH}_3)_2\text{CH}$), 25.0 (pinacol CH_3), 46.1 ($(\text{CH}_3)_2\text{CH}$), 51.2 ($(\text{CH}_3)_2\text{CH}$), 84.4 (pinacol C-O), 121.4 (q, $^3J_{\text{FC}} = 4$ Hz, ArC), 123.9 (q, $^1J_{\text{FC}} = 273$ Hz, CF_3), 124.1 (q, $^3J_{\text{FC}} = 4$ Hz, ArC), 132.5 (q, $^2J_{\text{FC}} = 33$ Hz, ArC-CF_3), 136.2 (ArC), 145.6 ($\text{ArC-CON}^i\text{Pr}_2$), 169.9 (CON^iPr_2); ^{11}B NMR (160.3 MHz, CDCl_3): δ = 29.8; ^{19}F NMR (470.3 MHz, CDCl_3): δ = -63.5 (s); IR (film): ν_{max} = 2978, 1627 (s), 1312 (vs), 1132 (vs) cm^{-1} ; MS (ES): m/z (%) = 400.2265 (100, $[\text{M} + \text{H}]^+$). $[\text{C}_{20}\text{H}_{30}\text{BF}_3\text{NO}_3]^+$ requires 400.2265; elemental analysis (%):

calcd. for $C_{20}H_{29}BF_3NO_3$: C 60.17, H 7.32, N 3.51; found: C 60.37, H 7.34, N 3.38.

N,N-Di-isopropyl-5-trifluoromethylbenzylamine-2-boronic acid **10**

To a stirred solution of **7** (1.00 g, 2.50 mmol) and $NaBH_4$ (0.95 g, 25.0 mmol) in dry THF (50 mL) under Ar was added $TMSCl$ (6.35 mL, 50.0 mmol) and the mixture stirred at reflux for 21 h. Reaction quenched by slow addition of 5% (w/v) HCl (7 mL) and THF removed *in vacuo*. A further portion of 5% (w/v) HCl (5 mL) was added (aqueous layer to pH 1) and extracted into Et_2O (3×15 mL). Et_2O extracts washed with 5% (w/v) HCl (5 mL) and combined aqueous phase washed with Et_2O (2×10 mL). Aqueous neutralised to pH 7 with NaOH (s) then 20% (w/v) NaOH and extracted into DCM (3×15 mL). Combined organic extracts were washed with brine (15 mL), dried over $MgSO_4$ and concentrated under vacuum. Recrystallisation from MeCN- H_2O afforded boronic acid **10** as a white crystalline solid (crystals suitable for single crystal X-ray analysis[†]); yield: 0.45 g (60%); mp 115–116 °C; 1H NMR (400 MHz, $CDCl_3$): δ = 1.14 (d, J = 6.8 Hz, 12H, $(CH_3)_2CH$), 3.13 (septet, J = 6.8 Hz, 2H, $(CH_3)_2CH$), 3.90 (s, 2H, Ar CH_2), 7.47 (s, 1H, ArH), 7.55 (d, J = 7.6 Hz, 1H, ArH), 8.10 (d, J = 8.0 Hz, 1H, ArH), 10.28 (br s, 2H, B(OH) $_2$); ^{13}C NMR (100.6 MHz, $CDCl_3$): δ = 19.8 ($(CH_3)_2CH$), 47.9 ($(CH_3)_2CH$), 51.9 (Ar CH_2), 123.8 (q, $^3J_{FC}$ = 4 Hz, ArC), 124.2 (q, $^1J_{FC}$ = 272 Hz, CF_3), 127.0 (q, $^3J_{FC}$ = 4 Hz, ArC), 132.0 (q, $^2J_{FC}$ = 32 Hz, ArC- CF_3), 137.3 (ArC), 143.2 (ArC); ^{11}B NMR (128.4 MHz, $CDCl_3$): δ = 28.5; ^{19}F NMR (376.3 MHz, $CDCl_3$): δ = -63.3 (s); IR (film): ν_{max} = 3324, 2978, 1328 (s), 1166 (s), 1112 (vs) cm^{-1} ; MS (ES): m/z (%) = 304.2 (100, $[M + H]^+$); elemental analysis (%): calcd. for $C_{14}H_{21}BF_3NO_2$: C 55.47, H 6.98, N 4.62; found: C 55.22, H 6.85, N 4.46.

General procedure for DoE on formation of *N*-benzylbenzamide

Benzoic acid (1, 3 or 5 mmol) was weighed into ReactArray tubes to give appropriate reaction concentration (0.1, 0.3 or 0.5 M) followed by catalyst **1** (1, 5.5 or 10 mol%). ReactArray azeotroping condenser set assembled, naphthalene (25 mol%) as a 0.5 M standard solution, and fluorobenzene or toluene were added to give a final reaction volume of 10.6 mL. Mixture heated to reflux under nitrogen and benzylamine (1, 3 or 5 mmol) was added. Reaction stirred at reflux with sampling at 4 h intervals. Samples were subjected to the following quench/dilution protocols:

- 0.1 M: 90 μ L into 910 μ L MeCN
- 0.3 M: 50 μ L into 1650 μ L MeCN
- 0.5 M: 100 μ L into 900 μ L MeCN, 176 μ L into 824 μ L MeCN

Samples were mixed and analysed by HPLC (MeCN (0.05% TFA) : water (0.05% TFA) 0 : 100 to 100 : 0 over 15 min; 1 mL min^{-1} ; t_r = 9.12 min). Naphthalene was used as an internal standard.

General procedure for catalyst screen on *N*-benzylbenzamide formation

The appropriate catalyst (0.233 mmol, 10 mol%) was manually weighed into each reaction vessel, followed by assembly of a

micro-Soxhlet apparatus loaded with activated 3Å molecular sieves under argon. Solid reagents were added using the ReactArray as standard solutions (0.5 M in fluorobenzene). Naphthalene (0.35 mmol, 15 mol%) and amine (2.33 mmol) were added to the reaction vessels at ambient temperature. The appropriate amount of fluorobenzene was then added to each reaction vessel in order to give a final reaction volume of 10 mL. After heating to reflux, carboxylic acid (2.33 mmol) was added to the stirred solution. Reactions were sampled (50 μ L) at 2 or 4 h intervals (24 or 48 h reaction time, respectively). Samples were quenched with MeCN (950 μ L), diluted once (50 μ L in 950 μ L MeCN) mixed and analysed by HPLC (gradient MeCN (0.05% TFA) : water (0.05% TFA) 0 : 100 to 100 : 0 over 15; 1 mL min^{-1} ; t_r = 9.12 min). Naphthalene was used as an internal standard, with response factors calculated automatically by ReactArray DataManager.

General procedure for isolation of amides (fluorobenzene)

A round-bottomed flask was equipped with stirrer bar, pressure equalising dropping funnel (in vertical neck) with a soxhlet thimble containing CaH_2 (~1 g), followed by a condenser. The appropriate carboxylic acid (5 mmol), followed by fluorobenzene (50 mL), and amine (5 mmol) were added, followed by **1** (117.6 mg, 0.5 mmol). The mixture was allowed to stir at reflux for 22, 24 or 48 h, before being concentrated under vacuum. The residue was then redissolved in DCM (25 mL), washed with brine (25 mL), 5% (w/v) HCl (25 mL), brine (25 mL), 5% (w/v) NaOH (25 mL), brine (25 mL), dried over $MgSO_4$, and the solvent evaporated under vacuum.

N-Benzyl-4-phenylbutyramide:¹⁷ yield: 0.86 g (68%)

N-4-Phenylbutyl-4-phenylbutyramide:¹⁰ yield: 1.03 g (70%)

1-Morpholin-4-yl-4-phenylbutan-1-one: yield: 0.78 g (67%)

1H NMR (400 MHz, $CDCl_3$): δ = 1.98 (quintet, J = 7.6 Hz, 2H, CH_2), 2.31 (t, J = 7.6 Hz, 2H, CH_2), 2.68 (t, J = 7.6 Hz, 2H, CH_2), 3.35–3.39 (m, 2H, morpholino), 3.58–3.68 (m, 4H, morpholino), 7.16–7.22 (m, 3H, ArH), 7.25–7.31 (m, 2H, ArH); ^{13}C NMR (100.6 MHz, $CDCl_3$): δ = 26.7 (CH_2), 32.2 (CH_2), 35.4 (CH_2), 42.0 (CH_2N), 46.1 (CH_2N), 66.8 (CH_2O), 67.1 (CH_2O), 126.1 (ArC), 128.5 (ArC), 128.6 (ArC), 141.7 (ArC), 171.6 (CON); IR (film): ν_{max} (inter alia) = 2856, 1647 (vs), 1433 (s), 1116 (s) cm^{-1} ; MS (ES): m/z (%) = 234.2 (100) $[M + H]^+$; elemental analysis (%): calcd. for $C_{14}H_{19}NO_2$: C 72.07, H 8.21, N 6.00; found: C 71.91, H 8.24, N 6.12.

N-(1-Phenylethyl)-4-phenylbutyramide:^{7f} yield: 0.71 g (53%)

N-Benzylbenzamide:¹⁸ yield: 0.53 g (50%)

N-Phenyl-4-phenylbutyramide^{7a}

To a stirred solution of 4-phenylbutyric acid (0.821 g, 5 mmol) in toluene (50 mL), was added aniline (0.46 mL, 5 mmol) followed by catalyst **4c** (11.8 mg, 0.05 mmol). The mixture was allowed to stir at reflux for 22 h, before being concentrated under vacuum. The residue was then redissolved in Et_2O (25 mL), washed with brine (25 mL), 5% (w/v) HCl (25 mL), brine (25 mL),

5% (w/v) NaOH (25 mL), brine (25 mL), dried over MgSO₄, and the solvent evaporated under vacuum; yield: 0.60 g (50%).

N-(1-Phenyl)ethylbenzamide¹⁹

Catalyst **1** (54.8 mg, 0.233 mmol) was weighed into a ReactArray tube, followed by assembly of a micro-Soxhlet apparatus loaded with activated 3Å molecular sieves under argon. Solid reagents were added using the ReactArray as standard solutions (0.5 M in fluorobenzene). Naphthalene (44.9 mg, 0.35 mmol), α -methylbenzylamine (301 μ L, 2.33 mmol) and fluorobenzene (4.63 mL) were added to the reaction vessel at ambient temperature. After heating to reflux, benzoic acid (0.285 g, 2.33 mmol) was added to the stirred solution. Reaction was sampled (50 μ L) at 4 h intervals over 48 h. Samples were quenched with MeCN (950 μ L), diluted once (50 μ L in 950 μ L MeCN) mixed and analysed by HPLC (gradient MeCN (0.05% TFA) : water (0.05% TFA) 0 : 100 to 100 : 0 over 31 min; 1 mL min⁻¹). Naphthalene was used as an internal standard, with response factors calculated automatically by ReactArray DataManager. Yield: 0.27 g (52%); HPLC: t_r = 16.10 min.

General procedure for isolation of amides (toluene)

The appropriate carboxylic acid (1 mmol) and catalyst **1** (23.5 mg, 0.1 mmol or 11.8 mg, 0.05 mmol) were weighed into ReactArray tubes followed by attachment of a ReactArray azeotropic condenser set. The appropriate amount of toluene was added to give a final reaction volume of 10 mL and the mixture heated to reflux under nitrogen. The appropriate amine (1 mmol) was added and the mixture stirred at reflux for 24 or 30 h, before being concentrated under vacuum. The residue was then redissolved in MTBE (10 mL), washed with 5% (w/v) HCl (10 mL), brine (10 mL), 5% (w/v) NaOH (10 mL), brine (10 mL), dried over MgSO₄, and the solvent evaporated under vacuum.

N-4-Phenylbutylbenzamide:¹⁰ yield: 0.18 g (71%)

Morpholin-4-yl-phenylmethanone:²⁰ yield: 0.04 g (21%).

N-(1-Phenyl)ethylbenzamide:¹⁹ yield: 0.16 g (71%).

N-Benzylpivalamide:^{7g} yield: 0.11 g (59%).

Acknowledgements

We thank the EPSRC for a research grant and DTA studentship (KA), and GlaxoSmithKline for CASE funding (KA) and the National Mass Spectrometry Service at Swansea.

References

- 1 A. W. Hofmann, *Chem. Ber.*, 1882, **15**, 977–978.
- 2 (a) J. A. Mitchell and E. E. Reid, *J. Am. Chem. Soc.*, 1931, **53**, 1879–1883; (b) D. Davidson and P. Newman, *J. Am. Chem. Soc.*, 1952, **74**, 1515–1516; (c) B. S. Jursic and Z. Zdravkovski, *Synth. Commun.*, 1993, **23**, 2761–2770.
- 3 (a) Y. I. Leitman and M. S. Pevzner, *Zh. Prikl. Khim.*, 1963, **36**, 632–639; (b) W. Walter, H. Besendorf and O. Schnider, *Helv. Chim. Acta*, 1961, **44**, 1546–1554.
- 4 (a) M. P. Vazquez-Tato, *Synlett*, **1993**, 506–506; (b) L. Perreux, A. Loupy and F. Volatron, *Tetrahedron*, 2002, **58**, 2155–2162.
- 5 (a) T. Ziegler, *Science of Synthesis*, ed. S. M. Weinreb, Thieme, Stuttgart, 2005, vol. **21**, pp. 43–76; (b) G. Benz, *Comprehensive Organic Synthesis*, ed. B. M. Trost, I. Fleming, Pergamon, Oxford, 1991, vol. **6**, pp. 381–417.
- 6 (a) A. Pelter, T. E. Levitt and P. Nelson, *Tetrahedron*, 1970, **26**, 1539–1544; (b) R. Latta, G. Springsteen and B. Wang, *Synthesis*, 2001, 1611–1613; (c) W. Yang, X. Gao, G. Springsteen and B. Wang, *Tetrahedron Lett.*, 2002, **43**, 6339–6342.
- 7 (a) K. Ishihara, H. Kurihara and H. Yamamoto, *J. Org. Chem.*, 1996, **61**, 4196–4197; (b) K. Ishihara, S. Ohara and H. Yamamoto, *Macromolecules*, 2000, **33**, 3511–3513; (c) K. Ishihara, S. Kondo and H. Yamamoto, *Synlett*, 2001, 1371–1374; (d) K. Ishihara, S. Kondo and H. Yamamoto, *Org. Synth.*, 2002, **79**, 176–185; (e) T. Maki, K. Ishihara and H. Yamamoto, *Org. Lett.*, 2007, **63**, 8645–8657; (f) T. Maki, K. Ishihara and H. Yamamoto, *Org. Lett.*, 2006, **8**, 1431–1434; (g) T. Maki, K. Ishihara and H. Yamamoto, *Tetrahedron*, 2006, **8**, 1431–1434.
- 8 P. Tang, *Org. Synth.*, 2002, **81**, 262–272.
- 9 (a) R. L. Giles, J. A. K. Howard, L. G. F. Patrick, M. R. Probert, G. E. Smith and A. Whiting, *J. Organomet. Chem.*, 2003, **680**, 257–262; (b) S. W. Coghlan, R. L. Giles, J. A. K. Howard, M. R. Probert, G. E. Smith and A. Whiting, *J. Organomet. Chem.*, 2005, **690**, 4784–4793; (c) A. J. Blatch, O. V. Chetina, J. A. K. Howard, L. G. F. Patrick, C. A. Smethurst and A. Whiting, *Org. Biomol. Chem.*, 2006, **4**, 3297–3302.
- 10 K. Arnold, B. Davies, R. L. Giles, C. Grosjean, G. E. Smith and A. Whiting, *Adv. Synth. Catal.*, 2006, **348**, 813–820.
- 11 G. Köbrich and P. Buck, *Chem. Ber.*, 1970, **103**, 1412–1419.
- 12 (a) M. Schlosser, F. Mongin, J. Porwisiak, W. Dmowski, H. H. Bükler and N. M. M. Nibbering, *Chem.–Eur. J.*, 1998, **4**, 1281–1286; (b) M. Schlosser and M. Marull, *Eur. J. Org. Chem.*, 2003, 1569–1575.
- 13 (a) For example: V. K. Aggarwal, A. C. Staubitz and M. Owen, *Org. Process Res. Dev.*, 2006, **10**, 64–69; (b) R. Carlson and J. E. Carlson, *Design and Optimization in Organic Synthesis*, Elsevier, Amsterdam, 2005.
- 14 The penalty for reducing the number of experiments is one factor interactions are aliased with three factor interactions, and two factor interactions are aliased with other two factor interactions.
- 15 The thermal reaction is not significant in either fluorobenzene or toluene in this case (0% and 5% conversion in 24 h, respectively).
- 16 T. Hudlicky, D. A. Frey, L. Koroniak, C. D. Claeboe and L. E. Brammer, *Green Chem.*, 1999, 57–59.
- 17 R. Verma and S. K. Ghosh, *J. Chem. Soc., Perkin Trans. 1*, 1998, 2377–2382.
- 18 N. Shangguan, S. Katukojvala, R. Greenberg and L. J. Williams, *J. Am. Chem. Soc.*, 2003, **125**, 7754–7755.
- 19 M. Noji, T. Ohno, K. Fujii, N. Futaba, H. Tajima and K. Ishii, *J. Org. Chem.*, 2003, **68**, 9340–9347.
- 20 J. D. Moore, R. J. Byrne, P. Vedantham, D. L. Flynn and P. R. Hanson, *Org. Lett.*, 2003, **5**, 4241–4244.

Achieving great heights

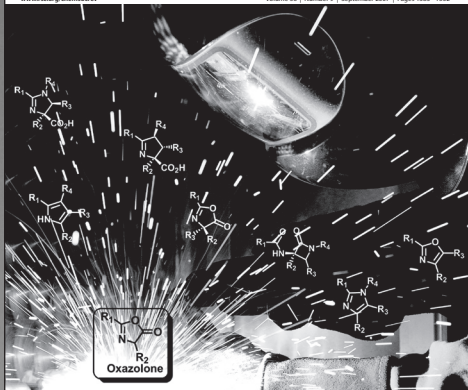
The latest impact
factor of 13.69*
says it all.

Chem Soc Rev

Chemical Society Reviews

www.rsc.org/chemsocrev

Volume 36 | Number 9 | September 2007 | Pages 1385–1532



RSC Publishing

TUTORIAL REVIEW
Jacob S. Fisk, Robert A. Mosay and
Janet J. Topik
The diverse chemistry of oxazol-5-
thione

TUTORIAL REVIEW
Ranjit Senanay and Steve Dong
The catalytic hydroamination of
alkynes



www.rsc.org/chemsocrev

Chemical Society Reviews publishes accessible, succinct and reader-friendly articles on topics of international, multidisciplinary and social interest in the chemical sciences. 12 monthly issues include special themed issues reviewing new areas of research, edited by a specialist guest editor. High visibility is ensured by indexing in a number of databases, including Medline.

Go online to find out more!

*2006 Thomson Scientific (ISI) Journal Citations Reports®

RSC Publishing

www.rsc.org/chemsocrev

Registered Charity Number 207890

Specialised searching

[View Online](#)

The graphical abstracting services at the RSC are an indispensable tool to help you search the literature. Focussing on specific areas of research they review key primary journals for novel and interesting chemistry.

requires specialised tools

Catalysts & Catalysed Reactions

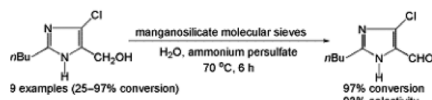
Catalysts and Catalysed Reactions covers all areas of catalysis research, with particular emphasis on chiral catalysts, polymerisation catalysts, enzymatic catalysts and clean catalytic methods.

The online database has excellent functionality. Search by: authors, products, reactants and catalysts, catalyst type and reaction type.

With Catalysts and Catalysed Reactions you can find exactly what you need. Search results include diagrams of reaction schemes. Also available as a print bulletin.

The screenshot shows the RSC Publishing website interface. It includes a search bar, navigation menus, and a list of articles. One article is highlighted:

11086 The green catalytic oxidation of alcohols in water by using highly efficient manganosilicate molecular sieves
 H. G. Manyar; G. S. Chauré; A. Kumar*
Green Chem., 2006, 8(4), 344-348



Registered charity Number 207890

For more information visit

RSC Publishing

www.rsc.org/databases

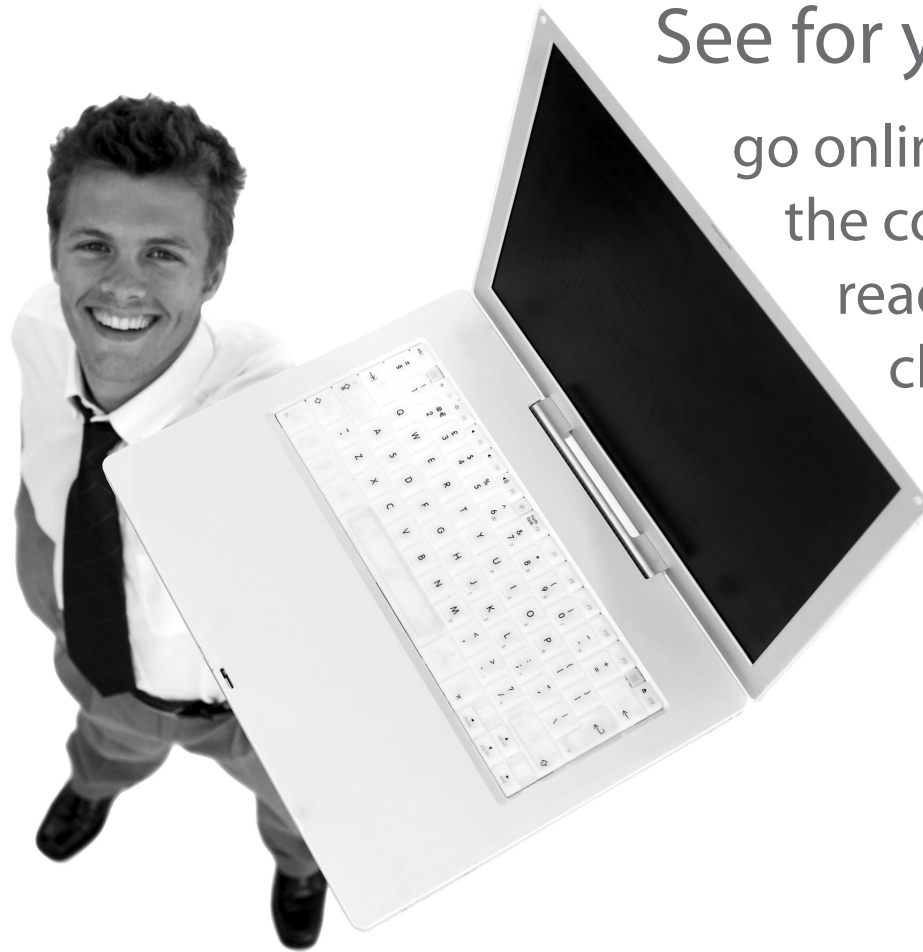
Registered Charity Number 207890

RSC eBook Collection

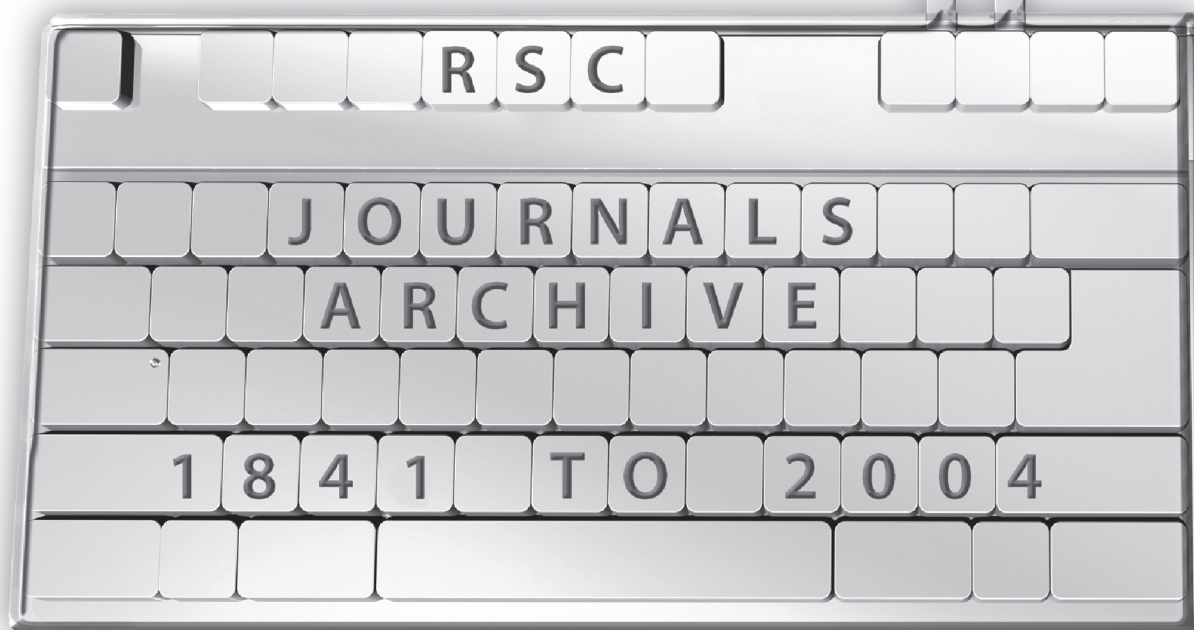
Access and download existing and new books from the RSC

- **Comprehensive:** covering all areas of the chemical sciences
- **Fully searchable:** advance search and filter options
- **Wide ranging:** from research level monograph to popular science book

See for yourself –
go online to search
the collection and
read selected
chapters
for free!



Chemical science research at your fingertips!



Featuring almost 1.4 million pages of ground-breaking chemical science in a single archive, the **RSC Journals Archive** gives you instant access to **over 238,000 original articles** published by the Royal Society of Chemistry (and its forerunner Societies) between 1840-2004.

The RSC Journals Archive gives a supreme history of top title journals including: *Chemical Communications*, *Dalton Transactions*, *Organic & Biomolecular Chemistry* and *Physical Chemistry Chemical Physics*.

As well as a complete set of journals with multi-access availability, the RSC Journals Archive comes in a variety of purchase options and available discounts.

For more information please contact sales@rsc.org

Celebrating the tenth year of the *Green Chemistry* journal

DOI: 10.1039/b718487p

This year *Green Chemistry* enters its tenth year of publishing. Since the first issue there have been a number of changes to the Journal, which has been growing from strength to strength. It is with thanks to our authors, the dedication of our referees and the guidance and enthusiasm of the Editorial and Advisory Board members that *Green Chemistry* has grown to be a high impact journal. This was recently emphasized by the ISI[®] 2006 impact factor of 4.192 for the Journal.

Looking back

Last year saw the start of the *Green Chemistry* sponsored lectures, which are designed to highlight green chemistry contributions at international conferences. The first of these was at the 90th Canadian Chemistry Conference in May and congratulations to Rick Danheiser who presented on “Organic Synthesis in Supercritical Carbon Dioxide and Related Environmentally Friendly Media”. The second was presented by Graham Hutchings at the 3rd International Conference on Green and Sustainable Chemistry in the Netherlands and was titled “Selective Oxidation Catalysis using Supported Gold and Palladium Nanoparticles”. A selection of papers from this meeting, including a contribution from Graham Hutchings, will be published in an issue of *Green Chemistry* early this year.

Looking forward

This year sees some changes to the Editorial Board, and we would like to sincerely thank departing board members Kyoko Nozaki and Roshan Jachuck for their contribution to the Journal during their time on the Editorial Board.

To mark the occasion of the tenth year of *Green Chemistry* we plan to publish a number of reviews representing the many areas of the subject green chemistry.

In this issue we are starting with the first review, a contribution from Professor Dr Arno Behr on the utilisation of

renewable resources (A. Behr, J. Eilting, K. Irawadi, J. Leschinski and F. Lindner, *Green Chem.*, 2008, **10**, DOI: 10.1039/b710561d).

This review is timely, as the chemical and biochemical conversion of renewable resources will undoubtedly continue to grow rapidly as a theme for green chemistry. The review highlights catalytic conversions of glycerol, the by-product of biodiesel production, to yield a range of important chemicals and materials. It demonstrates the broad potential of glycerol as raw material and also emphasises the need for efficient catalysts and catalytic processes to arrive at truly green routes starting from this renewable feedstock. Thus, it exemplifies nicely the importance of integrated product streams and synthetic pathway design, two major challenges to be met for a sustainable shift of the raw material basis.

Throughout the year we are organising celebrations for the 10th anniversary of the Journal and details of these events will be announced on the Journal website in due course. We hope that many of you will be able to join us for the celebrations.

News from the RSC

Award-winning technology and enhanced HTML articles

Launched in February 2007, *RSC Project Prospect* has had an exceptional first year. Bringing science alive via enhanced HTML articles in RSC journals, the project delivers: hyperlinked compound information (including downloadable structures) in text; links to IUPAC Gold Book terms; ontology terms linked to definitions and related articles; plus RSS feeds that include structured subject and compound information, enabling at-a-glance identification of relevant articles. As the only publisher able to offer these enhancements, we were delighted to be awarded the 2007 ALPSP/Charlesworth Award for Publishing Innovation, where judges

described *RSC Prospect* articles as “delightfully simple to use ... benefits to authors and readers are immediately obvious.” Around 1400 articles have now been published with enhanced HTML—to see for yourself, look out for the RSC Prospect icon on our website. Further developments to the project will be announced in 2008. Many of you have already told us how impressed you are with the project—www.projectprospect.org has examples of enhanced articles, feedback from the scientific community, plus the latest news.

Following feedback from journal readers a number of changes have been introduced across all RSC Journals. The *Green Chemistry* homepage now contains the contents list for the current issue, delivering the content you want to see as soon as you arrive at the site. Graphical abstracts are included as standard, allowing you to browse content much more conveniently. A more prominent and easy-to-use search box also makes finding published research much more intuitive. Advance Articles will soon also be available in pdf format.

For authors, the RSC Journal templates have been revised and updated to assist submission in a format similar to the journal layout. The guidelines for the use of colour in RSC Journals will be relaxed during 2008, and the decision on the free use of colour will be based on whether the use of colour *enhances* the scientific understanding of the figure (the old policy required the colour to be *essential*).

Energy & Environmental Science

RSC Publishing will be launching a new journal in summer 2008. *Energy & Environmental Science* will cover all aspects of the chemical sciences relating to energy conversion and storage and environmental science. Subscribers to *Green Chemistry* will have free online access to *Energy & Environmental Science* from launch. Visit the website for the latest news: www.rsc.org/ees.

'Green Chemistry book of choice' scheme

Launched in Spring 2007, the RSC eBook Collection offers scientists across the globe online access to a prestigious and wide ranging portfolio of chemical science books which span 40 years of research and opinion.

The RSC eBook Collection is testament to RSC's publishing innovation as well as the high quality of the content contained in our books. With further technical developments and new 2008 content being uploaded throughout the year, the RSC eBook Collection is set to become a key resource. To search the

Collection or for further information visit www.rsc.org/ebooks.

Scientists from all four corners of the globe are taking advantage of the *free* first chapter downloads and from January 2008, *Green Chemistry* will regularly highlight a book specifically for our readers through our 'Green Chemistry book of choice' scheme. More information is available on the *Green Chemistry* website.

If you would like to buy a print copy of the 'Green Chemistry book of choice' or other titles from the RSC, and you are an RSC author, editor or referee you can enjoy a special 25% discount on your

book purchase. You can redeem this offer online through the RSC Online Shop. To find out how to claim your exclusive discount, visit www.rsc.org/shop.

And finally...

We hope to have the opportunity to meet many of you during 2008. If you have any comments about the Journal please contact us at the following address: green@rsc.org.

Martyn Poliakoff, Chair of the Editorial Board

Walter Leitner, Scientific Editor

Sarah Ruthven, RSC Editor



Looking for that **special** chemical science research paper?

TRY this free news service:

Chemical Science

- highlights of newsworthy and significant advances in chemical science from across RSC journals
- free online access
- updated daily
- free access to the original research paper from every online article
- also available as a free print supplement in selected RSC journals.*

*A separately issued print subscription is also available.

Registered Charity Number: 207890

22030682

RSC Publishing

www.rsc.org/chemicalscience